

– An international journal for New Concepts in Global Tectonics –

NCGT JOURNAL

Editor-in-Chief: Bruce LEYBOURNE (leybourneb@iascc.org)



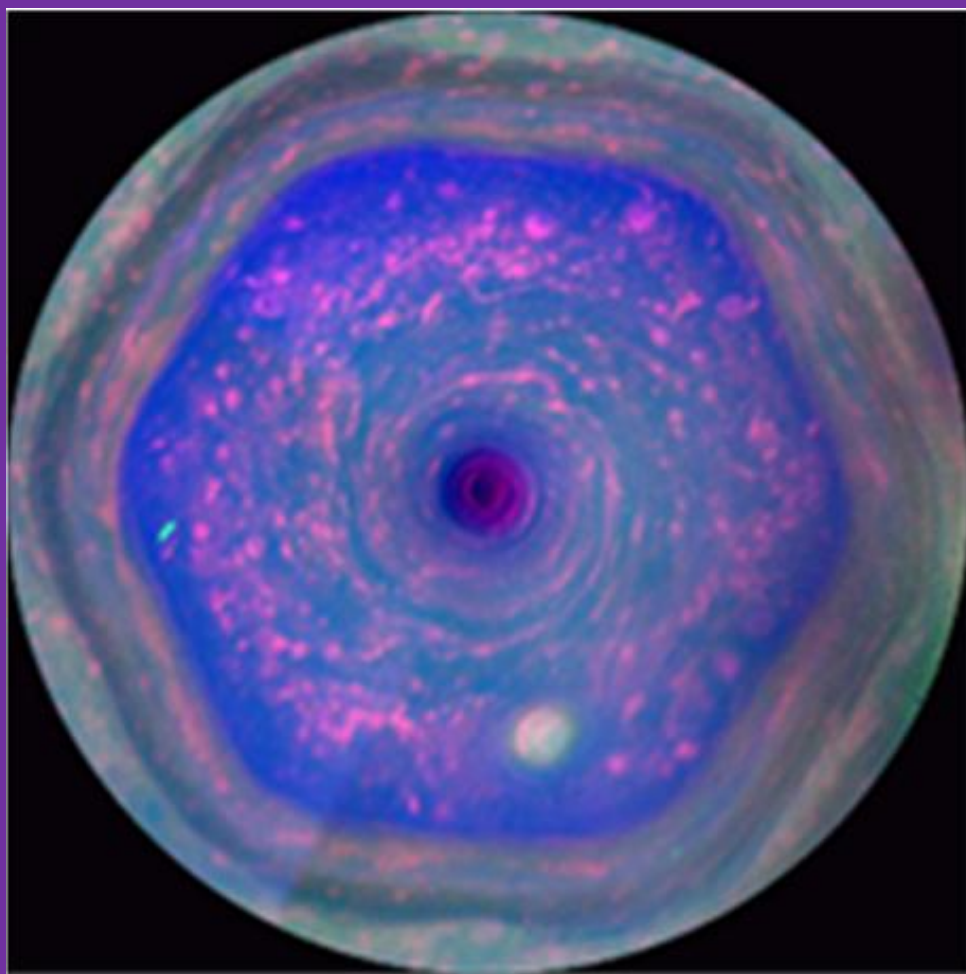
 **NCGT Journal**
New Concepts in Global Tectonics

Volume 14, Number 4
April 2026

Part 1

ISSN 2202-0039

WWW.ncgtjournal.com



Saturn's streaming hexagon

“In full view: This colorful view from NASA's Cassini mission is the highest-resolution view of the unique six-sided jet stream at Saturn's North Pole known as ‘the hexagon’. Image obtained on December 10, 2012 and released December 4, 2013.

Credit: NASA/JPL-Caltech/SSI/Hampton.” Figure and captions after Anonymous (2018f). NASA copyright free policy.

This issue : Fig .12 in The solar cycle and MiniMax - Effects on other planets. P 363.

Special Issue on
Air-Earth Currents



 **NCGT Journal**
New Concepts in Global Tectonics

Earth & Space

NCGT International Conference

September 21-24, 2026
Parma (Italy)

– *An international journal for New Concepts in Global Tectonics* –

NCGT



JOURNAL

Volume 14, Number 4, April 2026. ISSN 2202-0039.

EDITORIAL BOARD

Editor-in-Chief: Bruce LEYBOURNE, USA (leybourneb@iascc.org)
Co-Editor-in-Chief: Valentino STRASER, Italy (valentino.straser@gmail.com)
Masahiro SHIBA, Japan (shiba@dino.or.jp)
Giovanni P. GREGORI, Italy (giovannipgregori38@gmail.com)
Louis HISSINK Australia (louis.hissink@outlook.com)
Per MICHAELSEN, Mongolia (perm@must.edu.mn)
Biju LONGHINOS, India (biju.longhinos@gmail.com)
Vladimir ANOKHIN, Russia (vladanokhin@yandex.ru)

CONTENTS

PART 1

EDITOR's CORNER - Comments by Editor in Chief - Bruce Leybourne.....	229
Announcements on Upcoming Conferences - "CALL FOR PAPERS".....	229
Letters to the Editor.....	231
Online Book.....	232
Company Profiles.....	233

Article:

The Global Sun-Earth Circuit: Giovanni Pietro Gregori, Bruce Allen Leybourne, Gabriele Paparo†, and Maurizio Poscolieri.....	234
---	-----

Introduction –Anomalous Lesser Air-Earth Phenomena: Giovanni Pietro Gregori, Bruce Allen, Leybourne, Gabriele Paparo†.....	273
---	-----

The electrostatic Sun: Giovanni Pietro Gregori, Bruce Allen Leybourne.....	302
---	-----

About the NCGT Journal	316
-------------------------------------	-----

For donations, please feel free to contact the Research Director of the Geoplasma Research Institute, Mr. Bruce Leybourne, at leybourneb@iascc.org. For contact, correspondence, or inclusion of material in the NCGT Journal please use the following methods: *NEW CONCEPTS IN GLOBAL TECTONICS*. 1. E-mail: leybourneb@iascc.org (files in MS Word or ODT format, and figures in gif, bmp or tif format) as separate files; 3. Telephone, +61 402 509 420. **DISCLAIMER**: The opinions, observations and ideas published in this journal are the responsibility of the contributors and do not necessarily reflect those of the Editor and the Editorial Board. *NCGT Journal* is a refereed quarterly international online journal and appears in March, June, September and December. *ISSN number*; ISSN 2202-0039.

EDITOR'S CORNER: - Comments by Editor in Chief - Bruce Leybourne**Announcements on Upcoming Conferences - "CALL FOR PAPERS"****21-24 September 2026 – NCGT in Italy****Organized by Valentino Straser (valentino.straser@gmail.com)****Timetable for participating in the conference:**

Open abstract March 1, 2026

Abstract acceptance May 31

Payment due by June 15, 2026 (To organizing committee)

Publication of conference and abstract book September 1, 2026

September 21-24, 2026, International NCGT Conference - Parma, Italy

**Regarding information for authors:**

Abstract: 150 words (maximum)

Short CV: 300 words (maximum) and a photo.

For formatting and fonts, use NCGT Journal.

Abstract submission opens March 15, 2026

Conclusion: May 31, 2026

Confirmation of abstract acceptance: June 15, 2026

Information website about the city of Parma and its province:[homepage - Informazioni turistiche su Parma e provincia](#)

Attempting for hotel with a meeting room in the center of Parma less than 500 meters from the train station.

"Earthquake Forecasting with Space Weather between Heaven and Earth" summarizes the contents of the NCGT 2026 Conference scheduled in Parma from September 21 to 24, 2026. The NCGT team returns after fifteen years, to discuss Earth model innovations and scenarios for understanding geophysical processes and space weather effects. And, more traditionally, new models of Global Tectonics.

Understanding the Earth today means looking beyond the traditional boundaries of geology and geophysics, combining expertise ranging from electromagnetism to atmospheric physics to space weather. The "Earth & Space" conference was born with this objective: to propose an integrated interpretation of geophysical phenomena, exploring the role of electromagnetic signals as potential precursor indicators of seismic events and analyzing the contribution of new technologies for data observation and interpretation.

In recent decades, studies inspired by the global electric circuit model, a concept developed from the insights of scientists in recent decades, have highlighted how the Earth's atmosphere, ionosphere, and planetary surface constitute an electrically connected system. From this perspective, processes occurring in the lithosphere, including those preceding an earthquake, could produce measurable variations in electromagnetic fields and ionospheric properties.

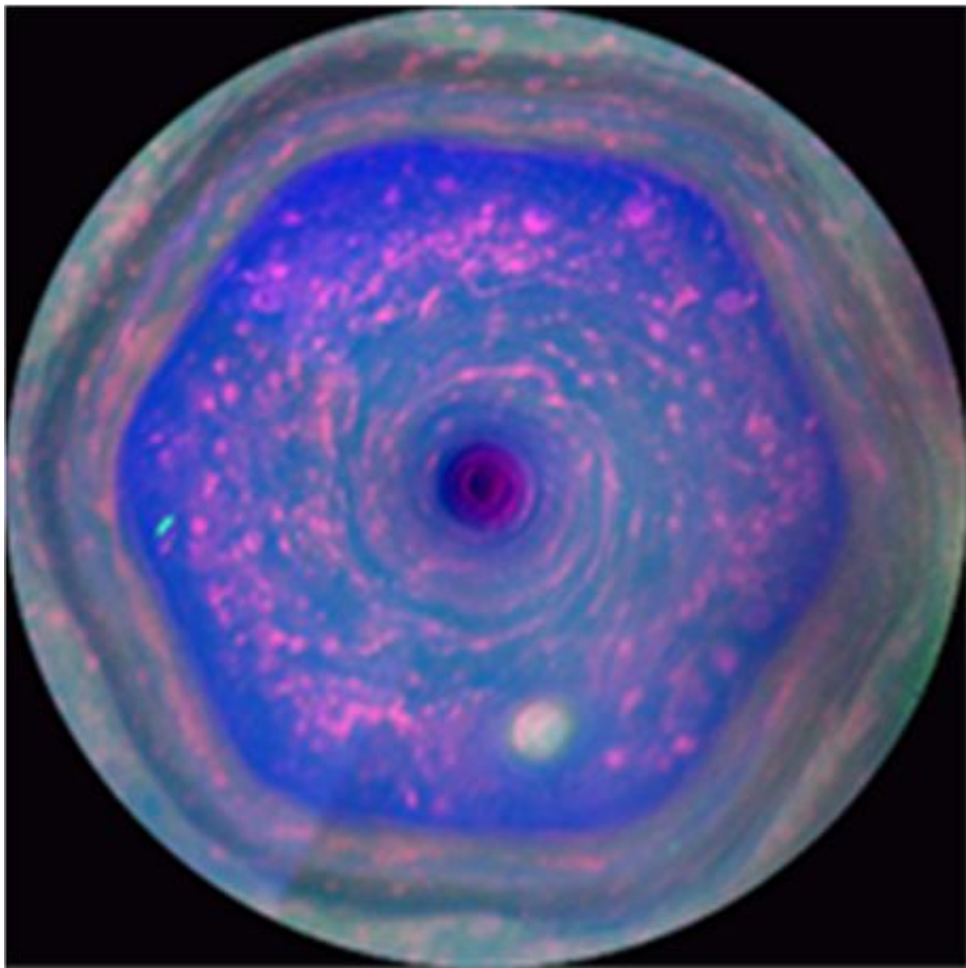
The conference aims to further analyze the so-called "candidate seismic precursors" of electromagnetic nature, evaluating their potential and limitations considering the latest scientific evidence. The integration of highly sensitive ground-based sensors, satellite networks, and ionospheric monitoring systems opens new perspectives in multi-parametric data collection and modeling of phenomena.

Special focus will be on the role of the Sun. Solar activity monitoring from NASA missions and international space weather programs, indicate influences in the ionosphere and Earth's magnetic field, have potential implications for climate and geodynamic systems. Understanding the interactions between the solar wind, the magnetosphere, and Earth's internal processes represents a crucial frontier for interpreting complex geophysical events from a systemic perspective. "Earth & Space" therefore proposes new interpretative concepts, encouraging us to move beyond compartmentalized visions to embrace a dynamic and interconnected model of the planet. Earth's evolution is not merely the result of endogenous forces but can be interpreted as the product of a continuous dialogue between space and the surface, between solar energy and deep-seated processes.

The conference is aimed at researchers, professionals, administrators, and citizens interested in understanding how new technologies and interdisciplinary models can contribute to a more advanced understanding of natural phenomena. It will provide an opportunity for scientific and cultural exchange to explore the future challenges of prevention, sustainability, and risk management on an increasingly complex planet.



- 1.) Straser - EQ forecasting (Abstracts requested)
- 2.) Leybourne - Stellar Transformer - Global Space Weather interactions (6 Abstracts in Editor's Corner within New Concepts in Global Tectonics Journal - Volume 12, Number 4, December 2024)
- 3.) Anokhin - Lake Ladoga - Siberia (2 Abstracts in Editor's Corner within New Concepts in Global Tectonics Journal - Volume 13, Number 1, March 2025 pp. 5-8, more abstracts requested)
- 4.) Longhinos - Indian Tectonics (Abstracts requested)



Cover Image : Saturn's streaming hexagon: “In full view: This colorful view from NASA's Cassini mission is the highest-resolution view of the unique six-sided jetstream at Saturn's North Pole known as 'the hexagon'. Image obtained on December 10, 2012 and released December 4, 2013. Credit: NASA/JPL-Caltech/SSI/Hampton.” Figure and captions after Anonymous (2018f). NASA copyright free policy. **This issue : Fig. 12 in The solar cycle and MiniMax - Effects on other planets. P 363.**

Letters to the Editor: Giovanni Gregori discusses research papers

In the present series of papers on air-earth currents, the set is composed of:

Gregori, G. P., B. A. Leybourne, and G. Paparo†. Introduction – Anomalous lesser air-earth phenomena,

Gregori, G. P., and B. A. Leybourne. The electrostatic Sun

Gregori, G. P., B. A. Leybourne, and J. R. Wright. The solar cycle and MiniMax

Gregori, G. P., and B. A. Leybourne. The solar cycle and MiniMax - Effects on other planets

The first paper discusses a few items that are generally considered of lesser interest, although they are strictly pertinent to the discussion of air-earth currents. Since they were not included while dealing with other facets of our discussion, they are here outlined for the sake of completeness.

The second paper deals with the electrical charge of the Sun and of the solar wind that, at present, are erroneously assumed having a neutral charge. In contrast, a correct discussion leads to an unprecedented and clear explanation of the sunspot cycle, and this is an essential aspect for several items related to air-earth currents.

The last two papers present a concise reminder about phenomena related to some anomalies of the sunspot cycle, which imply peculiar effects either on the Earth or on planets, mostly on the large gaseous planets.

The next special issue of NCGT will contain an important historical witness by Prof. Martin T. Hovland, and a large synopsis of all recently appeared papers that, either directly or indirectly, deal with several aspects of air-earth currents. Altogether these papers are a “monograph” (of over 1,700 pages) dealing with a topic that was lacking since the time of Gauss. We hope by this having fulfilled an important gap for a correct understanding of several crucial features of solar-terrestrial relations.

.

New Book

G. P. Gregori (born 1938), Degree in Physics (1961, Univ. of Milan),

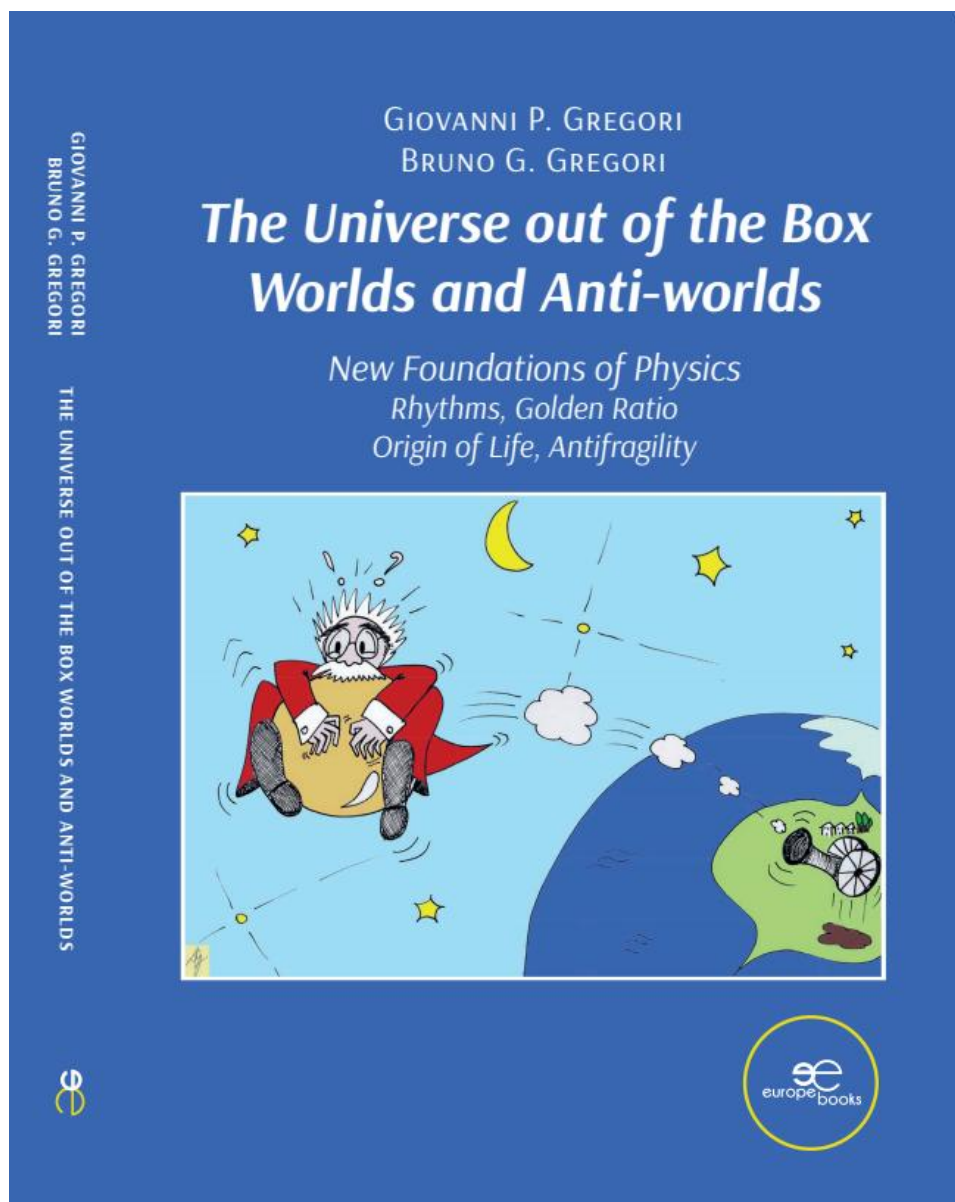
B. G. Gregori (born 1967), Degree in Medicine and Surgery (1992) and Specialization in Neurology (1999)

Science is suffering an identity crisis. Our “widespread scientific knowledge” is “static”.

Our mind dislikes uncertainty. Not relying on the mainstream is uncomfortable, but we gain better awareness of the world and of ourselves. This book is challenging. It stimulates the reader also on a psychological level, and tries to explain concepts that to most people consider abstruse. It is a journey where mind can dance between quantum physics, cosmology, theology, Greek philosophy and the mystery of life and death. Science is logic, and a scientist can never give up. Many present unsolved paradoxes can find a solution.

At present, we are biased by: 3 “original sins” in Newton’s principles, by an Einstein’s mistake, and by a misconception of “absolute” time and of the perception of time passing. A new formulation is presented, which is a substantial advancement compared to Galileo, Newton, Maxwell and Einstein.

<https://www.europebookstore.com/products/the-universe-out-of-the-box-worlds-and-anti-worlds-g-p-gregori-and-b-g-gregori/>



Company Profiles:

Tesla 3D, Inc. is an independent research and development company with a strong applied science foundation, enabling rapid and practical innovation in the energy and exploration sectors. While not a large enterprise, Tesla 3D, Inc. stays well informed about breakthroughs in electrical generation, storage, and mining technologies. When called upon, the company can comprehend complex challenges and develop strategic, real-world plans that effectively navigate regulations, funding mechanisms, and policies. Tesla 3D, Inc. actively contributes to national and industry advancement through volunteer leadership, including participation in the Homeland Security Taskforce focused on energy resilience and EMP (electromagnetic pulse) threats. The company also set a precedent by independently qualifying for federal Innovation (R&D) Tax Credits; demonstrating that small, agile innovators can leverage these incentives to streamline regulatory solutions and tackle critical infrastructure challenges. This involvement underscores Tesla 3D, Inc.'s commitment to advancing energy security and shaping the transformative role of technology in resource development. Founded: 2011 Colorado by R. Miller.

Geo-Transect LLP (www.tgeo.co.in) Geo-Transect LLP is a knowledge-driven geoscience consultancy, specializing in subsurface exploration and environmental intelligence across India. With core expertise in subsurface mapping, groundwater zonation, aquifer recharge quantification, coastal and shoreline analysis, landscape and topological planning, and island conservation, the firm delivers data-driven insights that empower sustainable planning and development. Representing the forefront of India's earth-science services sector, Geo-Transect blends scientific precision with advanced technologies to support governmental, industrial, and research-based initiatives across southern India and beyond. Integrating indigenous knowledge with global best practices, the firm is committed to environmental stewardship and responsible resource management. Guided by the ethos "With Wisdom in Nature," Geo-Transect envisions a future where scientific understanding harmonizes development with the natural world.

Stellar Transformer Technologies (<https://stellartransformertechnologies.com/>) is a private geophysical modeling company specializing in modeling the dynamic electro-magnetic Stellar Transformer interactions between Earth-Sun and planets within our solar system. Original research started in 1995 by the current owner and founder during investigations of the seafloor as a geophysicist with the Naval Oceanographic Office at Stennis Space Center. Leading to an understanding and application of new tectonic theories. Later research confirmed dynamic links to space weather affecting a myriad of environmental factors: such as everyday weather; hurricanes; tornadoes; sever weather outbreaks; earthquakes; global climate-change; and certain types of wildfire outbreaks from passing coronal mass ejections induced by internal core generated Electro-Magnetic Pulses (EMP). Current and planned services include mapping of Stellar Transformer circuits; innovative modeling of deep earth magnetics, forecasting Earth's natural hazards listed above; database development and more. Combining big data and AI to find inter-relationships. Developing algorithm inputs for forecasting, data visualization and simulations. All leading to new forecasting technologies. We are actively assisting the EMP Task Force power grid protection efforts with direct input and evaluation of EMP threats. Our company comprehends the complex challenges of geophysical modeling and development of real-world forecasting applications. Electro-magnetic or magnetic induction is the production of an electromotive force, or voltage, across an electrical conductor in a changing magnetic field. The Stellar Transformer Concept contends that simple step-down energy induction occurs between Sun and Earth, much like the transformer process that steps down your household energy from higher voltage transmission lines sourced from the power company. The Sun represents a large coil from the power company, while the Earth represents the smaller coil to your home. The larger coil element generally excites current into the smaller coil element by induction of "step down energy", although lesser feedback mechanisms occur due to the action/reaction principles. Layers within the Earth hold and release charge acting as condensers, or capacitance layers. Thus, the Earth operates somewhat like a battery where energy is either stored or released through time-change of state-of-matter. We combine new Geophysical Intelligence with AI for a winning combination of innovations that will bring new mitigation strategies for space weather to the forefront. Bringing a paradigm shift to the business community for global environmental forecasting based on solar and planetary effects. This will save lives and mitigate property damage using new science and innovative technologies. Many of these ideas were first presented at EU2015 - Electric Universe (<https://www.youtube.com/watch?v=IoggZhbxxhU>). Followed up at EU2016 with discussions on geometrical modeling applications, adhering to golden ratio principles (<https://www.youtube.com/watch?v=Q355Haapq-0>). Founded: 2023 in Colorado by Bruce Leybourne – Owner/Operator.

The Global Sun-Earth Circuit

Giovanni Pietro Gregori¹, Bruce Allen Leybourne², Gabriele Paparo^{1,3,†}, and Maurizio Poscolieri⁴

¹Former Senior Researcher at *IDASC-Institute of Acoustics and Sensors O. M. Corbino* (CNR), Rome, now merged into *IMM Istituto per la Microelettronica e Microsistemi* (CNR) Italy; and *ISSO-International Seismic Safety Organization*, Italy

²*GeoPlasma Research Institute-(GeoPlasmaResearchInstitute.org)*, Aurora, CO 80014, USA

³Associate *INVG*

⁴Former Director of *IDASC-Istituto di Acustica e Sensoristica O. M. Corbino* (CNR), Roma, at present retired *means*

Corresponding Author:

Giovanni Pietro Gregori
IDASC-Istituto di Acustica e Sensoristica O. M. Corbino (CNR), Roma, now merged into *IMM-Istituto per la Microelettronica e Microsistemi* (CNR) Italy
e-mail:

giovannipgregori38@gmail.com;

leybourneb@iascc.org

maurposc@gmail.com

† means deceased

Abstract: An ensemble of concepts is recalled that are needed for references in some articles of the present special issue. Owing to brevity purpose, no details can be given. The first item deals with historical information concerning air-earth currents. Then, the general perspective of the Earth model is illustrated. The next topics deal with some details about the Earth's interior and the generation of endogenous energy, and its propagation and transfer to Earth's surface with impact on geodynamics and on climate control. A few details are given about the "Pohlfluchtkraft", about the Pekeris force, and about a model for island arcs formation. A brief illustration is given of the large regions of anomalous large release of endogenous energy, i.e., Tuzo and Jason, related to the quatrefoil pattern, to the *DUPAL* anomaly, to diamond bearing kimberlites, to the Arctic cap, and to the Banda Sea. The next item deals with crustal stress monitoring and propagation, i.e., with acoustic emission (*AE*) minoring of the crust. The Appendix contains a brief review of the isotopic chemism of ocean basalt, referring to the concentration ratio of radioactive isotopes mostly concerning three elements, i.e., *Pb*, *Sr* and *Nd*. The *Pb* ratios refer to the ratios of ²⁰⁶*Pb*, ²⁰⁷*Pb*, ²⁰⁸*Pb* with respect to the stable isotope ²⁰⁴*Pb*. The *Sr* ratio refers to the radioactive isotope ⁸⁷*Sr* with respect to the stable isotope ⁸⁶*Sr*. The *Nd* ratio refers to the radioactive isotope ¹⁴³*Nd* with respect to the stable isotope ¹⁴⁴*Nd* (these plots are named tectonomagmatic discrimination diagrams). It is shown how to recognize 5 clusters. The usual "reservoirs" and "cocktails" model is here abandoned in favor of an "energy hierarchy" model, representative of the evolution of the basalt chemism associated to the upward penetration of sea-urchin spikes. A consequent rationale is detected, related to the geographical distribution of the basalt chemism, and also to the time-evolution of the basalt of the Andes.

Keywords: history – *IGRF* - global electrical circuit - Earth's endogenous energy – origin of the geomagnetic field - *TD* dynamo of the Earth and of planetary objects – water, Moho, serpentosphere - Earth's battery – *IC* and magpol state - soil exhalation – energy propagation to the Earth's surface – *ESI* mechanism - *CGDS* - climate control – three engines (physical, chemical, biological) – *LIPs* – *MORs* – origin and destruction of continents (Mortari cycle) – *WMT* – *FRs* – extinction events - Pohlfluchtkraft - Eötvös force - Pekeris force - island arcs – Tuzo & Jason – quatrefoil – basalt chemism - *DUPAL* anomaly – kimberlites - crustal stress - acoustic emission – flaw domain - tectonomagmatic discrimination diagrams – isotopic chemism - ocean basalt - 5 clusters - energy hierarchy - *H, D, N, A, SH* clusters - ³*He*/⁴*He* ratios - "reservoirs" and "cocktails" model – geographical distribution of basalt chemism – time evolution of Andes' basalt

Introduction

The present introductory paper illustrates a few concepts, needed as a reference by subsequent articles. It is a concise integration of Gregori and Leybourne (2021), as we do not repeat several concepts. We just add a few items, aimed to clarify additional facets required by the general rationale of air-earth currents. In addition, owing to brevity purpose, we can give no exhaustive proof concerning some item, because a full treatment ought to require a devoted long discussion to be given elsewhere. In some respect, the

result here given is a potpourri of relevant concepts and results that are more extensively illustrated elsewhere.

Historical premise concerning air-earth currents

Adrien-Marie Legendre (1785 and 1789; lived 1752-1833) first exploited the formalism of what we now call (respectively) Legendre's and associated Legendre's polynomials: they were the simplest analytical form of spherical harmonic (*SH*) functions.

Legendre's purpose was the study of the figures of the Earth and planets. Harmonic functions – rather than other

functions - were needed, as the gravitation potential satisfies the Laplace' equation.

Half a century later, Gauss (1836, ..., 1841) computed for the first time a *SH* expansion (*SHE*) of the magnetostatic potential of the Earth in terms of the Legendre's associated *SHs*. Since the magnetostatic potential satisfies the Laplace' equation, Gauss could transfer to the magnetic field **B** the identical mathematical knowhow exploited by Legendre for gravitation.

Gauss supposed - as a reasonable (at that time) working hypothesis - that the role can be approximately neglected of the air-earth electric currents **j**, at least when dealing with an average impact, computed over whole Earth. This was the historical origin of the present standard and well-known *IGRF* (*International Geomagnetic Reference Field*) models that are regularly computed for *IGA* every 5 years.

However, according to some recent evidence - which is extensively documented in the present special issue (mainly refer to Quinn et al., 2026) - an unexpected and as yet not fully acknowledged electromagnetic (e.m.) coupling exists between soil and ionosphere, with huge amounts of **j** that seem to flow due to soil exhalation, mainly in regions of fractured crust. This implies some serious concern about the physical significance and implicit approximation of every standard *IGRF*.

Only occasionally, such a reasonable Gauss working hypothesis was the object of discussion by some authors, who attempted to proof or to disproof it. A historical review would be too long of the attempts, proposals and partial evidences. Just refer, e.g., to the authoritative short note by Fukushima (1989) and - for the early discussion - see Chapman and Bartels (1940), or also several articles in Matsushita and Campbell (1967).

Consider only the leading and "generally agreed" set of assumptions that is authoritatively outlined by Chapman and Bartels (1940), who call air-earth currents "*vertical earth-currents*" and review the state-of-the-art.

Chapman and Bartels (1940) has been the reference source for generations of Earth scientists, and was considered the "generally agreed" explanation of phenomena. Concerning air-earth currents, no substantial improvement occurred during the subsequent several decades.

Whenever a correction to other measurements had to be introduced, in order to subtract the disturbance associated to air-earth currents, the reference physical interpretation always relied on the following argument.

Refer to two electrodes in ground, at different altitude on a hill-side. They recorded an average potential difference of $\sim 100 \text{ mV km}^{-1}$ with a **j** flowing in the electrode line toward the upper electrode. The steeper the line, the more constant and stable was **j**. In addition, they observed no dependence on geomagnetic activity, in contrast with what observed in horizontal lines (Burbank, 1905, Obergugenberger, 1926, Gish, 1933, Nippoldt, 1911).

This effect can be associated, maybe, with the geometrical factor, by which, if the **js** flow between Earth's surface and ionosphere, they obviously concentrate on the most elevated parts at Earth's surface. However, the physical explanation can be different.

Chapman and Bartels (1940) mention observations on a line located along the side of Vesuvius, where **j** was reported to flow upward during volcanically quiet periods, and downward at times of volcanic activity. However, compared to every other mountain, a volcano is substantially different.

The reversal of the **j** direction associated with volcanic activity is identified with the measurements of ions and dust released by the volcano, as measured by Palmieri (the second authoritative Director of *Osservatorio Vesuviano*; see Gregori et al., 2025t) and that were interpreted by Chapman and Bartels in a different way.

In any case, a volcano and a non-volcanic mountain cannot be compared with each other.

Chapman and Bartels (1940) remind about measurements carried out at the *Ben Nevis Observatory* in Scotland, where they measured an intense **j** that flows upward with clear summit, and downward when fog or clouds enveloped the summit.

This effect is a clear proof of the cloud screening of the ionospheric electric field **E**. In any case, these comments about the telluric currents - monitored on Vesuvius or on the summit of a mountain - must be interpreted by means of a combination:

- of the underground generator, which is supposed to supply volcanoes, although the sea-urchin spikes are a ubiquitous feature, and are responsible for the ubiquitous geothermal heat flow and exhalation of fluids from soil (see Gregori and Leybourne, 2021, and here below Table 1 and Fig. 3),
- of the sea-urchin structure,
- of the local topography, and
- of the instant electric charge of the ionosphere and cloud screening.

Chapman and Bartels (1940) warn, however, that Gish (1933) was skeptical about the interpretation of these measurements. "*If the **j** measured in the wires do actually flow in the soil from all sides of the mountain top, the circuit must be closed somehow. If it is assumed that the gradient has the same upward direction throughout the mountain, then the **j** should be closed through the air; a large **j** would go into the air on the summit. This, however, is exactly the opposite direction of the air-earth **j** observed in atmospheric electricity.*"

This statement relies on several arbitrary and unproven assumptions.

The first assumption is that the measured **j** cannot be a part of an electric circuit involving a geometrical size larger than the monitored mountain.

Another assumption is that **E** in air is the result of an ionospheric pattern - which was also arbitrarily believed to be originated by convection inside clouds, while it is a consequence if the Cowling dynamo (see Gregori et al., 2026d). In fact, the ionosphere cannot significantly change on the scale-size of a mountain. Hence, compared to ground, a mountain cannot behave differently from the

electrostatic viewpoint. Therefore, they guessed that all aforementioned observations were not reliable.¹

Chapman and Bartels (1940) comment that, if with fine weather the downward potential gradient in air is $\sim 1 \text{ V cm}^{-1}$, and if the average resistivity in the open air of $\sim 6 \times 10^{15} \text{ cm}$, a current-density $\sim 2 \times 10^{-16} \text{ A cm}^{-2}$ flows into ground from air. Similarly, concerning the aforementioned “uphill” currents, with a voltage of, say, $\sim 0.2 \text{ V km}^{-1}$, i.e., $\sim 2 \times 10^6 \text{ V cm}^{-1}$, and Earth of resistivity $\sim 10^5 \text{ } \Omega \text{ cm}$, there would be $\sim 2 \times 10^{-1} \text{ A cm}^{-2}$, which is $\sim 100,000$ times more intense than what Chapman and Bartels (*ibidem*) claim are the observed air-earth currents.

The wrong point in this argument is to liken air-earth currents inside three physical largely different environments, i.e., over ground, over a non-volcanic mountain, and over a volcano. For instance, it is nonsensical to compare air-earth currents on Aconcagua with air-earth currents on Ojos del Salado, because Aconcagua is the result of a tectonic process, while Ojos del Salado is a huge volcanic complex with a height almost identical to Aconcagua.

Chapman and Bartels (1940) claim, therefore, that one can envisage only two alternatives.

Either one assumes that the “uphill” \mathbf{j} is part of a circuit that closes in the interior of the mountain with a \mathbf{j} flowing downward.

Otherwise, they claim that one ought to appeal to systematic electrode effects, depending, e.g., on a variation of acidity of the soil with height. This could be a possible consequence of height-differences in erosion or weathering processes. That is, the mountain ought to operate like a chemical battery.

They warn, however, having attained no final decision concerning possible electrochemical or thermo-electrical processes.

This is obviously mere speculation. Indeed, everybody often wants to find an explanation, even though, in general, he does not try to inspect where his preconceived models and paradigms - or even the primary gnoseological approach - are correct, or ought rather to be revised in order to fit objective evidence of observations.

Finally, Chapman and Bartels (1940) remind about the experiment carried out in Finland by Lemström (1899) (see Gregori, 2020) by means of a “point-apparatus” on the tops of the Finnish mountains.

An area of several hundred square meters of the top of a mountain was covered with barbed wires, fastened on insulators connected - through a galvanometer - with an earthed plate in the valley. A downward current was detected, with numerous point-discharges that, at night, sometimes looked like St. Elmo's fire. However, Chapman

and Bartels (1940) simply claim that a credible explanation is by means of the normal atmospheric-electric vertical current. They don't specify, however, the reason of such “vertical currents”.

The great confusion is evident, while comparing with one another a few very different phenomena. Different articles in the present set of papers dealing with air-earth currents comment and discuss this remarkable and authoritative information. The scope is to give a hopefully correct assessment of the present knowledge dealing with “air-earth” currents.

The general perspective

We stress how it is possible to attempt and exploit the enormous source of clean electrostatic energy from the atmosphere. The focus is on practical procedures. In addition, we consider the reasons that forbade a previous development of such an achievement.

The key is the Sun-Earth electrical circuit (Fig. 1) that is supplied by the tidal action on the Earth, which is modulated by the encounters of the Solar System with clouds of matter inside the Galaxy - i.e., one deals with Galaxy - Sun - Earth Relations (Gregori, 2002; Gregori and Leybourne, 2021).

Fig. 2 is an outline of the mechanisms (see here below, and also Fig. 25 in Gregori and Leybourne, 2021 for additional explanation). Gravitation, through tidal interaction, supplies the *TD* (tide-driven) dynamo, which generates endogenous electric currents. A tiny fraction ($< 1\%$) produces the geomagnetic field \mathbf{B} , while the largest fraction decays by Joule heat, being the main source of endogenous heat. Table 1 and Fig. 3 show the resulting energy balance (after Gregori, 2020).

The Earth behaves like a “battery” that stores and discharges energy at different times, as the tidal action is steady, while the release of endogenous energy occurs by an intricate and time-delayed process (see below). The difference should be stressed with the surviving - unproven - concept of the Earth like a hot ball that cools on the *Ga* time scale, i.e., reminding about the model-Earth conceived by Buffon² who investigated cooling of bronze cannon balls.

The *TD* dynamo is typical of every planetary object that - similarly to the Earth - is composed of disjoint parts, and of a gravitational interaction characterized by a space gradient, by which the variation of gravitation through the body of the planetary object determines a relative motion of different component parts of the object. Since these parts, in general, are electrically charged, their relative motion is an effective dynamo driven by gravitation.

¹ Often scientists claim that observations are not reliable, when observations do not fit their expectation based on preconceived models and subconscious paradigms.

² Georges-Louis Leclerc, Comte de Buffon (1707-1788), famous French naturalist. Some recent investigation

partially revisits such a general, and more or less subconscious, feeling (see, e.g., Reimink et al., 2023, illustrated by Penn State, 2023).

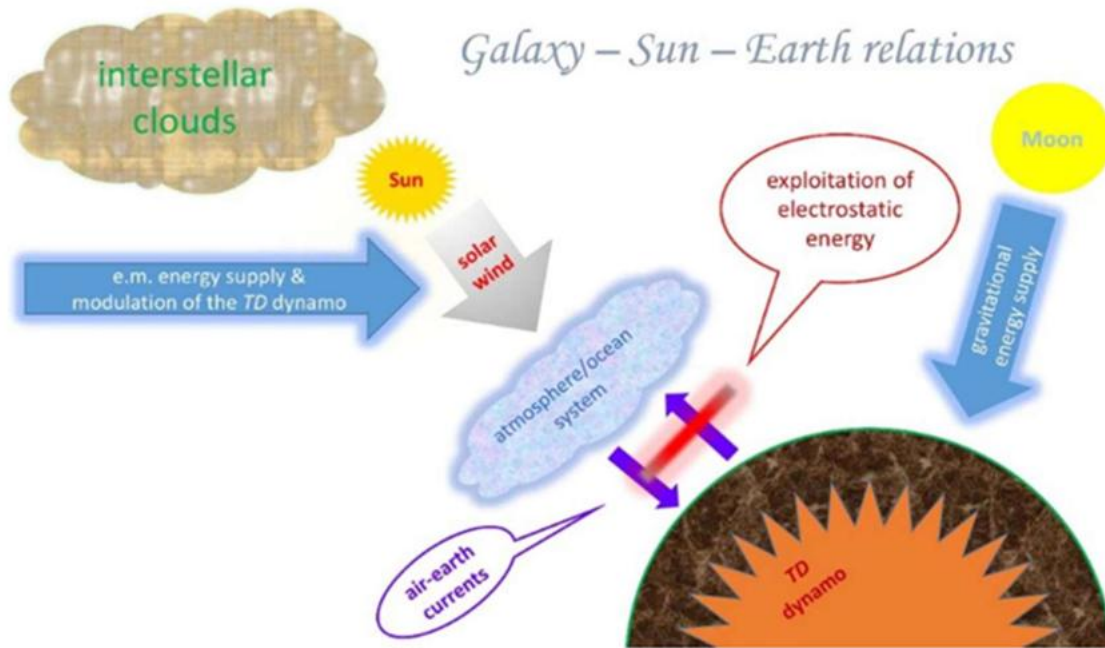


Fig. 1 - The global electrical circuit in Galaxy-Sun-Earth relations. See text. After Gregori (2020). With kind permission of Acoustics.

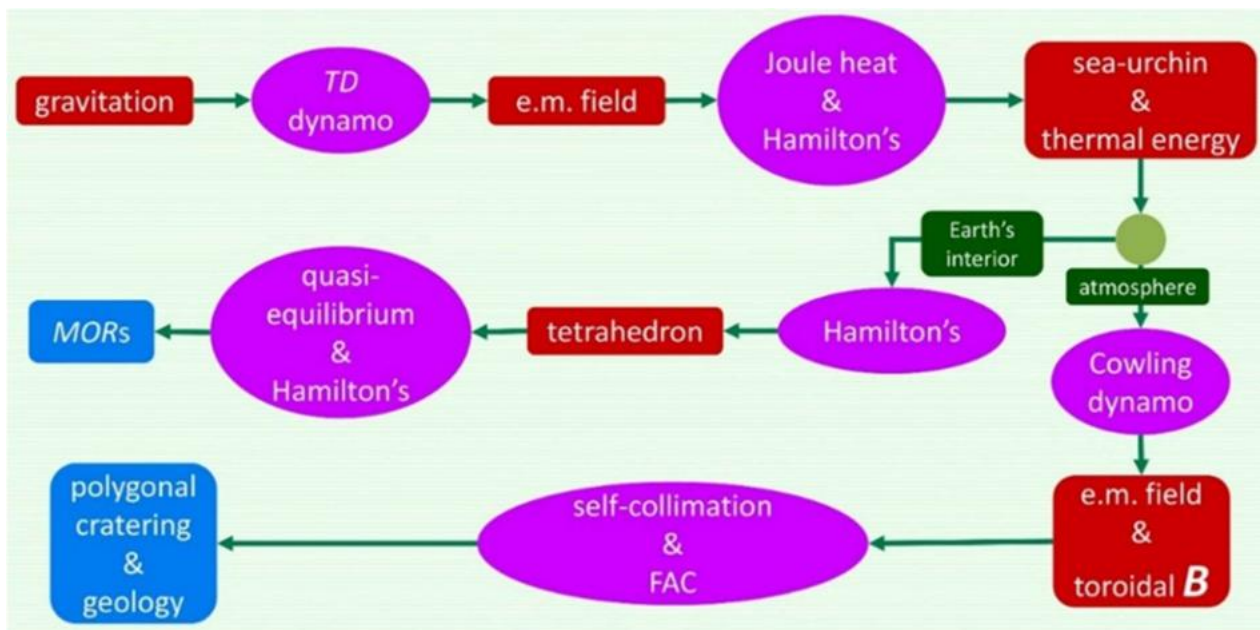


Fig. 2 – Mechanism and consequences on the Earth system associated to the Sun-Earth circuit.

Table 1. Endogenous energy of the Earth during the last few million years ($\times 10^{13}$ W)

Kind of Power	Estimate	Rough value	Percent
global heat flow measured across Earth's surface	4.42 ± 0.10	~ 4.42	$\sim 79\%$
tidal friction (total)	$0.4 \div 0.7$	~ 0.55	$\sim 10\%$
magmatic heat flux	$0.20 \div 0.39$	~ 0.3	$\sim 5\%$
metamorphic heat for transforming sedimentary and volcanic rocks	the same order of magnitude	~ 0.3	$\sim 5\%$
gravity sliding	2.5×10^{-2}	~ 0.025	$\sim 0.5\%$
seismic	$0.3 \div 3 \times 10^{-3}$		$\sim 0.5\%$
potential energy loss due to soil erosion	3×10^{-4}		$\sim 0.0\%$
Total		~ 5.56	100%

The energy balance of phenomena that occur in the case of the Earth are extensively discussed in Gregori (2002),

and are also briefly summarized in Gregori (2020). The available endogenous energy is found to be sufficient to

explain all phenomena observed on the Earth. The same mechanism applies to every other planetary object. A representative parameter - dealing with every given object - is the product of the diameter of the object times the local spatial gradient of gravitation. Tables 2 and 3 are borrowed after Gregori (2016),³ and see also Gregori and Leybourne (2021), show what objects can be characterized by a *TD* dynamo (see the last column of Table 3). Owing to brevity purpose, no comment can be here given concerning every case.

Four comments (at least) must be specified.

The energy balance - between sources and sinks - is presently focused, as a standard, on emphasizing the heat stored in the atmosphere. Conversely, Table 1 and Fig. 3 show that geothermal energy plays the leading role. The climate impact related to air-earth currents is briefly discussed and synthesized in Gregori and Leybourne (2025k).

One concern deals with the joint interaction of the **B** that is generated inside a planet, and the **B** that is generated inside all satellites of its satellite system. All satellites can influence one another, and also the central planet, in different ways. First, they interact through mutual tidal action that supplies every respective internal *TD*-dynamo, and, in any case, the global planetary magnetosphere results therefore from the sum of the *TD*-dynamo of every satellite.

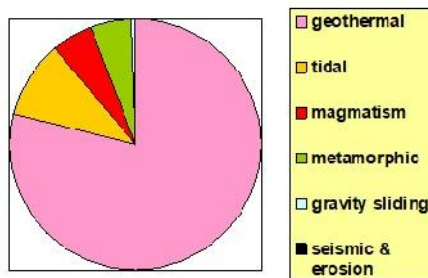


Fig. 3 - Relative role, during the last few million years, of different kinds of endogenous energy manifested in Earth phenomena (see Table 1). After Gregori (2020). With kind permission of *Acoustics*.

Another interaction can be associated to the electrostatic charge of every planetary object. If the total charge is not null, the orbital motion of the object, and also its spinning, are all sources of **B**. That is, altogether, the whole satellite system of a planet is an intricate sum of *TD*-dynamos that operate inside every object of the system, plus the **B** generated by the orbital motion and by the spinning of electrically non-neutral planet and/or satellites. In fact, unlike what is general believed, the solar wind is not neutral (see Gregori and Leybourne, 2026b). Hence, such a possibility cannot be ruled out.

Another concern deals with the time-variation of the efficiency of the *TD*-dynamo. One mechanism is through

the modulation of the intensity of the currents **j** induced in the mantle, which is the stator field of the *TD* dynamo. That is, the variation of the efficiency of the *TD* dynamo inside every given planetary object depends on the long-period e.m. induction by the solar wind through the “internal way” (see below).

An impressive variation of e.m. induction inside a planet or every satellite - or inside the whole planetary system - depends on the heliocentric distance. The Pluto/Charon binary system, owing to the large eccentricity of the orbit, is one impressive example of this kind. This effect explains several amazing features of the Hadean landscape, which rivals the most fanciful imagination of every most clever science-fiction writer (Gregori, 2016). That is, the magnetosphere of the planetary system of Pluto/Charon and of their four micro-satellites displays an intense seasonal dependence during the long Hadean year, with freezing and melt of oceans crossed by icebergs of other chemical components. Pluto/Charon is a natural laboratory surprisingly suited to test the various mechanism of generation of **B** fields in a composite planetary system.

An expressive implication of a *TD*-dynamo is the correlation with tectonism observed on the planetary object. This check applies fairly well to all objects inside the Solar System, as can be checked by a close inspection of Tables 2 and 3. A brief summary of this mechanism is as follows, anticipating a more detailed illustration given below.

Every kind of current **j** that is generated by any means inside any given object must expand in space as much as possible, due to Hamilton's. Finally every **j**-loop reaches some region where a rapid decrease occurs of the local electric conductivity σ , where the **j** decay by Joule heat. If a lesser bump occurs on the surface reached by the **j**-loops, the smaller the local radius of curvature of the surface, the greater the concentration of **j**, hence the greater the Joule heating. Thus, the **j**-loop can further propagate upward while the former bump shrinks. Finally, this give rise to the formation of a spike, and therefore the interior of the planetary object reminds about a sea-urchin. Refer to Gregori (2002) and to Gregori and Leybourne (2021) and references therein.

Bunches of sea-urchin spikes produce a spatial gradient of thermal expansion of the mantle. Thus, huge “hills” are formed, which are named superswells. The lithosphere slides on the slopes of superswells, over the lubricated surface of the asthenosphere. Geodynamics reminds therefore about a hot mud that slides on the slopes of the superswells. Different lithospheric slabs finally collide inside huge megasynclines, where continents and mountains are generated through over-thrust, and maybe also some partial folding. The complete incompatibility ought to be emphasized with any model based on a floating lithosphere - such as the standard, well known, and often contended and criticized plate tectonics that has to be totally rebutted.

present discussion. The value dealing with the Pluto/Charon system were computed after the observations carried out by the *NASA* probe *New Horizons*.

³ These tables were computed in 2004. Owing to their order-of-magnitude estimates, every eventual subsequent lesser improvement and updating in the evaluation of the input parameters is unessential for the

Table 2 - Intensity of the differential tidal pull acting on different objects in the Solar System (I)

<i>planet</i>	$TD_{Sp} (\times 10^{15})$	<i>satellite</i>	TD_{ps}	TD_{Ss}	$\sum [TD_{ps} + TD_{Ss}]$
Mercury	2.2011				
Venus	12.349				
Earth	6.0328				
Mars	0.097556	Moon	3.5960×10^{21}	2.0255×10^{13}	3.5960×10^{21}
		Phobos	2.7910×10^{10}	5.3227×10^3	2.7910×10^{10}
		Deimos	0.0196×10^{10}	0.6235×10^3	0.0196×10^{10}
Jupiter	149.44	Amalthea	1.4760×10^{13}	1.9432×10^5	1.4760×10^{13}
		Io	1.0979×10^{18}	1.8319×10^{11}	1.0979×10^{18}
		Europa	1.2575×10^{17}	8.4348×10^{10}	1.2575×10^{17}
		Ganymede	1.6141×10^{17}	4.3899×10^{11}	1.6141×10^{17}
		Callisto	1.9698×10^{16}	2.9198×10^{11}	1.9698×10^{16}
Saturn	6.0172	Mimas	1.7881×10^{14}	1.3796×10^6	1.7881×10^{14}
		Enceladus	2.9212×10^{14}	4.7219×10^6	2.9212×10^{14}
		Thetys	1.9326×10^{15}	5.9488×10^7	1.9326×10^{15}
		Dione	1.7331×10^{15}	1.1135×10^8	1.7331×10^{15}
		Rhea	1.8334×10^{15}	3.2174×10^8	1.8334×10^{15}
		Titan	2.8784×10^{16}	6.2979×10^{10}	2.8784×10^{16}
		Hyperion	6.6977×10^{10}	2.6087×10^5	6.6978×10^{10}
		Iapetus	4.6841×10^{12}	2.5361×10^8	4.6843×10^{12}
		Phœbe	5.5212×10^7	1.4384×10^5	5.5356×10^7
Uranus	0.049403	Ariel	2.6048×10^{15}	1.7575×10^7	2.6048×10^{15}
		Umbriel	8.4348×10^{14}	1.5372×10^7	8.4348×10^{14}
		Titania	7.7761×10^{14}	6.2408×10^7	7.7761×10^{14}
		Oberon	2.6829×10^{14}	5.1478×10^7	2.6829×10^{14}
		Miranda	1.6396×10^{14}	3.4882×10^5	1.6396×10^{14}
Neptune	0.014653	Triton	1.7624×10^{16}	1.6824×10^8	1.7624×10^{16}
		Nereid	8.5273×10^8	3.0488×10^4	8.5276×10^8
Pluto (aph.)	0.560×10^{-9}	Charon (aph.)	2.2214×10^{14}	0.286×10^6	2.2214×10^{14}
(perih.)	1.208×10^{-9}	(perih.)	2.2214×10^{14}	0.617×10^6	2.2214×10^{14}

In addition, when the interaction of different sea-urchin spikes is considered, the Hamilton's principle enters into play, and an explanation is thus surprisingly found for the geographical distribution of MORs (Mid-Ocean Ridges; Gregori and Leybourne, 2021).

It should be stressed that no explanation at all was ever proposed in the literature for such an impressive morphological feature of the Earth. In particular, this finding is relevant for the Digital Twins perspective, as it clearly envisages the deep location of an exact tetrahedron conductor that plays a crucial role in the e.m. coupling between solid Earth and solar wind (see also Leybourne et al., 2025).

Summarizing, every object with an endogenous and efficient TD-dynamo has an intense source of endogenous energy that produces a relevant amount of tectonism, and

this correlation seems to be verified by the present known association of tectonism with a **B** field of every given planetary object. Refer in detail to Tables 2 and 3.

The better known mechanism, generally reported in the literature, for **B** generation inside a star or a planet, is the MHD dynamo formerly proposed by Larmor in 1919/1920 for the Sun, and later applied to the Earth by Elsasser and Bullard. The MHD mechanism, however, leads to a self-blocking of the system, due to insufficient extraction of energy from the system. Therefore, the system ends into a self-blocking ("*Biermann blocking*"). Thermonuclear reactions inside a star continuously break the magnetic blocking, unlike inside a planet, where the MHD mechanism cannot be operative. See the detailed discussion given in Gregori (2002).

Table 3 -Intensity of the differential tidal pull acting on different objects in the Solar System (II)

<i>planet or satellite</i>	TD_{sp}	$\sum [TD_{Sp} + TD_{sp}]$	B (surface) (Gauss)	mean radius (km)	mean density ($g\ cm^{-3}$)	TD dynamo
Mercury		2.2011×10^{15}	0.002	2440	5.43	?
Venus		1.2349×10^{16}		6052	5.24	Y
Earth	1.3182×10^{16}	1.9215×10^{16}	0.5	6378	5.52	Y
Moon				1737.5 ± 0.1	3.344 ± 0.005	Y
Mars		1.0619×10^{14}		3397	3.93	Y
Phobos	8.5238×10^{12}			11.1 ± 0.15	1.867 ± 0.076	N
Deimos	0.1071×10^{12}			6.2 ± 0.18	2.247 ± 0.251	N
	8.6309×10^{12}					
Jupiter		5.2791×10^{19}	4.2	71492	1.33	Y
Amalthea	1.2365×10^{16}			83.45 ± 2.4 [$135 \times 84 \pm 75$]	0.849 ± 0.199	N
Io	4.2137×10^{19}			1821.6 ± 0.5	3.528 ± 0.006	Y
Europa	5.6327×10^{18}			1560.8 ± 0.5	3.013 ± 0.005	N
Ganymède	4.2885×10^{18}		0.02	2631.2 ± 1.7	1.942 ± 0.005	Y
Callisto	5.7133×10^{17}			2410.3 ± 1.5	1.834 ± 0.004	Y
	5.2642×10^{19}					
Saturn		1.3107×10^{18}	0.2	60268	0.69	Y
Mimas	5.2429×10^{16}			198.6 ± 0.6	1.165 ± 0.023	N
Enceladus	6.8206×10^{16}			249.4 ± 0.2	1.603 ± 0.345	Y
Thetys	2.1238×10^{17}			529.9 ± 1.5	0.991 ± 0.009	Y
Dione	1.8054×10^{17}			$559. \pm 5.$	1.490 ± 0.040	?
Rhea	1.3974×10^{17}			$764. \pm 4.$	1.240 ± 0.044	Y
Titan	6.5094×10^{17}			$2575. \pm 2$	1.881 ± 0.005	Y
Titan	6.5094×10^{17}			$2575. \pm 2.$	1.881 ± 0.005	Y
Iapetus	3.7989×10^{14}			$718. \pm 8.$	1.253 ± 0.168	?
Phœbe	2.9228×10^{10}			$110. \pm 10.$	1.3 ± 0.7	N
	1.3046×10^{18}					
Uranus		2.0232×10^{17}	~ 0.4	25559	1.32	Y
Ariel	1.1412×10^{17}			578.9 ± 0.6	1.665 ± 0.147	Y
Umbriel	3.6587×10^{16}			584.7 ± 2.8	1.400 ± 0.163	?
Titania	2.4999×10^{16}			788.9 ± 1.8	1.715 ± 0.044	Y
Oberon	8.9365×10^{15}			761.4 ± 2.6	1.630 ± 0.043	Y
Miranda	1.7635×10^{16}			235.8 ± 0.7	1.201 ± 0.137	Y
	2.0228×10^{17}					
Neptune		3.2066×10^{17}	~ 0.4	24766	1.64	Y
Triton	3.2065×10^{17}			1353.4 ± 0.9	2.061 ± 0.007	Y
Nereid	1.2352×10^{11}			$170. \pm 25.$	1.5	N
	3.2065×10^{17}					
Pluto		4.3511×10^{14}	yes (?)	1187	1.86	Y
Charon	4.3511×10^{11}		yes (?)	606	1.7	Y

Symbols for Tables 2 and 3

Units are [$km\ kg\ sec^{-2}$].

TD is a unique symbol expressing tidal deformation, while other symbols are as follows:

- S for Sun,
- s for satellite,
- p for planet,
- O for orbital object,
- C for central object,
- RO is for radius of the orbiting object,
- r is for mean radius of the object,
- F for gravitation force experienced by O due to the presence of C (or viceversa, due to action-reaction).

The definition of TD_{CO} depends on the diameter of O, and it implies that TD_{CO} is the tidal deformation exerted by C over O. Analogously, TD_{OC} is the corresponding feedback reaction, i.e., the tidal deformation exerted by O over C.

The feedback tide by the planets on the Sun was not computed, because, compared to the endogenous thermonuclear energy, the solar dynamo is only slightly controlled by the tide. In addition, the Sun can hardly be represented by a unique solid body. Even the radius of the photosphere is likely to be unreliable for the present kind of approximate computation.

Summarizing, inside large objects - such as inside a star - the MHD dynamo works fairly well, while the Biermann blocking is permanently disrupted by thermonuclear reactions. In contrast, in the case of less hot objects with no

endogenous thermonuclear reactions - but with disjoint components and with a tidal gradient that moves components with respect to one another - the **B** field is generated by a *TD*-dynamo, as formerly proposed in Gregori (2002). The mechanism generates in impressive amount of energy.

The resulting general picture is in terms of three engines that control Earth's climate. The *physical* engine is the *TD* dynamo. The *chemical* engine is the generation of the serpentosphere (see Gregori and Hovland, 2025). The *biological* engine is related to the role of the biosphere that plays a fundamental role in the carbon cycle (see Gregori and Leybourne, 2021, and Gregori and Hovland, 2025).

Also the water cycle plays a fundamental role. The uppermost more hydrated layer seems to be distinguished by underlying layer by a different speed of seismic wave – being typically called Moho. The deeper penetration of water produces really explosive chemical reactions with hydrated rocks – this is serpentinization with the formation of supercritical water (*ScriW*) and of the serpentosphere (Gregori and Hovland, 2025). The resulting hydrated rocks are dehydrated by the endogenous heat released by the physical engine. The new dehydrated rocks are ready for supplying the operation of the chemical engine, etc. The biosphere exists and flourishes due to the soil exhalation of carbon compounds from soil (CH_4 , CO_2 , etc.). Dead biosphere is later deposited on ocean floors, metamorphosed by endogenous heat, while soil exhalation releases carbon compounds that supply the biosphere, etc. (see Gregori and Leybourne, 2021, and Gregori and Hovland, 2025).

The serpentosphere is likely to be crucial also for the stress propagation of ultrasounds (*AE*, acoustic emission) below the crust, hence of crustal stress on the planetary scale (see below).

An additional general concept of solar-terrestrial relation is the distinction between “*external way*” and “*internal way*”. The external way is the generally considered effect of solar wind and solar radiation, from interplanetary space through the atmosphere until Earth's surface. This is better known as “*space weather*”. The “*internal way*” is related to the modulation by e.m. induction from the solar wind into the mantle, which determines a modulation of the efficiency of the *TD* dynamo, hence of the availability of endogenous heat that affects climate (see Gregori, 2002, 2020, and Gregori and Leybourne, 2021 and references therein)

Earth interior and endogenous energy

The nomenclature of the Earth's interior in the literature is sometimes contradictory. For clarity purpose, Fig. 4 summarize the terms that are here used. For additional details refer to Gregori and Leybourne (2021) or, e.g., to Reimink et al. (2023). The Moho is tentatively defined by a transition between a lower-to-higher speed of the seismic waves, consistently (perhaps) with a different water concentration in ground.

The asthenosphere is the upper layer of the mantle, and can be associated to - or identified with - the serpentosphere, i.e., the layer of unknown thickness where

water penetrates through dehydrated rocks (see Gregori and Hovland, 2025). An explosive chemical reaction, i.e., serpentinization, produces hydration and high fracturing of rocks, embedded in supercritical water (*ScriW*). Hence, the lithosphere drifts over the asthenosphere, which is a layer lubricated by *ScriW*. The asthenosphere has a high electrical conductivity σ . Moreover, owing to the Hamilton's variation principle (see Gregori et al., 2025e), every electric current **j** originated deep inside the Earth tends to expand as much as possible. Hence, the currents **j** that leak off from the *CMB* (core mantle boundary) expand as much as possible, i.e., up to the upper boundary of the upper boundary of the serpentosphere where they decay, and contribute to increase the local σ .

Owing to the increasing gravitational compression, temperature increases vs. depth through the mantle. Higher temperatures produce greater ionization, i.e., free electrons are available extracted from progressively deeper atomic shells. Electrons are stripped from their respective nucleus. The state-of-matter is no more solid – unlike what happens in the crust - because crystalline bonds no more exist. The large availability of electrons makes the medium highly conductive - i.e., a state occurs that, inside a large planet such as Jupiter, is conventionally called “metallic”. The Earth's mantle is therefore a fluid of decreasing viscosity vs. depth, being in a state that, more correctly, must be said to be “metallic”.

The outer core (*OC*) is basically completely fluid, or metallic - and S waves cannot propagate through it. In any case, the electrical conductivity σ in the deep Earth's interior can be estimated only with large error-bars, by means of computations of induced e.m. currents of very low frequency (see Fig. 4 of Gregori and Leybourne, 2021, and also Gregori, 2002, and references therein).

When the atomic nuclei are completely stripped of their electrons, the “naked” nuclei interact through their nuclear magnetic moments (see Gregori et al., 2025w, Gregori and Gregori, 2025). On the other hand, the present theoretical physics has several uncertainties concerning the detailed mechanism. The state-of-matter is, however, compact - because magnetic cohesion forces exist that are much stronger than crystalline bonds. Owing to the complete absence of electrons, the electrical conductivity σ is null. At the same time, nuclei experience a strong electrostatic repulsion, which is opposed by gravitational compression, while attraction by nuclear magnetic moments overwhelms Coulomb's repulsion. Call “*magpol*” such a state-of-matter, being acronym for “magnetic-polarized state”. Owing to the close alignment of all magnetic moments, all nuclear magnetic moments are compacted into some kind of “fibrous” pattern. In addition, the magpol state releases no photons, i.e., it is “*dark matter*”. Several different subtle meanings are associated to the term “dark matter”. “Dark matter” here simply denotes absence of photons, hence, we cannot directly observe it. The general feeling is that the largest fraction of matter in the universe ought to be “dark matter”. See Gregori et al. (2025w), and Gregori and Gregori, 2025.

Thus, the *IC* (inner core) of the Earth is the source for the leading part of the observed geomagnetic field, i.e., of

the dipole field. Let us stress the nonsensical generally reported reference to a “solid” state of the IC, speculated only because S waves cross through the IC. In fact, S waves

cross through the IC due to the strong magnetic coupling of nuclear magnetic moments.

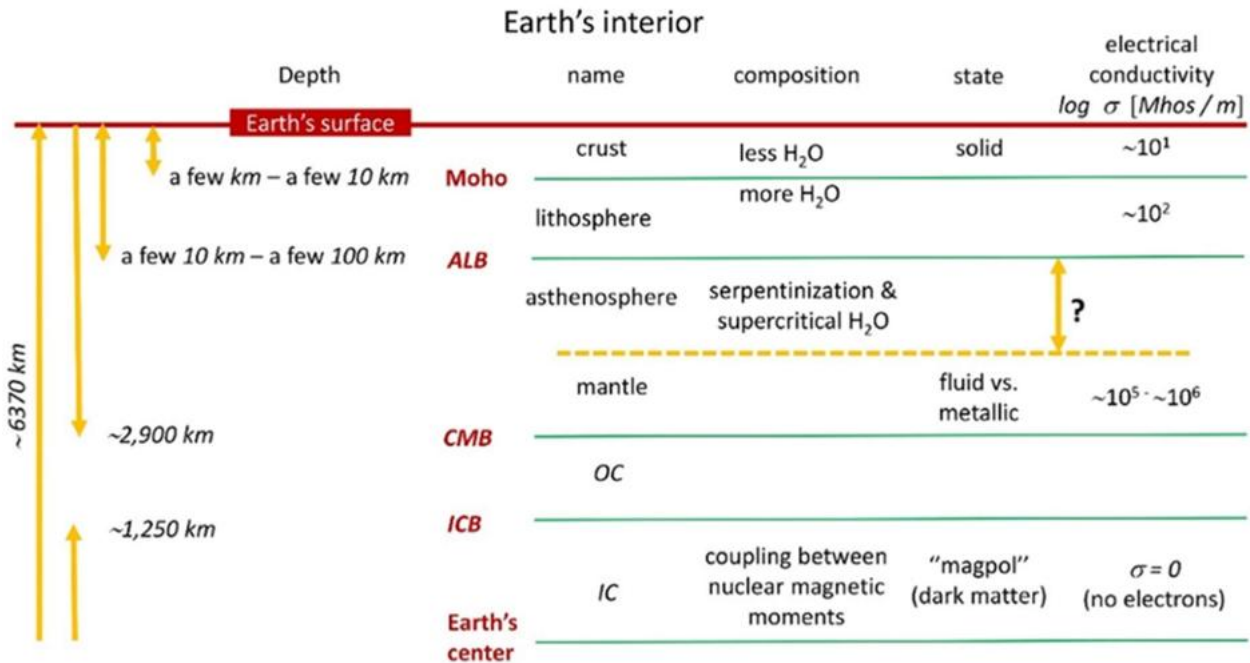


Fig. 4 – Conventional structure and names that are here adopted of the components of solid Earth.

Different component of Earth move with respect to one another, due to the varying tidal forces. Since various Earth's components are ionized, this process is the TD dynamo. The energy balance is impressive (see Fig. 3 and Table 1; and Gregori, 2002 and Gregori and Leybourne, 2021).

A crucial information derives from the so-called spatial spectrum of the geomagnetic field B (Loves, 1974; Nevanlinna, 1987), as expressed on the Lowes-Nevanlinna's (LN's) plot (Gregori, 2002, Fig. 5). When air-earth currents can be neglected, the B at Earth's surface (i.e., at $r = a$) is described by a potential, which is expressed in terms of a SHE. Every addendum of the SHE is associated to two indices. A couple of indices (i.e., degree n and order m) is associated to coefficients g_n^m and h_n^m that, in principle, can be arbitrary. In contrast, from a physical viewpoint, their trend vs. n and m reflects the physics of the dynamo. The m dependence reflects the choice of the frame of reference, unlike that n dependence, which is invariant with respect to change of frame of reference.

Fig. 5 has on abscissas n , and on ordinates the corresponding associated fraction of B^2 , when measured at $r = a$ and averaged over the entire planet - i.e., the ordinate is proportional to the mean magnetic energy density at Earth's surface associated to all terms of the SHE of the internal origin field and of a given degree n . Such a fraction is defined by considering, once at a time, every contribution by all terms, and for every fixed n by summing up over all $m = 0, 1, \dots, n$. The SHE considered in Fig. 5 is based on the B records collected by the MAGSAT satellite, epoch 1979.85, as these data are well suited for getting rid of the bias by crustal sources (Gregori et al., 1999).

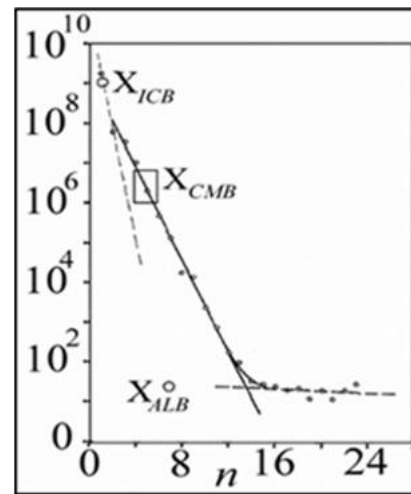


Fig. 5. Lowes-Nevanlinna's (LN's) plot. See the text for an explanation. The figure is redrawn after Gregori (2000c) and Gregori (2002). ESA copyright-free policy and kind permission of the late Wilfried Schröder.

All plotted points look aligned along 3 straight lines. One line through $n = 1, 2$ is called *Nevanlinna's line* (Nevanlinna, 1987) and is denoted by an index $k = 0$. The line $k = 1$ is called *first Lowes' line* (Loves, 1974) and it crosses through points $n = 3, 4, \dots, 13$. The third line, $k = 2$, is called *second Lowes' line* and it crosses through points $n = 14, \dots$. The three lines altogether are called LN lines (Gregori, 2002).

Focus on the energy balance, by considering that every j that is generated inside deep Earth must expand as much

as possible (by Hamilton's, see Gregori et al., 2025e). Therefore, assume that the three lines in Fig. 5 correspond to 3 spherical shells (ss) of currents that are defined like equivalent circuits suited for energy computation. Compute the \mathbf{j} that must flow on every ss, and compute the associated energy, which is function of the radius of the ss. Thus, find that the energy diverges, upon decreasing the radius of the ss, with an asymptote. The radius of the asymptote – which is related to the tilt of every LN line – surprisingly corresponds to the lower bound for the (seismically determined) radii R_{ICB} , R_{CMB} , and R_{ALB} , respectively of the ICB ($k = 0$, inner core boundary), of the CMB ($k = 1$, core mantle boundary), and of the ALB ($k = 2$, asthenosphere lithosphere boundary). The difference between every asymptote and the corresponding seismically determined radius is just a few percent. See Gregori (2002), Gregori et al. (2025m).

When considering SHEs that refer to different epochs, the tilt of every line changes vs. time, even by some relevant amount. However, every such a "historical" line always results to cross through some fixed cross-point denoted in Fig. 5 as X_{ICB} , X_{CMB} , and X_{ALB} , respectively. This implies that every line ought to be associated to some relevant change of the internal structure of the Earth, although always allowing for one specific n , and allowing for a corresponding energy contribution by that given n , which is invariant in time.

As far as R_{CMB} and R_{ALB} are concerned, the energy argument can be easily explained and understood. In fact, they correspond to the step-wise change of electrical conductivity σ (see Fig. 4 of Gregori and Leybourne, 2021), because the currents \mathbf{j} expand - and decay by Joule heat as soon as σ drops. In contrast, the difference - between R_{ICB} and the seismically determined IC radius - is a slightly larger percent than for R_{CMB} and R_{ALB} . In fact, R_{ICB} depends on the maximum and unknown compressibility of matter in the magpol state of the IC. Hence, the association with a hypothetical expanding \mathbf{j} -shell looks less appropriate – even though this is reasonable, as we are concerned only with energy estimates and balance.

During the last few centuries the values of R_{ICB} changed by a relevant amount, denoting that the energy that is produced by the TD dynamo is regularly stored inside the Earth's battery, through a change of the state-of-matter from the metallic state of the OC to the magpol state of the IC, and viceversa (Fig. 6). That is, the Earth behaves like a battery, where energy is stored or released through a change of state. The minimum value of R_{ICB} happened in AD 1790, corresponding to a geomagnetic jerk ("French Revolution jerk").

Energy transfer to Earth's surface and climate control

Refer to a given ss (e.g., at CMB), and consider a minor bump with respect to perfect spherical symmetry (Fig. 7a). Owing to Hamilton's (see Gregori et al., 2025e), the currents \mathbf{j} tend to concentrate on the top of such a bump, where they release a comparatively larger amount of Joule heat. However, the local thermal conductivity σ is very low and heat cannot propagate. Hence, the local temperature

increases, and also the local σ increases, by which, owing to Hamilton's, an additional and ever increasing amount of \mathbf{j} concentrate on the top of the bump. The process is self-amplifying. The mechanism looks like in the case of an "electric soldering iron" (ESI) that is pushed into a block of ice (Fig. 7a). The entire Earth ought thus to be depicted - in terms of the mass density - almost reminding about an onion, and - in terms of σ - reminding about a "sea urchin" or an "octopus", with every spike that shrinks while propagating upward.

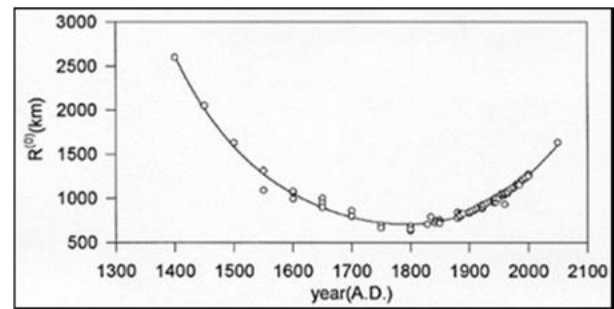


Fig. 6. Time variation of R_{ICB} and its interpolation by means of a 5th-order polynomial. Several SHEs are used. This is the apparent time variation during the last ~ 6 centuries of the geomagnetically determined values of R_{ICB} (in reality it is a lower bound limit for its physical value, implying a likely underestimate by, say, $\leq 5\%$). Plot formerly obtained in cooperation with Fabrizio T. Gizzi (after Gregori, 1997). With the kind permission of the late Wilfried Schröder

The mean speed of upward propagation is $\sim 10 \text{ cm year}^{-1}$ (dSBT law, Fig. 7b). In fact, de Santis et al. (2001) consider a "reorganization time" defined as follows. The geomagnetic potential V is defined by means of the Gauss' coefficients $\{g_n^m; h_n^m\}$ and by its SV (secular variation) \dot{V} defined by $\{\dot{g}_n^m; \dot{h}_n^m\}$. Consider the frequency f_n and the time τ_n defined by the ratio

$$f_n = 1/\tau_n = \frac{\sqrt{\langle \dot{V}_n^2 \rangle / \langle V_n^2 \rangle}}{F_n = |\text{grad } V_n|} \quad (1)$$

where the brackets denote averages, and f_n and τ_n do not depend on r . Following Stacey (1992), de Santis et al. (2001) remark that τ_n can be interpreted as a typical time associated with the "reorganisation" (due to diffusion) of some speculated initial \mathbf{j} -loop.

According to the rationale of the present study, such "reorganisation" should occur almost instantaneously, or the \mathbf{j} s ought to be induced, since their early generation, conforming with Hamilton's principle. Gregori (2002, p. 199-200) contains more extensive details and discussion. Interpret every τ_n as a ratio L_n/u_n between some typical linear dimension L_n and fluid speed u_n (absolute value). Choosing $L_1 \sim 1000 \text{ km}$ (i.e., some typical size of the core), $u_1 \sim 1 \text{ km year}^{-1}$ and $u_n \sim 6 \text{ km year}^{-1}$ for $n = 2, 3$. Thus, get Fig. 7b where the SHE terms with comparatively higher n evolve more rapidly vs. t .

On an intuitive ground, this fact derives from the ESI mechanism. In fact, for higher n , a smaller the curvature radius occurs of the sea-urchin spike or octopus' arm - or of the top point of the spike. Hence, a larger amount occurs of

Joule heat that is locally released per unit volume, and a faster heating occurs and a larger σ . Therefore, a comparative faster speed is expected of the upward propagation of the spike. It follows that such a *dSBT* law displays a slope that is related to the temporal variation of the upward propagation speed of the spike by the *ESI* mechanism. Note that the estimated speed is – as expected – of the same order of magnitude of the well-known standard drift of so-called ocean floor expansion.

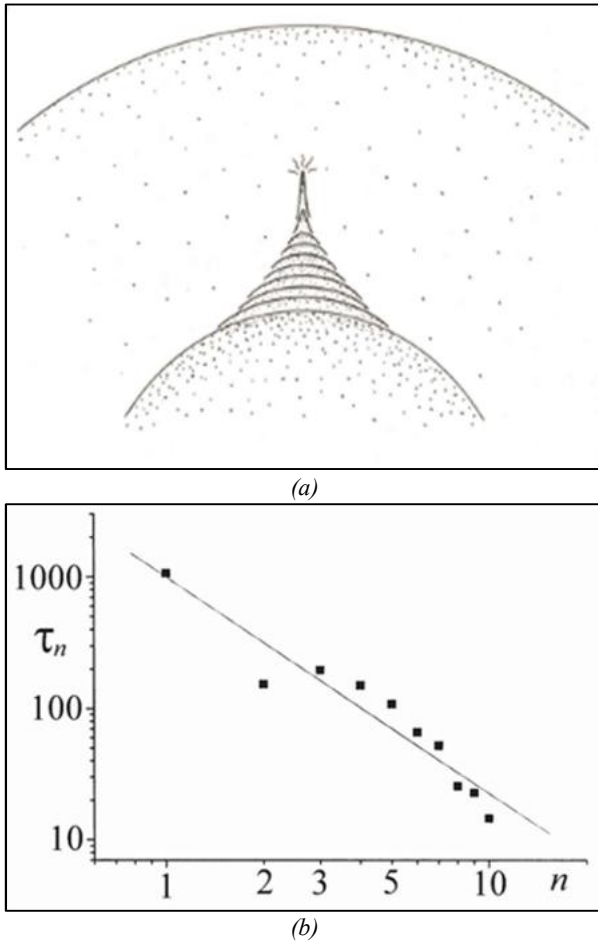


Fig. 7. (a) The *ESI* mechanism. See text. After Gregori (1993, 2002); (b) “Reorganisation times” τ_n [years] vs. n from the mean spatial spectrum of the 1960-1990 *DGRF* (log-log plot). The slope is ~ 1.64 and the regression coefficient is ~ 0.95 . This plot is called the *dSBT* (De Santis-Barracough-Tozzi) law. Redrawn after De Santis et al. (2003). After Gregori (2002). With kind permission of the late Wilfried Schröder

It should be stressed that \mathbf{j} flows along the spike like a DC current (see Gregori et al., 2025r, 2025t) - and owing to the Cowling dynamo (see Gregori et al., 2026d) it also experiences a self-collimation effect (Fig. 8). Such a propagation strictly implies no transport of matter (no magma, no ions, etc.), rather only - and strictly only - of electrons. That is, the process is merely electrodynamic, rather than thermodynamic.

When a sea-urchin spike approaches Earth's surface, as soon as it finds some fluids (water, oil, CO_2 , CH_4 , geogas, etc.), fluids transport heat by advection and ensure the energy balance. When the available fluids are insufficient,

the system warms up, and the spike further propagates upward, until it reaches some comparatively shallow depth where the equation-of-state permits melt. Thus, an additional fluid is formed, i.e., magma, that samples the chemism of the layer where it is formed (see below the mentions about the *DUPAL* anomaly). Then, magma operates like every other fluid, and transports heat by advection through effusion. Hence, as soon as some fluid (lava or other) is available, the electrodynamic process is transformed into a fluid-dynamic process. This whole process defines a volcano, and is the “calorimetric” explanation of volcanism. Note that the so-called magma chamber is a local phenomenon, and no connection exists between magma chambers of different volcanoes.

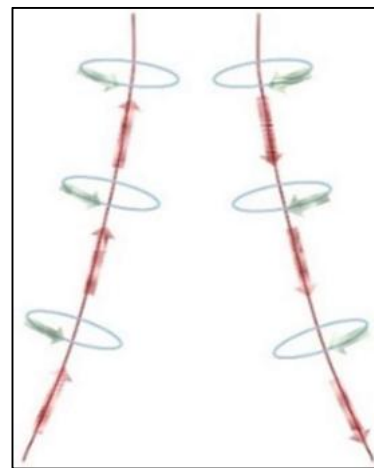


Fig. 8. Self-collimation, due to the Cowling dynamo, of the electric current \mathbf{j} that flows on one given side of a sea-urchin spike. Unpublished figure

For instance, an effective way to investigate the long-term time-variation of the release of endogenous energy of entire Earth is to consider the time lag that elapses between two subsequent periods of activity of a given volcano. That is, consider, for every given volcano, a log with (i) order number and (ii) date of every eruption activity period. Compute (iii) the time lag between successive eruption periods. Plot this time lag vs. the order number in the log. This is called “*Imbò histogram*”. It is thus found that volcanic activity displays a correlation with solar activity, and that the endogenous energy of the Earth displays the time variation that is synchronous - as displayed by different historical volcanoes of the world (see Gregori et al, 1992, 1994, and Gregori, 2002).

A general problem deals with the mapping of sea-urchin spikes. In general all devices to monitor local effects of soil exhalation are potential tools for such a mapping. However, in general, every phenomenon related to hot fluid exhalation is biased by the whims of fluid-dynamics through a porous medium. Direct reference to e.m. phenomena can rely either on geomagnetic anomalies (see, e.g., Gregori et al., 2025r, for volcanic areas) or on geomagnetic prospecting by a technique that can be called *CGDS* (canonical geomagnetic deep sounding). No exhaustive explanation was yet published (in preparation). One must rely on an array of simultaneously operated

magnetometers. By a suitable strictly rigorous data handling, it is possible to assess a local layering of the induced currents at different depths. Thus, a mapping can be attained of the relative underground “topography” of the local electrical conductivity σ . Higher frequency e.m. signals are associated to shallower depths. On the other hand, no exact association to the geometrical depth can be provided, as this depends on the unknown σ profile vs. depth at every given location.

Sea-urchin spikes have a twofold implication. On the one hand, they transfer energy from a large depth to Earth’s surface, through a flow of electrons that move at a speed comparable to light’s speed. On the other hand, the spikes act like effective antennae that permit e.m. coupling between deep Earth and the e.m. field induced by the solar wind. That is, the sea-urchin spikes get rid of the Faraday screening by the outer Earth’s layers. This justifies the solar control on volcanism (Gregori et al., 1992, 1994, and Gregori, 1997, 2002).

Related seemingly mysterious phenomena are sometimes reported, which are associated to invisible and undetected, transient, air-earth currents – which are not manifested by spectacular lighting, although they display phenomena inside some device that acts like an unusual detector of comparatively rare occurrences. Well known phenomena are fumaroles, or mud volcanoes etc. (see Gregori and Hovland, 2025), or wildfires (see Gregori and Leybourne, 2025i). We refer, rather, to other exceptional, although intense and anomalous occurrences (see Gregori et al., 2026b).

The mantle is locally heated, and experiences thermal expansion that determines the formation of uplifts (superswells⁴ and geotumors). The lithosphere slides down by gravity on the slopes and converges into megasynclines, thus causing geodynamics, seismicity, volcanism, formation of continents, and of orogens. The kinetic energy increases first, while some $\sim 50,000$ years later the consequent friction heat determines magma outpouring.

This model is called warm-mud tectonics (*WMT*; see Gregori, 2002 and Gregori and Leybourne, 2021). Note that plate tectonics relies on a model-Earth that is fluid, and the lithosphere floats on a fluid implying isostasy. In contrast, *WMT* envisages a reasonably “solid” mantle, which experiences thermal expansion that varies both in space and time, while the lithosphere slides on the slopes of some kind of huge hills, which are the superswells. Lithospheric slabs converge and collapse inside megasynclines, thus originating orogeny and the uplift of continents. Continents are eroded by weathering, and the cycle - of origin and death of a continents - is comparably rapid, with period between $\sim 100 - 200$ Ma and, likely, ~ 180 Ma (Mortari cycle). Note that *WMT* implies no isostasy on the planetary scale, while gravitational compensation is operative only on reduced scale-sizes.

A recent investigation (Zaccagnino et al., 2020) is particularly interesting, as it carries out an almost “local” monitoring of the instant astronomical influence on the deformation and motion of the lithosphere, while its slides

on the *ALB*. They use *GPS* records to monitor minor deformations locally induced on the lithosphere. *GPS* records are now accurate and, on long baselines, it is possible to measure secular motions of lithospheric slabs, as well as periodic tidal displacements. At present, > 20 year-long space-geodesy records are available and permit an accurate analysis of the contribution of the horizontal component of the body tide, which shifts the lithosphere. Zaccagnino et al. (2020) review the data. The lithospheric plates retain a non-zero horizontal component of the solid Earth tidal waves. The measured speed correlates with tidal harmonics. It is found that high-frequency semidiurnal Earth's tides are likely to contribute to lithospheric displacements, even though the residuals are still within the error of the present accuracy of *GNSS* (*Global Navigation Satellite System*) data. However, the low-frequency body tides show horizontal residuals equal to the relative motion among plates - and prove the astronomical input on the dynamics of the lithosphere. The lithosphere is found to move faster with nutation cyclicities of 8.8 and 18.6 years. This correlates to lunar apsidal migration and nodal precession. The high-frequency body tides are damped by the high viscosity of the asthenosphere. In contrast, “*low-frequency horizontal tidal oscillations are compatible with the relaxation time of the low-velocity zone and can westerly drag the lithosphere over the asthenospheric mantle*”. Zaccagnino et al. (2020) shows how tidal oscillations correlate with the seismic activity. Thus, a variable angular velocity can occur, when comparing different slabs of lithosphere, due to viscosity anisotropies at the *ALB*. In addition, let us remember (Gregori, 2002, and Gregori and Leybourne, 2021) that friction at the *ALB* experiences huge variations during the 27.4 ± 0.05 Ma cycle of the Earth electrocardiogram. Hence, the astronomical influence on lithospheric motions changed by a relevant amount during Earth’s history.

The Earth electrocardiogram, i.e., the 27.4 Ma cycle of the deep Earth’s interior is briefly illustrated in Gregori and Leybourne (1921). Rampino et al. (2021) carried out a multidisciplinary analysis that they summarize as follows. “*We performed spectral analyses on the ages of 89 well-dated major geological events of the last 260 Ma from the recent geologic literature. These events include times of marine and non-marine extinctions, major ocean-anoxic events, continental flood-basalt eruptions, sea-level fluctuations, global pulses of intraplate magmatism, and times of changes in seafloor-spreading rates and plate reorganizations. The aggregate of all 89 events shows ten clusters in the last 260 Ma, spaced at an average interval of ~ 26.9 Ma, and Fourier analysis of the data yields a spectral peak at 27.5 Ma at the $\geq 96\%$ confidence level. A shorter period of ~ 8.9 Ma may also be significant in modulating the timing of geologic events. Our results suggest that global geologic events are generally correlated, and seem to come in pulses with an underlying ~ 27.5 Ma cycle. ...*”

We stress that the 27.4 ± 0.05 Ma electrocardiogram cycle derived from the analysis of the volcanism of the

⁴ A more ancient term is megaundations.

Hawai'i hotspot, documented by the Hawai'i Emperor Seamount Chain, that is by a homogenous data set, while the Rampino et al. (2021) analysis relies on formal mathematical treatment of a heterogeneous database. In addition, the same analysis on the volcanism of the Hawai'i hotspot evidenced a regular cyclicity of ~ 14.0 Ma. It is noteworthy that - by means of a more heterogeneous database and by means of some intricate Fourier analysis - some cycles are found, even though with less accuracy, which match the result obtained by means of the homogeneous database of the volcanism of the Hawai'i hotspot.

Sea-urchin spikes represent the leading mechanism, or "channel", for the transfer - through fluid exhalation and related air-earth currents - of endogenous energy into the ocean/atmosphere system. The Earth operates like a battery that stores and releases energy at different times, by means of change of state (variation of the radius of the IC, see Fig. 6).

Two main cycles modulate the phenomenon. The most important periodicity, $\sim 27.4 \pm 0.05$ Ma, determines the Earth *electrocardiogram* (see Fig. 9 of Gregori and Leybourne, 2021) and it is explained by the timing of opening and closing of the "channels" associated to the charging/discharging of the battery. The other cycle, ~ 14 Ma, is of external modulation - i.e., probably due to the timing of the crossing of the galactic equator by the Solar System. In fact, the literature often reports about phenomena with a period close to ~ 14 Ma.

The Hawai'i volcanism seems to be the comparably more precise and unbiased proxy. However, when the Solar System crosses through the galactic equator, it collects meteoroids and comets. Hence, the astrobleme impact craters display - as expected - a similar well-known periodicity, although biased by error bars due to the need for a suitable meteoroid orbit, in order to cause a crater that we can detect on the geological time scale.

A different comment deals with geomagnetic field reversals (FRs). A FR is triggered by the occasional encounters of the Solar System with a cloud of interstellar matter (Gregori and Leybourne, 2021). The impact of a FR on the Earth's environment occurs through the generation of an extra amount of endogenous Joule heat (Gregori, 2002). The effect of every FR lasts a few to several thousand years. The peak of a heartbeat⁵ lasts a few million years.

The 27.4 Ma pace of the heartbeat is determined by time required by sea-urchin spikes to cross, by ESI mechanism, through the mantle. Therefore, every either small or large number of FRs can occur during the time lag between two successive heartbeats. The intensity of the heartbeat is modulated - as correctly checked by observations - by the integral effect of the several FRs occurred during the time lag, and suitably time-delayed

depending on the upward extension already attained by sea-urchin spikes (Gregori, 2002). A simultaneous anomalous trend is therefore expected to characterize geodynamics and climate. A LIP (large igneous province) was always generated on the occasion of every heartbeat of the Earth's electrocardiogram, and in general some great extinction event occurred, mainly involving the ocean fauna, due to increased ocean floor exhalation of CH_4 . At the same time, the new life forms emerged. That is, extinctions and new life forms are a persistent feature during the history of the Earth.

For instance, the P/Tr (Permian/Triassic) boundary event associated to the Siberian LIP occurred ~ 9 heartbeats ago.

Humankind is experiencing for the first time a heartbeat (Gregori, 2020), and the associated LIP is the birth of Iceland that 2 Ma ago did not exist. In fact, a movie was presented by Helman et al. (2001),⁶ based on a formerly classified database. Every frame of the movie was obtained by mapping the North Atlantic and by merging equal-age geomagnetic anomalies symmetrically located with respect to the northern section of the Mid-Atlantic-Ridge (MAR) in order to simulate the ocean floor at every given epoch before expansion. Iceland abruptly appears in the movie only ~ 2 Ma ago. Note that the eruption history of the hotspot is certainly older in terms of measured ages of rock samples,⁷ although a violent paroxysm of volcanic activity was seemingly associated with the present ongoing heartbeat.

Several features characterize the present heterogeneous distribution of the release of endogenous heat. Three main features can be recalled. A large region approximately centered on the Arctic cap is experiencing since a long time - on the geological time scale - an anomalous large endogenous heat release. The Banda Sea - at the crossing of several geodynamic actions related to the westward drift of Eurasia and to the sliding of the lithosphere on the slope of the Kerguelen superswell - is an area of anomalous endogenous heat release, manifested by a peculiar trend of wildfires (see Gregori and Leybourne, 2025i), and also being the likely site for the trigger of ENSO (El Niño Southern Oscillation; Leybourne et al., 2008).

Concerning the relationship with climate, Chen et al. (2015, their Fig. 4) investigated the relationship between climate temperature ($\delta^{18}O$) and occurrence-frequency of FRs computed inside a moving time-lag of 2 Ma with a time step interval is 0.1 Ma. As expected (according to the argument above), they found a correlation, including a periodicity of ~ 13 Ma - and also a less clear correlation with an approximate indicator of "tectonic plate subduction rate".

The release of endogenous energy has a twofold effect either on the Earth's interior, or on the ocean/atmosphere system. As far as the Earth's interior is concerned, the

⁵The term "heartbeat" was used also by Larson (1995), although with a different meaning, upon referring to the standard model - not here shared - of huge "plumes" slowly moving through the mantle, etc.

⁶ At the *International Workshop Global Wrench Tectonics - New theory of Earth evolution*, held in Oslo, 9-11 May, 2001, sponsored by FORTUN, RWE-DEA and hosted by Geir Lunde (see Lunde, 2001).

⁷ We are indebted to Franco F. Bonavia for this remark.

mutual interaction occurs between several continuously uplifting sea-urchin spikes (Gregori and Leybourne, 2021). The control is through the Hamilton's principle (Gregori et al., 2025e), and determines a tetrahedron pattern of the deep Earth alignments of spikes. In fact, owing to the long 27.4 Ma and 14 Ma cycles, the monitoring performed by the humans reminds about observing single frames of a high-speed movie. Every observed state represents a stage of quasi-equilibrium (Gregori et al., 2022, 2025w; Gregori and Gregori, 2025) while the natural system looks for final equilibrium. Owing to strict energy requirement, an exact tetrahedron pattern is envisaged inside deep Earth. The sliding of the lithosphere, due to WMT, substantially modifies the signature at Earth's surface of such an exact geometrical pattern. In any case, this mechanism seems to be the unique available physical explanation of the geographical distribution of MORs. See Gregori and Leybourne (2021) for additional details. A recent accurate investigation of the dynamics of South America was made by Espinoza and Iaffaldano (2023), which looks consistent with the aforementioned clockwise rotation.

In addition, a peculiar empirical association occurs between the Gulf of Mexico, hurricanes, SAA (South Atlantic Anomaly), lightning distribution, and a supposed "kingpin", altogether with be likely huge clockwise rotation of South America (see Gregori and Leybourne, 2021, 2025j; Leybourne et al., 2025).

As far as the ocean/atmosphere system is concerned, thermal convection occurs inside every fluid. Whenever the medium is ionized, every convection system generates an e.m. field by the Cowling dynamo (see Gregori et al., 2026d). The high conductivity of ocean water promptly damps every e.m. induced effect. In contrast, this phenomenon in the atmosphere results to be one of the main drivers for the control of climate. In addition, also the mysterious eigen-frequencies of the ocean-atmosphere system are to be considered that determine the large oscillation of the global climate system.

"Pohlfuchtkraft", Pekeris force, island arcs

The "Pohlfuchtkraft", or "Eötvös force" (Stacey, 1969; Jeffreys, 1976) is a classical concept, related to the model of fluid Earth according to isostasy. A floating lithosphere is subject to gravitation, to centrifugal force, and to Archimedean force. The resultant is an equatorward pull. This is the Pohlfuchtkraft, which is a strict requirement of plate tectonics.

In contrast, conceive the Earth like a plastic and deformable solid body. Compared to an ideal deformable body, the Earth is found to be excessively flattened. Hence, in some way, some matter ought to move poleward in order to restore a correct flattening. This is called "Pekeris force".⁸

On the other hand, the asymmetry between Northern and Southern Hemisphere is a matter of fact, which is most violently manifested by the tetrahedron pattern - or, equivalently, by the MORs planetary pattern, which is the

same (Gregori and Leybourne, 2021). Hence, unlikely in the Northern Hemisphere, the heat released by the Circum-Antarctic Ridge forbids a direct observation of the Pekeris force. This fact is relevant for a guessed model of island arc formation.

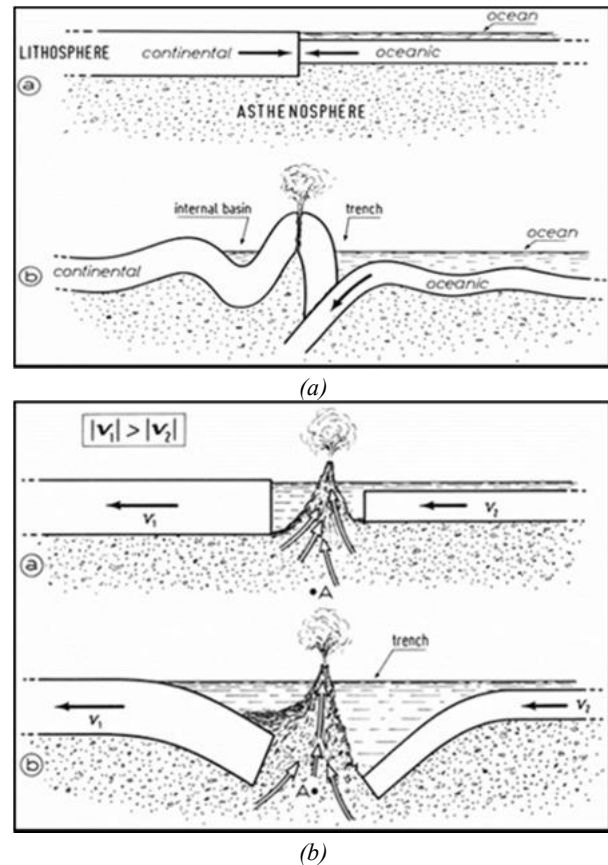


Fig. 9. Two slabs of lithosphere comparatively thicker (continental) and the other thinner (oceanic)-slide over the ALB. [upper]; (a) If $v_1 = v_2$, the two slabs move altogether with no interaction. [upper plot]. (b) If $v_1 \neq v_2$ and collide, overthrust and/or folding occurs. [upper plot]. If $v_1 > v_2$, the two slabs leave a gap in between. In this way [lower plot] (b) the lithosphere sinks into the mantle, while the absence of a "stopper" eventually permits the formation of a volcano. Unpublished figure.

In fact, consider the lithospheric slabs that drift on the ALB. Two contiguous slabs can move, relative to the asthenosphere, at comparatively equal or different velocity v . The effect is different in different cases (Fig. 9), leading either

- (i) to over-thrust and/or folding of collapsing slabs, or
- (ii) to the sinking of the two slabs due to local isostatic compensation.

Upon carrying out a detailed computation (not here given), a model results for the formation of an island arc. In addition, under reasonable approximations, it is found (Fig. 10) that a precise analytical relationship must exist - in every island arc - between the relative difference of v of the two slabs, the distance and the relative timing of formation

⁸ Refer to Jeffreys (1976), or, for thermal contraction, to Bott (1971), Collette (1974), and Turcotte (1974), ...

of every island, and the relative position (latitude and longitude) of the islands along the arc. No details are here given. At present, to our knowledge, no observational data are available to test such a model.

Note that this island arc model is consistent (i) with a westward drift of Eurasia, due to the loading tide of the Pacific Ocean on the Eurasian continental shelf, and (ii) with an efficient Pekeris force active in the northern Pacific Ocean. Also the Scotia arc formation is consistent with this model (Gregori and Leybourne, 2021).

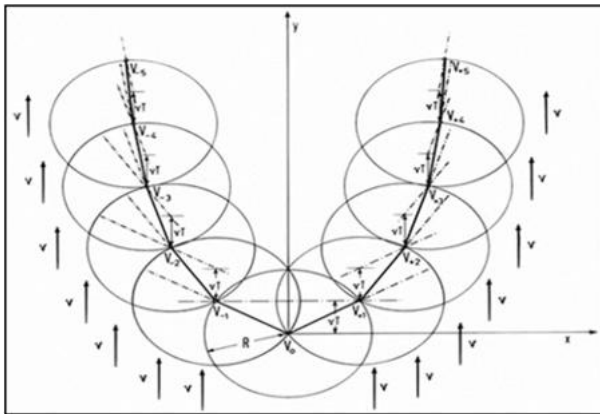


Fig. 10, Under reasonable assumptions it can be formally shown that the volcanic islands along an island arc ought to be located at a fixed relative distance (which is a well-known observed fact). A precise analytical relationship must occur between (i) The relative difference of v the two slabs, (ii) the distance, (iii) the relative timing of formation of every island, and (iv) the relative position (latitude and longitude) of the islands along the arc. No details are here given. This model is a possible explanation of the curvature of island arcs. However, as long as no observational data are available to check the model, this is only a speculative and unpublished figure.

“Tuzo”, “Jason”, *Quatrefoil*, DUPAL, kimberlites

A brief reminder is needed about some large-scale geomorphological features at Earth’s surface, which envisage the distribution of the release of endogenous heat flow. Refer, e.g., to Burke (2011) who, however, relies on the rationale of mantle convection, rather than on *WMT*. He claims that he has “*been able to show that deep-seated plumes of the past $\sim 5.5 \times 10^8$ years have risen only from narrow plume generation zones (PGZs) at the CMB mostly on the edges of two Large Low Shear wave Velocity Provinces (LLSVPs) that have been stable, antipodal, and equatorial in their present positions for hundreds of millions of years and perhaps much longer.*” He proposes the names “Jason” and “Tuzo” for the two huge bumps centered, roughly, in the Hawai’i and Botswana regions, respectively. The rationale here used explains these features, by means of *TD* dynamo, of Hamilton’s principle, of sea-urchin spikes, of tetrahedron, and of *WMT*.

In fact, owing to an almost endless number of indicators (also within deep Earth), some kind of quatrefoil pattern characterizes the endogenous heat release, with two maxima of upwelling heat, corresponding to “Jason” and “Tuzo” (Fig. 11; Gregori, 2002). Although the process is not thermodynamic - as it occurs in thermal convection - the

geometry of energy transfer, depending on the location of sea-urchin spikes (see Gregori and Leybourne, 2021), in some way seems to respond to a similar requirement as for the old-fashioned *OC* convection, envisaging a quatrefoil pattern, with two maxima in Hawai’i and Botswana. Fig. 11 is an expressive mnemonic representation of phenomena.

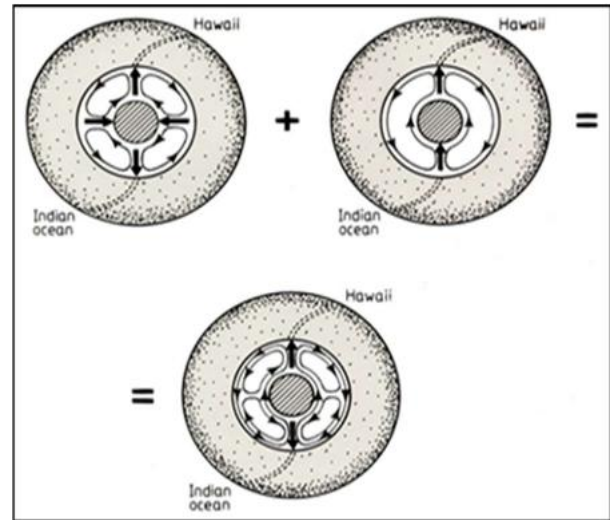


Fig. 11. Cartoon showing the lowest order and/or degree of “convection” cells to be expected inside the *OC*. The phenomenon, however, ought to be conceived to occur by an electrodynamic process, through sea-urchin spikes, rather than by thermal convection in the “metallic” *OC*. This figure is therefore only an expressive mnemonic tool, although it can be eventually misleading. After Gregori (2002). With the kind permission of the late Wilfried Schröder.

For instance, a region with a major relative maximum in every season of atmospheric concentration of CO_2 is around Botswana, according to the seasonal maps recorded by data of the *NASA* satellite *OCO-2* (see Gregori, 2020). The approximately antipodal Hawai’i region displays no corresponding relative maximum. In fact, *NASA* scientists interpret this absence of a maximum because of ocean currents that transport the exhaled CO_2 and originate a relative maximum elongated close to the Alaska coast.

A prominent phenomenon deals with the isotopic chemism of ocean basalt. A well-known feature is the so-called *DUPAL* anomaly, which is an acronym after the discoverers, Dupré (Stéphanie Dupré, *Institut Français de Recherche pour l’Exploitation de la Mer, (Ifremer)*, Department of Marine Geosciences, and Allègre (Claude Jean Allègre. 1937– Crafoord Prize, *Université Paris Diderot*, Paris VII). Standard plots are drawn dealing with the isotopic chemism (ratios of different isotopes) of *Sr-Nd-Pb*.

Our rationale is the aforementioned criterion by which the outpouring basalt represents the composition of the layer where basalt originates due to melting. If the mean Earth composition is reasonably uniform vs. latitude and longitude, the melt-depth depends on the intensity of the energy supply for the local sea-urchin spike. That is, the *DUPAL* anomaly is a curious features associated to air-earth currents according to their distribution in space during

the geological past. Only very few mentions can be here given about this item (see Gregori, 2002).

On an empirical basis an energy hierarchy is clearly envisaged, organised into five classes, according to the intensity of their presumable prime energy source. The classes are named (in decreasing intensity of primary energy supply), respectively: *H* (from Hawai'i), *D* (from *DUPAL*, extended over the entire Indian Ocean and over some part of the southernmost Atlantic Ocean), *N* (from normal or intermediate cluster), *A* (from Atlantic type), and *SH* (from St. Helena Island, while only one additional spot was found with the same chemism, roughly almost antipodal to St. Helena, i.e., in the Australs – Cook Islands).⁹

For the interested reader, some details are given in the Appendix. In fact, this analysis of the isotopic chemism of ocean basalt is unpublished. It was carried out in the early 1990s, by means of an intuitive, visual, pattern-recognition of clustering, where every plotted point was singly evaluated, derived from some plot available in the literature. The scant available database required a patient analysis. At present, a richer computerized database confirms the old analysis. However, the statistical analysis of the greater dataset hides some evidence of the former careful point-by-point investigation. The Appendix briefly illustrates the inferences of the early investigation.

In contrast, the interpretation is here reported, aimed to show the correlation with the bathymetry of the *MIR* (Mid Indian Ridge).

Klein and Langmuir (1987 and 1989) investigated the global systematics of basalt composition along *MORs*. They

focused on the relationship between basalt chemistry and ridge bathymetry, which they call “axial depth”. They filtered the database by averaging over segments of the ridge < 100 km long – but the actual length was decided in every case depending on natural segmentation. They also tried to give equal weight to different segments. Moreover, they considered a correction concerned with the low-pressure fractionation - a process by which the chemical composition of the basalt can undergo some relevant alteration. For such a purpose, they considered two reduced parameters, which they called *Na8.0* and *Fe8.0*. The *Na8.0* expresses the percent weight of *Na₂O* corrected for shallow fractionation and reduced to a concentration of *MgO* having a fixed value, arbitrarily pre-chosen at a weight of 8%. The definition of *Fe8.0* is analogous.

They plotted Fig. 12 that they obtained by means of a moving average over segments > 500 km long. They envisage three possible explanations, i.e., “*clinopyroxene fractionation, major element source heterogeneity, and varying extents of partial melting*”. They concluded as follows. “*Although there is evidence for the importance of all of these to some extent in various areas, the partial melting model alone provides a straightforward explanation of the first-order correlation between regional basalt chemistry and average depth ... The key point is that the overall global systematics are consistent with varying extents of melting at varying pressures, with basalts from the shallowest ridge segments produced by larger extents of melting deeper in the mantle.*”

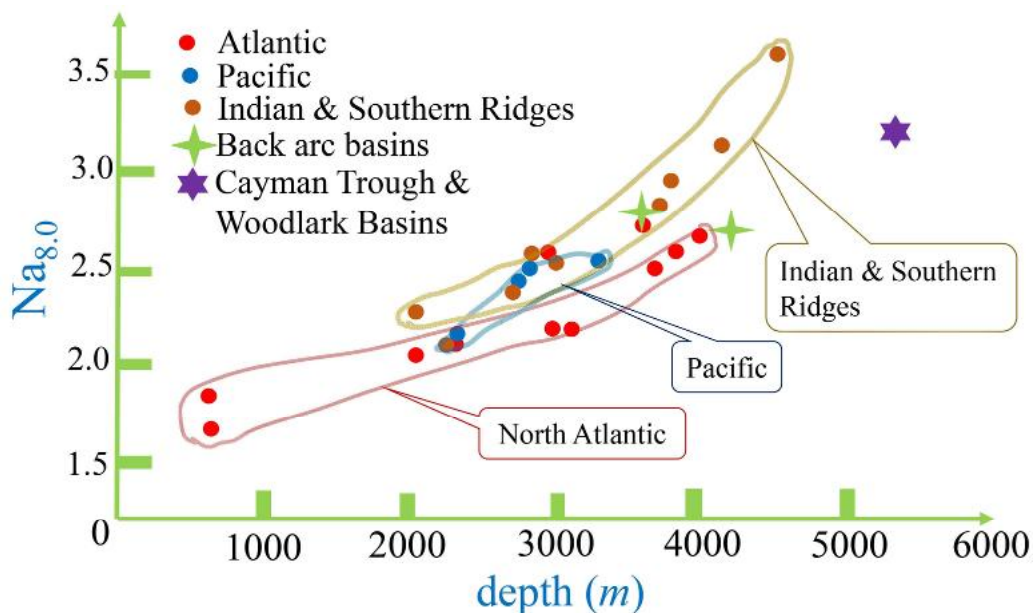


Fig. 12. “Long wavelength *Na8.0* vs. axial depth; data ... have been combined and, where sampling density permitted, averaged over > 500 km of ridge length; in particular hotspot centers and margins have been averaged together. $Na8.0 = Na_2O + 0.373 \times (MgO) - 2.98$, $Fe8.0 = FeO + 1.664 \times (MgO) - 13.313$. *Na8.0* and *Fe8.0* are calculated for samples with 5.0 – 8.5 wt%MgO; *CaO/Al₂O₃* are calculated for samples with > 5.0 wt%MgO.” Figure redrawn after Klein and Langmuir (1987).

⁹ In the literature the intermediate class, i.e., *N*, is often called *FOZO* (acronym for focal zone).

Melting beneath ridges is likely to occur by adiabatic upwelling of the mantle. [That is, a reduction of the lithostatic pressure permits melting according to the requirements of the equation-of-state.] In this case, for a given mantle composition, the amount of melt produced should be controlled largely by the temperature of the intersection of the mantle solidus." Therefore, "the global correlations of Fig. 12" should "reflect different extents of melting in response to variations in the temperature of the mantle."

They considered three possible mechanisms, synthesized by Fig. 13 and finally preferred the third one, and this looks reasonable as different regions of the mantle ought to display different temperatures at the same depth. Moreover, in their reply (Klein and Langmuir, 1989) to Brodholt and Batiza (1989), they further specified their interpretation, and showed Figs 14 and 15, by which they claimed that, wherever there is a larger temperature (at equal depth), there is a greater percent melt, hence a greater elevation of the ridge axis.

Refer to Fig. 12, and consider that, compared the North Atlantic, the MOR either in the Indian Ocean or in the South Atlantic - and also the southern ridges (i.e., in the area of the DUPAL anomaly) - all of them have a lower elevation - or equivalently a larger bathymetric depth. Hence, it can be concluded that they also have, at equal depth, a comparatively smaller percent melt or a lower temperature. That is, in Fig. 14b, the DUPAL anomaly looks like the Y case, unlike the North Atlantic MORB (which is the acronym for MOR basalt) that looks like the X case. That is, a weaker prime energy supply stops penetration at a lower depth, where heat accumulates until it causes melt. A more intense primary energy supply determines a penetration until a shallower depth, where melt occurs.

Consider how such a geochemical scenario can fit into the model here proposed. As already mentioned, suppose that a geochemical gradient exists (more or less steep) vs. radial distance from Earth's center, which applies - at least - when referring to shallow Earth's layers where, owing to the equation-of-state, melt occurs. That is, unlike what is generally speculated in the literature, instead of envisaging a chemical differentiation vs. the two dimensions along the Earth's surface, the chemical differentiation is supposed to occur solely vs. depth. However, it is very likely that both horizontal and vertical differentiation ought to occur. The concern is about collecting a reasonable amount of observations in order to get a realistic map of both trends.

Suppose that some sea-urchin spike pushes up through the surrounding medium. For instance, imagine that it rises from the CMB. Joule heat is released on the very top of every spike. Magma is eventually produced wherever

Joule heat is released, provided that its liquid state is compatible with the local pressure and equation-of-state (refer to Figs 13, 14, and 15).

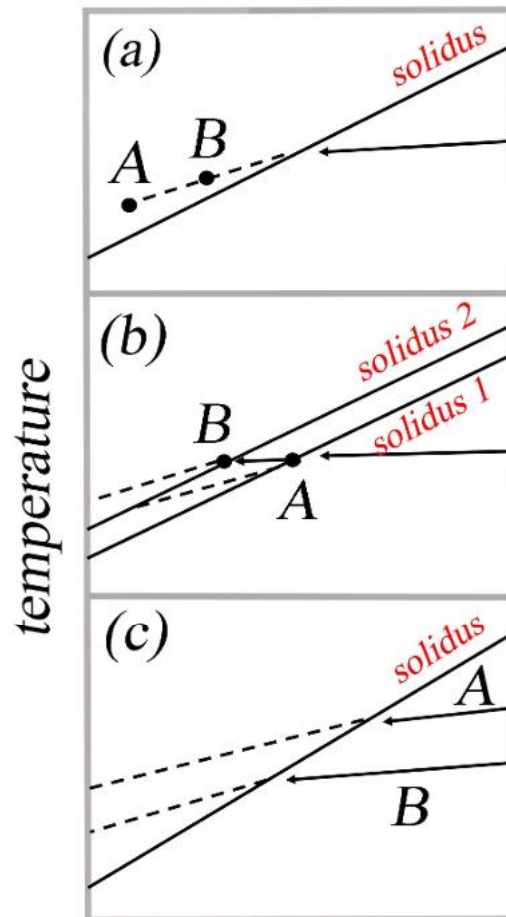


Fig. 13. "Schematic mantle pressure vs. temperature profiles. In Figs (a)-(c), 'A' and 'B' represent the paths followed to generate magmas erupted along shallow or deep ridges, respectively; (a) The mantle is characterized by a single thermal gradient, the solidus is intersected at the same pressure everywhere, but magmas segregate at different depths and therefore exhibit different extents of melting; (b) The mantle is characterized by a single thermal gradient but there are markedly different mantle compositions beneath different ridges; 'A' intersects the solidus deeper, due to its more fertile nature and melts more; 'B' represents more depleted mantle that intersects its solidus shallower and melts less; (c) Different regions of the mantle are at different temperatures at the same depth and therefore intersect the solidus at different pressures, depths and temperatures. 'A' represents a hotter region of the mantle which therefore intersects the solidus deeper and melts more; 'B' represents a cooler mantle region which intersects the solidus shallower and melts less ...Fig. (c) depicts our preferred model." Figure redrawn and captions after Klein and Langmuir (1987).

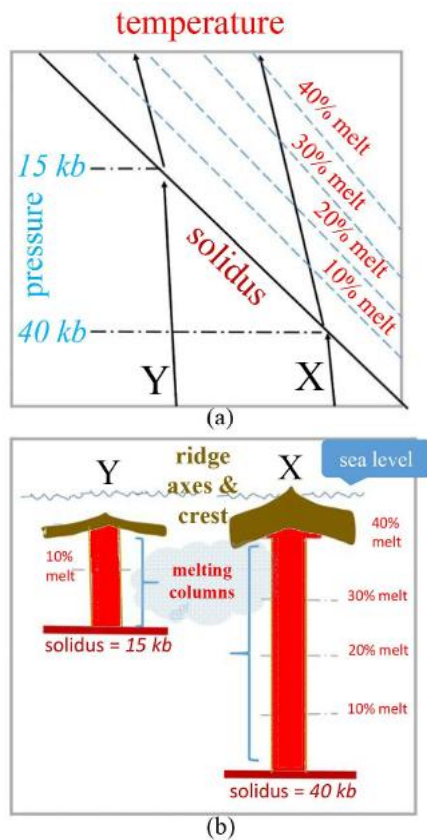


Fig. 14. "(a) Schematic drawing of mantle pressure vs. temperature. Path X represents a hotter parcel of the mantle that intersects the solidus at greater depth and undergoes great extents of melting upon ascent; path Y, a cooler parcel of mantle, intersects the solidus at shallower depth and melts less upon ascent; (b) Schematic cross-section of the oceanic crust and mantle resulting from the path X and Y in Fig. (a); light shading indicates the melting column ...; vertical ruling indicates the oceanic crust." Figure redrawn and captions after Klein and Langmuir (1989).

Note that the speculated primary components focus on a specific geochemical concern, dealing with the origin and composition of the Earth, since the time of its formation and with its subsequent chemical evolution. The general implicit rationale relies on the fact that MORs seem to rise from the CMB (due to the inferences from the SV of the geomagnetic field and from its WD, as discussed by Gregori, 1993; Gregori et al., 2025x). In contrast, several other volcanoes ought to be originated at the ALB supplied by friction heat. In addition, maybe, hotspot volcanism requires a specific independent consideration, as explained below.

Since the thermal conductivity is very low, heat must accumulate, the local temperature increases, hence also

the local pressure, until the solidus is crossed, after which melt occurs. The (T, p) track becomes the same as in Fig. 16a. Compared to the three cases considered in Fig. 13, this scheme is an additional case history.

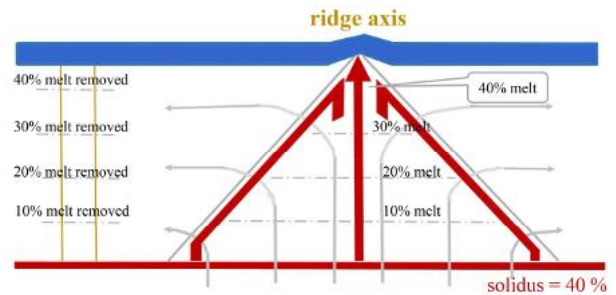


Fig. 15. "Schematic model of the melting zone beneath a ridge axis ... Light solid arrows show paths of upwelling and diverging mantle; heavy solid arrows show melt flow fields ...; dashed lines within melting zone show percent melting above solidus. The oceanic crust is indicated by the vertical ruling. The residual melting column resulting from the extraction of melt (stippled) is shown at left." Figure redrawn and captions after Klein and Langmuir (1989).

Therefore, in this model, the isolated volcanoes (OIB case) have a comparatively deeper heat source (point O). They are point-like "security fuses" that release heat and display a comparatively larger melt percent. The Hawai'i hotspot is, maybe, the best example of this kind. However, this model also applies to other less intense hotspots. Moreover, this phenomenon implies a comparatively long path of the thermal energy before its release at Earth's surface.

Diamond-bearing kimberlites deserve a mention. Fig. 17 shows an isotopic characterization of various kinds of basalt and of kimberlites. The figure was published in 1986, almost a historical witness of how the isotopic chemism of basalt can characterize different locations. Kimberlites look like some kind of aborted volcanoes, i.e., they seem typical of a DUPAL environment, with a "stopper" represented by a thick lithosphere (craton). Mitchell (1986) is an extensive review (see also Schulze, 1987). For instance, it is not a matter of chance if in 2006 the major diamond producer of the world has been Botswana. The process of diamond formation is still uncertain (e.g., see Coombs, 2016; Cook, 2019a; and references therein.). Several major diamond-bearing kimberlite provinces look like fields of "plugged" volcanoes (kimberlites), much like sea-urchin spikes that did not afford to outpour off the "stopper" represented by a thick continental craton. Diamond bearing kimberlites are observed in a large region referred to a large portion of the southern part of Africa, and in the Perth region in western Australia.

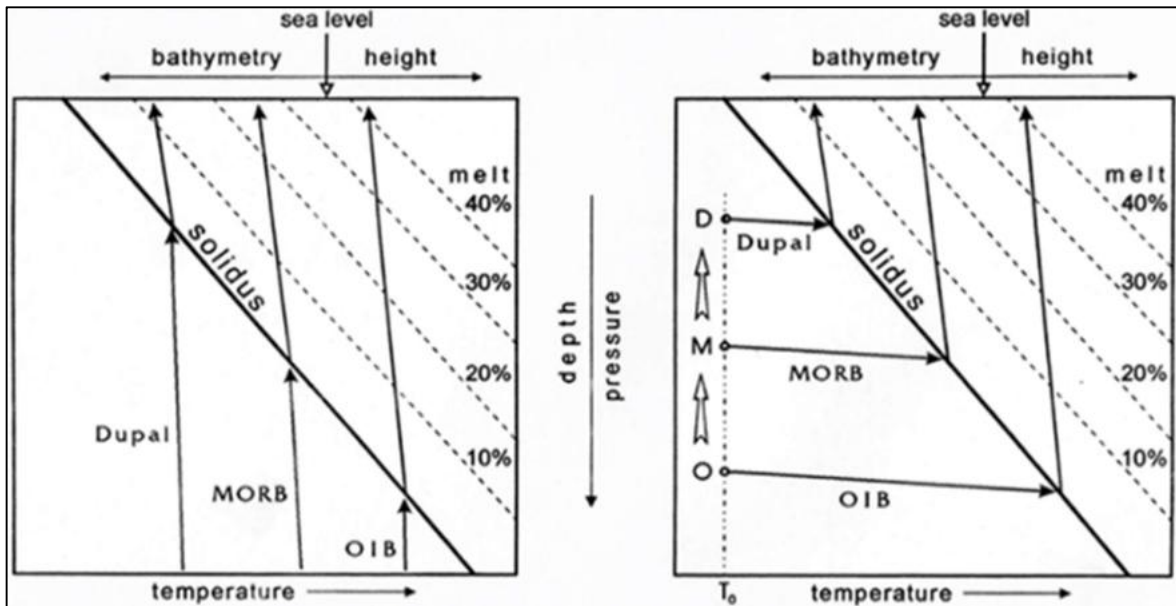


Fig. 16. (a) Re-drawing Fig. 14a (sketch, qualitative and out of scale) by distinguishing between OIBs that should be associated with a comparatively deeper heat source, thus producing a greater melt percent close to Earth's surface, hence a larger topographic elevation with respect to sea level. MORBs should be associated with a heat source of intermediate depth, thus producing an intermediate melt percent and an intermediate bathymetric depth. DUPAL's basalts should be associated with the shallowest heat source of the three cases, thus producing the smallest melt percent, hence the deepest bathymetry. This figure corresponds to the case of Fig. 13c-b) Fourth case, in addition to the three cases envisaged in Fig. 13. The electric circuit, supplied by the deep dynamo currents, is supposed to release Joule heat at the very top of the spike (almost like at the point of the *ES*). Three different possibilities are envisaged, by which the top of the spike reaches, respectively, either point O, M, or D. For simplicity, assume that the initial temperature T_0 is the same in all three cases. This makes little difference, as the local heating occurs due to the impossibility of releasing heat, other than by the very low thermal conduction. Hence, the local temperature increases together with the local pressure. The state of the system evolves until it reaches the solidus line, after which the track in the (p, T) diagram is identical to the case of Fig.16a. In this model the top of the spike must be deeper for the OIBs, intermediate for the MORBs and comparatively shallower for DUPAL's basalt. The Hamilton variational principle requires that the top of every spike must tend to penetrate upward. Hence, every point O must tend to approach a point M and every pointy M must tend to approach a point D. Hence, the isotopic geochemistry of OIBs, should (on the geologic time scale) become progressively more similar to MORBs and MORBs should become more similar to DUPAL's (such a last tendency seems to have been observed). Such a general trend, however, can be eventually stopped at some energy threshold.

Acoustic Emission (AE)

Monitoring crustal stress is fundamental to understand seismic precursors, and to release alerts. This entire topic is extensively discussed in Gregori et al. (2018) and the several references therein. Some reminder is also in Gregori (2020). We remind only about a few essential leading ideas.

The breaking of a molecular or atomic bond weakens the surrounding crystalline structure. Hence, the probability of occurrence of a subsequent breaking is higher where a bond already broke. Therefore, we can rely on an analysis of the fractal dimension of the time series of ultrasound signals that are monitored in solid ground

(i.e., "acoustic emission", *AE*). Observations clearly show that several-correlated *AE* signals are recorded at locations even much far apart from each other. On the other hand, ultrasounds damp off very rapidly in loose ground. Hence, they cannot propagate over any significant distance. In contrast, ultrasound easily propagate through fluid media. It happens, therefore, that local shallow and solid crustal blocks seem to be acoustically connected each other through the serpentosphere (see Gregori and Hovland, 2025), as *AE* can efficiently propagate through the serpentosphere.

In fact, if one monitors *AE* by means of a sensor inserted inside a rocky outcrop, the outcrop must be considered the terminal of a "natural probe" of unknown extension crossing through the crust and lithosphere. If

the records at different locations look correlated - even at a long distance from each other - this means that a stress crossed through the Earth generating ultrasounds inside the serpentosphere, to be later monitored by means of the “natural probes” associated to different rocky outcrops. This principle resulted realistic and heuristically very effective.

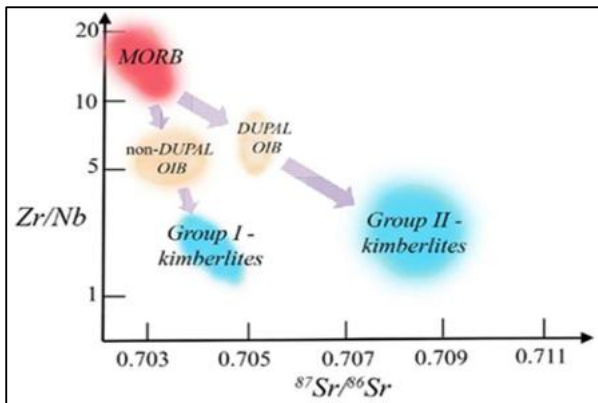


Fig. 17. Zr/Nb vs. initial $^{87}\text{Sr}/^{86}\text{Sr}$ for Group I and II kimberlites, compared to MORB and South Atlantic OIB. Redrawn after Le Roex (1986, Fig. 1, p. 243), also in Wilson (1989).

A peculiar effect deals with the propagation of crustal rupture according to a sequence that reminds about a domino effect. That is - on an empirical basis - it is found (Gregori, 2013a) that the breaking of a crystalline bond triggers the rupture of a nearby bond. The phenomenon is observed to occur at a typical speed of $\sim 10 \text{ cm sec}^{-1}$ independent of the medium - as every medium displays a similar behaviour, which is evidently typical of every solid structure.

Bond-yield occurs first on the smallest scale size, and produces a small flaw. The released AE are of a comparatively high frequency (HF), and are associated to the small flaw. Then, small flaws coalesce into increasingly larger flaws, while AE are released of progressively lower frequency (LF). That is, the progression of the loss of performance by the solid structure can be monitored by recording AEs at different frequencies, because HF AE precede progressively lower LF AE. This is, therefore, an important internal natural clock of the medium, and we are aware of no other internal clock of comparable reliability.

Differently stated, every given frequency is associated to some given size of the flaw that is responsible for the AE release. The true size of the flaw is unknown, although it is certain that a HF AE is associated to a “flaw domain” of smaller size than a LF AE is. The concept of “flaw

domain” applies to every phenomenon where a catastrophe of the system occurs first on a small scale, while a larger scale catastrophe occurs in a progressive time sequence.

In this respect, Bletery and Nocquet (2023) made a statistical investigation on the precursory phase of large earthquakes. They used GPS data and the measured displacements concerning 3026 high-rate GPS time series. They projected the records onto the direction of the expected slip at the hypocenter. They considered a time lag of 48 hours that preceded 90 earthquakes with moment magnitude ≥ 7 . They found “a ≈ 2 hour long exponential acceleration of slip before the ruptures, suggesting that large earthquakes start with a precursory phase of slip...” In any case, the scatter is relevant, and justifies some perplexing feelings of some authors.

In fact, the result is reasonable upon considering the diversity of every earthquake from all others. In contrast, the AE records, along a given active fault, are very precise and monitor the effect with a much specific timing. This was shown - as reported by Gregori et al. (2010) - upon analyzing the HF AE and LF AE records collected at Valsinni (in Southern Italy, at $\sim 354 \text{ km}$ from the epicenter) that preceded the L'Aquila earthquake (6 April 2009, $M_L = 5.8$, depth 8.8 km). The precursor - very clear - lasted about 15 days, consistently with a propagation of the microfracture along the Paganica fault. The stress propagation occurred as a domino-effect at a speed of $\approx 10 \text{ m sec}^{-1}$ (Gregori, 2013a). That is, in 15 days the microfracture covered $\sim 13 \text{ km}$, which is reasonable in terms of order of magnitude of the length of the active fault.

A curious feature is that the precursor was not clear in the AE records collected at the station of Orchi (a site in the municipality of Foligno in Central Italy), which is much closer to L'Aquila than Valsinni. The likely explanation is related to the so-called Anzio-Ancona line that some geologist guess should denote a deep fault separating the northern and southern part of the Italian peninsula. That is, L'Aquila and Valsinnin are on the southern crustal slab, while Orchi is on the northern crustal slab.

The L'Aquila precursor was found by an analysis *a posteriori*. We wanted to check the phenomenon by a permanent monitoring *a priori*, as reported by Gregori (2013). Both HF AE and LF AE were used, recorded at Valsinni, during September 2009 through December 2009 (inclusive). The analysis was routinely carried out every Monday, Wednesday, and Friday, using 2 or 3 days of data records of the previous days. The result clearly displays regular patterns that remind about the crustal “substorm” feature similar to the trend that preceded the L'Aquila earthquake. One “substorm” was observed

roughly beginning every week, although it was never completed, as it always stopped a few days before full completion. The reasonable explanation is that the crystal stress field changed due to the change in the boundary conditions of the crustal slab. Hence, the precursor is only an indicator of a crustal readjustment - which is very beneficial being a preventive of a possible earthquake, because it discharges the stress without giving rise to a catastrophic event. Only on one day, in October, the trend stopped only 1 or 2 *days* before full completion. Later we informally were informed that the Italian *Civil Protection*, which received the plots of our analysis in real time through its section of Potenza, considered the possibility of the occurrence of a seismic event at some site in peninsular Italy during the subsequent couple of days. However, later there was no concern when the “substorm” stopped its evolution before completion.

That is, the statistical study of Bletery and Nocquet (2023) is reliable. However, the duration of the precursor can vary greatly from case to case, depending on the linear extension of the active fault of concern. Only local *AE* permits monitoring of these phenomena with great precision, by means of the subtle analysis of feeble signals. This is the correct way to exploit the *Level 3* of the four-level approach to earthquake “prediction” explained below.

Summarizing, in principle, we can manage earthquake hazard in terms of four levels (Gregori et al., 2018).

Level 1 relies on monitoring of large-scale soil exhalation, e.g., by satellite (see Quinn et al., 2026; Parrot, 2025; Straser et al., 2026; Wu, 2025; Leybourne et al., 2025; Gregori et al., 2025t; Gregori and Leybourne, 2025i, 2025j).

Level 2 ought to rely on a planetary array of *AE* recording stations, aimed to monitor the large-scale crustal stress propagation, i.e., the occurrence of “*crustal storms*”, which last a few years each, with “quiet” intervals of several years (Gregori, 2013). An earthquake can strike a given region only when a crustal storm crosses through the area.

Level 3 ought to rely on a temporary *AE* array operated along an active fault, which is suspected to be the eventual location of a possible seismic event. A reliable alert of ~1 – 2 *days* can thus be attained.

Level 4 (to be checked, however) permits to forecast two time intervals - only a few minutes each - for the expected time instant of a possible shock in the area that, owing to previous levels, is known to be in hazard.

The interested reader ought to refer to the aforementioned references. In any case, monitoring crystal stress propagation is a fundamental aspect also to investigate the climate influence of soil exhalation over large regions, such as, e.g., on the Tibet Plateau and

through all China (see Gregori et al., 2025f, 2025g, 2025h, 2025i, 2025j).

Other applications were concerned with monitoring a viaduct (Gregori et al., 2013) and with studying the stability of blades of the super-attenuators of the *VIRGO* experiment (Braccini et al., 2002), with a solution that was later used also by the *LIGO* gravitational antennæ.

After writing the present paper, a paper was published (O’Ghaffari et al., 2023, illustrated by Chu, 2023). We report here a few statements loaned after Chu (2023).

“MIT scientists find the sounds beneath our feet are fingerprints of rock stability.

If you could sink through the Earth’s crust, you might hear, with a carefully tuned ear, a cacophony of booms and crackles along the way. The fissures, pores, and defects running through rocks are like strings that resonate when pressed and stressed. ...

Peč and his colleagues are listening to rocks, to see whether any acoustic patterns, or ‘fingerprints’ emerge when subjected to various pressures. In lab studies, they have now shown that samples of marble, when subjected to low pressures, emit low-pitched ‘booms’, while at higher pressures, the rocks generate an ‘avalanche’ of higher-pitched crackles. ...

The fact that rocks are brittle at the surface and more ductile at depth implies there must be an in-between - a phase in which rocks transition from one to the other, and may have properties of both, able to fracture like granite, and flow like honey. This ‘brittle-to-ductile transition’ (BDT) is not well understood, though geologists believe it may be where rocks are at their strongest within the crust. ...

He and his colleagues are studying how the strength and stability of rocks - whether brittle, ductile, or somewhere in between - varies, based on a rock’s microscopic defects. The size, density, and distribution of defects such as microscopic cracks, fissures, and pores can shape how brittle or ductile a rock can be

... the team turned to ultrasound, and the idea that, any sound wave traveling through a rock should bounce, vibrate, and reflect off any microscopic cracks and crevices... They found that the idea should work with ultrasound waves, at megahertz frequencies. [We used LF AE at 25 kHz, and HF AE at 200 kHz. Other groups use lower frequencies. Experiments on marble sample stressed in the lab were also reported by groups active in Japan and in St. Petersburg, but are not mentioned by O’Ghaffari et al., (2023), who also are seemingly not aware of the several investigations reviewed in Gregori et al. (2018), and several later related papers.]

‘This kind of ultrasound method is analogous to what seismologists do in nature, but at much higher frequencies,’ Peč explains. ‘This helps us to understand

the physics that occur at microscopic scales, during the deformation of these rocks.’ ... [We stress, however, that one must explain why very high ultrasound propagate through loose soil, i.e., the role of serpentosphere is crucial.]

In their experiments, the team tested cylinders of Carrara marble. ... As they slowly crushed each rock, the team sent pulses of ultrasound through the top of the sample, and recorded the acoustic pattern that exited through the bottom. When the sensors were not pulsing, they were listening to any naturally occurring acoustic emissions. [Guarniere (2003), in his PhD thesis - with referees G.P. Gregori and G. Paparo - crushed concrete cubes in a press in the lab, showing the effectiveness and importance of the domino effect, evidenced by means of fractal analysis.]

They found that at the lower end of the pressure range, where rocks are brittle, the marble indeed formed sudden fractures in response, and the sound waves resembled large, low-frequency booms. At the highest pressures, where rocks are more ductile, the acoustic waves resembled a higher-pitched crackling. [In fact, this is the aforementioned sequence of “flaw domain” of increasing size, due to coalescence.] *The team believes this crackling was produced by microscopic defects called dislocations that then spread and flow like an avalanche.*

‘For the first time, we have recorded the ‘noises’ that rocks make when they are deformed across this brittle-to-ductile transition, and we link these noises to the individual microscopic defects that cause them,’ *Peč says.* ‘We found that these defects massively change their size and propagation velocity as they cross this transition. It’s more complicated than people had thought.’

The team’s characterizations of rocks and their defects at various pressures can help scientists estimate how the

Earth’s crust will behave at various depths, such as how rocks might fracture in an earthquake, or flow in an eruption. [An exhaustive reply is given by the aforementioned 4 Level approach to crustal monitoring, for releasing seismic alerts.]

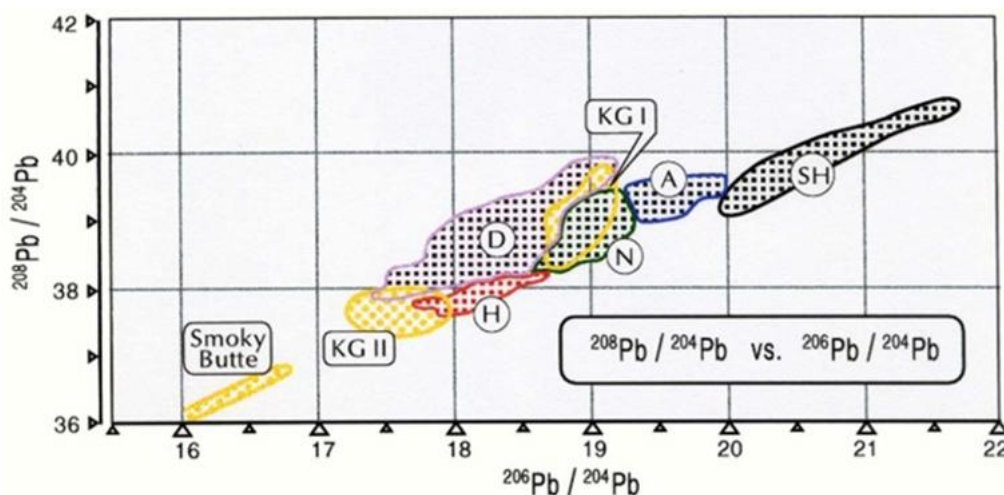
‘When rocks are partly fracturing and partly flowing, how does that feed back into the earthquake cycle? And how does that affect the movement of magma through a network of rocks?’ *Peč says.* ‘Those are larger scale questions that can be tackled with research like this.’ ...”

The state-of-the-art, which is outlined in the previous papers, looks much more a head than the naïve understanding envisaged by O’Ghaffari et al. (2023).

Appendix

Introduction

The present unpublished analysis was carried out in the early 1990s, by means of an intuitive, visual, pattern-recognition cluster-analysis in a 5-dimensional (5D) space. Every plotted point was singly evaluated, derived from a plot available in the literature. These several plots are usually called tectonomagmatic discrimination diagrams. The fragmentary and scant database required a patient analysis of point-by-point evaluation. At present, a richer computerized database is available - and the new plots confirm the old analysis. However, a statistical analysis of a greater dataset hides some evidence focused in the previous point-by-point investigation. The present Supplement shows the original plots and inferences, which were derived in the early investigation with a comparison with more recent data plots.



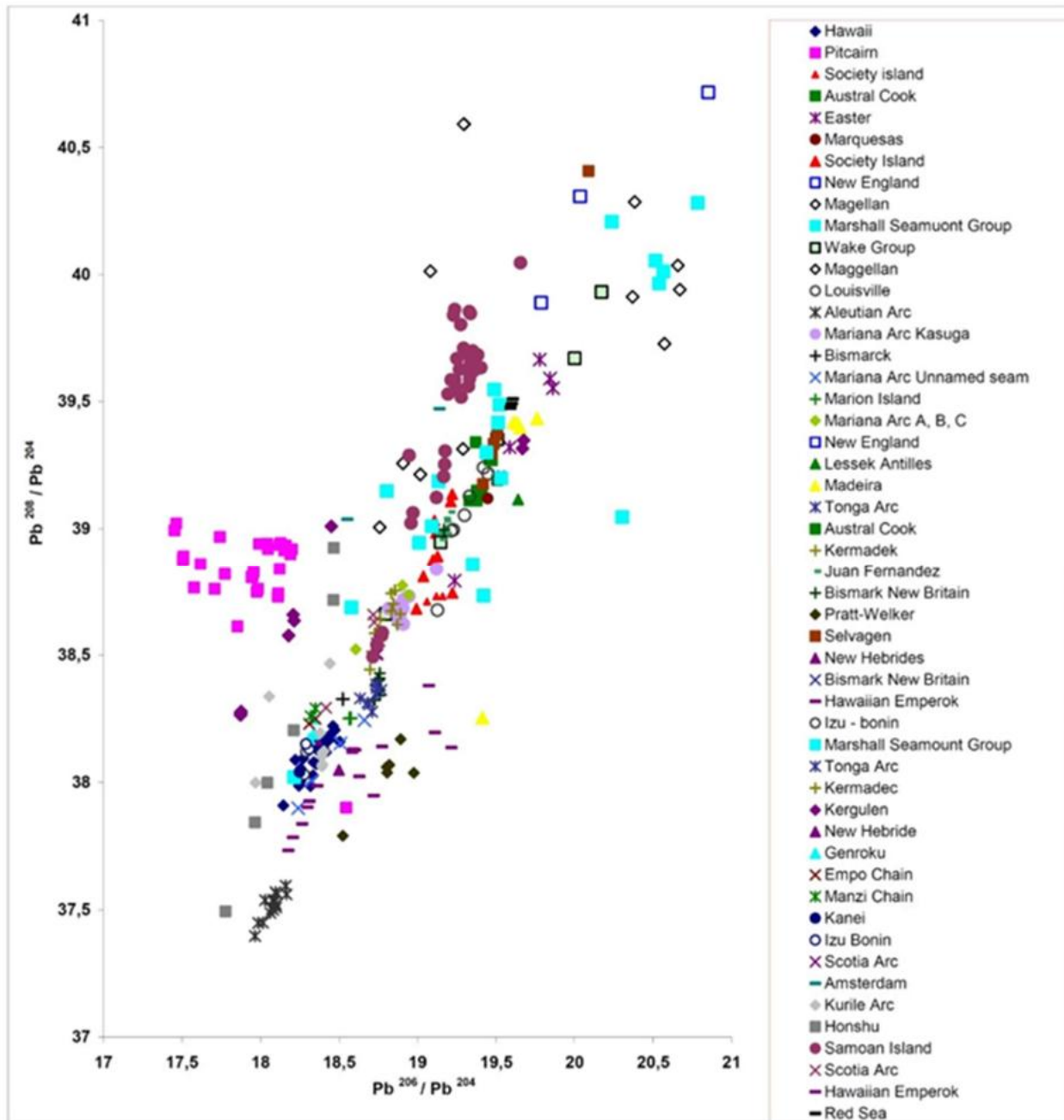


Fig. A-1 - Synthetic diagram plotting $^{208}\text{Pb}/^{204}\text{Pb}$ vs. $^{206}\text{Pb}/^{204}\text{Pb}$ showing samples of oceanic basalts into 5 clusters *H*, *D*, *N*, *A* and *SH*, respectively, plus cluster *IsAr* (island arc). (a) [upper diagram] Based on data from several diagrams appeared in the literature before ~1995. This figure is a 2D projection of observational points plotted in a 5D space. There is, however, no search for mutual consistency among all different (hand-drawn) Figs A-1 through A-5. Every figure was derived independent of others, and upon simple comparison between all diagrams that are synthesized by it. That is, any kind of *ad hoc* adjustment was avoided. Every apparent discrepancy between different figures is indicative of the uncertainty in the derivation of every (hand-drawn) figure. All points are part of a continuum. The proposed 5-cluster splitting is a simplifying way to characterize - or to label - every basalt sample. (b) [lower diagram] The same figure, drawn by computer and by means of a computerized database of basalt isotopic chemism, available on the web. Unpublished figure.

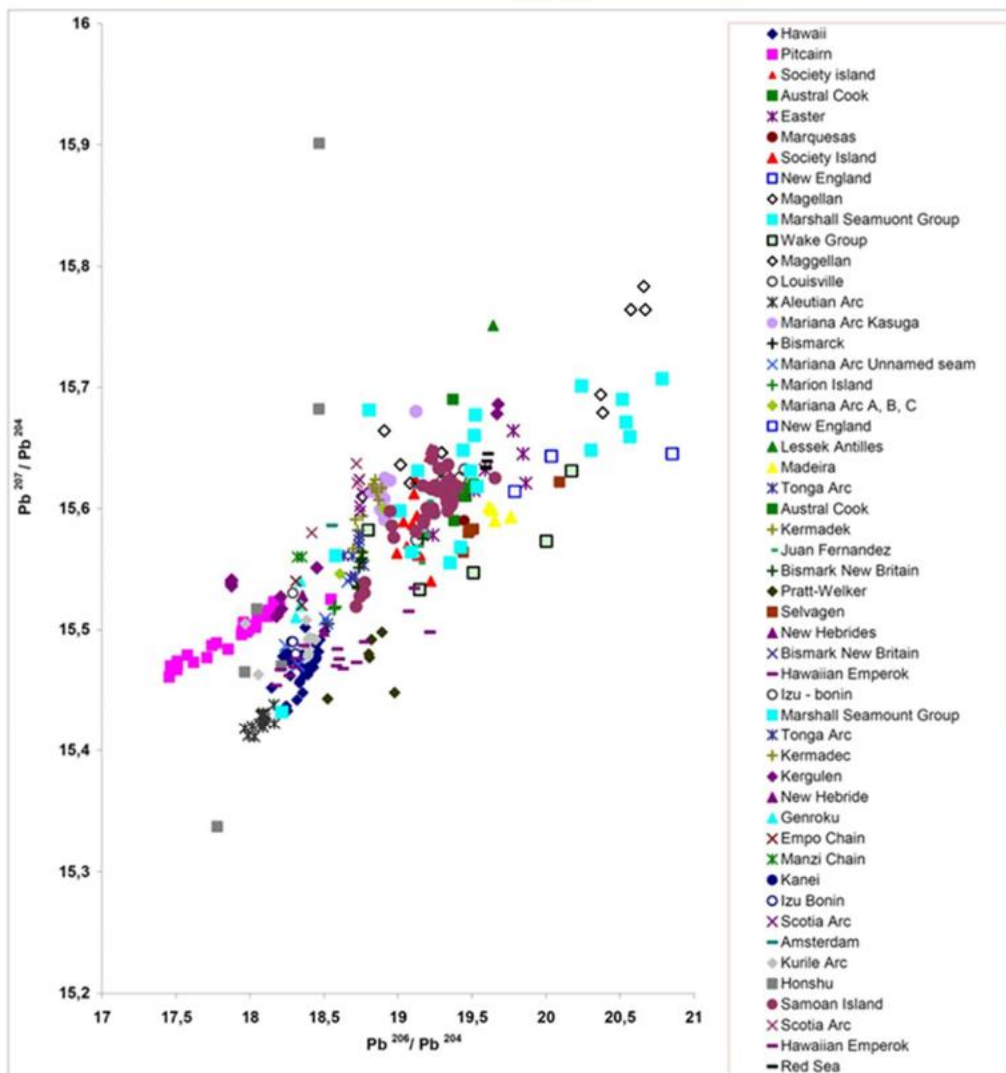
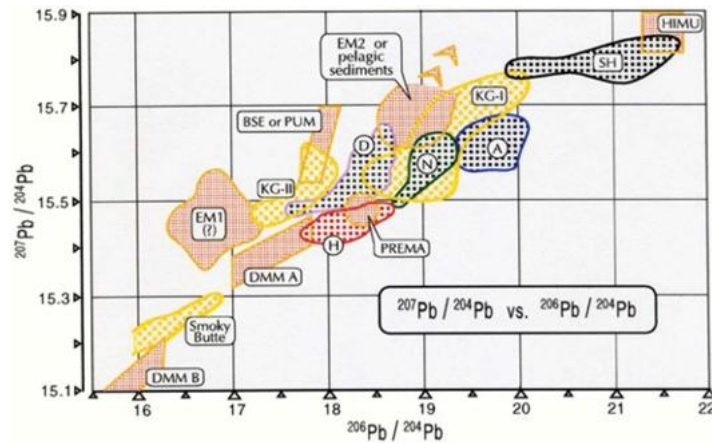


Fig. A-2 - The same as Fig. A-1 but referring to the $^{207}\text{Pb}/^{204}\text{Pb}$ vs. $^{206}\text{Pb}/^{204}\text{Pb}$ diagram. Unpublished figure.

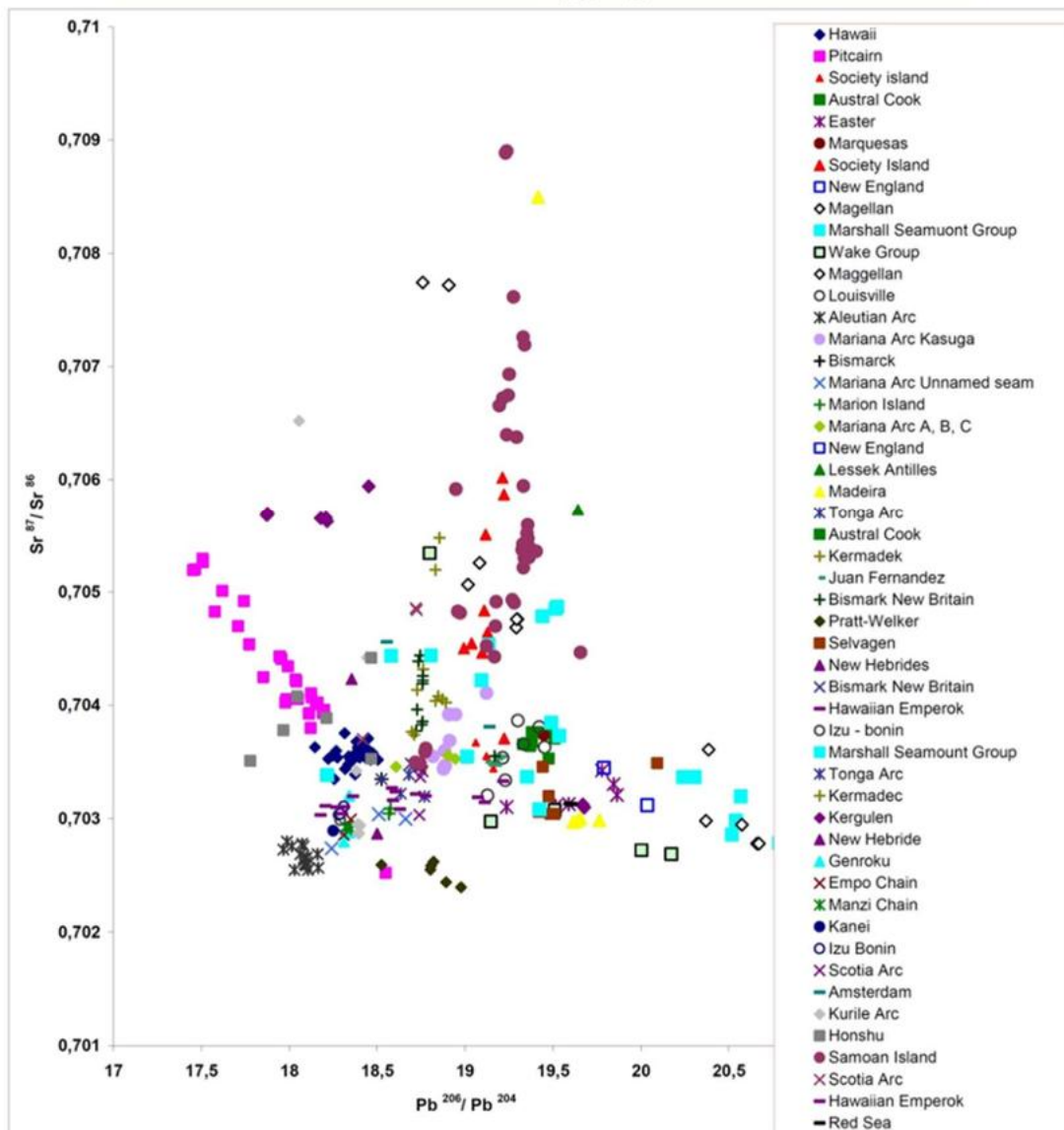
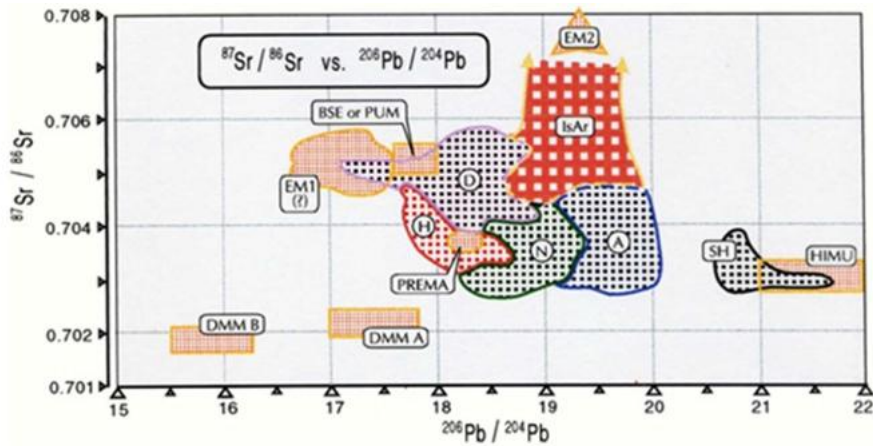


Fig. A-3 - The same as Fig. A-1 but referring to $^{87}\text{Sr}/^{204}\text{Pb}$ vs. $^{86}\text{Sr}/^{204}\text{Pb}$. Unpublished figure.

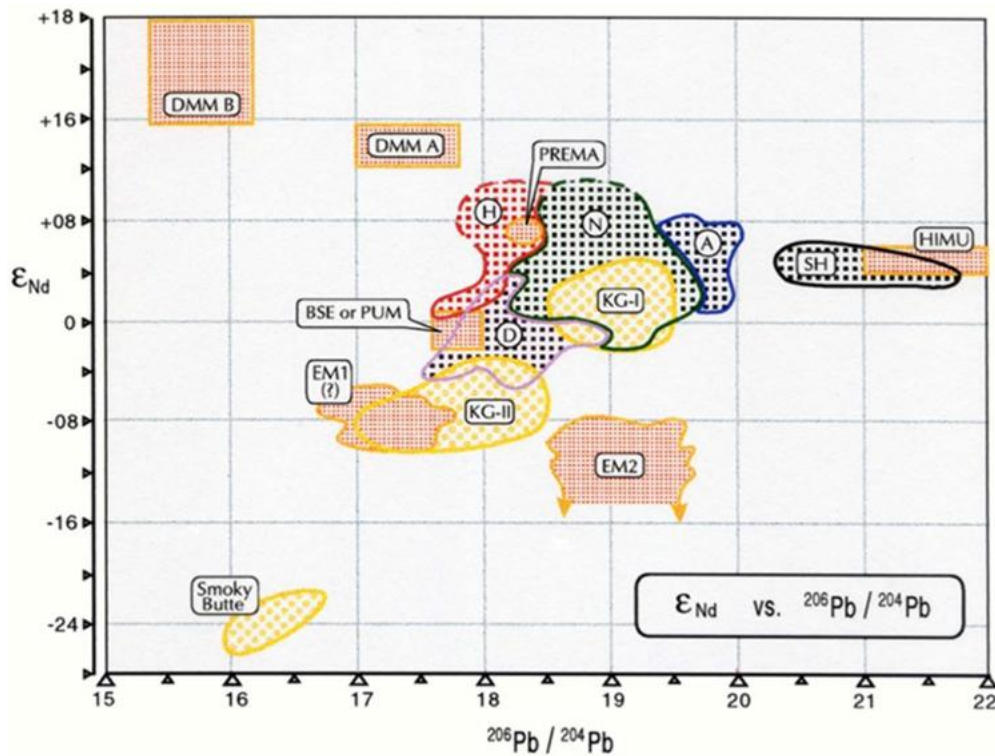


Fig. A-4 - The same as Fig. A-1 but referring to $^{143}\text{Nd}/^{144}\text{Nd}$ vs. $^{206}\text{Pb}/^{204}\text{Pb}$. Unpublished figure.

A standard and conspicuous database from all over the world is available of the isotopic concentration ratios of radioactive isotopes mostly concerning three elements, i.e., *Pb*, *Sr* and *Nd*. The *Pb* ratios refer to the concentration ratios of ^{206}Pb , ^{207}Pb , ^{208}Pb with respect to the stable isotope ^{204}Pb . The *Sr* ratio refers to the radioactive isotope ^{87}Sr with respect to the stable isotope ^{86}Sr . The *Nd* ratio refers to the radioactive isotope ^{143}Nd with respect to the stable isotope ^{144}Nd . In addition, it is usual to consider the quantities ϵ_{Sr} and ϵ_{Nd} , which are a different standard way used to express the aforementioned isotopic concentration ratios of *Sr* and *Nd*. See the formal original definition by De Paolo and Wasserburg (1976) (see also, e.g., Wilson, 1989 or Geyh and Schleicher, 1990).

Upon applying a cluster analysis to this database - and by considering only ocean floors for physical reason (see below) - a set of 5 clusters can be distinguished, on a mere phenomenological basis. Upon a closer inspection, these clusters reveal an “energy hierarchy”. A reasonable interpretation is in terms of a different primary energy supply. The clusters are denoted, respectively, in increasing order of energy, as:

(i) “SH” (after the St. Helena Island; only one additional spot was found with the same chemism,

approximately almost antipodal to St. Helena, i.e., in the Australs – Cook Islands);

(ii) “A” (after Atlantic type);

(iii) “N” as normal or intermediate cluster;

(iv) “D” (after DUPAL anomaly, extended over the entire Indian Ocean and over some part of the southernmost Atlantic Ocean); and

“H” (after Hawai’i)

The SH, A, N, D, and H clusters are an observational matter-of-fact. The evidence relies on Figs A-1 through A-5 (Gregori and Crisci, 1995) that, however, ought to be considered to be merely indicative. In principle, a formal approach should be carried out by cluster analysis and by computer. A search ought to be carried out for nD-clusters, by means of a file containing “all” available observations of isotopic ratios, as far as possible, depending on the available observational database. Figs A-1 through A-5 are rather only a few simple 2D projections of 5D objects. Every cluster eventually overlaps with others, when viewed from some given direction inside this 5D space. For every figure, the former 1990s hand-made plot is shown, altogether with the similar plot obtained by means of the present available dataset. M. Poscolieri drew these plots, relying on the database available some years ago.

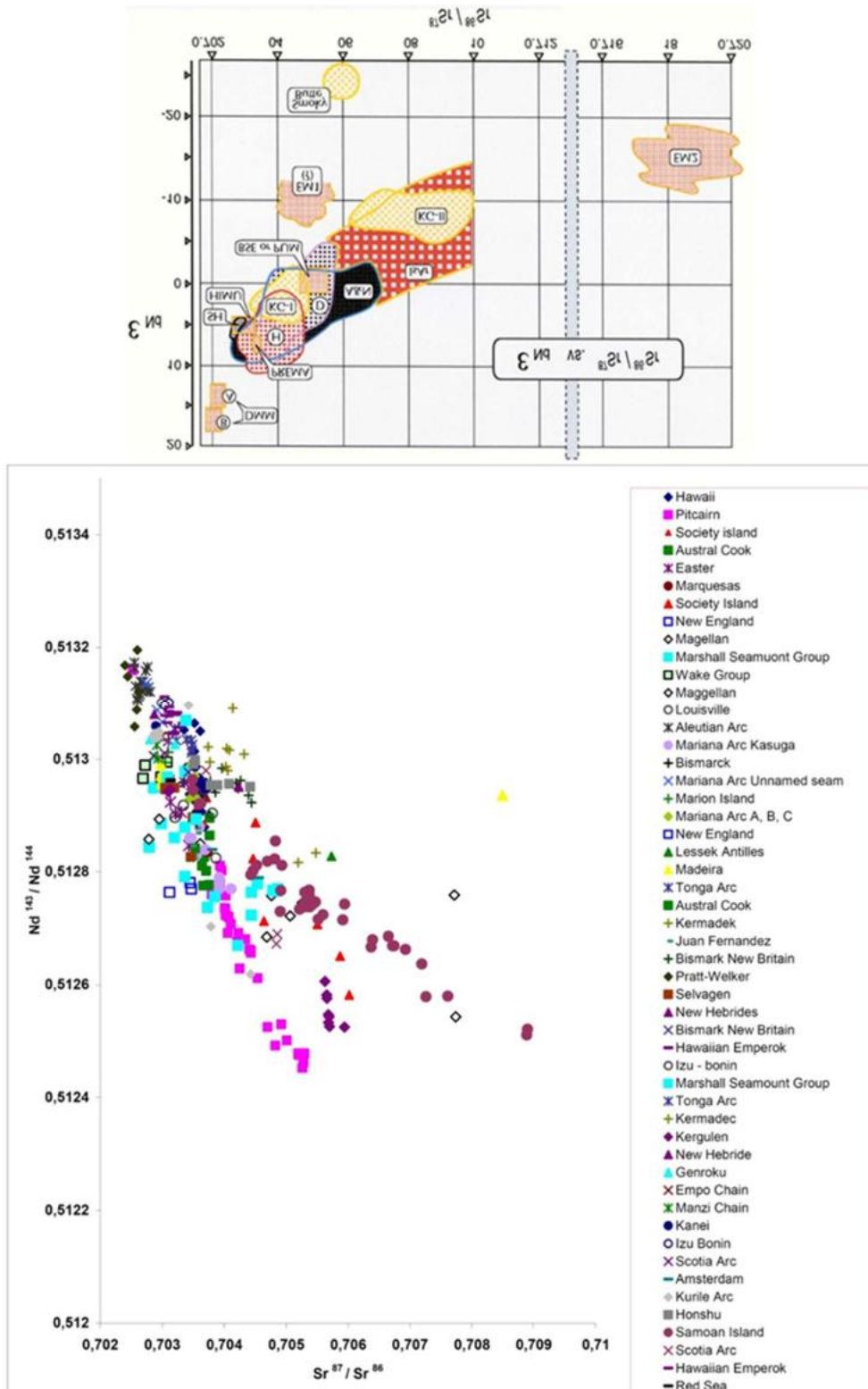


Fig. A-5 - The same as Fig. A-1 but referring to $^{143}Nd/^{144}Nd$ vs. $^{87}Sr/^{86}Sr$. Unpublished figure.

The agreement confirms the significance of the former hand-drawn figures that, however, contain some better indication, dealing with the geographical location of the site where the basalt samples were collected.

Several acronyms in these figures rely on some standard definitions that are found in the literature. They were envisaged on an empirical basis, and sometimes according to some speculated mechanism that some author considered as a working hypothesis. That is, some definitions rely on some tentative interpretation. Their definition (upon avoiding for brevity purposes any justification) is: “*BSE*” or “*PUM*” for bulk silicate Earth or primitive upper mantle, “*SHC*” St. Helena cluster, “*EM*” Enriched Mantle component (of two kinds), “*KG-II*” Kimberlites of Group II, “*PREMA*” Prevalent Mantle component, and “*DMM*” end-member “Depleted MORB Mantle”.

The literature contains a conspicuous amount of attempts to interpret these evidences. The generally reported rationale reminds us about a connoisseur who tries different cocktails and envisages the primary constituents. Thus, some acronyms deal with speculated primary ingredients that, maybe, might justify the observed ocean basalt chemism.

The $^{207}\text{Pb}/^{204}\text{Pb}$ vs. $^{206}\text{Pb}/^{204}\text{Pb}$ plots were drawn before the others. Some non-overlapping clusters could thus be envisaged and arbitrarily defined. Other analogous diagrams that were subsequently drawn were correspondingly managed, in order to account for eventual overlapping of different clusters.

Figs A-1 through A-5 are suggestive of 5 main clusters *H*, *D*, *N*, *A*, *SH*. In any case, the plotted points represent a distribution that is continuous in space. This separation into 5 discrete clusters is therefore a simple mnemonic scheme.

According to a simple straight analysis (not here shown), no clear correlation was found between the $^3\text{He}/^4\text{He}$ ratios and the *H*, *D*, *N*, *A*, *SH* clusters. Rather, the available $^3\text{He}/^4\text{He}$ ratios, which overlap with the *Pb*, *Nd*, *Sr* isotope data set, are distinguished in a larger subset with $^3\text{He}/^4\text{He} < 20$ and only 4 sites (i.e., Hawai’i, Iceland, Samoan Islands, and Easter Island) with $^3\text{He}/^4\text{He} > 25$. That is, the physical mechanisms seem to be different that originate a respective empirical distinction into different classes.

This whole scenario looks complicated. The basic approach, which is here adopted, relies on the geochemical isotopic evidence *per se*, in terms of the simplest viewpoint, with no need to speculate about chemical or isotopic differentiation, or about any

hypothesis concerning elementary “reservoirs” suited to compose different “cocktails”, etc.

A former hunch was found in Zindler and Hart (1986) - which deals with the imperfect alignment within a plane of the points plotted in Fig. A-6. Note that every such an isotopic ratio can eventually refer only to some averaged datum associated with every respective site. All points thus appear more or less clustered or scattered. The best known cluster is the *DUPAL* anomaly (*D*). For *DUPAL* definition see Hart (1984), based on Dupré and Allègre (1983).

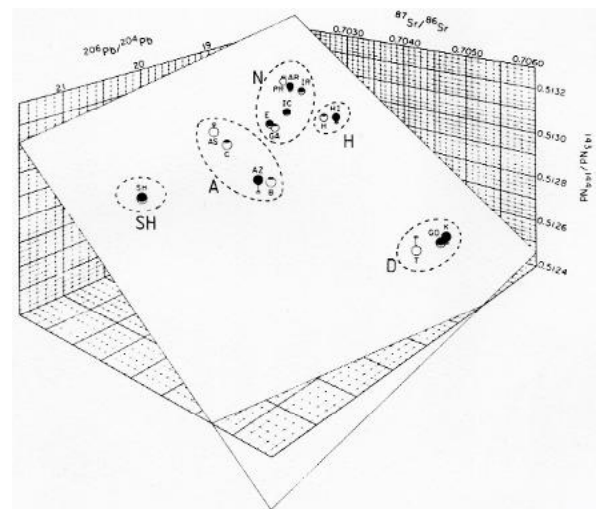


Fig. A-6 - 3D plot average plotting $^{206}\text{Pb}/^{204}\text{Pb}$, $^{143}\text{Nd}/^{144}\text{Nd}$ and $^{87}\text{Sr}/^{86}\text{Sr}$ for basalts from ocean ridges and islands, including the best-fit plane. Different symbols indicate the uncertainty of a single analysis. Acronyms are: *AR* - Mid-Atlantic Ridge (*MAR*); *AS* - Ascension; *AZ* - Azores; *B* - Bouvet Island; *C* - Canary Islands; *E* - Easter Island; *GA* - Galápagos; *GO* - Gough Island; *H* - Island of Hawai’i; *HI* - Hawai’ian Islands; *IC* - Iceland; *IR* - Indian Ocean ridges; *K* - Kerguelen Island; *PR* - East Pacific rise (*EPR*); *SH* - St. Helena Island; *T* - Tristan da Cunha Island. Data sources are given in Zindler et al. (1982). We modified the figure, shown by Zindler and Hart (1986) - while an older version is in Wilson (1989, p. 57) - by adding five closed dotted lines that show a proposed grouping into clusters *H*, *D*, *N*, *A* and *SH*, respectively. The figure with no cluster indication looks inexpressive. See text.

Other well-known clusters are tentatively indicated in Fig. A-6. That is, *SH* that is close to *HIMU*, and *H* that is generally acknowledged to have some peculiar characteristics of its own. The remaining points have been here arbitrarily divided into 2 clusters, by grouping the points for central Atlantic Ocean (cluster *A*), while leaving all other points within a cluster (*N*), which is here

arbitrarily called “normal” (but do not confuse it with *N*-type *MORB*).

Instead of the aforementioned “cocktail rationale” based on “reservoirs”, we rely on a criterion briefly called “energy hierarchy”. It is in terms of a different penetration of a sea-urchin spike, which samples some given deep layer, with its typical and different chemism. According to this energy hierarchy, every case history – from a feeble through a strong primary heat supply – will stop its penetration as soon as – owing to insufficient primary energy supply – it can no more propagate upward. Then, heat accumulates vs. time, until melt occurs. Whenever the spike affords to reach Earth’s surface, it releases the endogenous heat, and it eventually originates a large permanent magma emplacement (i.e., a hotspot and/or a large igneous province, *LIP*). Fig. A-7 shows the guessed “energy hierarchy”.

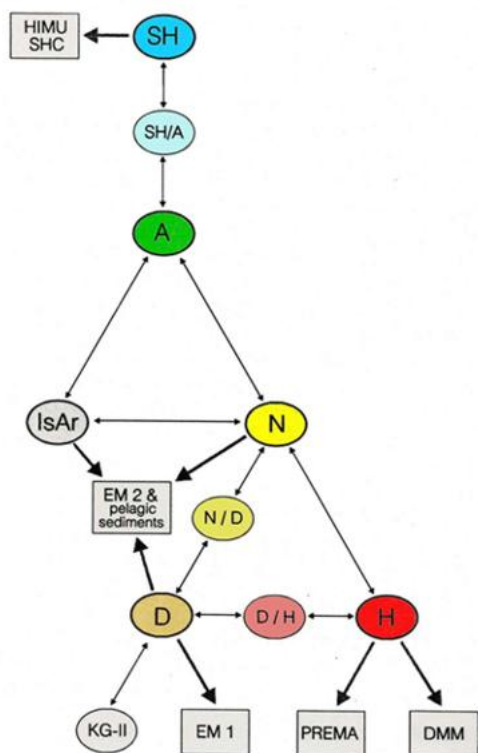


Fig. A-7 - Five-level hierarchy of primary energy supply for the generation of basalt, including upward propagation vs. time, thus producing thermal expansion and uplift of geotumors or superswells, according to *WMT*. See text. Unpublished figure.

The rationale behind the definition of a flow diagram, of the kind sketched in Fig. A-7 is called by Carlson (1994) “mixing hierarchy”. The reason is that the order

sequence and mutual relations between different clusters is interpreted in terms of some hierarchy.

Fig. A-7 includes all aforementioned clusters *H*, *D*, *N*, *A*, and *SH*, plus the new cluster “*IsAr*” (island arcs). Owing to the role of continental plate boundaries, island arc volcanism seemingly experienced a major contamination e.g., by some shallower layers. On the other hand, maybe, the anomaly could be related to the lithosphere that sinks into the trenches (see the aforementioned island arc model). Island arc volcanoes are therefore supplied by friction heat of the sinking lithosphere, and – compared to other volcanoes – they probe some layers deeper than the typical thickness of the lithosphere. In any case, according to the rationale of the present study, island arc volcanism is originated by boundary effects of lithospheric slabs, rather than by deep energy processes. Hence, the island arc chemism reflects “shallow” lithospheric features, while – compared to the thickness of the lithosphere – other kinds of volcanism can potentially sample much deeper layers. In any case, it does not mind whether chemical contamination is originated from the crust, or from subducted sediments, or from some intermediate-depth layers, etc. Hence, the “*IsAr*” cluster is located close to the speculated EM-II end-component (see Zindler and Hart, 1986).

The association of a given location with a given class is sometimes non-univocal, and some locations seems to partake to some “intermediate” chemism. For instance, *SH/A* includes basalts that have features that seemingly fall in between *SH* and *A*. In general, every site, which includes samples that partake into two clusters, can be included also into their corresponding “intermediate” cluster. In fact, 5 clusters are only a simplified discrete scheme of a continuum.

Moreover, the indicated association of clusters with geographical locations is only tentative, because more accurate geochemical analyses can eventually provide with new evidence that can envisage some different association.

Figs A-8 and A-9 show the geographical distribution of all clusters. Some regular trend is found – although, at a first glance, some apparent inconsistencies are evidenced. Fig. A-8 is the global plot, while Fig. A-9 shows a more detailed map for the SE Pacific Ocean. Separate maps dealing with the Mediterranean region are not here shown, as they ought to deserve a long devoted paper.

The color code is identical in all Figs A-8 and A-9. It is explicitly indicated in Fig. A-9. Whenever a few different clusters are to be indicated for one and the same site, this is shown either (i) by a few nearby full-circles, everyone with a different color, or (ii) by a few concentric

circles of different color. Either one representation or the other is arbitrary, with the aim to provide a better intuitive picture.

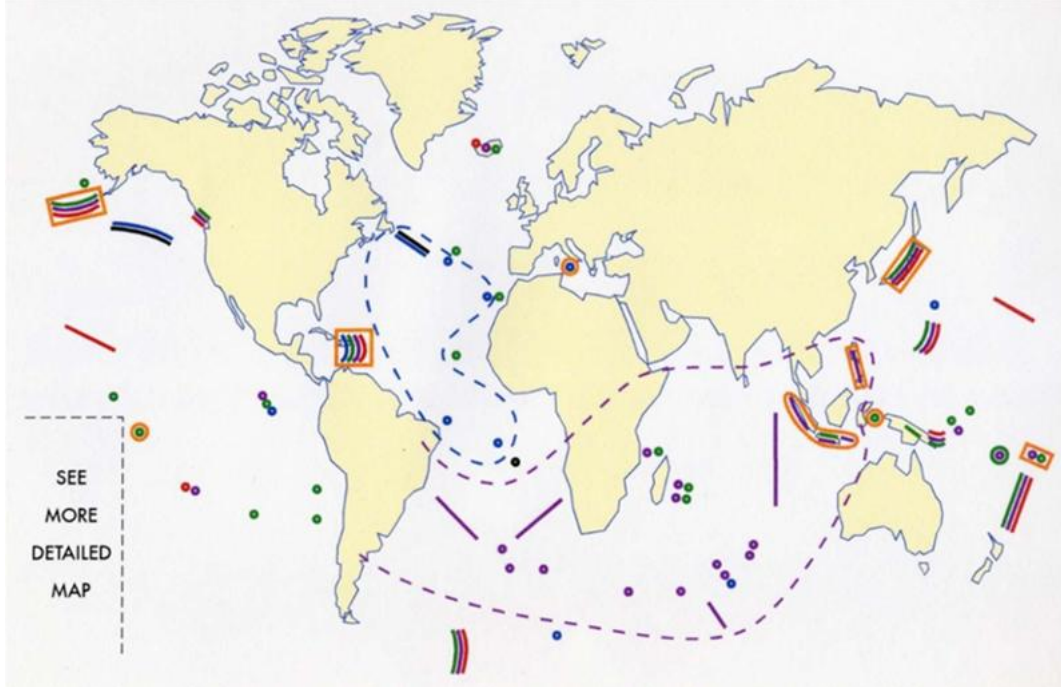


Fig. A-8 - Global plot of the geographical distribution of the 5 levels of the energy hierarchy of the isotopic chemism of basalt. The color code is indicated in Fig. A-9. See text. Unpublished figure.

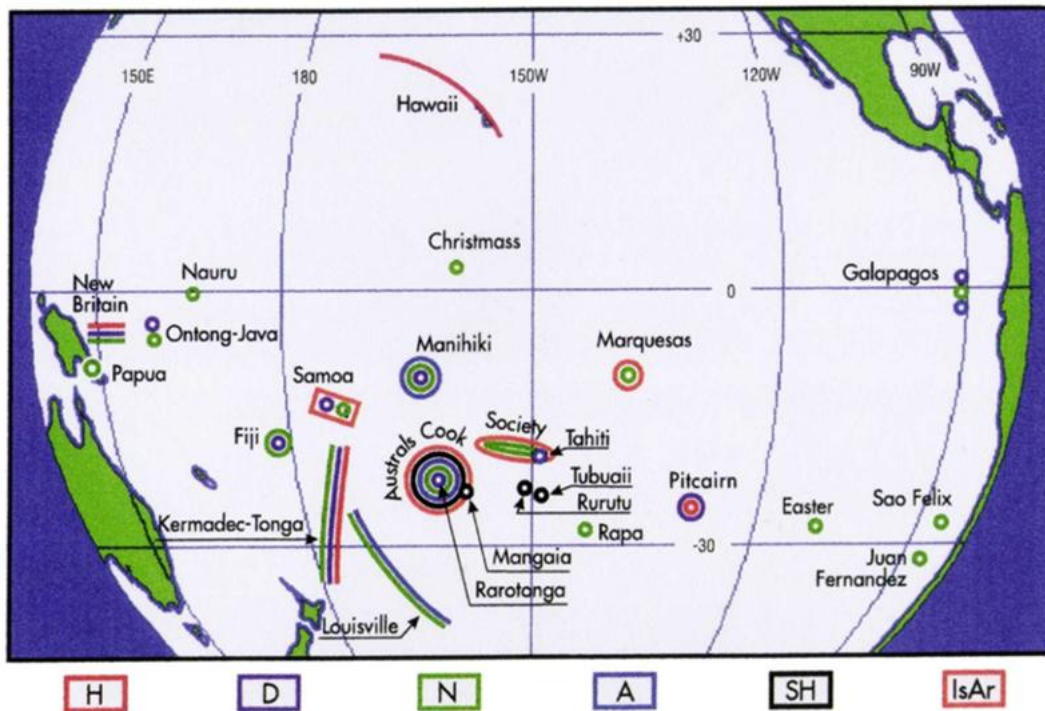


Fig. A-9 - Detail of Fig. A-8 referred to the SE Pacific Ocean. See text. Unpublished figure.

In addition, the isotopic chemism of basalt observed at a given site evolves in time, depending on the time-varying upward penetration of the sea-urchin spike. Hence, on the geological time scale the isotopic characterization of a site ought to evolve *vs.* time. The observed chemism displays therefore some cyclic evolution, which is typical of every sit, due to the recurrent heartbeats every $27.4 Ma$. In general, however, according to the available literature, this expected temporal evolution does not seem to have been investigated, apart at most a few exceptions (see below).

The general pattern of the variation *vs.* latitude and longitude looks smooth and regular. Two lines in Fig. A-8 enclose sets of sites that share a prevailing common character. One of these lines envelops *D* points (*DUPAL*'s area), beginning from the Philippines through the central and southern Indian Ocean, through southern Atlantic, until South America.

An intriguing feature is the apparent agreement of this line with the area in South Africa, South America, and even in western Australia, where either Group II kimberlites, or diamond-bearing formations, are found. This apparent correlation envisages the tentative suggestion that diamonds and *DUPAL*'s anomaly have a common or similar cause.

Another line is drawn to envelope the *A*-type points in central Atlantic Ocean.

Concerning Figs A-8 and A-9, the steep spatial gradient appears remarkable in the Australs Cook islands. In particular, it is remarkable, e.g., the transition between the *D* and *N* type of Rarotonga down through the *SH* type in Mangaia, Rurutu and Tubuai, with rock samples which smoothly cross through all clusters of intermediate energy.

These features are here interpreted in terms of a smooth continuous variation of the intensity of the prime energy supply, better than in terms of a smooth spatial variation of the primary "reservoir" for basalt. This tentative inference, however, implies that a large fraction (at least) of the observed basalt ought to have been emplaced directly from a source located at the sampling site, in contrast with the often reported hypothesis that basalts are generated at some site and then drift on the ocean floor.

These aforementioned two physical models (i.e., the "reservoir" rationale *vs.* the local spatial gradient of the primary supply of endogenous energy) can result to be sometimes contradictory with each other. Therefore, every case history ought to be considered independent of others.

Note that the *SH* restricted region around the Australs - Cook Islands is found to be approximately close to - slightly east of - the Osbourn Seamount ($\sim 76.7 Ma$) at the divide between the Kermadec Trench and the Tonga Trench. This is the ideal center of the approximate arc of circle, displayed by the segment of the Circum-Antarctic Ridge that gets closer to the South Pole. This fact is suggestive of a fixed hotspot located in this area that "pushed" far away the sea-urchin spikes located along the *MOR*. In addition, it also seemingly "pushed" another hotspot, which thus generated the whole track of the Louisville Ridge. This explanation can be in connection with the tetrahedron pattern (Gregori and Leybourne, 2021).

When the same analysis is tentatively applied to the continental basalt, the scenario looks more erratic, with no apparent guessed phenomenological ordered sequence. In fact, according to *WMT*, continents result from a convergence of lithospheric slabs into a megasyncline. Accordingly, they result from a complicated over-thrust of various lithospheric components. For instance, concerning South America, see Girardi et al. (2012) and Moreira Florisbal et al. (2012).

Concerning the time evolution of basalt chemism on the geological time scale, a reasonable expectation is that an early stage is *SH* is followed by a progressive chemism through *A*, *N*, *D* and *H*. Then, the "channel", which is represented by the conductive sea-urchin spikes, is closed for endogenous energy release. The cycle thus eventually re-starts beginning anew from *SH* etc.

An interesting case history is displayed in the Andes in central Chile. A timing of the isotopic chemism is shown in Fig. A-10, which can be tentatively interpreted as follows. The temporal evolution begins by a downward and rightward trend in this plot. Unfortunately, the *Pb* isotopic chemism is not reported by Yáñez et al. (2002) and it is not possible, by means of the *Sr* and *Nd* isotopic chemism alone, to get a clearer distinction between the different classes of basalts, according to their respective "energy hierarchy" cluster.

Start from the Late Oligocene - Early Miocene basalt ($\sim 33 - 15 Ma$), and presume that its melt occurred inside some comparably deeper layer. Maybe, this is *SH*. Then, the sea-urchin spike propagated upward, and generated a temporal sequence through the Early-mid Miocene basalt ($\sim 22.5 - 12 Ma$), the Late Miocene basalt ($\sim 12 - 5 Ma$), and the Quaternary basalt ($\sim 1.8 Ma$ through present). This ought to be a presumable sequence through *A*, *N*, *D*, and, maybe, it will end into *H*.

However, this is one full cycle of $\sim 27.4 Ma$. When one full cycle is completed, the endogenous heat can be

fully released through some kind of efficient “channel” for energy outflow. On every occasion of this kind, a *LIP* can be eventually generated. However, the release of endogenous energy is faster than its refill. Hence, the sea-urchin spike cools, and its electrical conductivity σ decreases. Thus, the electric “channel” is closed, and the Earth’s battery restarts to accumulate energy. By this, a new ~ 27.4 Ma cycle begins. Owing to this reason, the basalts that in Fig. A-10 refer to the Early Cretaceous ($\sim 141 - 118$ Ma) and to the Mid-Cretaceous ($\sim 118 - 88$ Ma) cannot fit within this rationale, because every such a time interval is $\gg 27.4$ Ma.

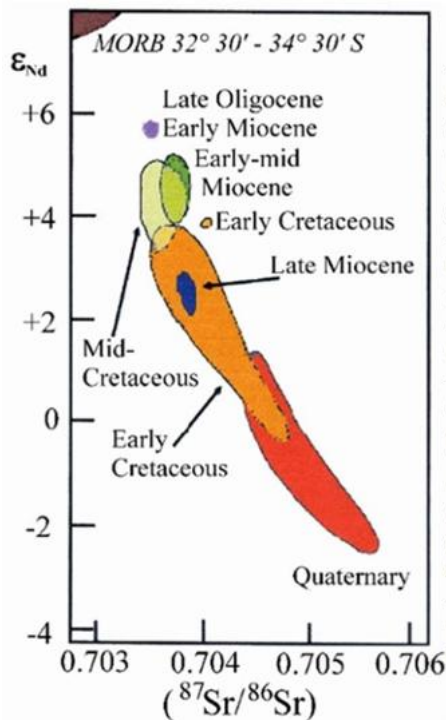


Fig. A-10 - “Isotopic ratios from central Chile basalts (Nyström et al., 1993), showing Oligo-Miocene lavas (Abanico Formation) being the less contaminated.” Figure (redrawn) and captions after Yáñez et al. (2002). AGU copyright free policy.

Another example of a very varied area in terms of isotopic chemism is given by the central Mediterranean region that, however - owing to brevity purpose - cannot be here considered.

In any case, isotopic ratios and “chemical geodynamics” - when suitably interpreted - are an effective hunch for the investigation of the third dimension (i.e., time) in Earth’s evolution. No list can be here given of several related references. For instance, concerning the variation of the Sr isotopic chemism of basalt along the Andes see, e.g., Cembrano and Lara (2009).

Diagrams dealing with other isotopic ratios cannot be drawn with any database of comparable size. We also attempted to draw some analogous figures by referring to

other couples of coordinate axes. However, according to the data available in the literature at that time, every dataset contains very few data, and can give no evidence about any possible cluster. A richer database is strictly required.

For comparison purpose, a few somewhat analogous attempts were carried out by other authors dealing with the isotopic chemism of basalt.

Hofmann (1997) made four similar plots (not here shown), the leading concern being, however, the search for some speculated original components that evolved since the time of Earth’s formation.

Turcotte and Schubert (2002) aimed to search for some clusters in three plots (not here shown). They display an approximate correspondence with the clusters here proposed - which, according to the rationale of Fig. A-7 is here called “energy hierarchy rationale”. For the interested reader, every Turcotte and Schubert (2002) cluster can be briefly denoted as *TS-* followed by either I, or II, ... or V. The approximate correspondence is $H \Leftrightarrow TS-II$, $D \Leftrightarrow TS-III$, $N \Leftrightarrow TS-I$, $A \Leftrightarrow TS-V$, and $SH \Leftrightarrow TS-IV$. Turcotte and Schubert (2002) identify their III cluster with *EM-I* and their cluster V with *EM-II*

The “energy hierarchy rationale” was proposed in December 1996 inside a long paper submitted to *Reviews of Geophysics*. That paper, which also contained the physical justification in terms of sea-urchin spikes, was rejected with no specific criticism or objection. The Turcotte and Schubert (2002) clusters were published six years later, although giving no physical explanation. However, Allègre and Turcotte (1985), as mentioned by Zindler and Hart (1986) and by Kellogg (1992), had envisaged 5 components or “reservoirs”, and - maybe - they were looking for observational evidence for their speculated 5-component chemism.

The physical interpretation, which is here proposed, is a substantial support for the physical meaning of the clusters - because, according to the present rationale, the clustering is found, as expected, to be closely correlated with the propagation of the endogenous energy up to Earth’s surface. In addition, also the *MIR* bathymetry enters into the physical explanation and analysis, as per Figs 13-16.

White (2010a) gave another analysis of the cluster of isotopic chemism of *OIB* and *MORB*. No figure is here shown, and no details concerning the interpretation is here mentioned that was given by White (2010a). The interested reader ought to refer to the original paper. In general, some interesting additional support for the hierarchy model here proposed derives from the four conclusions (not here mentioned) by White (2010a), although he interprets them in favor of the generally

agreed mantle-plume model, with related speculated geochemical inferences.

In addition, several studies in the literature deal with tectonomagmatic discrimination diagrams, referred however to limited regions or small areas. The huge number of papers is not here of concern. We just emphasize the relevance of chemism for understanding deep phenomena, when they are considered altogether with the general morphological information derived from other evidences, and upon avoiding – as far as possible – any *ad hoc* working hypotheses.

An additional tentative speculation derives from consideration of the very different tectonic setting of Æolian Islands compared to the Andes.

In the case of the Æolian Islands, volcanism is generated by the fact that the Italian peninsula is rotating counterclockwise, and it leaves a gap in the rear, by which it removes the lithospheric “stopper” that formerly “plugged” the endogenous pressure (Gregori and Leybourne, 2021). Hence, magmatism ought to be roughly similar to *OIB*.

In contrast, in the case of the Andes an over-thrust is in progress of the South American lithosphere on top of the Pacific ocean lithosphere. The process implies the generation of a large amount of friction heat, and an increase of the local electrical conductivity σ . A higher σ favors an upward propagation of the sea-urchin spikes that finally determine the depth where melt occurs.

However, a similar or approximately identical temporal sequence of the isotopic chemism of basalt is observed in both case histories. It seems therefore reasonable to conclude that the chemism is controlled by the upward propagation of sea-urchin spikes, independent of whether this occurs either (i) due to a lack of a “stopper” that “plugs” the endogenous pressure, or (ii) due to a local increase of σ caused by an external action (in the Andes case by the friction heat due to overthrust).

This observational evidence - and its associated tentative interpretation – needs for better investigation.¹⁰ Note that the depth units in Fig. A-7 are unknown, although one can manage some indicative value upon considering the order of magnitude of the speed of upward propagation of the spike. However, this would be very speculative. The comparison of the case histories of the Æolian Islands and of the Andes envisages however that, in any case, every source of the different kinds of chemism ought to be always inside the lithosphere (although the definition of “lithosphere” is *per se* somewhat ambiguous; not here discussed).

¹⁰ The existing literature only seldom reports isotopic ratios with sufficiently detailed time resolution (e.g., see Litvak et al., 2007). Some information on the

Acknowledgment

We want to acknowledge several friends and colleagues who often unconsciously contributed to the exploitation of the model and interpretation here envisaged.

All co-authors are particularly sad about the recent passing away of Gabriele Paparo (02/02/1949-07/04/2023).

G. P. Gregori expresses a profound and warm gratitude to the late Professor Wilfried Schröder for his always great encouragement.

Funding Information

The funding is derived from the respective institutions.

Author’s Contributions

This study derived from a long-lasting cooperation and discussion by the authors. The backbone draft was prepared by the G.P. Gregori, although a large number of ideas resulted from the emergence of long lasting discussions, and the paternity of ideas can be hardly separated. The late G. Paparo had a fundamental role in the exploitation of *AE* monitoring. M. Poscolieri contributed to *AE* investigations, and mainly to the discussion of the tectonics of the Earth and of other planetary objects. B.A. Leybourne contributed to the final re-evaluation and discussion of the entire study.

Ethics

This article is original and contains unpublished material. The authors declare that there are no ethical issues and no conflict of interest that may arise after the publication of this manuscript.

References

- Allègre, C.-J., and D.L. Turcotte, 1985. Geodynamic mixing in the mesosphere boundary layer and the origin of oceanic islands, *Geophysical Research Letters*, 12 (4): 207-210; DOI:10.1029/GL012i004p00207
- Bletery, Q., & Nocquet, J.-M., 2023. The precursory phase of large earthquakes. *Science*, 381(6655), 297-301. <https://doi.org/10.1126/science.adg2565>
- Braccini, S., C. Casciano, F. Cordero, F. Frascioni, G.P. Gregori, E. Majorana, G. Paparo, R. Passaquieti, P.

chemism of the Andean basalt is given by Stern (2004).

- Puppo, P. Rapagnani, F. Ricci, and R. Valentini, 2002. Monitoring the acoustic emission of the blades of the mirror suspension for a gravitational wave interferometer. *Physics Letters A*, 301 (5/6): 389–397; DOI:10.1016/S0375-9601(02)00991-X
- Brodholt, J.P., and R. Batiza, 1989. Global systematics of unaveraged mid-ocean ridge basalt compositions: Comment [on “Global correlations of ocean ridge basalt chemistry with axial depth and crustal thickness” by Klein, E.M. and C.H. Langmuir], *Journal of Geophysical Research, Solid Earth*, 94 (B4): 4231-4239; DOI:10.1029/JB094iB04p04231
- Burbank, J.E., 1905. Earth-currents and a proposed method for their investigation. *Terrestrial Magnetism and Atmospheric Electricity*, 10, (1), 23-49. <https://doi.org/10.1029/te010i001p00023>
- Burke, K., 2011. Plate tectonics, the Wilson cycle, and mantle plumes: geodynamics from the top, *Annual Review of Earth and Planetary Science*, 39: 1-29; DOI:10.1146/annurev-earth-040809-152521.
- Carlson, R.W., 1994. Mechanisms of Earth differentiation: consequences for the chemical structure of the mantle. *Reviews of Geophysics*, 32 (4): 337-361; DOI:10.1029/94RG01874
- Cembrano, J., and L. Lara, 2009. The link between volcanism and tectonics in the southern volcanic zone of the Chilean Andes: a review, *Tectonophysics*: 471, 96–113; DOI:10.1016/j.tecto.2009.02.038
- Chapman, S. and Bartels, J., 1940. *Geomagnetism*. 2 vol., Oxford Univ. Press, (Clarendon): London and New York. pp: 1-1049
- Chen, Jiasheng, V.A. Kravchinsky, and Xiuming Liu 2015. The 13 million year Cenozoic pulse of the Earth, *Earth and Planetary Science Letters*, 431: 256–263; DOI:10.1016/j.epsl.2015.09.033.
- Chu, J., 2023. Sonic signatures: how MIT geologists are mapping Earth’s hidden layers, *SciTechDaily*, issued October 14, 2023
- Cook, T., 2019a. Explaining the genesis of superdeep diamonds, *EOS, Transactions of the American Geophysical Union*, 100; DOI:10.1029/2019EO117779.
- Coombs, A., 2016. Mineral flaws clarify how diamonds form, *EOS, Transactions of the American Geophysical Union*, 97; DOI:10.1029/2016EO054833.
- De Paolo, D.J., and G.J. Wasserburg, 1976. Nd isotopic variations and petrogenetic models. *Geophysical Research Letters*, 3 (5): 249-252; DOI:10.1029/GL003i005p00249
- de Santis, A., D.R. Barraclough, and R. Tozzi, 2001. Spatial and temporal spectra of the geomagnetic field and their scaling properties. Submitted to *Physics of the Earth and Planetary Interiors*. Published, modified, in vol. 135 (2/3): 125-134; DOI:10.1016/S0031-9201(02)00211-X
- Dupré, B., and C.J. Allègre, 1983. Pb-Sr isotope variation in Indian Ocean basalts and mixing phenomena, *Nature*, 303: 142-146; DOI:10.1038/303142a0
- Espinoza, V., and G.P. Iaffaldano, 2023. Rapid absolute plate motion changes inferred from high-resolution relative spreading reconstructions: A case study focusing on the South America plate and its Atlantic/Pacific neighbors, *Earth and Planetary Science Letters*, 604: 118009; DOI:10.1016/j.epsl.2023.118009
- Fukushima, N., 1989. Memorandum on non-curl-free geomagnetic field. *Il Nuovo Cimento*, 12C (5): 541-546.
- Gauss, C.F., and *Königlichen Gesellschaft der Wissenschaften zu Göttingen*, 1877. Resultate aus den Beobachtungen des magnetischen Vereins. In *Werke* (pp. 595-596). Springer Berlin Heidelberg. https://doi.org/10.1007/978-3-642-49319-5_40
- Gauss, C.F., and W. Weber, 1836, ..., 1841. Resultate aus den Beobachtungen des magnetischen Vereins in Jahre 1836, ..., 1841 (6 Hefte): Göttingen and Leipzig. Some reprints in *Werke*, 5. Translations by E. Sabine in Richard Taylor, *Scientific Memoirs*, 2, London, R. J. E. Taylor, 1841
- Geyh, M.A., and H. Schleicher, 1990. *Absolute Age Determination. Physical and Chemical Dating Methods and their Application*. Springer Verlag, Berlin etc.; DOI:10.1007/978-3-642-74826-4; pp: 1-503
- Girardi, V.A.V., W. Teixeira, M. Mazzucchelli, and P.C. Corrêa da Costa, 2012. Sr-Nd constraints and trace-elements geochemistry of selected Paleo and Mesoproterozoic mafic dikes and related intrusions from the South American Platform: Insights into their mantle sources and geodynamic implications, *Journal of South American Earth Sciences*, 30: 1-18; DOI:10.1016/j.jsames.2012.09.006
- Gish, O.H., 1933. The problem of vertical earth-currents, *EOS, Transactions of the American Geophysical Union*, 14th annual meeting: 144-146.
- Gregori, G. P., 1997. Historical data and global change. Case studies. In W. Schröder (ed.), *Physics and Geophysics with Special Historical Case Studies (A Festschrift in Honour of Karl-Heinrich Wiederkehr)*. *Mitteilungen des Arbeitskreises Geschichte der Geophysik der DDG*, 16, Jahrgang (1997): (2/5): and Newsletter of IDCH-IAGA, (25), Science Edition / IDCH-IAGA / AKGGKP (Arbeitskreis Geschichte der Geophysik und Kosmischen Physik der DDG):

- Science Edition, Bremen Roennebeck and Potsdam, pp: 183-210
- Gregori, G. P., 2020. Climate change, security, sensors. *Acoustics*, 2: 474-504; DOI:10.3390/acoustics2030026. [<https://www.mdpi.com/2624-599X/2/3/26/htm>]
- Gregori, G. P., and B. A. Leybourne, 2021. An unprecedented challenge for humankind survival. Energy exploitation from the atmospheric electrical circuit, *American Journal of Engineering and Applied Science*, 14 (2): 258-291; DOI:10.3844/ajeassp.2021.258.291
- Gregori, G. P., and B. A. Leybourne, 2025i. Wildfires from the Banda Sea through Beijing and through Karakoram. *New Concepts in Global Tectonics, Journal*, 13, (6): 854-887
- Gregori, G. P., and B. A. Leybourne, 2025j. The energy supply to hurricanes. *New Concepts in Global Tectonics, Journal*, 13, (5): 731-786
- Gregori, G. P., and B. A. Leybourne, 2025k. The global climate change perspective. The glaciers proxy, *New Concepts in Global Tectonics, Journal*, 13, (2): 270-335
- Gregori, G. P., and B. A. Leybourne, 2026b. The electrostatic Sun. Present issue of *New Concepts in Global Tectonics, Journal*
- Gregori, G. P., and M. T. Hovland, 2025. Go for the anomaly – a golden strategy for discovery? Seepology & the origin and crucial role of the biosphere - Earth and planetary objects - Supercritical water and serpentinization. *New Concepts in Global Tectonics, Journal*, 13, (9): 1337-1491
- Gregori, G. P., B. A. Leybourne, and G. Paparo†, 2026b. Introduction – Anomalous lesser air-earth phenomena. Present issue of *New Concepts in Global Tectonics, Journal*
- Gregori, G. P., B. A. Leybourne, and J. R. Wright, 2026d. Generalized Cowling theorem and the Cowling dynamo. *New Concepts in Global Tectonics, Journal*, 14, (1): 90-112
- Gregori, G. P., B. A. Leybourne, and L. A. G. Hissink, 2018. Natural “catastrophes”: “forecast” and management deontological obligation and common sense, *New Concepts in Global Tectonics, Journal*, 6 (3): 327-346
- Gregori, G. P., B. A. Leybourne, Dong Wenjie, and Gao Xiaoqing, 2025i. Palæo- and archæo-climate in the Chinese subcontinent. In press in *New Concepts in Global Tectonics, Journal*, 13, (8): 1170-1233
- Gregori, G. P., B. A. Leybourne, Dong Wenjie, and Gao Xiaoqing, 2025j. Topics in palæoclimatology - The role of the biosphere for air-earth currents. *New Concepts of Global Tectonics, Journal*, 13, (8): 1234-1331
- Gregori, G. P., B. A. Leybourne, Dong Wenjie, and Gao Xiaoqing, 2025m. Energy release from ALB, CMB and ICB and secular variation. III – A physical analysis - Estimate of self-energies and radii & the LN law and related secular variation *New Concepts in Global Tectonics, Journal*, 13, (3): 378-409
- Gregori, G. P., B. A. Leybourne, U. Coppa, and G. Luongo, 2025r. Geomagnetic anomalies: double-eyes in volcanic areas, and lineaments. *New Concepts in Global Tectonics, Journal*, 13, (6): 887-919
- Gregori, G.P., 1993. Geo-electromagnetism and geodynamics: “corona discharge” from volcanic and geothermal areas. *Physics of the Earth and Planetary Interiors*, 77: 39-63; DOI:10.1016/S0031-9201(02)00211-X
- Gregori, G.P., 2000c. Galaxy-Sun-Earth Relations. The Dynamo of the Earth, and the Origin of the Magnetic Field of Stars, Planets, Satellites, and Other Planetary Objects. In A. Wilson, (ed.), The first solar and space weather conference. The solar cycle and terrestrial climate, *ESA SP-463*, European Space Agency, ESTEC, Noordwijk, The Netherlands, pp: 329-332
- Gregori, G.P., 2002. Galaxy – Sun – Earth relations. The Origin of the Magnetic Field and of the Endogenous Energy of the Earth, with Implications for Volcanism, Geodynamics and Climate Control, and Related Items of Concern for Stars, Planets, Satellites, and Other Planetary Objects. A Discussion in a Prologue and Two Parts. *Beiträge zur Geschichte der Geophysik und Kosmischen Physik*, Band 3, Heft 3: pp. 1-471 [Available at <http://ncgtjournal.com/additional-resources.html>]
- Gregori, G.P., 2013. Crustal storms of continental/planetary scale-Earth's battery and Earth's electrocardiogram, internal state, structure, and time variation, endogenous energy production and release, the role of solar modulation, and the "French Revolution" jerk, *New Concepts in Global Tectonics, Journal*, 1, (2): 40-64
- Gregori, G.P., 2013a. Space-time constraints on earthquake predictability - A 10 cm/sec “domino effect” typical of every fracture phenomenon, *New Concepts in Global Tectonics, Journal*, 1 (2): 23-39
- Gregori, G.P., 2016. The endogenous energy and the magnetic field of planetary objects. The Pluto/Charon binary system and its seasonal rejuvenation. *New Concepts in Global Tectonics, Journal*, 4 (3): 456-472
- Gregori, G.P., and B.G. Gregori, 2025. The universe out of the box - New foundations of physics -

- Rhythms, Golden Ratio, Origin of Life, Antifragility, Europe Books
- Gregori, G.P., and G.M. Crisci, 1995. The isotopic chemistry of basalts vs. melting depth. Geomagnetic correlations and a proposal for an explanation, (abstract 01875498), 1995 IUGG General Assembly, Boulder, Co.
- Gregori, G.P., B.A. Leybourne, Dong Wenjie, and Gao Xiaoqing, 2025f. The Tang Maocang school. The uplift of Himalaya – shallow geotherms – palæoclimate – endogenous heat. *New Concepts in Global Tectonics, Journal*, 13, (8): 1026-1039
- Gregori, G.P., B.A. Leybourne, Dong Wenjie, and Gao Xiaoqing, 2025g. The timing of the uplift of Himalaya and the Third Pole. *New Concepts in Global Tectonics, Journal*, 13, (8): 1040-1079
- Gregori, G.P., B.A. Leybourne, Dong Wenjie, and Gao Xiaoqing, 2025h. Shallow geotherms. *New Concepts in Global Tectonics, Journal*, 13, (8): 1080-1169
- Gregori, G.P., B.A. Leybourne, U. Coppa, and G. Luongo, 2025t. Lightning and volcanic plumes. *New Concept of Global Tectonics*, 13, (6): 920-967
- Gregori, G.P., B.A. Leybourne, W. Soon, and V. Straser, 2025e. The heuristic meaning of variational principles. *New Concepts in Global Tectonics, Journal*, 13, (6): 920-967
- Gregori, G.P., C.W. Monckton of Brenchley, W. Soon, R. Tattersall, A. D'Amico†, G. Zimatore, V.M. Velasco Herrera, B.A. Leybourne, and Z.A. Oziewicz‡, 2022. The golden Ratio, variational principles, cyclic and wave phenomena, and quanta. In H. M. Colin Garcia, J-de-J. Cruz Guzman, L. H. Kauffman, and H. Makaruk, (eds), *Scientific Legacy of Professor Oziewicz, selected papers from the International Conference "Applied Category Theory Graph-Operated-Logic"* held in honor of Professor Zbigniew Oziewicz in Memoriam (August 25th to 27th, 2021), World Scientific, Series on Knots and Everything; DOI:10.1142/9789811271151.0018: 363-389; <http://ncgtjournal.com/additional-resources.html>
- Gregori, G.P., F.F. Bonavia, and B.A. Leybourne, 2025x. Geoelectrical geology in North America, *New Concepts in Global Tectonics, Journal*, 13, (2): 252-269
- Gregori, G.P., G. Ventrice, S. Pinori, G. Alessandrini, and F. Bianchi, 2013. Structural ageing of a cable-stayed bridge during load-test: The overall effect monitored by acoustic emission. In W. Sikorski, (Ed.), *Acoustic Emission—Research and Applications*; InTech: 2013; ISBN 978-953-51-1015-6, DOI:10.5772/54840; pp: 35–30
- Gregori, G.P., M. Poscolieri, G. Paparo, S. De Simone, C. Rafanelli, and G. Ventrice, 2010. "Storms of crustal stress" and AE earthquake precursors, *Natural Hazards and Earth System Sciences*, 10: 319–337
- Gregori, G.P., M.T. Hovland, B.A. Leybourne, S. Pellis, V. Straser, B.G. Gregori, G.M. Gregori, and A.R. Simonelli, 2025w. Air-earth currents and a universal "law": filamentary and spiral structures - Repetitiveness, fractality, golden ratio, fine-structure constant, antifragility and "statistics" - The origin of life, *New Concepts in Global Tectonics, Journal*, 3, (1): 106-225
- Gregori, G.P., V. Banzon, and R. Leonardi, 1994. The cycles of volcanoes, and the global synchronism of the time variation of their heat source. In W. Schröder, and M. Colacino (eds), *Geophysics: past achievements and future challenges. Newsletter of IDCH-IAGA*, (20), Science Edition / IDCH of IAGA, Bremen-Roennebeck, pp 152-191.
- Gregori, G.P., V.P. Banzon, R. Leonardi, and G. de Franceschi, 1992. Geomagnetic activity versus volcanic cycles and their forecasting. Application to Etna and Vesuvius. In W. Schröder, and J.-P. Legrand, (eds), *Solar Terrestrial Variability and Global Change*; IDCH of IAGA, Bremen-Roennebeck, pp: 188-222
- Gregori, G.P., Wen-Jie Dong, F.T. Gizzi, and Xiao-Qing Gao, 1999. The separation of the geomagnetic field originated in the core, in the asthenosphere, and in the crust. *Annali di Geofisica*, 42 (2): 191-209
- Guarniere, S., 2003. *L'emissione acustica come strumento diagnostico di strutture a varia scala*, unpublished PhD Thesis, University of Messina; pp: 1-144
- Hart, S.R., 1984. A large-scale isotope anomaly in the Southern Hemisphere mantle, *Nature*, 309: 753-757
- Helman, M., S. Knott, L. Vergara, G. Richardsen, and E. Kariström, 2001. Plate Reconstructions of the North Atlantic Region and the Geological History of the Norwegian Sea. In G. Lunde, (ed.), *Proceedings of the workshop on Global wrench tectonics. New theory of Earth evolution*, Oslo, Norway, 9-11 May, 2001, <http://www.earthevolution.org>, <https://adsabs.harvard.edu/full/2000ESASP.463..329G>
- Hofmann, A.W., 1997. Mantle geochemistry: the message from oceanic volcanism, *Nature*, 385: 219-229; DOI:10.1038/385219a0
- Jeffreys, Sir H., 1976. *The Earth, its origin, history and physical constitution*. VI edition, Cambridge Univ. Press, Cambridge etc., pp: 1-574
- Kellogg, L.H., 1992. Mixing in the mantle. *Annual Review Earth Planetary Science*, 20: 365-388; DOI:10.1146/annurev.earth.20.050192.002053
- Klein, E.M., and C.H. Langmuir, 1987. Global correlations of ocean ridge basalt chemistry with axial depth and crustal thickness. *Journal of*

- Geophysical Research., Solid Earth*, 92 (B8): 8089-8115; DOI:10.1029/JB092iB08p08089
- Klein, E.M., and C.H. Langmuir, 1989. Local versus global variations in ocean ridge basalt composition: a reply, *Journal of Geophysical Research., Solid Earth*, 94 (B4): 4241-4252 DOI:10.1029/JB094iB04p04241
- Larson, R.L., 1995. Le superpanache du Crétacé moyen, *Pour la science*, (210): 90-94. Italian translation "Un superpennacchio alla metà del Cretaceo" *Le Scienze*, (320): 80-84
- Le Roex, A.P., 1986. Geochemical correlation between southern African kimberlites and South Atlantic hotspots. *Nature*, 324, (6094): 243-245; DOI:10.1038/324243a0.
- Legendre, A.-M., 1785. Recherches sur l'attraction des sphéroïdes. *Mémoires. des savants étrangers*, 10: 411-434. Written in 1782
- Legendre, A.-M., 1789. *Mémoires. de l'Académie. des Sciences, Paris*: 372-454. Written in 1790, published in 1793
- Lemstrøm, S., 1899. Earth-currents and electrical currents in the atmosphere and their relations to the Earth's magnetism, *Öfvers. F. Vet. Soc.*, 41: 45 pp.
- Leybourne, B.A., D.W. Johnson, and G.P. Gregori, 2025. Arc-blast as static electricity or interplanetary lightning short circuits in Stellar Transformers. A plausible North American scenario, *New Concepts in Global Tectonics, Journal*, 13, (2): 229-251
- Leybourne, B.A., N.C. Smoot, G.P. Gregori, G. Paparo, and M.I. Bhat, 2008. Tectonic spiral structures of the Tethyan Vortex Street: GRACE geoid interpretations and African lightning teleconnections. *Proceedings of the International Geological Congress*, 2008 Oslo, Norway.
- Litvak, V.D., S.Poma, and S. Mahlburg Kay, 2007. Paleogene and Neogene magmatism in the Valle del Cura region: new perspective on the evolution of the Pampean flat slab, San Juan province, Argentina, *Journal of South American Earth Sciences*, 24: 117-137; DOI:10.1016/j.jsames.2007.04.002
- Lowes, F.J., 1974. Spatial power spectrum in the main geomagnetic field, and extrapolation to the core. *Geophysical Journal of the Royal Astronomical Society*, 36: 717-730. <https://doi.org/10.1111/j.1365-246x.1974.tb00622.x>
- Matsushita, S., and W.H. Campbell, 1967. *Physics of Geomagnetic Phenomena*. 2 vol., Academic Press, New York, etc., pp.: 1-1398
- Mitchell, R.H., 1986. Kimberlites: mineralogy, geochemistry and petrology. Plenum Press, New York; DOI:10.1007/978-1-4899-0568-0, pp.: 1-442
- Moreira Florisbal, L., V. de Assis Janasi, M. de Fátima Bitencourt, L.V. Stoll Nardi, and L.M. Heaman, 2012. Contrasted crustal sources as defined by whole-rock and Sr-Nd-Pb isotope geochemistry of neoproterozoic early post-collisional granitic magmatism within the Southern Brazilian Shear Belt, Camboriú, Brazil, *Journal of South American Earth Sciences*, 39: 24-43; DOI:10.1016/j.jsames.2012.06.013
- Nevanlinna, H., 1987. Notes on global mean-square values of the geomagnetic field and secular variation, *Journal of Geomagnetism and Geoelectricity*, 39 (3), 165-174 <https://doi.org/10.5636/jgg.39.165>
- Nippoldt, A., 1911. Über das Wesen des Erdstroms, *Meteorologische Zeitschrift*, 46: 244-261.
- Nyström, J.O., M.A. Parada, and M. Vergara, 1993. Sr-Nd isotope compositions of Cretaceous to Miocene volcanic rocks in Central Chile: a trend towards a MORB signature and reversal with time. *Proceedings of the 2nd International Symposium on Andean Geodynamics* (Oxford), extended abstract volume: pp: 411-414
- O'Ghaffari, H., M. Peč, T. Mittal, U. Mok, H. Chang and B. Evans, 2023. Microscopic defect dynamics during a brittle-to-ductile transition, *Proceedings of the National Academy of Sciences*; 120 (42). <https://doi.org/10.1073/pnas.2305667120>
- Obergugenberger, V.F., 1926.... der Anathomie und Philosophie - Bosl, DBE - III 673: 286-287 Obermayer, Josef (1851, 1 1926), Weinhändler – Strätz. [See *Deutscher Biographischer Index*]
- Parrot, M., 2025. DEMETER observations of the variations of the global electric circuit under various constraints, *New Concepts in Global Tectonics, Journal*, 13, (2): 355-366; ID 530865; DOI:10.1155/2013/530865
- Penn State, 2023. Shaking foundations: new research contradicts established theories on Earth's crust evolution, *SciTechDaily*, issued September 27, 2023
- Quinn, J. M., † G. P. Gregori, and B. A. Leybourne, 2026. Satellite monitoring of air-earth currents. *New Concepts in Global Tectonics, Journal*, 14, (1): 6-89
- Rampino, M.R., K. Caldeira, and Yuhong Zhu, 2021. A pulse of the Earth: a 27.5-Myr underlying cycle in coordinated, *Geoscience Frontiers*, 12 (6): 101245; DOI:1016/j.gsf.2021.101245
- Reimink, J.R., J.H.F.L. Davies, J.-F. Moyen, and D.G. Pearson, 2023. A whole-lithosphere view of continental growth, *Geochemical Perspective Letters*; DOI:10.7185/geochemlet.2324
- Schulze, D.J., 1987. Kimberlite geology: kimberlites, mineralogy, geochemistry and petrology. Roger H. Mitchell. Plenum, New York, pp:1-442, *Science*, 236 (4802): 729-729.

- Stacey, F.D., 1969. *Physics of the Earth*, 324 pp., John Wiley and Sons, Inc., New York, etc. II ed., 1977, pp.: 1-413, III ed., 1992, pp.: 1-513
- Stacey, R.D., 1992. Managing the unknowable: strategic boundaries between order and chaos in organizations, John Wiley & Sons, pp.: 1-240
- Stern, C.R., 2004. Active Andean volcanism: its geologic and tectonic setting, *Revista Geologica De Chile*, 31 (2): 161-206
- Straser, V., G. Cataldi, and D. Cataldi, 2026. Space weather related to potentially destructive seismic activity, *New Concepts in Global Tectonics, Journal*, 14, (2), 220-224
- Turcotte, D.L., and G. Schubert, 1982. *Geodynamics: Applications of Continuum Physics to Geological Problems*, John Wiley & Sons, New York; pp:1-450
- White, W.M., 2010a. Oceanic island basalts and mantle plumes: the geochemical perspective. *Annual Review of Earth and Planetary Sciences*, 38: 133–160; DOI:10.1146/annurev-earth-040809-152450
- Wilson, M., 1989. *Igneous Petrogenesis. A Global Tectonic Approach*. Unwin Hyman, London, etc.; DOI:10.1007/978-94-010-9388-0; pp: 1-466
- Wu, Hong-chun, 2025. Jet stream's disturbances as possible precursors of earthquakes, preprint
- Yañez, G., J. Cembrano, M. Pardo, C. Ranero, and D. Selles, 2002. The Challenger-Juan Fernández-Maipo major tectonic transition of the Nazca-Andean subduction system at 33-34 S: geodynamic evidence and implications, *Journal of South American Earth Sciences*, 15: 23-38
- Zaccagnino, D., F. Vespe, C. Doglioni, 2020. Tidal modulation of plate motions, *Earth-Science Reviews*, 205: 103179; DOI:10.1016/j.earscirev.2020.103179
- Zindler, A., and S.R. Hart, 1986, Chemical geodynamics, *Annual Review of Earth and Planetary Sciences*, 14: 493–571
- Zindler, A., E. Jagoutz, and S. Goldstein, 1982. Nd, Sr and Pb isotopic systematics in a three-component mantle: a new perspective, *Nature*, 298: 519-523
- CGDS - canonical geomagnetic deep sounding
CMB - core mantle boundary
D – energy hierarchy class of DUPAL type
DGRF - Definitive Geomagnetic Reference Field
DMM - end-member Depleted MORB Mantle
dSBT – DeSantis – Barraclough – Tozzi law
DUPAL - acronym for Dupré and Allègre, from its discoverers
E - Easter Island
EM - Enriched Mantle component (of two kinds)
ENSO - El Niño Southern Oscillation
EPR - East Pacific rise
ESI - electric soldering iron (mechanism)
FAC – field aligned currents
FOZO – Focal Zone
FR – field reversal (geomagnetic)
GA - Galàpagos
GNSS - *Global Navigation Satellite System*
GO – Gough Island;
GPS – *Global Positioning System*
H - energy hierarchy class of Hawai'i type
H - Island of Hawai'i;
HF -high frequency
HI – Hawai'ian Islands;
HIMU – synonymous of SHC; basalt (or mantle component) with comparatively high ratio $\mu = {}^{238}\text{U}/{}^{204}\text{Pb}$
IAGA – *International Association of Geomagnetism and Aeronomy*
IC – Iceland
IC -inner core
ICB - inner core boundary
Ifremer - *Institut Français de Recherche pour l'Exploitation de la Mer*
IGRF - International Geomagnetic Reference Field
IR - Indian Ocean ridges;
IsAr – island arcs
K – Kerguelen Island;
KG-II - kimberlites of Group II
LF - low frequency
LIGO - *Laser Interferometer Gravitational-Wave Observatory*
LIP – large igneous province
LLSVP - Large Low Shear wave Velocity Province
LN – Lowes-Nevanlinna (law or plot)
magpol – magnetic polarization (state of matter)
MAGSAT - *Magnetic field Satellite, Applications Explorer Mission-C or AEM-C or Explorer 61*, a NASA/USGS
MAR - Mid-Atlantic-Ridge
MHD – magneto-hydro dynamics
MIR - Mid Indian Ridge
MOR – Mid-Ocean Ridge

Acronyms

- A – energy hierarchy class of Atlantic type
AE - acoustic emission
ALB - asthenosphere lithosphere boundary
AR - Mid-Atlantic Ridge
AS - Ascension;
AZ - Azores;
B – Bouvet Island;
BDT - brittle-to-ductile transition
BSE - bulk silicate Earth
C - Canary Islands;

MORB - MOR basalt
N - energy hierarchy class of normal or intermediate cluster type
OC - outer core
OCO-2 - *Orbiting Carbon Observatory 2*, a *NASA/JPL* satellite
OIB - ocean island basalt
P/Tr – Permian/Triassic boundary extinction event also known as the End-Permian Extinction and colloquially as the Great Dying
PGZ - plume generation zone
PR - East Pacific Rise
PREMA - Prevalent Mantle component
PUM - primitive upper mantle
SAA - South Atlantic Anomaly
ScriW - supercritical water
SH - energy hierarchy class of St. Helena Island type
SH – spherical harmonic (function)
SH/A includes basalts that have features that seemingly fall in between SH and A
SHC - St. Helena cluster
SHE – spherical harmonic expansion
ss - spherical shell (of currents)
SV - secular variation of the geomagnetic field
T - Tristan da Cunha Island
TD - tide-driven (dynamo).
TS - Turcotte and Schubert
VIRGO - large Michelson interferometer designed to detect gravitational waves, named after the Virgo Cluster, a cluster of ~1,500 galaxies, ~50 *MLY* from Earth
WD – westward drift (of the geomagnetic SV)
WMT – warm mud tectonics

Introduction – Anomalous Lesser Air-Earth Phenomena

Giovanni Pietro Gregori^{1,2}, Bruce Allen Leybourne², Gabriele Paparo^{1,3†}

¹IDASC-Istituto di Acustica e Sensoristica O. M. Corbino (CNR), Roma, now merged into IMM-Istituto per la Microelettronica e Microsistemi (CNR) and ISSO-International Seismic Safety Organization, Italy

²GeoPlasma Research Institute-(GeoPlasmaResearchInstitute.org), Aurora, CO 80014, USA

³Associato INGV, Roma †

Corresponding Author: G. P. Gregori, IDASC-Istituto di Acustica e Sensoristica O. M. Corbino (CNR), Roma, now merged into IMM-Istituto per la Microelettronica e Microsistemi (CNR);
Email: giovannipgregori38@gmail.com
leybourneb@iascc.org

† means deceased

Abstract: Several lesser and often unnoticed phenomena are a clear indication of air-earth currents. We attempt to give a reminder of some best-known occurrences, and of several less known and eventually rare phenomena, although it is almost impossible to give an exhaustive list.

Keywords: Elmo fire - Andes lights - hot weather flashes - deep ocean fauna beaching - lightning - energy of volcanoes - lava lakes - sulphur lakes - water caldera lakes - ³He/ ⁴He – Mars - microbiology – geysers CH₄ bubbling - “limnic” volcanism - Cameroon Volcanic Line - Lake Nyos - Lake Monoun - basalt chemism - gravity anomaly in Africa - lakes chemistry - kinematics of west-central Africa - explosive eruptions monitored by satellite - the Caronia phenomenon - wildfires in West Central Africa

Introduction

Some phenomena are associated to air-earth currents and are not illustrated here in detail. For instance, some mysterious phenomena are sometimes reported, which are associated to invisible and undetected, transient air-earth currents – which are not manifested by spectacular lighting, although they display observable features inside some “device” that acts like an unusual detector of comparatively rare occurrences. Well known phenomena are fumaroles, or mud volcanoes etc. (see Gregori and Hovland, 2025), or wildfires (see Gregori and Leybourne, 2025i). We refer, rather, to other exceptional, eventually intense occurrences.

St. Elmo fires (Fig. 1) were formerly observed on the mast of vessels. The surface of the mast is covered by a thin sheet of salted water, i.e., by a conductor, and the mast point is the tallest point on the conducting flat sea-surface.



Fig. 1. St. Elmo fire on the top of a clock tower. After Marcuse (1903), who borrowed it from *L'atmosphère* by Camille Flammarion (lived 1842-1925), a French astronomer and renowned popular science writer, very active after 1862. Copyright extinguished.

Wildfires are well known and are discussed in Gregori and Leybourne (2025i). Less known are all phenomena generally named *TLEs* (transient luminous events; see Gregori and Leybourne, 2026g) that, however, in general represent phenomena that occur above clouds, while clouds are an active segment (through Cowling dynamo, see Gregori et al., 2025d) of the soil-ionosphere electrical circuit. A huge literature is now available on *TLEs* and cannot be reviewed here.

Less known is the phenomenon of “Andes lights” that the countrymen of the Po Valley call “hot weather flashes”. This is “corona discharge” effect with a large cross-section, which is sometimes observed, and which involves the spatial range of a mountain massif. During very hot days, it happens that a large heat release occurs from ground that was warmed by sunlight. This release causes a huge convection cell through the atmosphere. A large upwelling plume is thus eventually raising from all over a mountain massif. This causes an increase of the atmospheric electrical conductivity σ . A repeated occurrence of flashes is thus sometimes observed, although these flashes can be seen only from a suitable distance, which is needed in order to monitor the effect integrated over a large volume. Differently stated, this is like a St. Elmo fire, although spread out over the area of a mountain massif (e.g., the Monte Bianco and/or the Monte Rosa massif in western Alps) that is observed by countrymen in the Po Valley at 200 – 250 km from the massif. People staying just underneath the convection cell cannot detect these luminous events, due to lack of luminosity contrast. That is, these phenomena are air-earth currents associated to convective motions above large spatial gradients of crust warmed by solar radiation.

On other occasions this phenomenon can be likened to a prolongation through air of the electrically conducting “spikes” underground, i.e., the “sea-urchin spikes” (see Gregori et al., 2025a, and Gregori and Leybourne, 2021).

Hence, this is a faint phenomenon that can be observed by naked eye only under suitable conditions.

Other phenomena are sometimes reported according to non-professional witness. Therefore, there is need for a suitable care before accepting their report. No systematic collection exists of information – that, however, could be valuable to understand the long-range trend of the changes of release of endogenous heat on the planetary scale that control climate change (see Gregori et al., 2025a, and Gregori and Leybourne, 2021).

It must be stressed that the general feeling is incorrect that claims that unusual phenomena are “a matter of coincidence”. In fact, phenomena never repeat themselves, and a correlation observed at one time does not imply that the same association must occur every other time. Thus, e.g., an earthquake precursor is eventually real, although only some earthquakes have a similar precursor, while others have different precursors. This rule holds for the association of every other singular or exception phenomenon.

For instance, let us remind about a recent occurrence. Between 15 and 16 September 2022 a flash flood struck the Italian Region Marche, mainly involving the provinces of Ancona, Pesaro, and Urbino, causing in a few hours 12 victims, a missing woman, 50 injured, 150 displaced people and damages for 2 billion Euros. The greatest damage involved, however, is located within an unusually very restricted area. Meteorologists claimed that they are incapable to forecast such a kind of events, because - as they stressed - in this case only ~40 km apart it did not even rain. In fact, a map (Fig. 2)¹ of the seismic events – only of lesser intensity, hence not perceived by the inhabitants - shows that this specific restricted area suffered by a temporary abnormal crustal fracturing. This permitted an intensified soil exhalation that altered the thermal regime in the atmosphere. Hence, precipitations were enhanced through the Cowling dynamo (see Gregori et al., 2025d).

On the other hand, this occurrence does not imply that every flash flood must be triggered by a local anomalous soil exhalation. In any case, a much better understanding must rely only whenever an array is eventually operative of recorders of shallow geotherms (see Gregori et al., 2025h) that are suited to monitor locally the time variation of soil exhalation.

Deep ocean fauna beaching

Remind about deep ocean fauna beaching - such as giant squids or octopuses - that escape from waters polluted by an excess soil exhalation of CH_4 . The phenomenon derives from the heating of CH_4 clathrates, due to increase of heat released from ocean floors. Every kind of fauna that is subjected to live with some high environmental pressure - i.e., up to ~ several 100 atm, or ~ several 10 megaPa - has no reason to escape to shallow waters. When this fauna reaches shallower layer, it dies by embolism.



Fig. 2 – Map of lesser earthquake occurred in Italy between 14 September 2022 until 18:28:14 UTC of 17 September 2022. After the online seismic catalogue of INGV.

The phenomenon is similar to several of the most violent extinction events that often involved mainly the ocean life, while the beings living on land were eventually almost unaffected. The concern is not about the occasional report of these rarely observed events, rather about the apparent clustering in time and space of these reports referring to different parts of the world that denotes a planetary increase of release of endogenous energy.

Only recently this topic has been the object of some scientific literature. For instance, a few mentions are given in Anonymous (2015ax). Choi (2016h) illustrates as follows the paper by Paxton (2016), relying also on an interview with that author, and he shows Figs 3 and 4.



Fig. 3. “On October 1, 2013, a 9 m long giant squid washed ashore in the Spanish community of Cantabria. Credit: Enrique Talledo, www.enriquetalledo.com.” Figure and captions after Choi (2016h). NASA copyright free policy.

¹ We are indebted to Claudio Rafanelli for calling our attention on this peculiar observational detail.



Fig. 4. “In 1954, two men in Norway inspected a 9.2 m long giant squid. Credit: NTNU Museum of Natural History and Archeology, via Wikimedia Commons.” Figure and captions after Choi (2016h). NASA copyright free policy.

“... Specimens recognizable as giant squid (*Architeuthis dux*) have been found washed up onshore since at least 1639. However, these sea monsters ... are so elusive that they were largely thought to be mythical until they were first photographed alive in their natural environment in 2004. Ever since giant squid were discovered, there has been considerable speculation as to how large they can get. In a previous analysis of more than 130 specimens, scientists said that none exceeded 13 m in length. Suggesting that giant squid could grow larger was ‘a disservice to science’, they said. Still, prior studies estimated that hundreds of thousands of giant squid may live in the ocean, which would suggest that there are plenty of chances for giant squid to grow larger than previously suggested ...

Now, a statistical analysis from Paxton suggests that giant squid may plausibly reach 20 m in total length. This new study extrapolated the maximum sizes this species might reach by both examining a variety of categories of data and examining as much data taken directly from specimens of the creature as was available. ... The data Paxton analyzed included 164 measures of mantle (body) length; 39 measures of standard length, which included the lengths of their bodies as well as the lengths of the longest of their arms; and 47 measures of total length, which included the lengths of their bodies as well as the lengths of the tentacles ... Paxton also examined 46 instances where beak, or mouth, size was measured along with mantle length. He found that beak size could help predict mantle length, confirming previous studies.

All in all, Paxton found that it was statistically plausible that giant squid could have mantle lengths of about 3 m

and total lengths of 20 m ... Paxton noted that there are claims that giant squid can grow to be 30 m long ... To help resolve that question, there are people in New Zealand and Spain who fairly regularly collect specimens of giant squid ...

Another study, McClain et al. (2015), suggested that it’s human nature to exaggerate the sizes of the ocean’s giants. The study found that people overestimate measurements for whales, sharks and squid ... “

Paxton’s (2016) claims that *Architeuthis dux* is among the largest known invertebrates, even though we lack a consensus on their maximum size. He reports a statistical investigation on *Architeuthis dux*, and claims that “squid of at least 2.69 m (99.9% prediction interval: 1.60 – 3.83 m) mantle length (ML) may be handled by large bull sperm whales but perhaps not females.” The distinction of size depends on the definition. In addition to ML, the length can be considered between the tip of mantle to end of arms. However, also the total length can be considered from tip of mantle to end of tentacles. The longest reliably measured ML of 2.79 m, while the standard generally reported length 10 m can be plausibly extended even to 20 m total length. Hickok (2018) shows Fig. 5 referring to a finding, on August 25, 2018, on a New Zealand beach of a ~ 4.2 m size squid.



Fig. 5. “These divers were easily dwarfed by the giant squid they found. Credit: Daniel Aplin.” Figure and captions after Hickok (2018). NASA copyright free policy.

“... A representative from the New Zealand Department of Conservation told ... that the divers most likely found a giant squid (*Architeuthis dux*) and not a colossal squid (*Mesonychoteuthis hamiltoni*) ... Both species of squid are formidable sea creatures, with giant squid typically reaching 5 m long, according to the Smithsonian, and the colossal squid reaching over 10 m long, according to the International Union for Conservation of Nature. Scientists know very little about these deep-sea-dwelling species, because the animals are so rarely seen. Most observations come from the occasional specimen washing ashore, as in this case, or getting accidentally captured by fishers. The enormous tentacled creature’s cause of death is unknown ... the squid appeared unscathed except for a scratch that was so tiny that the diver ‘wouldn’t think that’s what killed it’. When the divers checked the squid out again after their dive, they thought it had shrunk a little, but no animals had decided to make a meal out of the dead beast ... “

A statistical estimate has been attempted of these giant squids' distribution. Coro et al. (2015) claim that reports of *Architeuthis* are available even before the 16th century, while only recently it was observed for the first time live in its habitat. *Architeuthis dux* has been the object of particular attention from biologists. On the other hand, the distribution of these animals is still poorly understood. Most information derives from stranded animals or stomach remains. Coro et al. (2015) "estimate the potential distribution of *A. dux* at global scale, with relative high resolution (1 degree)." They claim to "combine information using feed-forward neural networks", and that their "model is the most similar to an expert drawn map respect to other models ... "

According to the viewpoint of the present study, timing, and location of beaching ought to be recorded, as they should be a significant indication of a severe increase of geogas exhalation from the ocean floor that ought to be correlated - on the long-time range and on some wide regional scale - with geodynamic, seismic and volcanic activity, and also with the possible extinction of some unknown deep ocean species.

In addition, some impressive events are often reported that imply the beaching of hundreds of cetaceans, seemingly with no reason (see e.g., Hickok, 2018e). No explanation is given, although a likely guess is that a reason could be perhaps originated by some kind of environmental pollution due to ocean floor exhalation. In fact, an intense exhalation from the ocean floor can determine a rapidly deadly environment. However, a smaller exhalation can change the ecosystem, hence the nutritional environment. Cetaceans suffer from starvation and seek food, approaching the coast and eventually washing up dead on the beach. Maybe, this occurred in California (Hickok, 2019).

"For a few months twice a year, the waters off California are home to graceful gray whales migrating north or south between the coast of Mexico and the Bering Sea. This year, however, it seems that fewer whales are surviving the journey north. Two dead gray whales washed up on the shores of Northern California beaches on Tuesday (April 16, 2019), which means 8 have been found around California's Bay Area since the beginning of the year; 7 in just the past two months. So far this year, a total of 30 dead gray whales have washed up on the West Coast: 8 in Washington, one in Oregon and 21 in California.

Those numbers are unusually high ... Gray whales (Eschrichtius robustus) make one of the largest migrations of any species ... the whales cruise by California, Oregon and Washington between March and early June on their trip north from the coast of Baja California, Mexico, to the cool, food-rich waters of the Bering and Chukchi seas, north of Alaska. They'll make their return trip south, back to Mexico, in December and January. ... This year, there have been far more reports of gray whales swimming closer to shore and spending more time in bays, marinas and harbors ... they're so skinny and emaciated ...In Northern

California, 3 out of 4 of the dead whales that have been examined so far appear to have died of starvation and the fourth was killed by a ship strike ... "

Maybe, it is not coincidence that this anomalous observation occurs while endogenous energy release seems anomalous during the period that immediately follows the MiniMax period (see Gregori and Leybourne, 2025c; Gregori et al., 2025c). During this period relevant climate anomalies are observed, along with geodynamics and seismicity anomalies, and, maybe, also volcanic anomalies. These phenomena deserve great attention as they can be important indicators of the changing "climate". At present, this is - however - only speculative.

It is unfortunate, however, that this important observational information about fauna beaching is presently neglected by the generally accepted "official science". This kind of exceptional events, or extreme conditions, are normally considered a matter of sensational curiosity, a "mystery" almost like *UFOs*,² etc. Conversely, these sporadic occurrences - analogously to earthquakes, floods, volcanic eruptions, landslides, iceberg detachment, etc. - deserve suitable systematic records to be used for scientific investigation, as every extreme event has a specific reason that determines its occurrence.

Suitable account ought to be given for the presently available detection efficiency, and for the space- and time-coverage of the detecting network and facilities (e.g., even some huge volcanic eruptions, perhaps, may be almost unnoticed, when they occur in some area with no population).

Lightning strokes

Even a catalogue of trees (or buildings or other) that suffered by a lightning strike ought to be kept within data centers, similarly to the information stored about earthquakes, volcanic eruptions, floods, etc. Even the ancient Romans kept records of the sites that appeared prone to being stricken by lightning discharges, although their concern was ritual in honor of Jupiter (see Fig. 6).



Fig. 6. "Fulgur Dium", fulgural box found in Rome at Castro Pretorio. Drawing by M. Melis reproduced by Pietrangeli (1951). These boxes were built at sites that were struck by some remarkable (or, maybe, repeated?) atmospheric electric discharges, as these sites were considered sacred to Jupiter, the God who launched lightning flashes. After Pavese (1992). Reproduced with kind permission of the *Pontificia Accademia Romana di Archeologia*.

Also in this respect, as already mentioned above, suitable consideration ought to be given for the three concurrent factors: the presence of a sea-urchin spike, a

² A pioneer, or beginner, concerning unidentified celestial objects (very often *TLEs*) has been, maybe, Charles Hoy

Fort (1874-1932), who wrote ten novels, only one of which was actually published (Feminò, 2008).

sufficient electrostatic charge of the ionosphere, and suitable electrical conductivity in the atmospheric condenser (Gregori et al., 2025a, and Gregori and Leybourne, 2021). The spike is a local feature, unlike the electrostatic charge of the ionosphere that simultaneously characterizes some large area.

Trees that are stricken by lightning discharges are considered a comparatively common phenomenon, which is not worthy of being recorded. The concern is, however, about why these phenomena occur at some given time, and only very seldom, although their frequency seemingly increases synchronously over some comparatively wide area. A more reliable, uniform, and objective information could be available by means of dense arrays of recorders of atmospheric potential-gradient - of the correct kind as discussed in Gregori and Leybourne (2026d). As long as no arrays are available of this kind, the information is important that is provided by the density of trees stricken by lightning discharges.

Nothing occurs by chance, and we must collect a statistical database and investigate it accordingly, much like what is presently done for earthquakes, floods, landslides, snowslides, volcanic eruptions, hurricanes or tornadoes, wind surges, etc. and several kinds of so-called extreme events. The statistical distribution of lightning is discussed in Gregori and Leybourne (2025j).

The energy of volcanoes

For future reference, we must distinguish different forms of energy associated with volcanism. Six kinds of energies are to be distinguished, being respectively associated with:

- (i) velocity and mass of ejected fragmental material (kinetic energy);
- (ii) changes of height of the magma column (potential energy);
- (iii) heat of the lava, pyroclastics, and gases (thermal energy);
- (iv) earthquakes and tremors;
- (v) tsunami and tornadoes related to the eruption;
- (vi) opening of the eruptive channels and deformation of the crust.

According to Yokoyama (1957), “we may take into account - for order of magnitude estimates - only thermal energy because energies of other kinds do not contribute much to the total sum of the energies”. Rezanov³ (1980) quotes a total energy of $\sim 1.8 \times 10^{15} \text{ J}$ that - according to E.K. Markhinin - ought to be needed to powder $\sim 1 \text{ km}^3$ of rock into particles with a diameter of $\sim 10^{-6} \text{ m}$. The thermal energy E_{th} can be computed in Joules as follows

(according to Bullard,⁴ 1984, who reports a formula by Yokoyama, 1957, adopted also by Hédervári,⁵ 1963 and others)

$$E_{th} = V \rho (\alpha T + \beta) \quad (1)$$

where V is the volume of the ejecta, ρ is the density, T is the temperature, $\alpha = 0.25 \text{ cal [g } ^\circ\text{C]}^{-1} = 1.05 \times 10^3 \text{ J [Kg } ^\circ\text{C]}^{-1}$ is the specific heat of lava, and $B = 50 \text{ cal g}^{-1} = 2.09 \times 10^5 \text{ J kg}^{-1}$ is the latent heat of lava. Williams and McBirney⁶ (1979) state that the heat energy amounts to $\sim 1.4 \pm 0.3 \times 10^6 \text{ J kg}^{-1}$ of erupted mass. They also claim that, for all practical purposes, $\sim 1.6 \pm 0.4 \times 10^6 \text{ J kg}^{-1}$ is “a reasonable estimate of the energy involved in erupting a given mass of volcanic rock”. Rezanov (1980) states that the total thermal energy is $\sim 3.5 \times 10^{18} \text{ J km}^{-3}$ of lava, which corresponds to $\sim 3.5 \times 10^6 \rho^{-1} \text{ J kg}^{-1}$, where ρ is the density (in g cm^{-3}) of the lava. Thus, the Rezanov’ (1980) and the Williams and McBirney’s (1979) values are identical if $\rho \cong 2.5 \text{ g cm}^{-3}$.

The energy of subsurface explosions can be calculated by means of the empirical relation

$$M = 3.65 + \log Y \quad (2)$$

where M is the magnitude of the seismic shock and Y is the energy in [kton of TNT], or [cal $\times 10^9$], or [4.187 $\times 10^{12} \text{ J}$], to be compared with the seismic energy of an earthquake

$$\log E = 9.9 + 1.92 M - 0.024 M^2 \quad (3)$$

where M is the Gutenberg-Richter magnitude, and E is expressed in *ergs*. Thus, the seismic energy is only $\sim 2 \times 10^{-4}$ times the total energy of an explosion, although it varies greatly with depth, because shallow levels are less efficient for shock transmission (Williams and McBirney, 1979).

Gorshkov (1959 and 1960) compared the atmospheric pressure wave generated by volcanic explosive eruptions with the analogous wave generated by a nuclear weapon test of known power.⁷ He used the following formula for the Bezymianny explosion (see below) (energy in *Joules*)

$$E = 1.25 \times 10^{20} \cdot \sin \phi \cdot \sum \frac{A^2 t}{2} \quad (4)$$

where ϕ is the distance of the barograph (in degrees from the source), and A and t are the amplitude and duration of each half wave of the barogram. He also considered (according to Bullard, 1984) “that in a hydrogen bomb blast not more than $\sim 0.3\%$ of the entire energy goes into the air wave”, and “he concluded (without giving any evidence) that in a volcanic eruption the amount would be about $\sim 10\%$ ”.

In fact, a general misunderstanding deals with the problem of gas-driven vs. thermal-driven volcanism. “ ...

³ Igor Aleksandrovich Rezanov (1927-2006).

⁴ Fred Mason Bullard (1901-1994), American Professor of volcanology.

⁵ Péter Hédervári (1931-1984), geophysicist, scientific populariser, amateur astronomer.

⁶ Howel Williams (1898-1980), American geologist and volcanologist; Alexander R. “Mac” McBirney (1924–2019), a pioneer in the application of fluid dynamics in volcanology and igneous petrology.

⁷ Previous measurements of sound shocks caused by violent eruptions had been investigated by Sassa (1936, p. 40-41) by means of seismographic records on smoke-paper, collected at a station located $\sim 7.5 \text{ km}$ from the crater. He found a linear relation between the amplitude of the seismographic records and the maximum distance (up to $\sim 700 \text{ m}$) of rock fragments ejected from the volcano.

The writer is not able to say positively that volcanism is a derivative of earthquakes and prefers to say that both are equally the derivatives of the same rank from the thermal energy contained in the bottom of the crust or the mantle.” (Yokoyama, 1957, p. 106).

Bullard (1984, p. 508-509), however, referring to an explosive eruption in Kamchatka, states: “... the energy of the March 30 explosion was $\sim 4 \times 10^{23}$ ergs. The thermal energy released in the Bezymianny eruption, calculated in the conventional manner, is about $\sim 2.2 \times 10^{25}$ ergs. Thus, the explosion energy is only about $\sim 2\%$ of the total thermal energy of the eruption, a calculation which led Gorshkov to conclude: ‘... the main active agent of the eruption is the heat energy of the magma, and gas only serves to transform this energy into an explosive one’ (1959, p. 108). This is contrary to the prevailing view, as stated in a quotation from Perret that ‘Gas is the active agent and the magma is its vehicle’ (1924, p. 59).”

This Perret’s viewpoint is also confirmed (Bullard, *ibid.*, p. 35) by the following statement by Thomas A. Jaggar:⁸ “*volcanism everywhere has unity; gas is the prime mover.*” This belief reminds about the myth of an Earth likened to a Buffon’s cooling cannon ball (Gregori et al., 2025a), which - on the *Ga* time scale - releases gas from its deep interior. In contrast with the aforementioned contradictory result by Gorshkov, this same Perret’s and Jaggar’s concept is still emphasized by some volcanologists, such as, e.g., by Krafft⁹ (1991) and by the editorial comments included within its Italian translation appeared in 1993.

The Gorshkov conclusion was further confirmed by himself by means of the analysis of the explosion of Mount Shiveluch occurred on 12 November 1964 (see Table 1 below, where his revised percent values are lowered to $< 1\%$).

Bullard (1984) also contains several details about several historical eruptions including the important aforementioned case history of Bezymianny, for which Rezanov (1980) gives the following description.

“On Kamchatka, at the center of the Klyuch group of giant volcanoes, there is a relatively small cone (3085 m) that was not given a name because of its lack of interest, and which figures in the catalogue of volcanoes as ‘Nameless’ [Bezmyanny]. It was thought to be an extinct volcano.

Underground shocks registered at the Klyuchi volcanological station, ~ 45 km away, signalled its awakening. The eruption began at dawn on 22 October, 1955. Clouds of white smoke which appeared on the eastern slope of the Klyuchi volcano were spotted from Klyuchi. Then ash began to fall. In a few days the dark plume of material reached a height of ~ 8000 m. Great flashes of lightning were seen within the monstrous cloud at night. Explosions, one more powerful than the other, did not cease throughout November. On some days the pall of ash hanging above the volcano was so thick that it blotted out

the Sun. Lamps were burning in the houses in Klyuchi, and vehicles drove with their lights on. In a month the volcano’s crater widened from ~ 250 to ~ 800 m.

At the end of November activity subsided, eruptions were less and less frequent and weaker, but a dome of viscous lava began to grow inside the crater. The pressure reached such a force that a long-hardened ancient dome adjoining the volcano gradually rose by nearly ~ 100 m and shifted south-east.

Finally, on 30 March, 1956, a gigantic explosion occurred. A fiery column slanting east at an angle of $\sim 30^\circ$ was thrown up above the volcano. A column of black smoke also rose obliquely that hid the peaks of the mountains within a few minutes. The cloud of ash surged upward and sideways, like an immense fan, reaching a height around $\sim 40,000$ m ... In Ust-Kamchatsk, 120 km from the volcano, this cloud covered the whole horizon. It appeared to be impenetrably black; only its light edges were bright golden in the rays of the setting Sun. Four hours after the explosion a jet of gas was noted, flung up above the black blanket to a height of $\sim 45,000$ m.

Soon the ash cloud covered the Klyuchi station. Ash began to fall out, at first big, separate grains up to ~ 3 mm in diameter. It seemed as if big hailstorms were striking the window panes. Gradually the fallout increased and soon such an impenetrable darkness set in that it was impossible to see anything immediately in front of one’s eyes. The area covered by ash was ~ 400 km long and ~ 100 to ~ 150 km wide. The total volume of ash was at least $\sim 5 \times 10^8$ m³.

A full idea of the catastrophe that had occurred was only got after the area round the volcano could be visited. Nameless had altered out of all recognition. From a regular, slightly truncated cone it had been converted into a semicircular caldera. The old dome, raised in the first stage of the eruption, had now vanished. On the site of the peak and the south-eastern slope of the mountain there gaped a huge crater in the shape of a crescent ~ 1500 by ~ 2000 m. The peak of the volcano had been blown away by the explosion, and its height reduced by almost ~ 200 m.

Over a stretch of > 10 km everything was buried beneath a half-meter layer of volcanic sand. The blast of this sand had stripped the bark from trees within a radius of ~ 30 km. All the thin trees had been broken. A house, the volcanologists’ base (fortunately uninhabited), located ~ 12 km from the site of the eruption, was literally wiped off the face of the Earth; not a single plank of it remained.

Under the immense thickness of red-hot sand falling from the sky the snow began to melt rapidly, causing powerful mud flows that ripped off slabs of rock weighing hundreds of tons, and surged along the valleys, smashing everything in their path.

⁸ Thomas Augustus Jaggar, Jr. (1871-1953), American volcanologist, founder of the Hawai’ian *Volcano Observatory*, and its director during 1912-1940.

⁹ Catherine Joséphine "Katia" Krafft (- 1991) and her husband, Maurice Paul Krafft (1946-1991), Alsatian French volcanologists died in a pyroclastic flow on Mount Unzen, in Japan, on June 3, 1991.

Table 1. Detailed energies, and other data, for two explosive eruptions

Parameters of the eruption	Bezymianny		Mount Shiveluch	
energy of the explosion wave (Joules and percent)	$3. \times 10^{15}$	0.08%	1.8×10^{14}	0.01%
kinetic energy (Joules and percent)	1.2×10^{17}	3.06%	$1. \times 10^{17}$	5.26%
thermal energy (Joules and percent)	3.8×10^{18}	96.86%	1.8×10^{18}	94.73%
explosive, plus kinetic, plus thermal energy (Joules and percent)	3.9×10^{18}	100. %	1.9×10^{18}	100.0%
initial velocity of the explosion ($m \text{ sec}^{-1}$)	360 – 500		280 – 310	
initial pressure (atm)	1500 – 3000		800 – 1000	
amount of ejected material (km^3)	2 – 2.5		1.5	

After the paroxysm of March 30 the final phase of the eruption began. Two domes began to rise in the huge new crater. When G.S. Gorshkov, chief of the Klyuchi volcanological station, climbed Nameless, the first of them had reached a height of $\sim 320 \text{ m}$. The eruption ended in November. It had taken place in a completely uninhabited locality, so the biggest volcanic catastrophe of our century did not claim a single human life.”

The Gorshkov analysis referring to the explosions of Bezymianny, 1956, and Mount Shiveluch, 1964, are listed in Table 1 (according to Gorshkov, modified from Rezanov, 1980).¹⁰ The total volume of ejecta is comparable to the St. Helens 1980 eruption ($\sim 2.8 \text{ km}^3$) and to the Pompei eruption of Vesuvius ($\sim 3 \text{ km}^3$), for which “Plinian eruptions” are called the events with an amount of ejecta of the order of $\sim 1 \text{ km}^3$. Summarizing, the errors are large, sometimes even by more than one order of magnitude (Williams and McBirney, 1979), so that Fudali and Melson (1970) believe to be unrealistic even to attempt to estimate relations between the energy of the eruption and the calculated gas pressure. As well, it is nonsensical to correlate the total energy of an eruption with either its explosive energy, or the size of its crater or caldera, because large volumes of outpouring magma associated with large thermal energies can, or cannot, be associated with large explosive energies. Indeed, there is a great variability of morphology of volcanic eruptions, ultimately depending on the different local setting of the crust and lithosphere, and on the local amount of energy supply.

Fig. 7 synthesizes the different energies released before and during the St. Helens eruption occurred on 18 May 1980.¹¹

Lava lakes, sulphur lakes, water caldera lakes

Let us consider in some detail some comparatively seldom observed phenomena that are generally considered

like curiosities or whims of nature. These “curiosities” look like a logical confirmation of the entire rationale for air-earth currents that is here proposed. Their explanation is consistent with the rationale envisaged in Gregori et al. (2025a) and in Gregori and Leybourne (2021). Every case history is a different phenomenon, sometimes looking like an amusing whim of nature, much like several other phenomena appear to us, such as, e.g., a rainbow, or a charming sunset, or several other atmospheric optical phenomena including the very wide variety of polar aurora displays, or a ball lightning (BL; see Gregori and Leybourne, 2026e), etc.

We refer to volcanic phenomena, i.e., lava lakes, sulphur lakes, and “limnic” volcanism, while mud and asphalt volcanoes are extensively discussed in Gregori and Hovland (2025).

Lava lakes

Lava lakes are not a permanent feature of any one given volcano. They are occasional although very spectacular features. In some respect, they can be likened to natural strainmeters¹² dealing with some comparatively shallow layer. However, they cannot be considered a reliable high-time-resolution gauge suited to monitoring the time changes of the endogenous energy supply. In reality, both effects simultaneously play a role, i.e., (i) a change of the geometry of the “bottle” that contains the fluid magma, and/or (ii) a time variation of the endogenous heat supply.

The power radiated by lava lakes can be estimated either by satellite remote sensing (e.g., Landsat Thematic Mapper, LTM, by means of its bands 5 and 7, at $1.55 - 1.75$ and $2.08 - 2.35 \mu\text{m}$, respectively; a pixel has 30 m size; Glaze et al., 1989) or by ground-based measurements of their radiant energy. Concerning satellite measurements, an actual test for a ground signature was possible by measurements carried out on Erta’Ale, a lava lake first discovered in 1967 in the Danakil depression.

¹⁰Concerning permissions, since 2008-2009 either direct or indirect contact seems impossible with MIR Publishing house.

¹¹ Concerning permission to reproduce this figure, copyright is not of Scientific American, rather it is the authors. Le Scienze did not reply. Robert Wayne Decker passed away in 2005, and we got no address for Barbara Decker. We presume the figure can be reproduced.

¹²A strainmeter is composed of a drill hole, e.g., several hundred to a few thousand meters deep, with a tube filled with oil. The oil level monitors, with a high sensitivity, the strain of the crust, and it allows detection of even the minor harmonics of the tidal deformation of the Earth. See, e.g., Rikitake (1976).

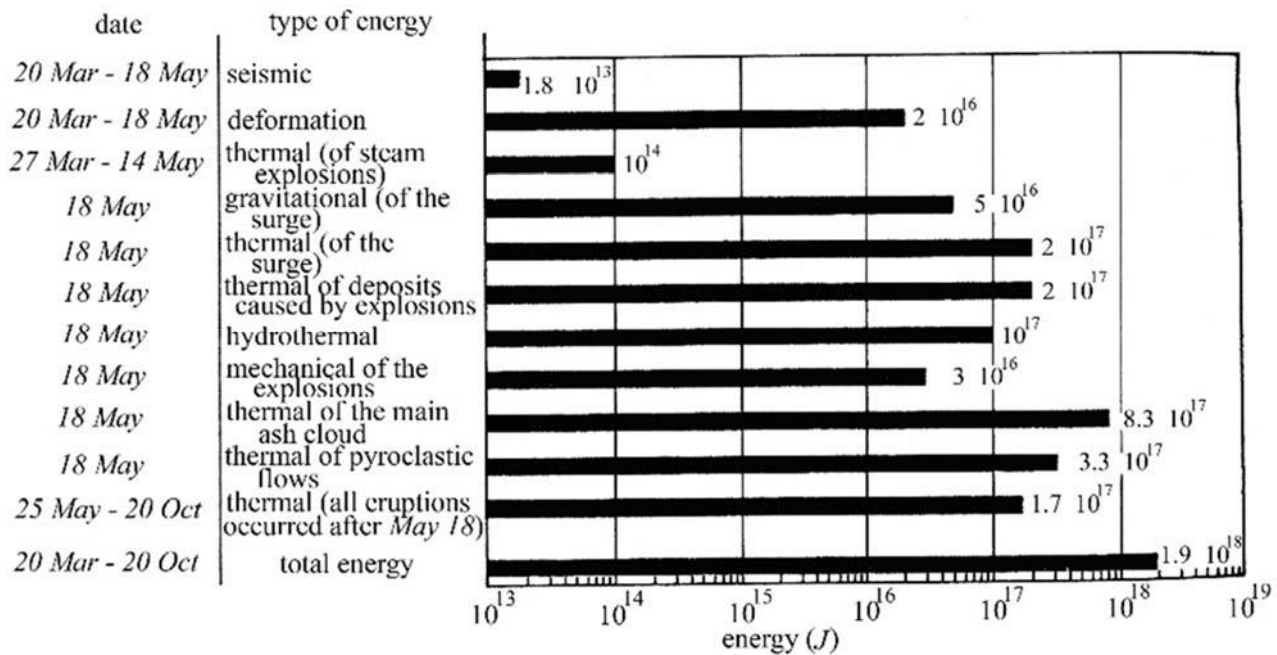


Fig. 7. Representation of six types of energy released during eruptive events of Mount St. Helens (dates are indicated on the left). The seismic, deformation, and thermal energies of explosions of steam were released during the period preceding the eruption of 18 May. Energies are in logarithmic scale, and the bottom line shows the total energies released between the start of the eruption until its end in October 1980. After Decker and Decker (1981).

There is some concern about recognizing (by satellite) the radiant energy of a true lava lake, compared to the effect of simple fumarolic activity. The phenomenon, however, is not constant in time and, at most, one should actually compare among each other only “simultaneous” records, where “simultaneous” means “*apart some suitable (although a priori unknown) time lag*”. IR images, however, clearly recognize lava flows (e.g., Fig. 8).



Fig. 8. “The Landsat 8 satellite captured IR hotspots representing two distinct lava flows on the volcano. Credit: Joshua Stevens/ NASA Earth Observatory.” Figure and captions after Deamer (2017). NASA copyright free policy.

In general, a lava lake has a tiny surface, compared to the area of the whole volcanic edifice. This is shown, e.g.,

by another image of Mount Erebus, in Antarctica (a NASA Earth Observatory image; Doermann, 2023). That is, only one sea-urchin spike at a time affords to reach Earth’s surface – just like an erupting boca of every volcano. Occasionally, the local topography determined the formation of a lava lake.

Nyiragongo’s seems to radiate one order of magnitude more than the other measured lava lakes of other volcanoes. Tazieff¹³ (1975 and references therein) reports about the variations of the level of Nyiragongo. It displays some important changes of several ten meters amplitude, elapsing a week or a month, plus other less important phenomena of the order of one meter up to half a dozen of meters, elapsing a fraction of an hour up to one hour. Sometime lava appears inflating by a few tens of centimeters in a matter of seconds (Tazieff, 1975).¹⁴

The total power radiated by a lava lake depends on its instant extension, and on its temperature, which depends both on its heat budget and refill, and on the process whereby heat is transported up to its surface, i.e., through advection. The extension of its surface depends on its level, which depends on the crustal strain.

A volcanic lava lake is a strainmeter with a very deep hole (a few kilometers at least) and with a time-varying temperature of the fluid that fills it. Therefore, the most significant datum is the power released per unit surface, which is directly related to the lava temperature, and which is implicitly corrected for the variations of the level and extension of its surface. On the other hand, concerning

¹³ Haroun Tazieff (1914-1998), Tatar, Belgian and French volcanologist and geologist. He was also a government adviser and French cabinet Minister.

¹⁴ Volcano “inflation” and “deflation” can be monitored, e.g., on Vesuvius, by means of AE records (see Gregori et al., 2025a, and Paparo et al., 2004).

direct temperature measurements, Tazieff (1975, and references therein) reports about - and discusses the causes of - substantially different measured temperatures, depending on the varying morphological features of the surface of the lava lake that looks more or less fluid, hence more or less radiating. That is, this variability of the apparent surface temperature - and the irregular variability of the appearance of its surface - imply some limitations for the possibility to detect the time variation the primary heat supply. As long as the lava lake is fluid, owing to convection, the sensitivity is high, but the sensitivity rapidly decreases when its surface solidifies. The actual occurrence of convection within the lake was shown by the movement of the floating "island" that was sometimes observed on the surface of Nyiragongo's lava lake.

At present, better observation facilities of several volcanoes permit monitoring the likely ongoing birth process of a new lava lake. For instance, Smets et al. (2014) report about a red glow that since June 2013 through April 2014 was visible on top of Nyamulagira, the westernmost volcano of the Virunga Volcanic Province, in the western branch of the East African Rift. Betz (2015a) reports about the use of a "unique seismic signatures to track the cyclic rise and fall of lava inside Hawai'i Volcanoes National Park's Overlook crater" (Fig. 9).



Fig. 9. "Over the past 7 years, the 'Overlook crater' near the summit of Kilauea volcano has grown from just 35 to more than 200 m wide and now hosts one of the largest lava lakes in the world (shown here). Recent research sheds light on gas-piston activity that may have contributed to the dramatic rise and fall of lava columns connected to the crater. Credit: USGS." Figure and captions after Betz (2015a). AGU and USGS copyright free policy.

In terms of an analogy, let us refer to water lakes in summit calderas. The same principle idea of strainmeters cannot be applied, because water precipitation and evaporation largely depend on the temperature and on meteorological factors. In addition, Simkin and Siebert (1994) comment as follows about crater lake explosions. "Water and hot magma make an explosive combination, and a summit crater lake on an active volcano places these two components in dangerous proximity. Lake water adds to the danger by contributing, in an eruption, the mudflows that can devastate the volcano's outer slopes and beyond. The Costa Rican volcano Poás has had at least 38 crater

lake eruptions, with one (in 1910) reportedly shooting a fountain of water 4 km in the air. Ruapehu, in New Zealand, has recorded the most crater lake eruptions (48), with Aso (46) close behind, but the most devastating has been Java's Kelut, where extensive efforts to drain the lake have successfully reduced its danger after 10 fatal eruptions claimed many thousands of lives."

The subsurface interaction of water with magma is called phreatomagmatic. Valentine et al. (2014) investigated the hazard associated with this phenomenon and summarizes as follows their findings. "Experiments over a wide range of energies show that for a given energy there is a depth below which an explosion will be contained within the subsurface (not erupt), and there is a corresponding shallower depth that will optimize ejecta dispersal. We combine these relationships with constraints on the energies of phreatomagmatic explosions at maar-diatreme volcanoes and show that most eruptions are likely sourced by explosions in the uppermost ~ 200 m, and even shallower ones (< 100 m) are likely to dominate deposition onto tephra rings. Most explosions below ~ 200 m will not erupt but contribute to formation of, and to the vertical mixing of materials within, a diatreme (vent structure), with only rare very high energy explosions between ~ 200 and ~ 500 m erupting. Similar constraints likely apply at other volcanoes that experience phreatomagmatic explosions."

Note that also the most violent catastrophic volcanic explosions partake to the same category of phreatomagmatic phenomena, as water is a relevant component of underground fluids at every depth, maybe mostly down to the Moho (see Gregori et al., 2025a). Much deeper phenomena involve serpentization, and the formation of the serpentosphere (see Gregori and Hovland, 2025).

A case history of "hydro-volcanic eruption" dealt with Mt. Otake, a stratovolcano (elevation 3067 m) located in central Honshu, Japan (35° 54' N, 137° 29' E) as reported by Sano et al. (2015).

"Mt. Ontake in central Japan suddenly erupted on 27th September 2014, killing 57 people with 6 still missing. It was a hydro-volcanic eruption and new magmatic material was not detected. There were no precursor signals such as seismicity and edifice inflation. It is difficult to predict hydro-volcanic eruptions because they are local phenomena that only affect a limited area surrounding the explosive vent. Here we report a long-term He anomaly measured in hot springs close to the central cone.

³He is the most sensitive tracer of magmatic volatiles. We have conducted spatial surveys around the volcano at once per few years since November 1981. The ³He/ ⁴He ratios of the closest site to the cone stayed constant until June 2000 and increased significantly from June 2003 to November 2014, while those of distant sites showed no valuable change.

These observations suggest a recent re-activation of Mt. Ontake and that ³He enhancement may have been a precursor of the 2014 eruption. We show that the eruption was ultimately caused by the increased input of magmatic volatiles over a ten-year period which resulted in the slow

pressurization of the volcanic conduit leading to the hydro-volcanic event in September 2014.” They illustrate their He measurements by means of Fig. 10. See also other related figures, not here shown, concerning the greatly intricate seismic and tectonic environment.

Another related concern deals with the interaction between lava and an ice sheet. An unprecedented specific detailed investigation was carried out on the 2010 Eyjafjallajökull eruption (Fig. 11). It was the first eruption where it has been possible to “document, in a lot of detail, what happens as the lava flow is moving under ice for a pretty good distance ... When the heat from lava rapidly melts ice at the top of a mountain, torrents of meltwater can cascade below, overwhelming glacial lakes and causing extensive flooding downstream ... In addition, when moving meltwater mixes with mud and ash, the flowing slurry (called a lahar) can pose extreme dangers. Like torrents of volcanic ‘concrete’...

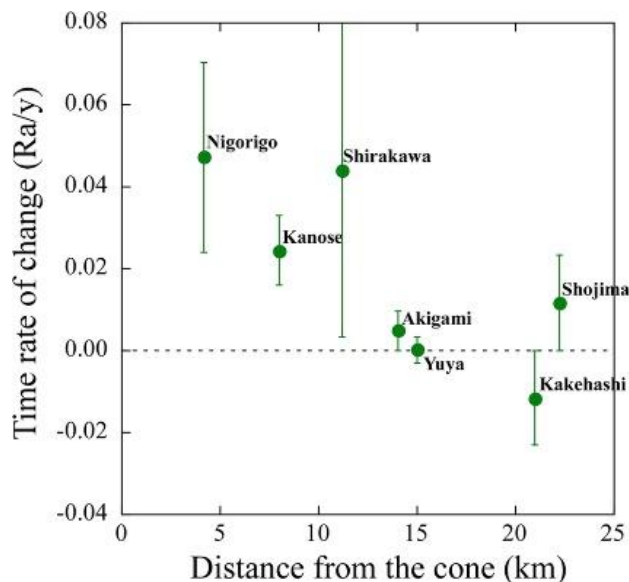


Fig. 10. “Correlation diagram between time rate of $^3\text{He}/^4\text{He}$ change since 2003 to 2014 and distance of the sampling site from the central cone of Mt. Ontake.” Figure and captions after Sano et al. (2015). With kind permission of *New Concepts in Global Tectonics, Journal*.

... the risk from meltwater was greatest during the initial explosive phase of the eruption, when vast amounts of ice melted, triggering torrential bursts. These sudden releases could overflow glacial lakes below, causing severe floods called jökulhlaups, ... one of the largest hazards associated with volcanic eruptions in Iceland. Later, when the lava began to move beneath the glacier, the flow of lava mixed with water carved channels under the ice, localizing and limiting potential dangers and allowing meltwater to escape more regularly. When lava interacts with ice, it solidifies into different forms, such as pillow lava. The ice cools the skin of the lava rapidly, creating a glassy, smooth exterior. The still-molten interior pushes through this skin and itself rapidly cools, forming distinctive bulbous lumps ... The locations where the pillow lava gives way to other lava forms along the slopes of a volcano give scientists an

indication of how far glaciers extended at the time of past eruptions.

Other aspects of ice-influenced lava can tell researchers about the temperature and characteristics of the lava as it emerged. For instance, as opposed to relatively smooth contours of hardened Eyjafjallajökull lava that had penetrated the ice, the roughly 10% that flowed on top of the glacier or beside it formed fields of sharp, jagged “a’a” lava ... “ (Deatrick, 2016).

The investigation was carried out by Oddsson et al. (2016), who summarize as follows their inference. “During the 2010 Eyjafjallajökull eruption in South Iceland, a 3.2 km long benmoreite lava flow was emplaced subglacially during a 17 day effusive-explosive phase from April 18 to May 4. The lava flowed to the north out of the ice-filled summit caldera down the outlet glacier Ggjökull. The flow has a vertical drop of ~ 700 m, an area of ~ 0.55 km², the total lava volume is ~ 2.5 × 10⁷ m³ and it is estimated to have melted 10 – 13 × 10⁷ m³ of ice.

During the first 8 days, the lava advanced slowly (< 100 m day⁻¹), building up to a thickness of 80 – 100 m under ice that was initially 150 – 200 m thick. Faster advance (up to 500 m day⁻¹) formed a thinner (10 – 20 m) lava flow on the slopes outside the caldera where the ice was 60 – 100 m thick. This subglacial lava flow was emplaced along meltwater tunnels under ice for the entire 3.2 km of the flow field length and constitutes 90% of the total lava volume. The remaining 10% belong to subaerial lava that was emplaced on top of the subglacial lava flow in an ice-free environment at the end of effusive activity, forming a 2.7 km long “a’a” lava field. About 45% of the thermal energy of the subglacial lava was used for ice melting; 4% was lost with hot water; ~ 1% was released to the atmosphere as steam. Heat was mostly released by forced convection of fast-flowing meltwater with heat fluxes of 125 – 310 kW m⁻².”

However, some non-understood items deal with the groundwater hydrologic regime. Yapa (2016) “observed > 100 l sec⁻¹ continuous flows in many water springs along the Andean volcanic range, some occurring a distance of 10 – 20 km away from the possible source (in Arequipa and Ayacucho, Perú and in Chimborazo, Ecuador). Given that these are strato-volcanoes with high silica lava flows, one would not expect subterranean lava tube formations in these mountains. Moreover, these springs maintain such flows even when the peaks are without snow or when streams are dry, indicating some large subterranean reservoirs feeding them. Are solidification cracks in volcanic rocks sufficient to explain such phenomena?” That is, water reservoirs underground are much extended.

Sulphur lakes

As far as Volcan Poás in Costa Rica is concerned, it has the seemingly best-known liquid-sulphur lake. This topic shifts the focus on the role of water mixed with ground, i.e., on mud volcanism (extensively discussed in Gregori and Hovland, 2025), to be eventually characterized by a specific chemistry. This liquid-sulphur lake was already reported by Sapper (1903) in terms of three-color paintings based on his own drawings that show some kind of a geyser activity.

Much more detailed information on this sulphur lake¹⁵ is given by Oppenheimer and Stevenson (1989) who report about a progressive rapid drop occurred over a two-year period until April 1989, when only scattered boiling mud remained, leaving large bodies of molten sulphur after the disappearance of the last water from the lake. They also suggest “that their formation resulted from removal of the overlying water, which allowed lake sediment temperatures to rise above the liquidus of the elemental sulphur deposits contained within them. The sulphur ponds bubbled

vigorously because of the flux of hot gases from below, which kept them molten at a temperature of ~ 116 °C. The low viscosity of sulphur at this temperature is likely to have been critical in enabling its migration through the lake sediments to collect at fumarole vents ... The temperature of the molten sulphur, measured by thermocouple, was ~ 116 °C (J. Barquero, personal communication), well below the boiling point of sulphur (~ 444 °C).”

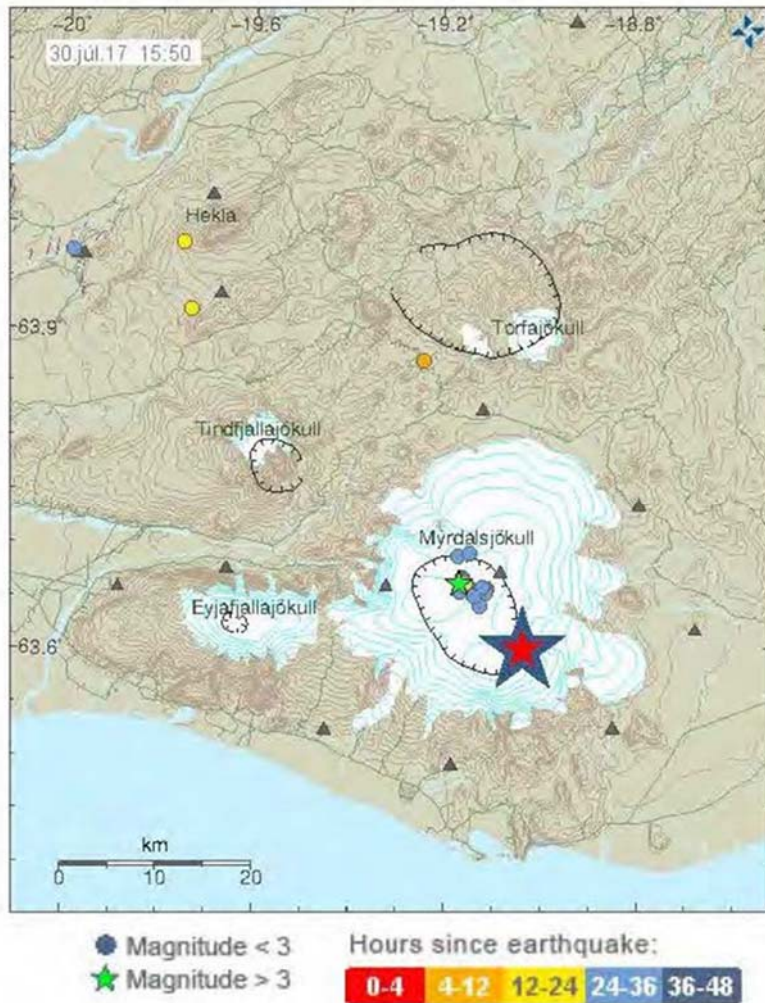


Fig. 11. “Map of Southeast Iceland, showing two major glaciers, Eyjafjallajökull and Myrdalsjökull, covering the ‘E’ and Katla volcanoes, respectively. The green star indicates the location of two $M \geq 3.0$ quakes plus swarm of smaller earthquakes (blue and yellow circles) under Katla on July 30, 2017. Another swarm of small quakes (not shown) was present July 29 to the left of the green star. These all followed the $M = 4.5$ quake (red star) that occurred on July 17, 2017. Map source: Icelandic Met Office. $M = 4.5$ location via USGS.” Figure and captions after Casey (2017). With kind permission of *New Concepts in Global Tectonics, Journal*.

No previous report on sulphur lakes is seemingly available, although several sulphur-related minor morphological features were reported from a few well-known volcanoes. However, concerning Volcan Poás, Rymer and Brown (1989) monitored large gravity variations, which they interpreted in terms of substantial structural changes of the magma chamber and of the plumbing line - while according to the rationale of the present study they ought to be explained in terms of suitable

phase changes related to variations of the primary energy supply, and consequent mass transfer.

A recent investigation (Hynek et al., 2018) found that this lake hosts only one type of organism, a case history of extremophiles that is interesting in order to study the possibility of elementary life forms on Mars or on other planetary objects. Hynek et al. (2018) summarize their study and stress the analogy with a Mars geochemical environment. In fact, hydrothermal and mineralogy alteration of the sulphur lake displays a style consistent with

¹⁵ Information, bibliography and links to specific volcanic lakes - including several papers on Volcan Poás - can be found at <http://pasternack.ucdavis.edu/lakes.htm>.

the relicts of hydrothermal systems on Mars. The lake is located on an active volcano, showing high-temperature fumaroles (up to 980 °C) and an ultra-acidic lake. At present, this lake – named Laguna Caliente – shows a most dynamic environment, characterized by frequent phreatic eruptions. The temperatures range from near ambient to almost boiling, a *pH* range of –1 to 1.5, with a wide range of chemistries and redox potential.

Also on Mars, some analogous acid-sulfate hydrothermal systems were likely to display similar dynamics. These environments are equally challenging to life. The microbiology of Laguna Caliente was sampled for the first time in November 2013. “*The diversity of the microbial community was surveyed via extraction of environmental DNA from fluid and sediment samples followed by Illumina sequencing of the 16S rRNA gene. The microbial diversity was limited to a single species of the bacterial genus Acidiphilium. This organism likely gets its energy from oxidation of reduced sulfur in the lake, including elemental sulfur.*” Owing to the environment that is guessed to have existed in the past on Mars, the same type of organism can be significant for the search for past or present life on Mars. See also Gregori et al. (2025w) and Gregori and Gregori (2025)..

Similar phenomena are concerned with the entire study of mud volcanoes of every kind and size, including fumaroles. Mud and/or asphalt volcanoes are discussed in Gregori and Hovland (2025). A continuum exists between the opposite extremes of (i) mere volcanic summit water lakes and (ii) gas exhalation in fumaroles.

Water caldera lakes

A present, water volcanic lakes are the object of a systematic investigation. Among the world’s 714 Holocene-aged (i.e. $\leq 10,000$ years old) volcanoes – which are listed in the *Catalog of Active Volcanoes of the World* - only ~ 12% has a lake of this kind (Rowe et al., 1992a, 1992b). Both the endogenous (i.e., the volcano structure, e.g., substratum permeability and crater shape) and exogenous forces (i.e., volcanic heat flux vs. atmospheric cooling and precipitation vs. evaporation) are the crucial drivers that are operative in the sub-environment of a given crater. These phenomena determine lake chemistry, which is indicative of its volcanic activity and of geo-hydro-chemical processes.

Pasternack and Varekamp (1997) and Varekamp et al. (2000) proposed a genetic classification scheme for volcanic lakes, based on morphological characteristics of natural lakes and models of ideal lakes. They avoided, however, simple descriptive features. Rather, they referred to the threshold of processes. They envisaged therefore 3 quantitative levels of classification - i.e., absolute energy, hydrodynamic mixing regimes, and chemistry. Concerning the first 2 levels, they used a perfect mixing, steady-state energy/mass balance model, which implies some *a priori* physical constraints. The several fluxes - associated with volcanic/geothermal inflow, radiative fluxes, conductive heat loss at the lake surface, evaporative heat loss, and the energy used to heat entering meteoric waters – were equated and solved iteratively assuming a steady-state temperature

of the lake. In addition, mass balance for water was imposed. The lake surface area was dominant. Precipitation rate and catchment area are essential for lake survival and for maintaining water balance.

A new model was proposed by Terada and Hashimoto (2017) that partially revises some previous belief. They summarize as follows their result. “*We use a numerical model to investigate the factors that control the presence or absence of a hot crater lake at an active volcano. We find that given a suitable pair of parameters (e.g., the enthalpy of subaqueous fumaroles and the ratio of mass flux of the fluid input at the lake bottom to lake surface area), hot crater lakes can be sustained on relatively long timescales.*

Neither a high rate of precipitation nor an impermeable layer beneath the lake bottom are always necessary for long-term sustainability. The two controlling parameters affect various hydrological properties of crater lakes, including temperature, chemical concentrations, and temporal variations in water levels. In the case of low-temperature crater lakes, increases in flux and enthalpy, which are a common precursor to phreatic or phreatomagmatic eruptions, result in an increase in both temperature and water level. In contrast, a decrease in water level accompanied by a rise in temperature occurs at high-temperature lakes.

Furthermore, our model suggests that crater geometry is a key control on water temperature. For lakes with a conical topography, a perturbation in the water level due to trivial non-volcanic activity, such as low levels of precipitation, can cause persistent increases in water temperature and chemical concentrations, and a decrease in the water level, even though subaqueous fumarolic activity does not change. Such changes in hot crater lakes which are not caused by changes in volcanic activity resemble the volcanic unrest that precedes eruptions.”

Scenarios of breaking processes were investigated for the definition and assessment of different lake types. The entire discussion and modeling is largely concerned with chemical processes that can explain several morphological, physical and geochemical features. These items are outside the main concern of the present study, and no additional mention is here given.

At the opposite extreme, no discussion and review can be here given of the wide scenario of the several evidences dealing with soil outgassing. See, however, Gregori and Hovland (2025). For instance, just as an example, see Fig. 12 that shows a diffuse fumarolic and geyser extensive occurrence in Kamchatka that is one of the present volcanically most active regions. Therefore, it displays a varied morphology of geothermal phenomena.

Only in comparatively recent times did this seemingly “rare” phenomena attracted the attention of the scientific community. For instance, even the observation of ball lightning (BLs) is a direct detection of faint soil exhalation (see Gregori and Leybourne, 2026e). More specifically, we remind about three main key issues, dealing, respectively, with CH_4 , with CO_2 , and with the coupling between subsoil phenomena and the atmosphere up to the ionosphere and magnetosphere.

The exhalation of CH_4 and of CO_2 is basically ubiquitous, at every latitude and longitude. Its energy supply on the deep ocean floors is the likely primary energy source for a continuous regeneration of life. This unexpected and impressive result is a finding of the investigations carried out during several decades by Martin Hovland. These items are extensively reported in Gregori and Hovland (2025) (see also Gregori, 2020 and references therein). In addition, the natural exhalation of CH_4 is the primary fuel for wildfires (see Gregori and Leybourne, 2025i). Also CH_4 bubbling is sometimes reported. For instance, see Fig. 13 (see also Walter et al., 2006) dealing with permafrost thaw exhalation, which is the phenomenon that originates the huge increase of CO_2 atmospheric concentration in springtime (see Gregori, 2020 and references therein).



Fig. 12. Valley of Geysers, Kamchatka. Courtesy of Yuri V. Marapulets (private communication, 2013).

“Limnic” volcanism

Steady and smooth CH_4 exhalation is generally detected even in areas that were not expected to be significant for oil availability (see Gregori and Hovland, 2025). These findings, however, are consistent with the guessed role of the biosphere in the evolution of Earth’s crust. This smooth and steady outgassing - but also the varied fumarole activity, or mud volcanism, etc. - originates different manifestations of the release of endogenous energy. The morphology of every phenomenon of this kind critically depends on the local structure and composition of the lithospheric and crustal setting. Some anecdotic reports can be mentioned. Comparatively almost irrelevant events of abrupt soil exhalation are sometimes reported, although they cause no limnic eruption and therefore are generally considered like curiosities, unnoticed by the scientific community. Just like examples, we report some information that we could occasionally collect, almost by chance.

A few years ago, in the town of Marino, on the Vulcano Laziale south of Rome, a few tens of cows, closed inside a pen inside a small valley, were found asphyxiated. The likely cause was an abrupt gas exhalation from soil. Only a few years before, another case history (Dr. Mario Mattia, private communication) dealt with a gentleman, who listened a strong and frequent roar underneath his house, located on the main square of the town of Lanuvio, also on

the Vulcano Laziale not far from Marino. The owner instructed a formal legal action against unknown people. He was concerned about somebody who could be illegally excavating a tunnel underneath his house. Dr. Mario Mattia is a professional physicist of sound, who was commissioned by the Court to carry out a legal assessment of the phenomenon. Subsequent official inspection by authorities assessed that no digging was in progress.



Fig. 13 - [upper figure] “ CH_4 bubbling in an interior Alaska abrupt thaw lake. CH_4 bubbles released by ebullition from thaw bulbs beneath thermokarst lakes are seasonally trapped in winter lake ice forming white bubble patches. High bubbling rates of particularly strong ebullition seeps known as hotspots maintain ice-free holes in winter lake ice. Ebullition hotspots are indicative of abrupt thaw environments, where the rapid (decadal-scale) transformation of terrestrial permafrost to deep thaw bulbs beneath lakes fuels anaerobic decomposition of ^{14}C -depleted soil organic carbon and the release of ^{14}C -depleted CH_4 in bubbles ... Diameters of the ice-free hotspot holes shown in this October 17, 2016 photograph are between 0.4 – 0.9 m.” Figure and captions after Walter Anthony et al. (2018). Reproduced with kind permission of Nature Communications, (CC BY 4.0). [lower figure] “Bubbles of CH_4 mark a lake where permafrost is melting below and quickly releasing greenhouse gases into the atmosphere. Credit: Katey Walter Anthony/University of Alaska Fairbanks.” Figure and captions after Bartels (2018d). NASA copyright free policy.

The reason of the phenomenon was an intense exhalation of geogas in this volcanic area. A similar case history deals with the site of Orchi (literally “Ogres”). The name of this site derives from a frequently heard roar

underground. This area, close to Foligno in central Italy north of Rome, is to be considered generally geothermal, with much seismicity (it is very close to the epicenter of the Colfiorito earthquake and not very far from the epicenter of the Amatrice/Norcia seismic crisis of August-October 2016). Orchi is the location of an AE recording station, generously hosted and operated for over a decade in the basement of the private house of the renowned painter Alfredo Raponi. See Gregori et al. (2025a) and references therein.

In August 2013, close to the Fiumicino airport of Rome, a few episodes of vents were reported with fluid bubbling from underground. Consider that the whole region of peninsular Italy which is west of the Apennines - unlike the region east of the Apennines - is characterized by conspicuous geothermal flow associated with volcanism. Two of these vent episodes were spontaneous, one inland and one offshore, and one was artificially triggered. Two scientific papers deal with these features.

Ciotoli et al. (2013) claim that they “assessed that this gas, analogous to other minor vents in the area, is dominantly composed of deep, partially mantle-derived CO₂, as in the geothermal gas of the surrounding Roman Comagmatic Province. Increased amounts of thermogenic CH₄ are likely sourced from Meso-Cenozoic petroleum systems, overlying the deep magmatic fluids. We hypothesize that the intersection of NE-SW and N-S fault systems, which at regional scale controls the location of the Roman volcanic edifices, favors gas uprising through the impermeable Pliocene and deltaic Holocene covers ... “ In reality, also a temporary increase occurred of the local endogenous heat supply.

Sella et al. (2014) report that on 24 August 2013 they drilled a shallow borehole at the same spot. “Following by hours” this suddenly originated a new fumarole with CO₂-rich gas, water, and mud. The fumarole was located at a crossroad along the fenced area of the Fiumicino international airport of Rome. In recent and past years similar occurrences have been reported or scientifically documented. Sella et al. (2014) claim that they “used five borehole ..., analyzed the stratigraphy of these and other nearby cores, acquired a 2D seismic refraction tomogram, and performed chemical and isotopic analyses of water samples collected from aquifers intercepted by two drilled boreholes”. Thus, they found that gases are mainly entrapped at ~ 40 – 50 m depth in a mid-Pleistocene gravel horizon, which contains a confined aquifer that stores the endogenous upwelling gases. The gravel is confined by two silty-clayey units. Sella et al. (2014) also inform that while writing their paper additional similar artificially triggered degassing events were observed off the Fiumicino village in connection with the construction of the new harbor.

Note that, in any case, a time variation of the endogenous energy supply is effective over some large area. In addition, these changes are long-period phenomena. On the other hand, all these anecdotic phenomena seemingly imply - consistently with the Caronia house’s fires (see below) - a small space-scale of a possible, or presumable, local sea-urchin spike.

Early in May 2009, in the town of Riesi in Sicily, located south of Caltanissetta approximately halfway towards the sea, abruptly the ground floor temperature in a house warmed up, up to ~ 88 °C ... The tectonic setting of Sicily (Fig. 14) is much complicated, and the presence of several sea-urchin spikes appears much more reasonable.

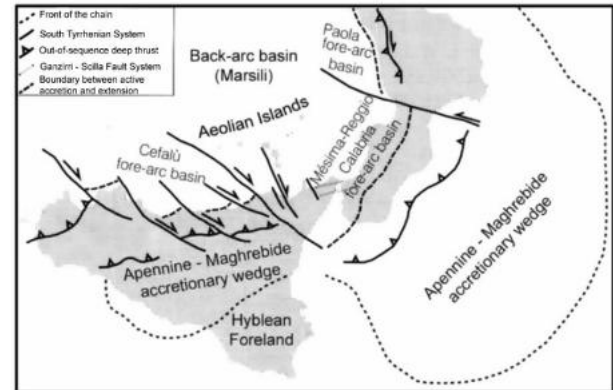


Fig. 14. “Neotectonic scheme. The South Tyrrhenian system is the superficial expression of the continental collision and causes the segmentation of the fore-arc system. The south-eastward migration of the Calabrian arc provokes the formation of a physiographic boundary characterized by normal faults. This structure is visible both on land and on seismic lines and separates the regimes of active accretion and extension (after Guarneri and Carbone, 2003).” Figure and captions after Parotto and Praturlo (2004). With kind permission of Società Geologica Italiana.

To our knowledge, no systematic - more or less spatially dense - monitoring or inventory of these phenomena was ever attempted - that, maybe, can be reliably monitored in an objective way by a suitable array of AE (acoustic emission) recorders (see Gregori et al., 2025a). In addition, this outgassing activity in volcanic areas ought to be closely correlated with the standard minor seismic activity, normally characterized by weak and frequent shocks – such as typically occurs in volcanoes. That is, concrete possibilities exist to monitor these seemingly curious or unusual phenomena that, however, are presumably much more frequent than presently believed. In general, soil outgassing is likely to occur with large space and time gradients, on a wide variety of scale sizes. However, owing to the difficulty of monitoring it, only a small fraction of this relevant climate driver can be investigated.

A particularly effective “sensor”, or a way of detecting time-integrated soil exhalation, occurs whenever a crater lake, with its water, operates like the security valve of a pressure cooker, whereby the gas release occurs abruptly like a real volcanic eruption of gas. That is, the water of the lake is the “device” that accumulates a non-measurable phenomenon until it reaches a threshold when it can be detected as a violent release. This kind of phenomena includes geysers and, more seldom, “limnic volcanoes”. The occurrence and location of a limnic volcano derives from the balance between two concurrent causes: endogenous heat source and water availability. The heat source must be intense - compared to the available endogenous fluids and water - because heat transport must be limited in order to allow for energy accumulation in the

system. On the other hand, if fluids do not afford, either smoothly or impulsively, to transport enough endogenous energy, heat must accumulate until magma is formed, thus leading to standard volcanism.

The best-known case histories of limnic volcanism appear to occur (maybe) close to the boundaries of regions of comparatively high endogenous heat release. The surface morphology is often associated with a maar, i.e., a volcanic crater, formerly originated by an explosion in an area of low relief, which in general is more or less circular, often containing either a lake, or a pond, or marsh.

West central Africa is a particularly intriguing - and dramatic - case history (Fig. 15). The Mount Oku massif along the Cameroon Volcanic Line (CVL) contains numerous maars and basaltic cinder cones, aligned in a deeply dissected area. Two crater lakes, Lake Nyos to the north and Lake Monoun to the south (~ 100 km ESE of Lake Nyos, part of the Bambouto Volcanic Field), originated catastrophic events of abrupt gas release.

Remember that this area is located right on the intense doublet of geomagnetic anomaly shown in Fig. 6 of Gregori et al. (2025s), and it is the likely site of an alignment of strong sea-urchin spikes.

On 15 August 1984 a gas release at Lake Monoun killed 37 people¹⁶ and it was explained by an overturn of the stratified lake water, triggered by an earthquake and landslide. In March 1985, Haraldur Sigurdsson, J.D. Devine, and F. Tchoua investigated the August 1984 event. A summary of their information is as follows.¹⁷ “On 15 August at about 23:30, several people heard a loud noise or explosion from the Lake Monoun area and there were unconfirmed reports that an earthquake was felt that day at a town ~ 6 km N of the lake. The gas cloud was emitted from the E part of the lake, where a crater ~ 350 m in diameter and at least ~ 96 m deep is located. Victims of the cloud were in a low-lying area and had apparently died between 03:00 and dawn. No autopsies were performed and the exact causes of death are unknown; all bodies had suffered skin damage (corrected from first-degree burns). Persons on the fringes of the cloud reported that it smelled bitter and acidic. From 06:30 until it dissipated by 10:30, the whitish, smoke-like cloud remained 0 – 3 m above the ground. Vegetation was flattened within ~ 100 m of the lake’s east end, indicating that a water wave as much as ~ 5 m above lake level was associated with the event.

Lake Monoun is near the center of a volcanic field that includes at least 34 recent craters, and there is evidence that eruptive activity has occurred there as recently as a few hundred years ago. However, the chemistry of the lake water and sediments, the uniformly low lake temperature (~ 23 – 24 °C), and the absence of new tephra in or around the lake suggested to the research team that the August 1984 event was not the result of an eruption or a sudden ejection of volcanic gas from the lake. Gradual emission of CO₂ from volcanic vents is thought to have led to a buildup of HCO₃ in the lake. An earthquake or internal seiche is thought to have upset the density stratification of

the lake, triggering its overturn and catastrophic exsolution of CO₂, which suffocated the victims. Explanations of the cloud’s acid odor and the agent of victims’ skin damage are uncertain.”

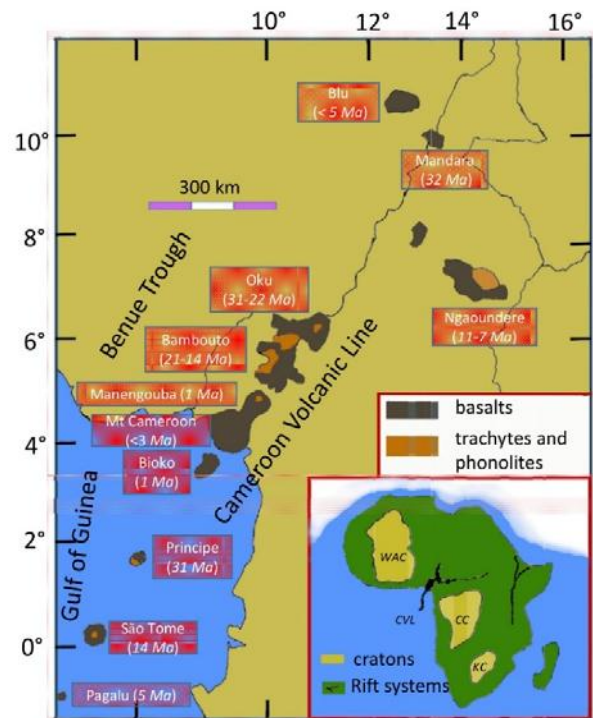


Fig. 15. Sketch map of the Cameroon Volcanic Line (CVL). Ages refer to the volcanoes of the continental sector (Gouhier et al., 1974; Fitton and Dunlop, 1985; Njilah, 1991; Marzoli et al., 2000; and Aka et al., 2004), and to the onset of the basaltic volcanism on the oceanic islands (Lee et al., 1994a). Inset: the cratons are West African Craton (WAC), Congo Craton (CC) and Kalahari Craton (KC). Pagalu is also called Annobon, Mt Cameroon includes volcano Etinde. Biu denotes a Plateau. The Fouban shear zone connects Oku with Ngaoundere. Figure simplified redrawn based on similar figures in Marzoli et al. (2000) and Aka et al. (2004).

On 21 August 1986 an analogous event occurred in the Lake Nyos, which is ~ 1,800 m across and ~ 208 m deep, inside one of the maars, formed ~ 400 years ago during an explosive eruption of CO₂. The 21 August 1986 event killed at least 1,700 people and 845 people were hospitalized. A rumbling was reported lasting ~ 15 – 20 sec, with “rotten eggs smell”, which caused loss of consciousness, while > 3,000 cattle were killed. The lake turned rusty red, but vegetation remained essentially unaffected. The cloud traveled inland ~ 25 km from the lake. A wave flattened vegetation, including a few trees, stripping the peninsula at the left. The gas emission was estimated as ~ 1 km³ of CO₂. The overturn of stratified waters was explained by phreatic explosions or by injection of hot endogenous gas. Victims died of CO₂ asphyxiation, and CO₂ is believed to be of magmatic origin (Sano et al., 1990). However, no direct volcanic activity was involved.

¹⁶Kling et al. (1987), Sigurdsson (1987), Sigurdsson et al. (1987), also Tchoua (1983) and Holloway (2000).

¹⁷See Smithsonian Institution Global Volcanism Program Website, 1999, SEAN 10:08.

The CO_2 was stored in the lake's hypolimnion, i.e., in the dense, bottom layer of water in the thermally-stratified lake, below the thermocline. Typically, it is the coldest layer of a lake in summer, and the warmest layer during winter. It is isolated from surface wind-mixing during summer, and usually no photosynthesis can occur inside it, due to insufficient solar irradiance.

On the night of 21 August 1986, a large jet of gas and water erupted from Lake Nyos lasting several hours. The jet was over 100 m high, while the heavy, lethal gas swept down the slope. Thus, 1746 people died by asphyxiation in the villages below the lake. Only 6 over 1000 inhabitants survived in the village of Lower Nyos, 3 km below the lake. Also, at Subum, more than 10 km distant, asphyxiation deaths were common. A wave damage occurred along most of the southern shore and reached 25 m above lake level with a maximum of over 80 m at one point. However, the evidence shows that volcanism was the direct cause of the tragedy. In fact, this is proven by the sediments on the lake bottom that remained undisturbed, by the cool lake waters, while the water samples contained almost no volcanic gases other than CO_2 , and almost no suspended sediment was observed at least below the upper 10 m. In addition, the lethal gas cloud was cool that flooded the valley below the lake, while no evidence is suggestive of caustic volcanic gases. The most important finding was perhaps that the lake was highly stratified, displaying a distinct "chemocline", with embedded in it a dense, lower layer, rich in CO_2 and ions, which rarely mixed with the lighter, fresher water above it.

Hence, by the end of 1986, the general feeling was that Lake Nyos experienced a previously unknown type of eruption - a "limnic", or lake-water eruption. This was believed to trigger some disturbance that raised CO_2 -saturated bottom water across a chemocline, until reaching a depth of lower hydrostatic pressure. The CO_2 solubility decreases with decreasing pressure. Hence, the CO_2 release is explosive. Thus, the researchers envisaged that a similar limnic eruption probably occurred at Lake Monoun, 95 km south of Lake Nyos, causing 37 deaths on 15 August 1984 (Sigurdsson et al., 1987).

Subsequently, it was possible to explain in better detail how such a limnic eruption might proceed. Gas, forced out of solution by a heat source below the lake (they speculated a body of cooling magma; we claim, rather, that the source was a bunch of sea-urchin spikes) dissolves in water and flows along rock fractures. When the upwelling water reached the lake, the dissolved gas would be largely depleted of reactive components, becoming ~ 98 – 99% CO_2 . However, the CO_2 -rich water, owing to the greater density, would remain near the lake bottom, and cannot mix with the fresher water above it. An unstable equilibrium occurs as long as some perturbation raises the saturated bottom water into the lower-pressure, shallow regions, thus causing the dissolved gas to 'exsolve', or bubble out of solution. Therefore, the resulting gas-water mixture was forced upward by buoyancy, and - by this - CO_2 continued to exsolve. This phenomenon increases the mixture's buoyancy, favoring additional dense CO_2 -rich bottom water that is thus siphoned up into the eruption conduit, sustaining

the reaction. Some objection was raised, however, mostly because it is not clear how such a process is limited to only a portion of the lake, such as reported by eyewitnesses at Lake Nyos. In any case, a decade of observations of the post-eruption evolution of Lake Nyos confirmed the limnic eruption hypothesis as the most likely explanation. Thus, the probable conditions were assessed in the lake just prior to the eruption.

Kling et al. (1987) give additional details. A series of rumbling sounds - lasting perhaps 15 to 20 sec - frightened people on 21 August at about 21:30, in the immediate area of the lake. They came out of their homes. A bubbling sound was reported by one observer, who walked to a vantage point. He saw a white cloud rising from the lake together with a large water surge. Many reports were given of an odor of "rotten eggs or gunpowder", felt with a warm sensation, while they rapidly lost consciousness. The survivors awakened from 6 to 36 hours later and felt weak and confused. They also found oil lamps gone out, although they still contained oil. In addition, their animals and some family members were dead. In addition, birds, insects, and small mammals were not seen for 48 hours at least, while the plant life looked essentially unaffected. In fact, now it is well-known that an excess of CO_2 concentration favors plants growth.

People from the surrounding area on the morning of 22 August started the task of recovery and burial. Only on the morning of 24 August two Swiss missionary helicopter (*Helimission*) pilots inspected the area. Thus, the "outside world" was informed about the tragedy. The lake surface looked calm, littered with floating mats of vegetation. The usual clear blue color of the lake looked rusty red (Fig. 16). The vegetation damage denoted a water surge that washed up the southern shore to the height of ~ 25 m. The spillway at the northern end of the lake was overflowed by a water surge 6 m high. On the southwestern shore, a fountain of water or froth had splashed over an 80 m-high rock promontory. The event killed 3000 cattle.

Kling et al. (1987) carried out chemical analyses on the gases of the lake and of some springs in the area. They make the following interesting comment. They distinguish three possible sources for the gas released on 21 August, i.e., volcanic, magmatic, or biogenic. They associated volcanic gas with high-temperature, eruptive processes. In contrast, they claim that "magmatic" gas below the Earth surface should be released from magma - while we claim that the heat source is a bunch of sea-urchin spikes. This gas, when it reaches Earth's surface, is relatively cool, and has lost the reactive constituents, e.g., sulphur and chlorine compounds and CO. The biogenic gas derives from decomposition of organic matter. Kling et al. (1987) state that, according to their data, the bulk of the gas had a low temperature envisaging a "magmatic" origin. In addition, they specify that, according to geophysical and geochemical evidence, the mantle source region of basaltic Cameroon magmas - i.e., the top points of the bunch of sea-urchin spikes - is at > 90 km depth (Gumper and Pomeroy, 1970; Fitton and Dunlop, 1985).

Therefore, according to the rationale of the present study, this phenomenon is not simply associated to an

increase of the endogenous energy supply. Rather, it is related to an effect connected to gas solution inside some deep layer, with variation of gas solubility following a change of the local pressure. Indeed, those authors correctly specify the exact meaning of their wording. Terms like “magmatic” vs. “volcanic” could be confusing if no specification is given. According to the rationale of the present study, an equivalent (and better) concept could be by specifying that in either case an endogenous heat source is the primary driver. Some gas (or in general any other fluid) is eventually heated at some comparatively large depth, and it transports heat by advection. Since its geometrical path - through the fissures and pores of the overlying strata - is sufficiently long, the gas loses its temperature and reactive constituents, before arriving at Earth’s surface. This is the gas that Kling et al. (1987) call of “magmatic” origin. Instead, when the gas heating occurs at comparatively shallower depth, they state that the gas is of “volcanic” origin.



Fig. 16. Lake Nyos, Cameroon. The 1986 limnic eruption “might be due to a previously unknown type of non-volcanic eruption coming from the rusty stain of the lake’s normally clear blue waters. The stain suggested that the lake’s iron-rich bottom waters had mixed with the oxygen-rich surface waters ... (Photo courtesy of George Kling, University of Michigan).” Figure and captions after Ladbury (1996). Reproduced as kind courtesy of George Kling, *University of Michigan*.

These lethal catastrophes occurred in a region (Africa) with some generally very thick lithosphere, although this region is crossed by the deep fracture of the CVL. They claim that magmas ought to be at $> 90 \text{ km}$ depth. Maybe, similar events could not occur in areas where the primary heat source is much shallower, because in those cases the gas should be “volcanic”, while in Africa it was “magmatic”, and perhaps these limnic eruptions (seemingly) strictly require a “magmatic” gas.

In this same respect, Ladbury (1996) concludes and enquires whether we deal with a unique system. In fact, the only known limnic eruptions occurred within $\sim 100 \text{ km}$ of each other. Can other lakes experience similar catastrophes?

“Anthropologist Eugenia Sahnklin of Trenton State College in Trenton, New Jersey, has found some evidence of similar past events in the folklore of Cameroon’s Northwest Province and plans to carry out more exhaustive studies in the near future.”

In Japan, during part of the year, Lake Mashu shows a buildup of CO_2 in its bottom waters. On the other hand, winters in Japan are colder, and on a yearly basis the dense surface water can mix across the chemocline. In contrast, the Cameroon lakes experience no such yearly mixing occurs. However, as Ladbury (1996) points out, Kling stressed that both Lakes Nyos and Monoun erupted during the cool rainy season, which have been the trigger for a disturbance that caused mixing.

The refugee camps along the Zaïre-Rwanda border is close to a more threatening candidate lake. This is Lake Kivu - with an area of $\sim 2370 \text{ km}^2$, with a maximum depth of $> 485 \text{ m}$. It contains over 700 times gas than in Lake Nyos. Lake Kivu has on its floors several active volcanoes and has a stratified structure similar to the two Cameroon lakes. However, Lake Kivu is certainly much more stable than Lakes Nyos and Monoun. Hence, procedures were already carried out to extract CH_4 (and CO_2), by means of procedures similar to that ones that were used for degassing the Cameroon Lakes. Ladbury (1996) specifies that “Tietze, who in 1981 proposed a scheme for taping Lake Kivu’s $\sim 6.3 \times 10^{10} \text{ m}^3$ of CH_4 , estimates the reserves to be worth \$20 billion.” Moreover, according to Kling, a sediment core in Lake Kivu shows a ~ 4000 year old layer with a high concentration of fish bones and debris from the lake shore. Ladbury (1996) states that this may be suggestive of a past occurrence of a limnic eruption at Lake Kivu. Ladbury (1996) reports a Kling statement: “if this were to happen today, at least a million people in the Kivu basin could be affected”.

In any case, Ladbury (1996) wonders what surprises are to be expected in Cameroon’s Northwest Province if Lakes Nyos and Monoun are the only two lakes that experience limnic eruptions.

In late 2001 a webcam was placed at Lake Nyos to monitor the degassing effort. The entire area has been the object of extensive geochemical investigations, concerning both gas exhalation aspects and basalt chemism. The fascinating - and comparatively recently born - discipline of basalt chemism, i.e., of chemical geodynamics is discussed in Gregori et al. (2025a). In any case, the timing of lava eruption along the CVL showed that - as shown in Fig. 15 - its pattern does not indicate a sequence of volcanic activity associated with one hotspot and a lithospheric slab moving on top of it. Rather, the morphology clearly indicates that it was a regional occurrence, i.e., just like it has to be expected following the upheaval of a geotumor, and consistently with the model of WMT (warm mud tectonics), and with the geomagnetic anomaly alignment of Fig. 6 of Gregori et al. (2025s).

Nnange et al. (2001) investigated the isostatic compensation mechanism of the region of the Adamawa dome and found that it seems to be over-compensated. The reason might be a low-density material and “*probably an upwarping of the plate above the low density materials at depths.*” Nnange et al. (2001) also recall a similar “*dynamic compensation observed in similar uplifts in Africa, e.g., the broad East African plateau.*” In any case, they stress that such a compensation mechanism is consistent with a hot, low-density asthenosphere beneath the uplift.

The aforementioned lake Kiwu is located at the border between Rwanda and the Democratic Republic of Congo. It is ~ 2,000 times larger than Lake Nyos. As already stressed, it appears particularly intriguing from the viewpoint of the present study. It contains ~ 10³ times more gas than Lake Nyos, and ~ 1/5 of this gas is CH₄. Nyos, Monoun, and Kiwu are reported as being the only three lakes in the world containing high concentrations of dissolved gas in their bottom waters. Their location appears curiously to fall right on the boundary of the anomalous and approximately circular area of Zaïre, where a gravity low (Fig. 17), and an anomalous lightning activity (Figs 1 and 8 of Gregori et al., 2025v), envisage the presence of a huge bunch of sea-urchin spikes. That is, at the boundary of this huge bunch of spikes, the endogenous heat is comparatively lower - hence the local subsoil fluids are sufficient to ensure the energy balance with no need to produce a new *ad hoc* fluid (magma). Hence, limnic volcanism is observed at these boundaries, rather than lava effusion.

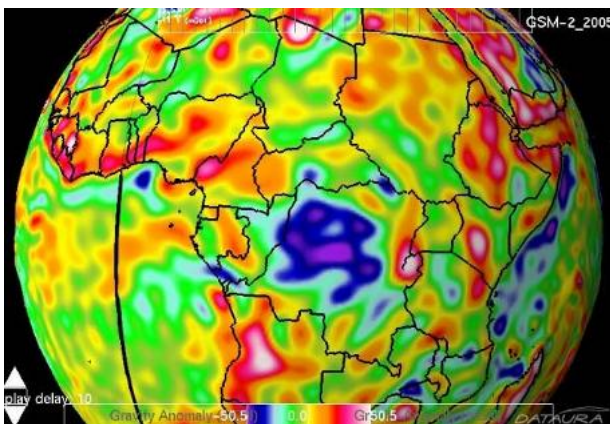


Fig. 17. Gravity anomaly map for Africa by GRACE data (Image by Dataura and Geostream Consulting; Data source =NASA).

These dramatic events triggered an unprecedented great increase of interest for the chemistry of volcanic lakes.¹⁸ The hazard is greater in summer, because a higher rainfall is associated with more clouds and less solar heat input,

¹⁸This shows that an endless number of new disciplines can eventually be started. We apologize for not being even aware of several presently “less known” branches of Earth’s sciences that ought to be considered in the framework of the present study and that are here unduly forgotten.

¹⁹This information has been borrowed from a power-point, retrieved on the web, of a presentation given by Dmitri

hence a lower lake surface temperature, which implies a lesser stability of the lake. Wind, internal wave, rock fall, ... are additional possible triggers.

IAVCEI has now established the *International Working Group on Crater Lakes (IWGCL)*. Many papers appeared and are appearing in the literature, dealing mainly with the chemistry of lacustrine exhalation. It is impossible to review here these studies that are outside the mainly geophysical character of the present study. The interested reader may refer, e.g., to Le Guern and Sigvaldason (1989), Kusakabe (1994), Varekamp et al. (2000), Déruelle et al. (2007), Varekamp and Van Bergen (2008), Descy et al. (2012), Schmid and Wüest (2012), ... and references therein.

Pumping experiments (e.g. Schmid et al., 2003, 2006; Halbwegs et al., 2004; Kling et al., 2005; Kusakabe et al., 2008) have also been carried out in the Lake Nyos, aimed to prevent the hazard deriving from thermal layering inside the lake. Also, patents and projects have been envisaged for CO₂ extraction from lakes etc. (e.g., Wüest et al., 2012). Only a limited and synthetic information is here given about the chemistry of these lakes.¹⁹

Let us consider only He, because noble gases are chemically easier. In contrast, the C and N chemistry and their isotopes are more closely related to the difficult problems of the biogeochemical cycles. However, these items are outside the general framework of the present study. According to a recent report (Metcalf, 2017), “*large underground reserves of He in East Africa are at least twice as large as first reported, ... The discovery of pockets of He in the Great Rift Valley region of Tanzania was announced late last year. The initial samples from gas seeps in the area indicated that the underground deposits contained an average of 2.6% He, mixed mostly with N ... But new measurements from the Tanzanian gas seeps now show He concentrations of up to four times the earlier average value, ... a second independent assessment of the underground He resource in Tanzania now amounts to 2.8 × 10⁹ m³... It takes millions of years for pockets of the gas, like those found in Texas and Tanzania, to accumulate underground, and the gas escapes easily into the atmosphere after use ...*

... the scientific team ... identified the location of likely He pockets in Tanzania, using a new theory of He production by underground heat sources - such as the volcanoes in Tanzania’s Rift Valley region - which can set the gas free from where it slowly forms inside ancient rocks. ... the He deposits were within a ‘Goldilocks Zone’ for He production, about 200 km from the volcanic zone around Tanzania’s Mount Rungwe ... “

Rouwet and Minoru Kusakabe at the 26th ECGS Workshop AVCOR 2007, on “*He – C – N isotope systematics of dissolved gases in Lake Nyos and Monoun (Cameroon, Western Africa)*” . AVCOR is the acronym for Active Volcanism and Continental Rifting, and ECGS for European Center for Geodynamics and Seismology.

Concerning *He* isotopes, ^3He is believed to be primordial ^4He is radiogenic, derived from the decay of ^{235}U , ^{238}U , ^{232}Th and ^{40}K , and the ratio $R \equiv ^3\text{He}/^4\text{He}$ of every given sample is usually referred to its value in air (with $\text{He} \sim 5 \text{ ppm}$) $R_a \equiv 1.4 \times 10^{-6}$. Typical values are $^3\text{He}/^4\text{He} = 8 \pm 1 R_a$ in *MORB*, $^3\text{He}/^4\text{He} < 0.01 R_a$ for radiogenic *He* (Mamyrin and Tolstikhin, 1984), and $^3\text{He}/^4\text{He} = 11 - 37 R_a$ at hotspots. Concerning *CVL*, the first measurements were carried out only after the Nyos-Monoun disasters (Sano et al., 1987, 1990), and it was found $^3\text{He}/^4\text{He} = 5.39 - 5.75 R_a$ in Lake Nyos, $^3\text{He}/^4\text{He} = 3.56 R_a$ in Lake Monoun, $^3\text{He}/^4\text{He} = 2 - 7 R_a$ in springs (Aka et al., 2001, 2001a), and $^3\text{He}/^4\text{He} = 3.9 - 7.11 R_a$ in rocks (Aka et al., 2004).

Aka et al. (2004) carried out a detailed investigation of the isotopic chemism along the *CVL*. They plot (not here

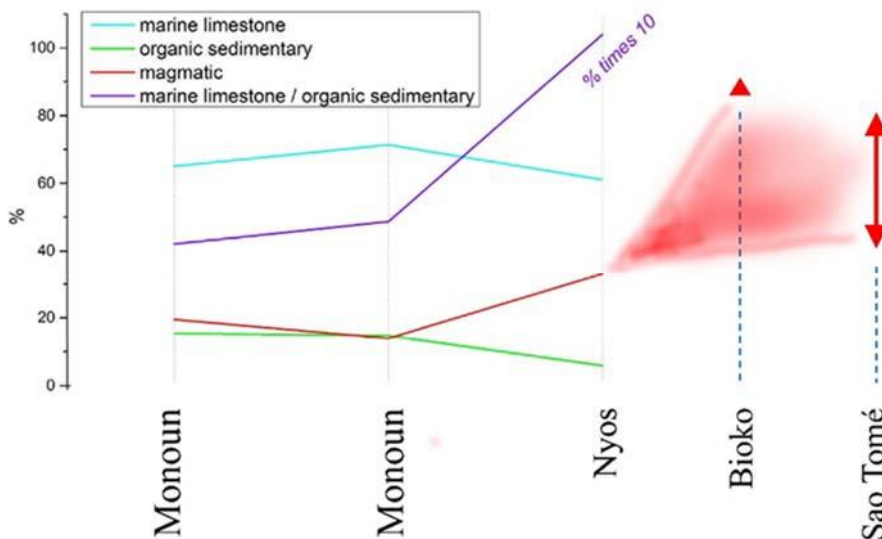


Fig. 18. Origin of *C* in the Monoun Lake, in the Nyos lake, and in the islands of Bioko and São Tomé. The islands have a comparatively greater percentage of magmatic origin. The data sources are Sano and Marty (1995) and, for Bioko and São Tomé, Aka et al. (2001). Unpublished figure.

The Monoun and Nyos lakes events had a greater percent of marine limestone *C* than of magmatic *C*. In general, both *He* and *C* data resulted stable (as expected) during 21 years measurements after the catastrophe. The *He* data fit with other measurements in free gases and in rock inclusions. It was found that $^3\text{He}/^4\text{He} \sim 3.6$ (for Monoun) $< ^3\text{He}/^4\text{He} \sim 5.7 <$ (for Nyos) $< ^3\text{He}/^4\text{He} \sim 6.8$ (expected for the NE extreme of *CVL*). Concerning *C*, it was found that magmatic *C* in volcanic arcs (4 – 20%) $<$ magmatic *C* in Nyos and Monoun (14 – 33%) $<$ magmatic *C* in *MORB* type volcanism ($> 82\%$), in SW of *CVL*.

In addition, consider also that the *CVL* is close to the triple-junction, with continental breakup occurred 130 Ma ago, i.e., to the triple rupture of the lithosphere that caused the detachment of Brazil from Africa. It is also located on the aforementioned geomagnetic anomaly doublet of Fig. 6 of Gregori et al. (2025s). That is, the Cameroon region is presumably characterized by a comparatively higher

shown) the location of the measured samples, and the variation along the *CVL* of $^3\text{He}/^4\text{He}$, $^{206}\text{Pb}/^{204}\text{Pb}$, and $^{208}\text{Pb}/^{204}\text{Pb}$, respectively, showing a substantial difference between the *CVL* and other basalts. No mention is here given about the *C* and *N* isotopic chemism. Instead, only the estimated different origin of *C* is shown in Fig. 18. Note - compared to *CVL* - the considerably larger contribution of magmatic (hence, radiogenic) sources in the volcanic islands. The two volcanic islands are Bioko and São Tomé. Bioko ($3^\circ 30' N$, $8^\circ 42' E$), also spelled Bioco, native name Otcho, is traditionally called Fernando Pó, and it is 32 km off the west coast of Cameroon. São Tomé is located a few degrees south of it ($0^\circ 20' 10'' N$, $6^\circ 40' 53'' E$). See Fig. 15.

geothermal flow. That is, the entire central and southern Africa ought to be the site of a comparatively higher geothermal flow. Therefore, limnic phenomena - such as Lake Nyos' - in some ways are a witness of some kind of intermediate condition between "normal" or "smooth" and "steady" geothermal flow vs. a typical "volcanic" environment.

The kinematics of west-central Africa was investigated by Ubangoh et al. (1998) by evaluating the *VGP* (virtual geomagnetic pole)²⁰ on samples from 154 sites in the continental sector of the *CVL*. They found six *VGPs*, belonging to rocks that - according to K-Ar dating - correspond to $\sim 0.4 - 0.9 \text{ Ma}$, $\sim 2.6 \text{ Ma}$, $\sim 6.5 - 11 \text{ Ma}$, $\sim 12 - 17 \text{ Ma}$, $\sim 20 - 24 \text{ Ma}$ and $\sim 28 - 31 \text{ Ma}$, respectively. They comment that "the results are in general agreement with other palaeomagnetic poles from Oligocene to recent formations in Africa. The first three poles for rocks formed between $\sim 0.4 - 11 \text{ Ma}$ are not significantly different from the present geographical pole. Together with other African poles for the same period, this suggests that

measured *B* at a given site is the field of a pure Earth's dipole.

²⁰ *VGP* is a frequently used concept in archæo- and palaeomagnetism, and is defined by assuming that the

the African continent has moved very little relative to the pole since ~ 11 Ma. The other three poles for rocks dated between ~ 12 – 31 Ma are significantly different from the present geographical pole, showing a ~ 5° polar deviation from the present pole in the Miocene and ~ 13° in the Middle Oligocene.”

The comparative geodynamics of Africa and South America was studied by Silver et al. (1998) who concluded that “*although the African plate’s NE-ward absolute motion slowed abruptly ~ 30 Ma ago, the South Atlantic’s spreading velocity has remained roughly constant over the past ~ 80 Ma, thus requiring a simultaneous westward acceleration of the South American plate.*” They interpret their evidence in terms of plates “*coupled to general mantle circulation*”. In contrast, according to the rationale of the present study, this is rather the expected trend of the lithosphere, while it slides down the slope of the Atlantic MOR superswell (Gregori and Leybourne, 2021, and Gregori et al., 2025a). Indeed, this is the same conclusion here inferred from several evidences - and it is the reason of the present high geodynamic activity of South America, including the rapid clockwise rotation of South America (Gregori and Leybourne, 2021; Gregori and Leybourne, 2025j).

Silver et al. (1998) refer to the hotspot reference frame. This issue is relevant. They consider the relative dynamics between MAR (Mid-Atlantic Ridge) and several hotspots of the Atlantic basin. They stress that all evidences are suggestive of a westward motion of MAR in a hotspot reference frame. The definition of the reference frame is crucial, and it should deserve a long discussion that cannot be given here. For the present purpose, the hotspot reference frame can be intuitively considered to be approximately – although not exactly - “fixed” to the mantle (Gregori and Leybourne, 2021).

Similarly to the Iceland hotspot, the Tristan da Cunha hotspot, seems to drift eastward relative to the MAR. At present, both hotspots are overlain by crust that was formed at the time of anomaly 6, ~20 Ma ago. The Azores hotspot is located some 200 km east of the adjacent MAR, analogously to nearly all other proposed Atlantic hotspots. The New England hotspot in the Great Meteor-Atlantis seamounts is located a few hundred kilometers east of the MAR. The Sierra Leone, Circe, Shona, and Discovery hotspots are isotopically distinct, and display a similar eastward-displaced position relative to MAR. Compared to the Iceland or Tristan da Cunha hotspots, the dynamic history of these hotspots is less known. However, all evidences are compatible with a westward drift of MAR relative to Atlantic hotspots occurred since at least 30 Ma. Silver et al. (1998) further comment that the South America’s higher drift velocity is correlated with the increased cordilleran activity along its western edge that began ~ 30 Ma ago, which is consistent with the clockwise rotation of South America (Gregori and Leybourne, 2021, and Gregori et al., 2025a).

Refer to the aforementioned discussion on the energy of volcanic phenomena. The roles must be considered of the energy associated with gas, compared to all others volcanic ejecta. The energy transported by the eruption gases *per se*

is of the order of ~ 1% of the total energy release. These events - such as Lake Nyos and other similar eruptions - show that, as far as no effusive release of lava occurs, gases (or hot fluids) are in any case the carriers for energy transport – and the source of relevant air-earth currents. However, only a tiny fraction of the released energy is manifested in the form of explosive gases, while the largest amount is expended to produce a mechanical work on solid matter, by giving it a corresponding amount of kinetic (and thermal) energy.

Several items of this kind deal with phase changes, chemical processes, etc. All these items are not specifically of direct concern for the present discussion. The aforementioned discussion gives a feeling of the difficulty of dealing with the processes that control soil exhalation and outgassing.

A summary

Summarizing, lava lakes - like every kind of volcanic lake - are typical of a “volcanic” environment. In contrast, a volcanic lake (either composed of lava, or of sulphur, or of water) cannot be considered a simple “strainmeter”, because it has a time varying structure, also depending on the time variation of its primary supply, and on the physicochemical processes associated with exhalation from some deeper Earth’s layers. In addition, it suffers from explosions, and in any case by water evaporation, which depends on temperature.

In general, these different morphological manifestations of release of endogenous energy are much influenced by the composition of the crust, by various amounts of water content, and by the local chemistry of the crust. Therefore, they are not suited to monitor the variations of the primary endogenous energy supply.

The best presently available example of a lava lake monitored by means of satellite is, perhaps, Lascar, a 5641 m high volcano in northern Chile (see the review by Mouginiis-Mark et al., 1993 with several pictures). However, the improved satellite monitoring facilities permit an ever-increasing capability to monitor these “point-like” features.

Lascar was reported as having during historical time only minor fumarolic activity, but no major eruption. On 16 September 1986, a powerful explosive eruption occurred, although - owing to the inaccessible site - it was reported only from Salta, Argentina, 285 km from the volcano, where ash fall was recorded. Therefore, this event destroyed the pre-existing lava lake. LTM maps allow for 30 m resolution on ground. A few pictures allowed to assess the temporal evolution of the whole phenomenon, although it is not possible to distinguish clearly between a lava lake and a hot fumarolic activity. The geostationary meteorological satellite GOES (Geostationary Operational Environmental Satellite weather satellite system 1975-1990s) provided with ~ 1 km resolution images in the visible range (0.55 – 0.75 μm) that helped to monitor the downwind dispersal of the eruption cloud. The eruption lasted less than ~ 5 min and the cloud rose up to ~ 15 km height. Thermal IR GOES images also allowed to investigate the cloud temperature.

This behavior of Lascar shows how the calorimetric criterion - i.e., reminding about the energy balance of a security valve of a pressure cooker - applies to volcanic phenomena, although on a time scale much longer compared to the time scale of human life.

Lava lakes are biased by several unknown factors. However, independent of every drawback, satellite monitoring vs. time of the few volcanic lava lakes that exist, over time can provide important information related to deep Earth's processes, at least for monitoring short-range temporal changes of the primary heat supply: lava lakes are actual "windows" open to deep Earth.

In general, lava lakes have often been an intermittent phenomenon in historical times. Piton de la Fournaise had a lava lake in 1801 when it was visited by Bory de Saint Vincent (Krafft, 1991). Halemaumau was active when the Europeans first visited Kīlauea in 1823 and it remained molten until comparatively recent times (see Fig. 9 for an analogous lake). Masaya (Nicaragua) had a lava lake intermittently during the past ~ 450 years. At present, information is reported, e.g., about a couple of lava lakes in Africa (Erta'Ale and Nyiragongo), and one in Antarctica (Erebus; first seen by Ross in 1841 during a violent eruption; its molten lava lake exists since at least 1972; see also Doermann, 2023). Due to the local uncomfortable environment, they are very difficult to permanently monitor with ground-based observations. Only Halemaumau, i.e., the Kīlauea lava lake, is monitored by a renowned volcanic observatory, but a few decades ago its surface solidified. Concerning Nyiragongo - one of Africa's most notable volcanoes - in 1977 the lava lake, in its deep summit crater, drained catastrophically through its outer flanks. Extremely fluid, fast-moving lava flows killed 50 to 100 people, and several villages were destroyed. On January 18, 2002 a river of molten rock poured from its lake, and a day after it erupted, killing dozens, swallowing buildings and forcing hundreds of thousands to flee the town of Goma. The flow continued into Lake Kivu.

Simkin and Siebert (1994) specify that "lava lakes are known from 31 volcanoes, with Kīlauea accounting for a third of the 93 recorded lava lake eruptions ... The Nyiragongo Lake ... also provided useful information during its 49 year existence, and lava lakes were still active at Erta'Ale ... , Masaya ... , and Erebus ... in 1994 ... Drilling through the crusts of such lakes as they solidified has provided valuable data on the cooling history and fractionation of magma (Peck et al., 1979; Wright et al., 1976)."

Francis et al. (1993) investigated the heat supply to lava lakes and volcanoes, by considering them as an almost permanent active phenomenon. Their rationale is in terms of deep reservoirs of magmas, magma chambers, plumbing lines, etc., which are hypothesized to be the primary heat supply for every surface manifestation. That is, they consider the supply to volcanoes in terms of a pipeline network with lava flowing inside it, reminding about the water-pipe network in a house. This ("plumber") model is manifestly in contrast with the rationale here adopted of a Joule (or friction) local heat supply to volcanism. In any case, they exploit some considerable amount of modeling,

and compare the estimated powers and energy of different lava lakes.

Stromboli - owing to its Strombolian activity that seemingly persists since at least three millennia - is a particularly intriguing case history. Francis et al. (1993) comment as follows. "Giberti et al., (1992) calculated that ~ 200 kg sec⁻¹ of magma must be supplied to the upper parts of Stromboli's edifice, to sustain heat losses through degassing and conduction, and to account for the inferred gas flux. They suggested that this supply might come either from a deep mantle source or from convective overturn of large magma chamber; however, U-series isotopic disequilibria studies for both Stromboli and Etna suggest that the residence time for shallow magma is only several tens years ... indicating that their persistent surface manifestations cannot be sustained by convective circulation between surface vents and un-replenished reservoirs. Even a conservative interpretation of the thermal and gas flux data therefore implies that new magma must be supplied to these and similar volcanoes at rates of hundreds or thousands of kilograms per second. Whenever the inferred steady-state supply of mantle-derived magma exceeds the rate of eruption, formation of sub- and/or intra-volcanic intrusive complexes is indicated."

In contrast, it is here proposed that the heat supply to all these volcanic phenomena requires no external magma input. Rather, electric currents- supplied by the TD (tide-driven) geodynamo - release Joule heat directly at some shallow depth. This speculation can be investigated by means of geo-e.m. (electromagnetic) records carried out during several years in volcanic and geothermal areas. In addition, this explanation seems consistent even with the lightning flashes that are observed inside volcanic plumes (see Gregori et al., 2025t).

Harris and Ripepe (2007) made an extensive review of the Stromboli activity and modeling, by combining seismic, infrasonic and thermal records. They inferred some constraint on the shallow system geometry and on the dynamics of the explosive events. They model "chamber depths, gas and magma fluxes, shallow system magma residence times, explosion source depths, and the rise/ejection velocities of ascending gas slugs and ejecta." They interpret the Strombolian phenomenon "in terms of the coalescence of gas within the magma to form large gas slugs ... ". They find "that gas coalescence occurs at a depth of ~ 260 m, with a typical event frequency of ~ 9 hour⁻¹. Infrasonic and thermal data show the explosion source to be located 20 – 220 m below the vent. Thermal data give emission velocities for the ejected fragments of 8 – 20 m sec⁻¹, which converts to gas jet velocities of 23 – 39 m sec⁻¹." These features can fit very well in the aforementioned interpretation which is here proposed. Harris and Ripepe (2007) also recognize that "eruptions ... can be grouped into two characteristic types (simple and complex - each of which characterizes a particular crater, NE and SW, respectively) ... The system does, however, appear robust, maintaining its characteristic Strombolian eruption style after significant effusive phases and more energetic explosive events."

The Caronia phenomenon

Sicily has a peculiar tectonic setting (Fig. 14) and some unusual phenomena are sometimes reported. For instance, remind about the town of Riesi mentioned above, located south of Caltanissetta. Abruptly the ground floor temperature in a house warmed up to $\sim 88^{\circ}\text{C}$.

A very similar phenomenon - although of comparatively negligible intensity but localized on the space size of a house - was observed in January 2004 at the site Canneto di Caronia (in the province of Messina, along the coast of Sicily, approximately halfway between Messina and Palermo; Canneto di Caronia is a small fraction of the town of Caronia, a fraction with only ~ 40 inhabitants; Fig. 19). This phenomenon was an almost point-like occurrence, a unique experiment, performed with a great spatial and temporal resolution, where the local inhabitants were the unwilling, although very accurate, "detectors". They were only frightened, with no consequence for their safety.



Fig. 19. Canneto di Caronia is just along the beach in the town of Caronia, located only several tens of kilometers from the volcanic archipelago of the Aeolian Islands. The background map is a detail of a chart in Drago and Boroli (1995).

The report here given relies on an inspection required by the Italian *Civil Protection* to two of the authors (GPG and GP). Abruptly, large fires simultaneously spread out from all plug-ins of the electrical circuit of a house. A few other nearby houses experienced similar, though less violent, phenomena. For several weeks or a few months, these occurrences continued - more or less continuously - with a variety of morphologies, even changing the frequency band of the leading e.m. perturbation. It was later claimed that analogous effects continued in the subsequent years ... but mass media no more reported news about this ...

All these occurrences, including also some repeated reported beaching of dead marine fauna, seemingly nicely fit into the aforementioned rationale. A few animals were found dead on the beach, and the authorities assessed that the likely cause appeared being a lack of oxygen (i.e., it was a presumable geogas exhalation from soil). In addition, exactly in those same days, marine circulation reversed direction in the Adriatic Sea - from the normal counterclockwise state to clockwise direction - denoting an abrupt anomalous increase of geothermal heat flow from

the sea floor. Moreover, the strong Stromboli paroxysm (see Gregori and Paparo, 2006) had shortly preceded this Caronia phenomenon, denoting a generalized anomalous increase of release of endogenous heat during those several months in the central Mediterranean area. A few months after Caronia, the atmospheric temperature throughout Europe was exceptionally high. Maybe, it is only a coincidence, but all these relevant climatic anomalies could be related to one another, and they could be caused and supplied by a unique prime trigger and energy source.

The national - and some international - mass media extensively reported about these Caronia events. Even exorcists were called ... No full official complete explanation was given by authorities, other than some vague mention about some presumable classified anthropic actions - a hypothesis that evidently cannot be checked by scientists. This is an easy "comment" when no other explanation is available. After a few years, the authorities claimed that even the "official" explanation in terms of mysterious manmade actions was no more credible. Hence, no "official" explanation remains.

This entire phenomenon, however, can be very simply explained by natural causes. These occurrences are probably not rare, although they can be detected only whenever and wherever, owing to a lucky circumstance, some manmade device - such as a house located at the correct site - is available like a reliable and efficient measuring instrument.

For instance, Rubino et al. (2012) monitored abyssal temperature and velocity in the framework of the *Neutrino Mediterranean Observatory (NEMO)*, located south of Sicily in the Ionian abyssal plain of Eastern Mediterranean. They detected abyssal vortices at depths $> 2,500\text{ m}$. "*The eddies consist of chains of near-inertially pulsating mesoscale cyclones/anticyclones. They are embedded in an abyssal current flowing towards NNW. The paucity of existing data does not allow for an unambiguous determination of the vortex origin. A local generation mechanism seems probable, but a remote genesis cannot be excluded a priori.*"

These phenomena are likely to occur at several locations, and comparatively frequently, although displaying an eventually very different morphology. It would be surprising if these events did not occur. Their understanding can be fundamental even for the unprecedented use of a natural, and maybe even exploitable, energy source, such as, e.g., geothermal flux on sea floors. Hence, it is worthwhile considering this Caronia 2004 event in better detail, due to its relevance for subsequent discussion. It is some kind of "test" study experiment.

Canneto di Caronia is a narrow strip, with a cross-section of several tens of meters, comprised between a DC electrified railway and the Tyrrhenian coast. It comprises only a few ten houses. Mostly one house was stricken. A nearby house, some ten meters apart, suffered by lesser consequences. That is, the phenomenon has a large spatial gradient, and it significantly changes on the scale-size of the order of $\sim 10\text{ m}$. Let us refer to the house that suffered by the strongest effect. GPG and GP had the opportunity to

make a personal inspection a few days after the event. The house is almost on the beach, and a very thin salt layer is likely to be located outside the insulator of every electric wire, while - as a standard - a conspicuous amount of humidity is in the air (which is the typical condition at every site very close to seacoast). The entire set of different events can be interpreted analogously to a St. Elmo fire. It is a “corona effect”, where electric currents flow inside the conductors of the house, including also the electric currents flowing outside the plastic insulator around the wires of the electrical circuit of the house. The house is only composed of a ground floor, plus a simple roof. It is constructed of cement bricks, with no steel reinforcement. Hence, it has no Faraday cage that protects it. The standard internal electric circuit for the power supply is composed, of flexible plastic tubes embedded in the walls, and the wires are inserted inside the tubes.

The first phenomenon was manifested like abrupt flames, coming out simultaneously from all plug-ins. The flames produced black strips on the walls, everyone ~ 0.5 – 1 m long. All (much frightened) people were evacuated. Upon a detailed inspection of the wires, it clearly appeared that they surprisingly suffered by no excess electric current inside them. Rather, the plastic cover appeared to have melted and caused fire, while the wire was incredibly intact.²¹

The owner of the house took off the wires of the electrical circuit from their plastic tube. The phenomenon was repeated, but it struck the water pipes. Curiously, the water pipes and the electric boiler were intact. The boiler was held to the wall by “L” shaped nails, of a few centimeters size, handmade. The nails had points and were hammered into small plastic sticks inserted into the wall. The “corona effect” caused sparks outgoing from the sharp points of the “L” nails. Sparks melted the plastic of the rod. Flames were thus produced, and the wall had a few tens of centimeter black strips around the nails.

The owner did not want to abandon his house. He took off the furniture, and he put a mattress in the middle of the living room, where he could eventually sleep. The mattress had steel springs inside. The fire hit the mattress. Upon simple direct inspection it appeared evident that the trigger of the fire was right from the points of the steel-springs, clearly originated by sparks outgoing from them.

For the sake of completeness, it should be mentioned that the owner of the house also mentioned that he was acquainted with fishing in a small boat. He used a compass, which seemingly resulted in being abruptly unreliable. No scientific check could be made for this. He obviously was somewhat shocked, and – perhaps - his report was not fully reliable, although his report appeared reasonable. On the other hand, nobody knows whether, if during similar very localized events some local features of geomagnetic

anomalies can eventually abruptly change on some very small spatial scale.

In the subsequent days, the phenomenon changed. According to extensive information by mass media, several car alarms were reported, within a slightly larger area (a few kilometers in linear extension), to be activated for no apparent reason. Automatic closures of cars abruptly closed or opened with no command, etc. Everything appeared like in the case that a natural e.m. signal, of frequency varying in time, was more or less erratically and seemingly randomly generated. Maybe, on a speculative basis, the change of frequency might be consistent with a supposedly upward penetration of the sea-urchin spike (see Figs 7 and 8 of Gregori et al., 2025a), by which the resonance frequency of the underground electric circuit is consequently changed. If this guess is correct, the area was therefore affected by a comparatively rapid increase of endogenous heat release vs. time.

Concerning the biosphere, somebody claimed that several dead fish were seen in the sea not far from this site, and a dog and a chicken were found dead on the beach. They reported (but we had no official report about this) that the dog was excessively putrefied, while the chicken could be analyzed.²² It was reported that they found that the chicken died by lack of oxygen. Hence, the likely cause is anomalous soil exhalation of geogas.

Finally, the authorities decided to set up more efficient grounding for every house, although they put no lightning rod. This was a hazard, because, if the phenomenon is going to be eventually repeated while somebody takes a shower, with no lightning rod he would be inside the electric circuit of the St. Elmo fire, with potential likely lethal consequences.

In addition, they carried out measurements aimed to monitor spontaneous potentials by means of long cables between land and the shelf offshore. They found no anomalous result. This is reasonable, because one can measure the effects of an intense electric air-earth current (a lightning or other) only while the discharge is ongoing. Measuring effects either before or after the strike is useless.

The Caronia phenomenon was a real unexploited first case history in the poorly explored realm of e.m. coupling between soil and ionosphere. It was very intriguing evidence of air-earth currents. It was unfortunate that this very rare event - which is very likely to be frequent in nature, while only very seldom can we detect it - was not investigated and monitored. Thus, the amount of energy being associated with an almost permanent St. Elmo fire could not be measured. This kind of phenomena can be considered as a test experiment, aimed at carrying out a very accurate and unprecedented investigation of the details of the involved mechanisms, also upon considering the potential exploitation of these phenomena as a possible

²¹ Private communication by Bruno Azzerboni, Professor of *Electrical Technology* at the *Faculty of Engineering* of the *University of Messina*, whom we thank.

²² According to the information this analysis was carried out by the *RIS, Reparto Indagini Scientifiche* of

Carabinieri, the most authoritative Italian national institution for scientific investigations concerning criminal events.

renewable energy source (see Gregori and Leybourne, 2025l).

Remote sensing by satellite provides an excellent coverage – such as, e.g., SST (sea surface temperature) changes in the Gulf of Mexico that give energy to hurricanes (see Gregori and Leybourne, 2025j). The spatial resolution, however, is limited by the size of the pixel. For instance, consider Fig. 20 and compare with Fig. 17.

Forest fires are monitored by the *Moderate Resolution Imaging Spectroradiometer (MODIS)* on NASA's *Terra* satellite. Fig. 21 shows the monthly mean map for June 2004. Whether the fires are natural or agricultural, they are a source of air-earth currents. A more extensive discussion of wildfires is given in Gregori and Leybourne (2025i).

Conclusion

Air–earth currents are a ubiquitous phenomenon, displaying large spatial gradients, on a very small scale, and implying huge amounts of often unnoticed exhalation phenomena. They are an essential component in the global climate atmospheric electrical circuit, and it is almost impossible to account for all of them. Every phenomenon requires careful consideration before discarding it as being irrelevant. A monitoring array – based also on unusual reports – can be very useful to integrate satellite remote sensing monitoring that gives only spatially averaged information on the pixel size, and a time resolution

compatible with satellite orbit.

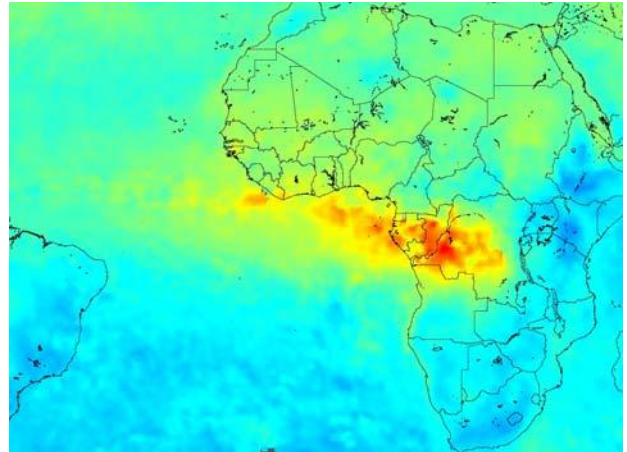


Fig. 20 - Forest fires in West Central Africa, June, 2004. False-color image showing CO in the lower atmosphere averaged for the entire month of June 2004. The unit here is molecules $CO\ cm^{-2}$. CO is a good tracer of pollution and is produced as a by-product of the combustion associated with wildfires and agricultural fires. Based on records by the *Measurements Of Pollution In The Troposphere (MOPITT)* instrument aboard NASA's *Terra* satellite. NASA image by Jesse Allen using data courtesy of NCAR/UCAR MOPITT instrument team. NASA copyright free policy. With kind UCAR permission ("Fair Use").



Fig. 21 - Fire maps for June 2004, based on observations from the *Moderate Resolution Imaging Spectroradiometer (MODIS)* on NASA's *Terra* satellite. NASA copyright free policy.

Acknowledgement

We want to acknowledge all co-workers that, in different ways and at different times, contributed to the exploitation of the analyses mentioned in the present study. We are also thankful for the warm encouragement we had from several outstanding scientists. We thank Dr. Mario Mattia for information on the Lanuvio anomalous soil exhalation. We thank Bruno Azzerboni, Professor of

Electrical Technology at the *Faculty of Engineering* of the *University of Messina*, for discussion on the Caronia phenomenon.

Funding Information

G. P. Gregori retired since 2005. G. Paparo retired in 2004, and suddenly died in 2023 after having edited the present paper. B.A. Leybourne is a semi-retired independent researcher.

Author's Contributions

This study derived from a long-lasting cooperation and discussion by the authors. The backbone draft was prepared by the first author, although a large number of ideas resulted from the emergence of long-lasting discussions, and the paternity of ideas can be hardly separated. G. Paparo made a relevant contribution in the discussion of the Caronia phenomenon. B.A. Leybourne contributed to the final discussion and setting of the whole paper.

Ethics

This article is original and contains unpublished material. Authors declare that there are no ethical issues and no conflict of interest that may arise after the publication of this manuscript.

References

- Aka, F. T., M. Kusakabe, and K. Nagao, 2001a. New K-Ar ages for Lake Nyos maar, Cameroon. Implications on hazard evaluation. *Géosciences au Cameroun*, 1: N1A
- Aka, F.T., K. Nagao, M. Kusakabe, H. Sumino, G. Tanyileke, B. Ateba, and J. Hell, 2004. Symmetrical helium isotope distribution on the Cameroon Volcanic Line, West Africa, *Chemical Geology*, 203 (3/4): 205-223; DOI:10.1016/j.chemgeo.2003.10.003
- Aka, F.T., M. Kusakabe, K. Nagao, and G. Tanyileke, 2001. Noble gas isotopic compositions and water/gas chemistry of soda springs from the islands of Bioko, São Tomé and Annobon, along with Cameroon Volcanic Line, West Africa, *Applied Geochemistry*, 16 (3): 323-338; DOI:10.1016/S0883-2927(00)00037-8
- Anonymous*, 2015ax. Giant squid surfaces in Japanese harbor. *EarthSky*, issued Dec 29, 2015
- Bartels, M., 2018d. Melting permafrost below Arctic lakes is even more dangerous to the climate, NASA warns, *Space.com*, issued Aug 18, 2018
- Betz, E., 2015a. Hawaii's swelling lava lake charts a volcano's hidden plumbing EOS, *Transactions of the American Geophysical Union*: 96, DOI:10.1029/2015EO042055
- Bullard, F.M., 1984. *Volcanoes of the Earth. II Revised Edition*, University of Texas Press, Austin, pp: 629
- Casey, J.L., 2017. Is Katla ready to erupt? *New Concepts in Global Tectonics, Journal*, 5 (3): 460-463
- Choi, C.Q., 2016h. School-bus-size giant squid may be lurking deep in the sea, *Live Science*, issued May 25, 2016
- Ciotoli, G., G. Etiope, F. Florindo, F. Marra, L. Ruggiero, and P. E. Sauer, 2013. Sudden deep gas eruption nearby Rome's airport of Fiumicino, *Geophysical Research Letters*, 40 (21): 5632-5636; DOI:10.1002/2013GL058132
- Coro, G., C. Magliozzi, A. Ellenbroek, and P. Pagano, 2016. Improving data quality to build a robust distribution model for *Architeuthis dux*, *Ecological Modelling*, 305: 29-39; DOI:10.1016/j.ecolmodel.2015.03.011
- Critelli, S., 1999. The interplay of lithospheric flexure and thrust accommodation in forming stratigraphic sequences in the southern Apennines foreland basin system, Italy. *Rendiconti Lincei. Scienze Fisiche e Naturali*, sezione 9, 10: 257-326
- Deamer, K., 2017. 'Gateway to hell': volcano caught spewing lava in satellite image, *Live Science*, issued Jan 31, 2017
- Deatrick, E., 2016. Eyjafjallajökull gave lava and ice researchers an eyeful, *EOS, Transactions of the American Geophysical Union*: 97, DOI:10.1029/2016EO055113
- Decker, R.W., and Decker, B., 1981. The eruption of Mount. St. Helens, *Scientific American*, 244 (3): 68-80. Italian translation "Le eruzioni del Mount St. Helens", *Le Scienze*, 26 (153): 14-27
- Déruelle, B., I. Ngounouno, and D. Demaiffe, 2007. The 'Cameroon hot line' (CHL): a unique example of active alkaline intraplate structure in both oceanic and continental lithospheres, *Comptes Rendus Geoscience*, 339 (9): 589-600
- Descy, J.-P., F. Darchambeau, and M. Schmid, 2012. Lake Kivu: past and present, *Lake Kivu, Aquatic Ecology Series*, 5: 1-11
- Doermann, L., 2023. The towering inferno: Mount Erebus' dramatic emergence from the Antarctic clouds, *SciTechDaily*, issued November 29, 2023
- Drago, M., and A. Boroli, (eds), 1995. *Grande atlante geografico d'Europa e d'Italia*, Istituto Geografico De Agostini, Novara, pp: 256+LXXVII
- Feminò, F., 2008. Fort, l'apostolo dell'incredibile, *Le Scienze*, (478): 111-111
- Fitton, J.G., and H.M., Dunlop, 1985. The Cameroon line, West Africa, and its bearing on the origin of oceanic and continental alkali basalt, *Earth and Planetary Science Letters*, 72: 23-38
- Francis, P., C. Oppenheimer, and D. Stevenson, 1993. Endogenous growth of persistently active volcanoes. *Nature*, 366: 554-557
- Fudali, R.F., and W.G. Melson, 1970. Ejecta velocities, magma chamber pressure and kinetic energy associated with the 1968 eruption of Arenal volcano. *Bulletin of Volcanology*, 35: 383-401
- Giberti, G., C. Jaupart, and G. Sartoris, 1992. Steady-state operation of Stromboli volcano, Italy: constraints on the feeding system. *Bulletin of Volcanology*, 54: 535-541
- Glaze, L., P.W. Francis, and D.A. Rothery, 1989. Measuring thermal budgets of active volcanoes by satellite remote sensing. *Nature*, 338: 144-146
- Gorshkov, G.S., 1959. Gigantic eruption of volcano Bezymianny. *Bulletin of Volcanology*, ser. 2, 20: 77
- Gorshkov, G.S., 1960. Determination of the explosion energy in some volcanoes according to barograms. *Bulletin of Volcanology*, ser. 2, 23: 141
- Gouhier, J., J. Nougier, and D. Nougier, 1974. Contribution à l'étude volcanologique du Cameroun ('Ligne du Cameroun'-Adamaoua). *Annales de la Faculté des Sciences, Université de Yaoundé, Cameroun*, 17: 69-78
- Gregori, G.P., and M.T. Hovland, 2025. Go for the anomaly – a golden strategy for discovery? *Seepology & the*

- origin and crucial role of the biosphere - Earth and planetary objects - Supercritical water and serpentinization. *New Concepts in Global Tectonics, Journal*, 13, (9): 1337-1491
- Gregori, G.P., 2020. Climate change, security, sensors. *Acoustics*, 2: 474-504; DOI:10.3390/acoustics2030026.[https://www.mdpi.com/2624-599X/2/3/26/html]
- Gregori, G. P., and B. A. Leybourne, 2021. An unprecedented challenge for humankind survival. Energy exploitation from the atmospheric electrical circuit, *American Journal of Engineering and Applied Science*, 14 (2): 258-291; DOI:10.3844/ajeassp.2021.258.291
- Gregori, G. P., and B. A. Leybourne, 2025c. The solar cycle and MiniMax - Effects on other planets Present issue of *New Concepts in Global Tectonics, Journal*
- Gregori, G. P., and B. A. Leybourne, 2026d. Measuring the electric field at ground. *New Concepts in Global Tectonics, Journal*, 14, (2): 120-128
- Gregori, G. P., and B. A. Leybourne, 2026e. The physics of electrical discharges – I. Small-scale phenomena - Fog - atmospheric precipitation – BLs. *New Concepts in Global Tectonics, Journal*, 14, (2): 129-152
- Gregori, G. P., and B. A. Leybourne, 2026g. The physics of electrical discharges – III. Sparks and lightning - electrostatics of the ionosphere – TLEs - plasma jets collimation – Birkeland currents & sea-urchin spikes - stellar and galactic alignments. *New Concepts in Global Tectonics, Journal*, 14, (2): 171-207
- Gregori, G. P., and B. A. Leybourne, 2025i. Wildfires from the Banda Sea through Beijing and through Karakoram. *New Concepts in Global Tectonics, Journal*, 13, (6): 854-887
- Gregori, G. P., and B. A. Leybourne, 2025j. The energy supply to hurricanes. *New Concepts in Global Tectonics, Journal*, 13, (5): 731-786
- Gregori, G. P., and B. A. Leybourne, 2025l. Conclusion – Exploitation of the electrostatic energy of the atmosphere, *New Concepts in Global Tectonics, Journal*, 13, (2): 336-343
- Gregori, G.P., and G. Paparo, 2006. The Stromboli crisis of 28÷30 December 2002. *Acta geodaetica et geophysica Hungarica*, 41 (2): 273-287
- Gregori, G. P., B. A. Leybourne, and F. F. Bonavia, 2025v. The origin of lavakas. *New Concepts in Global Tectonics, Journal*, 13, (5): 787-811
- Gregori, G. P., and B. A. Leybourne, 2025c. The solar cycle and MiniMax - Effects on other planets. Present issue of *New Concepts in Global Tectonics, Journal*
- Gregori, G. P., B. A. Leybourne, and J. R. Wright, 2026d. Generalized Cowling theorem and the Cowling dynamo. *New Concepts in Global Tectonics, Journal*, 14, (1): 90-112
- Gregori, G. P., B. A. Leybourne, Dong Wenjie, and Gao Xiaoqing, 2025h. Shallow geotherms. *New Concepts in Global Tectonics, Journal*, 13, (8): 1080-1169
- Gregori, G. P., B. A. Leybourne, G. Paparo†, and M. Poscolieri, 2025a. The global Sun-Earth circuit. Present issue of *New Concepts in Global Tectonics, Journal*
- Gregori, G. P., B. A. Leybourne, U. Coppa, and G. Luongo, 2025t. Lightning and volcanic plumes. *New Concept of Global Tectonics*, 13, (6): 920-967
- Gregori, G. P., M. T. Hovland, B. A. Leybourne, S. Pellis, V. Straser, B. G. Gregori, G. M. Gregori, and A. R. Simonelli, 2025w. Air-earth currents and a universal “law”: filamentary and spiral structures - Repetitiveness, fractality, golden ratio, fine-structure constant, antifragility and “statistics” - The origin of life, *New Concepts in Global Tectonics, Journal*, 3, (1): 106-225
- Gregori, G.P., and B.G. Gregori, 2025. *The universe out of the box - New foundations of physics - Rhythms, Golden Ratio, origin of life, antifragility*, Europe Books
- Guarnieri, P., and S. Carbone, 2003. Assetto geologico e lineamenti morfostrutturali dei bacini plio-quadernari del Tirreno meridionale. *Bollettino della Società Geologica Italiana e del Servizio Geologico d'Italia*, 122: 377-386
- Gumper, F., and P.W. Pomeroy, 1970. Seismic wave velocities and Earth structure on the African continent. *Bulletin of the Seismological Society of America*, 60: 651-668
- Halbwachs, M., J.-C. Sabroux, J. Grangeon, G. Kayser, J.-C. Tochon-Danguy, A. Felix, J.-C. Béard, A. Villeveille, G. Vitter, P. Richon, A. Wüest, and Hell, 2004. Degassing the “Killer Lakes” Nyos and Monoun, Cameroon, EOS, *Transactions of the American Geophysical Union*, 85 (30): 281-285; DOI:10.1029/2004EO300001
- Harris, A., and M. Ripepe, 2007. Synergy of multiple geophysical approaches to unravel explosive eruption conduit and source dynamics – A case study from Stromboli, *Chemie der Erde*, 67: 1–35
- Hédervári, P., 1963. On the energy and magnitude of volcanic eruptions. *Bulletin of Volcanology*, ser. 2, 25: 373-386
- Hickok, K., 2018. Divers find enormous, creepy squid on New Zealand beach, *Live Science*, issued Aug 27, 2018
- Hickok, K., 2018e. 145 pilot whales found dead on remote New Zealand beach. Nobody knows why, *Live Science*, issued Nov 27, 2018
- Hickok, K., 2019. Why are so many gray whales washing up dead on California's coast? *Live Science*, issued Apr 18, 2019
- Holloway, M., 2000. The killing lakes, *Scientific American*, 283, July: 92-99
- Hynek, B.M., K.L. Rogers, M. Antunovich, G. Avarad, and G.E. Alvarado, 2018. Lack of microbial diversity in an extreme Mars analog setting: Poás Volcano, Costa Rica, *Astrobiology*; DOI:10.1089/ast.2017.1719
- Kling, G.W., M.A. Clark, G.N. Wagner, H.R. Compton, A.M. Humphrey, J.D. Devine, W.C. Evans, J.P. Lockwood, M.L. Tuttle, and E.J. Koenigsberg, 1987. The 1986 Lake Nyos Gas Disaster in Cameroon, West Africa, *Science*, 236 (4798): 169-175; DOI:10.1126/science.236.4798.169
- Kling, G.W., W.C. Evans, G. Tanyileke, M. Kusakabe, T. Ohba, Y. Yoshida, and J.V. Hell, 2005. Degassing Lakes Nyos and Monoun: Defusing certain disaster,

- Proceedings of the National Academy of Sciences of U S A*, 102 (40): 14185-14190
- Krafft, M., 1991. Les feux de la Terre. Histoire des volcans. Gallimard, Paris. English translation: Volcanoes: fire from the Earth, published by Harry N. Abrams, New York in 1993, pp: 207. Italian translation: I vulcani. Il fuoco della Terra (with additions) published by Universale Electa/Gallimard, Scienze, 1993, pp: 192
- Kusakabe, M., (ed.), 1994. Special issue: geochemistry of crater lakes, *Geochemical Journal*, 28 (3): 137-138 (Preface)
- Kusakabe, M., T. Ohba, Issa, Y. Yoshida, H. Satake, T. Ohizumi, W.C. Evans, G. Tanyileke, and G.W. Kling, 2008. Evolution of CO₂ in Lakes Monoun and Nyos, Cameroon, before and during controlled degassing, *Geochemical Journal*, 42 (1), Special Issue: Geochemistry of volatiles in the solid Earth and their release to the atmosphere: 93-118; DOI:10.2343/geochemj.42.93
- Ladbury, R., 1996. Model sheds light on a tragedy and a new type of eruption. *Physics Today*, 49 (5): 20-22
- Le Guern, F., and G.E. Sigvaldason, (eds), 1989. Special issue: the Lake Nyos Event and Natural CO₂ Degassing, I, *Journal of Volcanology and Geothermal Research*, 39 (2/3): 95-275
- Lee, D.C., A.N. Halliday, J.G. Fitton, and G. Poli, 1994a. Isotopic variations with distance and time in the volcanic islands of the Cameroon line: evidence for a mantle plume origin. *Earth and Planetary Science Letters*, 123: 119-138
- Mamyrin, B.A., and I.N. Tolstikhin, 1984. Helium isotopes in nature, Elsevier (Develop. Geochem., vol. 3), Amsterdam etc., pp: 273
- Marzoli, A., E.M. Piccirillo, P.R. Renne, G. Bellieni, M. Iacumin, J.B. Nyobe, and A.T. Tongwa, 2000. The Cameroon Volcanic Line revisited: petrogenesis of continental basaltic magmas from lithospheric and asthenospheric mantle sources, *Journal of Petrology*, 41 (1): 87-109
- McClain, C.R., M.A. Balk, M.C. Benfield, T.A. Branch, C. Chen, J. Cosgrove, A.D.M. Dove, L.C. Gaskins, R.R. Helm, F.G. Hochberg, F.B. Lee, A. Marshall, S.E. McMurray, C. Schanche, S.N. Stone, and A.D. Thaler, 2015. Sizing ocean giants: patterns of intraspecific size variation in marine megafauna. *PeerJ*, 3: e715; DOI:10.7717/peerj.715
- Metcalfe, T., 2017. Huge underground cache of helium in Africa could avert global shortage, *Live Science*, issued Oct 6, 2017
- Mouginis-Mark, P J., D.C. Pieri, and P.W. Francis, 1993. Volcanoes. In Atlas of satellite observations related to global change, Gurney, R.J., J.L. Foster, and C.L. Parkinson, (eds), Cambridge University Press, Cambridge etc., pp: 341-357
- Njilah, I.K., 1991. Geochemistry and petrogenesis of Tertiary-Quaternary volcanic rocks from Oku-Ndu area, N.W. Cameroon. Unpublished Ph.D. Thesis, University of Leeds
- Nnange, J.M., Y.H. Poudjom Djomani, J.D. Fairhead, and C. Ebinger, 2001. Determination of the isostatic compensation mechanism of the region of the Adamawa dome, west central Africa using the admittance technique of gravity data. *African Journal of Science, Technology, Science and Engineering Series*, 1 (4): 29-35
- Oddsson, B., M.T. Gudmundsson, B.R. Edwards, T. Thordarson, E. Magnússon, G. Sigurðsson, and B. Oddsson, 2016. Subglacial lava propagation, ice melting and heat transfer during emplacement of an intermediate lava flow in the 2010 Eyjafjallajökull eruption, *Bulletin of Volcanology*, 78: 48-; DOI:10.1007/s00445-016-1041-4
- Oppenheimer, C., and D. Stevenson, 1989. Liquid sulfur lakes at Poás volcano. *Nature*, 342: 790-793
- Paparo, G., G.P. Gregori, A. Taloni, and U. Coppa, 2004. Acoustic emissions (AE) and the energy supply to Vesuvius - "Inflation" and "deflation" times. *Acta Geodaetica et Geophysica Hungarica*, 39 (4): 471-480; DOI:10.1556/AGeod.39.2004.4.14
- Parotto, M., and A. Praturlo, 2004. The southern Apennine arc, Special Volume of the Italian Geological Society for the IGC 32, Florence-2004, pp: 33-58
- Pasternack, G.B., and J.C. Varekamp, 1997. Volcanic lake systematics-I. Physical constraints, *Bulletin of Volcanology*, 58 (7): 528-538
- Pavese, M.P., 1992. Historical geophysics of ancient ages and the contribution of Latin epigraphy. In W. Schröder, and J.-P. Legrand, (eds), *Solar terrestrial variability and global change*, Interdivisional Commission on History of IAGA, Bremen-Roennebeck, pp: 263-279
- Paxton, C.G.M., 2016. Unleashing the Kraken: on the maximum length in giant squid (*Architeuthis* sp.), *Journal of Zoology*, 300 (2): 82-88; DOI:10.1111/jzo.12347
- Peck, D.L., T.L. Wright, and Robert W. Decker, 1979. The lava lakes of Kilauea, *Scientific American*, 241 (October): 114-128
- Perret, F.A., 1924, The Vesuvius eruption of 1906. Carnegie Institution of Washington, Publication 339, Washington D.C.
- Pietrangeli, C., 1951. Bidentalìa. *Atti della Pontificia Accademia Romana di Archeologia, Rendiconti*, 25-26: 37-51
- Rezanov, I.A., 1980. Catastrophes in the Earth's History, Mir Publ., Moscow. Revised English edition published in 1984, pp: 167
- Rikitake, T., 1976. Earthquake prediction. Elsevier, Amsterdam etc., pp: 357
- Rowe, G.L., S. Ohsawa, B. Takano, S.L. Brantley, J.F. Fernandez, and J.H. 1992b. Using crater lake chemistry to predict volcanic activity at Poas Volcano, Costa Rica, *Bulletin of Volcanology*, 54: 494-503
- Rowe, G.L., S.L. Brantley, M. Fernandez, J.F. Fernandez, A. Borgia, and J.H. Barquero, 1992a. Fluid-volcano interaction in an active stratovolcano: the crater lake system of Poas Volcano, Costa Rica, *Journal of Volcanology and Geothermal Research*, 49: 23-51
- Rubino, A., F. Falcini, D. Zanchettin, V. Bouche, E. Salusti, M. Bensi, G. Riccobene, G. De Bonis, R. Masullo, F. Simeone, P. Piattelli, P. Sapienza, S. Russo, G. Platania,

- M. Sedita, P. Reina, R. Avolio, N. Randazzo, D. Hainbucher, and A. Capone, 2012. Abyssal undular vortices in the Eastern Mediterranean basin, *Nature Communications*, 3: article no. 834; DOI:10.1038/ncomms1836
- Rymer, H., and G. Brown, 1989. Gravity changes as a precursor to volcanic eruption at Poás volcano, Costa Rica. *Nature*, 342: 902-905
- Sano, Y., and B. Marty, 1995. Origin of carbon in fumarolic gas from island arcs, *Chemical Geology*, 119 (1/4): 265-274; DOI:10.1016/0009-2541(94)00097-R
- Sano, Y., H. Wakita, T. Ohsumi, and M. Kusakabe, 1987. Helium isotope evidence for magmatic gases in Lake Nyos, Cameroon, *Geophysical Research Letters*, 14 (10): 1039-1041; DOI:10.1029/GL014i010p01039
- Sano, Y., M. Kusakabe, J.-I. Hirabayashi, Y. Nojiri, H. Shinohara, T. Njine, and G. Tanyileke, 1990. Helium and carbon fluxes in Lake Nyos, Cameroon: constraint on next gas burst, *Earth and Planetary Science Letters*, 99 (4): 303-314; DOI:10.1016/0012-821X(90)90136-L
- Sano, Y., T. Kagoshima, N. Takahata, Y. Nishio, E. Roulleau, D.L. Pinti, and T.P. Fischer, 2015. Ten-year helium anomaly prior to the 2014 Mt Ontake eruption, *Nature*, *Scientific Reports*, 5: article no. 13069; DOI:10.1038/srep13069
- Sapper, K., 1903. Esplorazione della crosta terrestre. Article within the encyclopedia *Universo ed Umanità, Storia dei progressi umani nella conoscenza e nel dominio delle forze naturali*, ed. by H. Kraemer et al., vol. I: 17-292. Italian translation from the German, with notes by Luigi de Marchi et al., printed by Casa Editrice Dottor Francesco Vallardi, Milano
- Sassa, K., 1936. Micro-seismometric study on eruptions of the volcano Aso. *Memoirs of the College of Science, Kyoto Imperial University*, 19 (1): 11-56 (+4+3)
- Schmid, M., A. Lorke, A. Wüest, M. Halbwachs, and G. Tanyileke, 2003. Development and sensitivity analysis of a model for assessing stratification and safety of Lake Nyos during artificial degassing. *Ocean Dynamics*, 53 (3): 288-301
- Schmid, M., and A. Wüest, 2012. Stratification, mixing and transport processes in Lake Kivu. In *Lake Kivu, Aquatic Ecology Series*, 5: 13-29
- Schmid, M., M. Halbwachs, and A. Wüest, 2006. Simulation of CO₂ concentrations, temperature, and stratification in Lake Nyos for different degassing scenarios, *Geochemistry, Geophysics, Geosystems*, 7 (6); DOI:10.1029/2005GC001164
- Sella, P., A. Billi, I. Mazzini, L. De Filippis, L. Pizzino, A. Sciarra, and F. Quattrocchi, 2014. A newly-emerged (August 2013) artificially-triggered fumarole near the Fiumicino airport, Rome, Italy, *Journal of Volcanology and Geothermal Research*, 280: 53-66; DOI:10.1016/j.jvolgeores.2014.05.008
- Sigurdsson, H., 1987. Lethal gas bursts from Cameroon crater lakes, *EOS, Transactions of the American Geophysical Union*, 68 (23): 570-573
- Sigurdsson, H., J.D. Devine, F.M. Tchoua, T.S. Presser, M.K. W. Pringle, and W.C. Evans, 1987. Origin of the lethal gas burst from Lake Monoun, Cameroon, *Journal of Volcanology and Geothermal Research*, 31: 1-16
- Silver, P.G., R.M. Russo, C. Lithgow-Bertelloni, 1998. Coupling of South American and African plate motion and plate deformation, *Science*, 279 (5347), 60-63; DOI:10.1126/science.279.5347.60
- Simkin, T., and Siebert, L., 1994. *Volcanoes of the World*. Geosciences Press, Inc. Tucson, pp: 349
- Smets, B., N. d'Oreye, and F. Kervyn, 2014. Toward another lava lake in the Virunga volcanic field? *EOS, Transactions of the American Geophysical Union*, 95 (42): 377-378
- Tazieff, H., 1975. *Niragongo ou le volcan interdit*, Flammarion, pp: 288
- Tchoua, F.M., 1983. The phreatomagmatic explosions of Monoun, *Revue scientifique et technique*, 3: 87-97
- Terada, A., and T. Hashimoto, 2017. Variety and sustainability of volcanic lakes: response to subaqueous thermal activity predicted by a numerical model, *Journal of Geophysical Research Solid Earth*, 122: 6108-6130; DOI:10.1002/2017JB014387
- Ubangoh, R.U., I.G. Pacca, and J.B. Nyobe, 1998. Palaeomagnetism of the continental sector of the Cameroon Volcanic Line, West Africa, *Geophysical Journal International*, 135 (2): 362-374; DOI:10.1046/j.1365-246X.1998.00635.x
- Valentine, G.A., A.H. Graettinger, and I. Sonder, 2014. Explosion depths for phreatomagmatic eruptions, *Geophysical Research Letters*, 41 (9): 3045-3051; DOI:10.1002/2014GL060096
- Varekamp, J.C., and M.J. Van Bergen, (eds), 2008. *Volcanic lakes and environmental impacts of volcanic fluids*, *Journal of Volcanology and Geothermal Research*, 178 (2): 131-330
- Varekamp, J.C., G.B. Pasternack, and G.L. Row Jr., 2000. Volcanic lake systematic, II. Chemical constraints, *Journal of Volcanology and Geothermal Research*, 97 (1/4): 161-179; DOI:10.1016/S0377-0273(99)00182-1
- Walter Antony, K., T. Schneider von Deimling, I. Nitzte, S. Frolking, A. Emond, R. Daanen, P. Anthony, P. Lindgren, B. Jones, and G. Grosse, 2018. 21st-century modeled permafrost carbon emissions accelerated by abrupt thaw beneath lakes, *Nature Communications*, 9 (1): article number 3262; DOI:10.1038/s41467-018-05738-9
- Walter, K.M., S.A. Zimov, J.P. Chanton, D. Verbyla, and F.S. Chapin, III, 2006. Methane bubbling from Siberian thaw lakes as a positive feedback to climate warming, *Nature*, 443: 71-75; DOI:10.1038/nature05040
- Williams, H., and McBirney, A.R. 1979. *Volcanology*, Freeman, Cooper and Co., San Francisco, pp: 397
- Wright, T.L., D.L. Peck, and H.R. Shaw, 1976. Kilauea lava lakes: natural laboratories for study of cooling, crystallisation, and differentiation of basaltic magma, *AGU Monograph*, 19: 375-390
- Wüest, A., L. Jarc, H. Bürgmann, N. Pasche, and M. Schmid, 2012. Methane formation and future extraction in Lake Kivu. *Lake Kivu, Aquatic Ecology Series*, 5: 165-180

- Yapa, K., 2016. Mechanism behind high flows in water springs in volcanic rock formations? Research Gate (question, unpublished)
- Yokoyama, I., 1988. Poynting vector in geomagnetic and geoelectric variations, *Journal of geomagnetism and geoelectricity*, 40, 105-110

Acronyms

- AE - acoustic emission
- AVCOR - Active Volcanism and Continental Rifting
- BL - ball lightning
- CC - Congo Craton
- CVL - Cameroon Volcanic Line
- DNA - deoxyribonucleic acid
- e.m. - electromagnetic
- ECGS - *European Center for Geodynamics and Seismology*
- GOES - *Geostationary Operational Environmental Satellite*
- IAVCEI - *International Association of Volcanology and Chemistry of the Earth Interior*
- INGV - *Istituto Nazionale di Geofisica e Vulcanologia*
- IWGCL - *International Working Group on Crater Lakes*
- KC - Kalahari Craton
- LTM - *Landsat Thematic Mapper*
- MAR - Mid-Atlantic Ridge
- ML - mantle length (of a squid)
- MODIS - *Moderate Resolution Imaging Spectroradiometer* aboard NASA's *Terra* satellite
- MOPITT - *Measurements Of Pollution In The Troposphere*, instrument aboard NASA's *Terra* satellite.
- MOR - Mid-Ocean Ridge
- MORB - MOR basalt
- NEMO - *Neutrino Mediterranean Observatory*
- RIS - *Reparto Indagini Scientifiche*
- SST - sea surface temperature
- TD - tide-driven (geodynamo)
- Terra - (*EOS AM-1*) multi-national, NASA scientific research satellite in a Sun-synchronous orbit around the Earth, flagship of the *Earth Observing System (EOS)*
- TLE - transient luminous event
- UCAR - *University Corporation for Atmospheric Research*
- USGS - *United States Geological Survey*
- VGP - virtual geomagnetic pole
- WAC - West African Craton
- WMT - warm mud tectonics

The electrostatic Sun

Giovanni Pietro Gregori^{1,2}, Bruce Allen Leybourne²

¹IDASC-Istituto di Acustica e Sensoristica O. M. Corbino (CNR), Roma, now merged into IMM-Istituto per la Microelettronica e Microsistemi (CNR) and ISSO-International Seismic Safety Organization, Italy

²GeoPlasma Research Institute-(GeoPlasmaResearchInstitute.org), Aurora, CO 80014, USA

Corresponding Author: G. P. Gregori, IDASC-Istituto di Acustica e Sensoristica O. M. Corbino (CNR), Roma, now merged into IMM-Istituto per la Microelettronica e Microsistemi (CNR);
Email: giovannipgregori38@gmail.com
leybourneb@iascc.org

Abstract: The old-fashionable and generally agreed paradigm of an electrically neutral solar wind is untenable, according to the present knowledge and understanding of the expansion of the solar corona. The surviving paradigm is a heritage of the pre-*MHD* (magneto-hydro-dynamics) age that ended with Alfvén in the 1950s. The Sun is very likely to release a positive charged solar wind, while the electrostatic reset of the Sun occurs cyclically, through the emission of huge electrons fluxes from van de Graaff accelerators. This is a simple and straightforward explanation of the sunspot cycle, and of the related implications for electron polar auroræ. In addition, the morphological features of the Pluto/Charon binary system, including their 4 tiny rocky satellites, is found to be an excellent and unexpected natural laboratory suited to test the mechanisms of the interaction between solar wind and different kinds of planetary objects.

Keywords: electric charge of the solar wind – sunspot cycle - van de Graaff accelerators – *MHD* age – Parker spiral – MiniMax - Pluto/Charon binary system – singular morphology and orbital plane – Pluto/Charon mini-satellites orbital plane and fast spinning

Introduction

Universal gravitation, and the axiomatics of the principles of dynamics, were speculated by Newton in 1687, i.e., almost two centuries before the Maxwell's axiomatics (in 1865) for electromagnetic (e.m.) phenomena. However, fluid dynamics remained treated in terms of neutral matter alone, until the formulation of magneto-hydro-dynamics (*MHD*) by Alfvén in 1950. That is, almost 3 centuries elapsed after Newton before dealing with fluids in terms of the combined action of gravitation and electromagnetism.

Therefore, all models for planetary system formation - and for cosmology - were developed during three centuries with a strong bias in favor of gravitation, while the e.m. interaction was considered as an optional additional "perturbation". In particular, the interplanetary environment was considered rigorously empty, and eventually occasionally crossed by clouds of matter released by the Sun (see Gregori et al., 2026a).

Given such a scenario, the Parker¹ (1958) model for solar corona expansion looks with all its innovative and revolutionary perspective. Human minds require "simple" or "beautiful" theories or models. A "simple" theory can explain some facets of reality, though not all of them. Different schemes, or approximations, lead to different

theories. The Parker (1958) model of solar corona expansion was constructed by *MHD*, and it was confirmed by *in situ* observations. It has been a great intuition and achievement, confirmed by "ground truth". This was a real milestone suited to get rid of several uncertainties and possible logical ambiguities.

However, this "beautiful" model cannot explain several transient phenomena that appear to be a steady, rather than an exceptional, occurrence. That is, the scatter with respect to average is much more important than the average *per se*. In the ultimate analysis, the primary logical "flaw" relies in the discrete nature of the solar corpuscular radiation, opposite to the continuum approximation implied by *MHD*.²

In particular, since it is impossible to smear one single electron or proton in infinitesimal parts – as electrons or protons must be treated, rather, like quantum particles - the "logical monster" of "reconnection" of *B*-field-lines had to be introduced in order to save in some way the continuum formalism of *MHD*. Hence,³ the $\text{div } \mathbf{B} = 0$ Maxwell's law was violated. Otherwise, a particle-particle interaction must be used, instead of *MHD*.

No formal treatment is here discussed of the *MHD* computation of any model. In addition, it is impossible to include in the present study a review of the ongoing

¹ Eugene N. Parker (1927-).

² Concerning the bias implied by the continuum approximation, with respect to the quantized structure of nature see Gregori et al. (2022, 2022a, 2022b, 2022c, 2022d, 2022e).

³ The symbols for classical vector differential operators are as follows. [Historical symbol (here used) \Leftrightarrow most

frequently used]: scalar product $\mathbf{v} \times \mathbf{w} \Leftrightarrow \mathbf{v} \cdot \mathbf{w}$; vector product $(\mathbf{v} \wedge \mathbf{w})_k \Leftrightarrow (\mathbf{v} \times \mathbf{w})_k$; $(\text{grad } f)_j \Leftrightarrow \nabla f$; divergence $\text{div } \mathbf{v} \Leftrightarrow \nabla \cdot \mathbf{v}$; curl $(\text{curl } \mathbf{v})_j$ or also $(\text{rot } \mathbf{v})_j \Leftrightarrow (\nabla \times \mathbf{v})_k$; Laplacian $\Delta f \Leftrightarrow \nabla^2$ or $\nabla \cdot \nabla$.

investigations on several structural details of the expanding solar corona and of its embedded B_{int} – i.e., interplanetary B , which is also called interplanetary magnetic field (*IMF*) or heliospheric magnetic field (*HMF*).

For instance, refer to Owens and Forsyth (2013) who introduce this difficult topic, and state that the *HMF* "is the means by which the Sun interacts with planetary magnetospheres and channels charged particles propagating through the heliosphere. As the *HMF* remains rooted at the solar photosphere as the Sun rotates, the large-scale *HMF* traces out an Archimedean spiral. This pattern is distorted by the interaction of fast and slow solar wind streams, as well as the interplanetary manifestations of transient solar eruptions called Coronal Mass Ejections (CMEs). On the smaller scale, the *HMF* exhibits an array of waves, discontinuities, and turbulence, which give hints to the solar wind formation process."

Owens and Forsyth (2013) warn, however, that "while some of this material, such as the Parker spiral, is mature and established enough to part of standard textbooks on space physics, other areas are very much developing ... a number of *HMF* reviews already exist, so we have tried to focus on aspects of the *HMF* where our knowledge is rapidly evolving: the outer heliosphere, the solar cycle variations, the link to solar wind formation, long-term variations in the *HMF*, etc. "

Therefore, no attempt is here made to deal with these rapidly evolving items, while following the steadily ever-increasing amount of observational material that is discussed by devoted meetings and monographs. Therefore, as far as the present paper is concerned, interplanetary or magnetospheric phenomena are to be considered only a lengthy additional detail and/or some kind of mathematical supplementary technicality.

Similarly, there is no concern about the complicated - and often still incompletely understood - phenomena associated with large-scale variations of the solar wind flow, as a response to violent solar dynamic events. This kind of topic is better suited for a study on solar physics than for items dealing with Earth's science.

In general, the leading focus is here on the assessment of one essential - more or less conscious - paradigm that almost unbelievably seems to be "generally accepted", and that has a crucial impact in the present "generally agreed" understanding of Sun-Earth relations. The paradigm is the assumption of the neutral electric charge of the solar wind.

Indeed, there is no concern about the fact that some "mean" electric charge must be null. The concern is rather about the minimum scale-size in spacetime that has to be considered in order to find a null "mean".

The focus is therefore on the solar wind - rather than on phenomena that accelerate it. In general, only some items are highlighted almost like flashes, while every item ought to be the object of a devoted very long monograph. However, no such details are needed here.

A preliminary warning is rather needed. In general, a mathematical formulation of the solar wind depends on the approximations that are chosen in order to get a theory that can be managed by our available algorithms (refer to Fig.

1). Every chosen model can justify a few facets of observations, etc. However, one must refrain from the temptation to consider a given model like a "paradigm". A fundamental critical feeling must always be applied in order to remain in contact with reality: this is the leading criterion of the present whole discussion.

The crucial point is that, in contrast with the present generally accepted belief, no sound reason, either observational or theoretical or physical, requires that the solar wind must be electrically neutral on a strictly instant and point-like basis. Electrical neutrality must hold when averaging over suitable and non-vanishing time-lags and space-volumes. The concern is therefore about assessing the size of these time-lags and space-volumes.

No "revolutionary" viewpoint is implied, and no new "paradigm" has to be introduced, as the electrostatic repulsion argument is always firmly taken into account.

It can be stated, as it is here shown, that the Earth - and other planetary objects - are the most effective monitoring devices for a concrete - although indirect - assessment of the role of electrostatic phenomena in the solar wind. In addition, whenever the comparison is to be made between different planetary objects, the different relevance of every planetary object (satellite through comets) is closely related to its size.

Scatter vs. mean trend both in space and in time

The Parker (1958) model for the expansion of the solar corona has to be considered as a representation of the mean trend of a very intricate phenomenon. In fact, following the early proposal by Larmor (1919, 1920) and Larmor and Joseph (1919), every star is a very efficient *MHD* dynamo, supplied by the intense internal thermal convection maintained by thermonuclear reactions.

The Cowling dynamo (see Gregori et al., 2026d) generates a violent self-confinement, by which, in the case that the e.m. interaction ought to prevail, the star would be permanently closed in a pattern firmly confined by a toroidal magnetic field B . Owing to the Biermann blocking, even photons would have difficulty to be released. For instance, the B inside sunspots is so large that electrons cannot cool, because they are strongly trapped by B (Biermann, 1941).

This statement is, however, paradoxical, as energy must be released, due to the enormous energy production by thermonuclear reactions. Hence, the stellar *MHD* dynamo permanently explodes in order to achieve a thermodynamic release of endogenous energy, and thus to satisfy energy balance. Owing to this reason the B of the Sun and of stars – as it is well-known - cannot be regular and smooth both in space and time – such as, e.g., the B of the Earth or of several other planets.

Therefore, solar evaporation is dominated by kinetic energy, inside a highly conductive medium due to the great availability of free electrons. This implies the well-known effect of "frozen-field" that was first envisaged by Alfvén (1950).

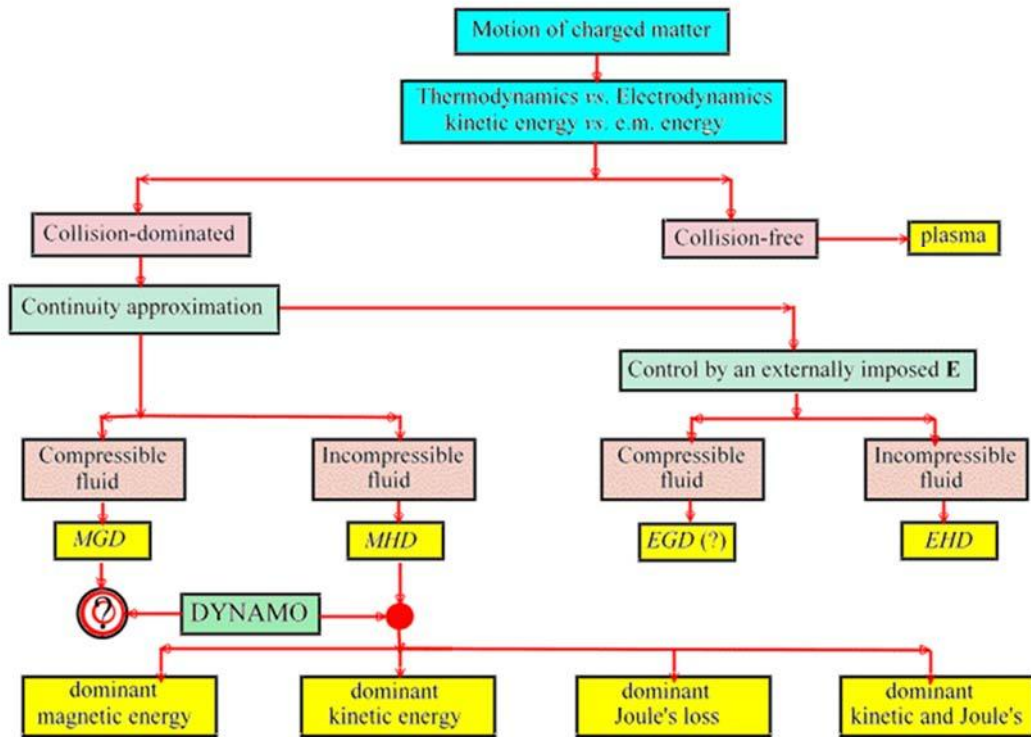


Fig. 1 - Different conventional definitions dealing with the motion of charged particles, and four possible dynamo scenarios. The choice of either one scenario or another depends on the kind of dominating energy. The standard homogeneous dynamo (for the Earth interior or for a star) is essentially always supposed to be composed of an incompressible fluid, hence it relies on *MHD*. In the case of a compressible fluid (e.g., for the ionospheric dynamo) it should rely on *MGD* (magneto-gas-dynamics). The case of control by an externally applied electric field E seems to be, in general, of no concern, likewise *EHD* and *EGD* (electro-hydro-dynamics or electro-gas-dynamics). After Gregori (2002). With kind permission of the late Wilfried Schröder.

The sketch of Fig. 2 shows one simple pattern of the electric current j and of the B that is transported by the thermal expansion of hot matter. The great scatter, however, must be considered of B , when it is observed at the photosphere. Hence, different regions of the photosphere are found to be associated with B directions that are either towards or away from the Sun, resulting in the well-known classical sector structure of the Parker spiral (Fig. 3).

The "heliospheric neutral sheet" (*HNS*) is a well-known and important morphological feature of interplanetary environment (Fig. 4). However, in general, the literature only seldom stresses that during "quiet" Sun – i.e., when the total number of sunspots looks to be lower – a clustering occurs of sunspots into very few, or sometimes even just one, large ensembles.

The corresponding interplanetary sector structure, which is "normally" characterized by four sectors (toward → away → toward → away), shifts to a two-sector pattern (toward → away). This fact is observed in the photographs of the solar corona during solar eclipses that appear more regular and less scattered during "quiet" Sun than during "active" Sun.

In addition, during a full rotation of the solar corona (say, roughly, ~ 27 days with small changes vs. heliocentric latitude), the Earth - or every planetary object - experiences either 4 or 2 crossing with the *HNS*. The 2-

crossing pattern corresponded to the so-called MiniMax Sun (Clette et al., 2014; Gregori et al., 2026c).

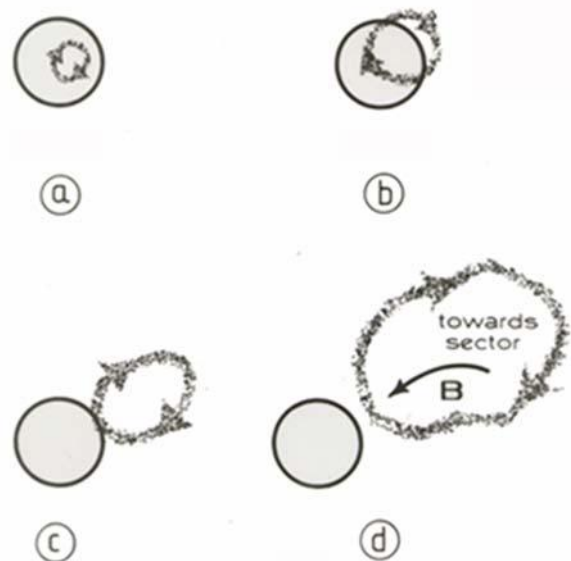


Fig. 2 – A CME projects through space j -loops that characterize the well-known classical observed Parker spiral pattern of interplanetary environment. Unpublished figure.

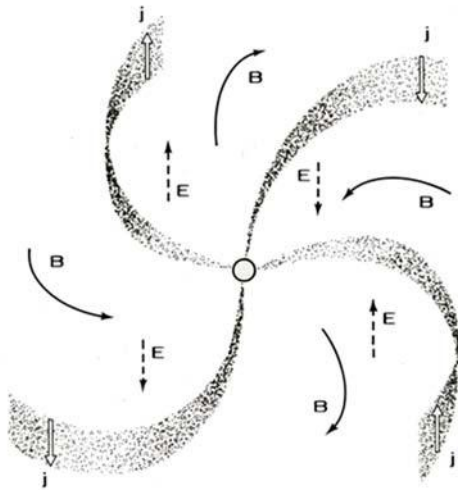


Fig. 3 - Interplanetary space is characterized by the well-known observed spiral pattern of B_{int} that, owing to the almost infinite conductivity σ of the solar wind and to the frozen-in approximation - according to the Alfvén's theorem - is associated to a corresponding pattern of the interplanetary electric field E_{int} . In addition, owing to the Maxwell's relation $curl \mathbf{B} = \mathbf{j}$, some kind of huge "blades" of currents \mathbf{j} (called "heliospheric neutral sheet", HNS) must separate the different interplanetary sectors. Unpublished figure. The leading role must be emphasized that is played by the kinetic energy originated by the explosion of the solar confinement.



Fig. 4 - An artist's concept of the HNS, which becomes wavier when \mathbf{B} flips on the surface of the photosphere. After Phillips (2013b). NASA copyright free policy.

In addition, this has implications on the e.m. induced \mathbf{j} inside planetary objects, with an effect on the efficiency of their respective internal TD (tide driven) dynamo (Gregori and Leybourne, 2021; Gregori et al., 2026a). In fact, an increased efficiency of the TD dynamo occurs inside every planetary object. Therefore, anomalous Earth's climate features and anomalous Sun (MiniMax), are to be expected to be correlated with anomalous phenomena observed, e.g., also in the atmosphere of the large gaseous outer planets, etc. Differently stated, nothing happens by chance, and a logical relation can always be found between much different and apparently unrelated observations. The MiniMax is a crucial item in the control of the solar-

terrestrial relations and of the atmospheric electric circuit. See Gregori et al. (2026c) and Gregori and Leybourne (2026c).

All this refers to the *mean* picture of the whole solar expansion phenomenon, while - in reality - a leading role is played by single events that characterize the scatter of the system with respect to the mean trend. Compared to planetary objects, scattered phenomena have a very large size. Planetary objects react, therefore, to every single event, rather than to the mean background. That is, the concern is about the space-size and the time-lag to be considered.

The size of planetary objects

Consider Fig. 5 that is similar to several other often reported figures aimed to compare the relative size of the Earth and of solar eruptions. The dramatic pattern that can be observed on the photosphere is sometimes shown in greater detail, such as, e.g., in Fig. 6. See also impressive images in Chitta et al. (2023), illustrated by *European Space Agency* (2024).

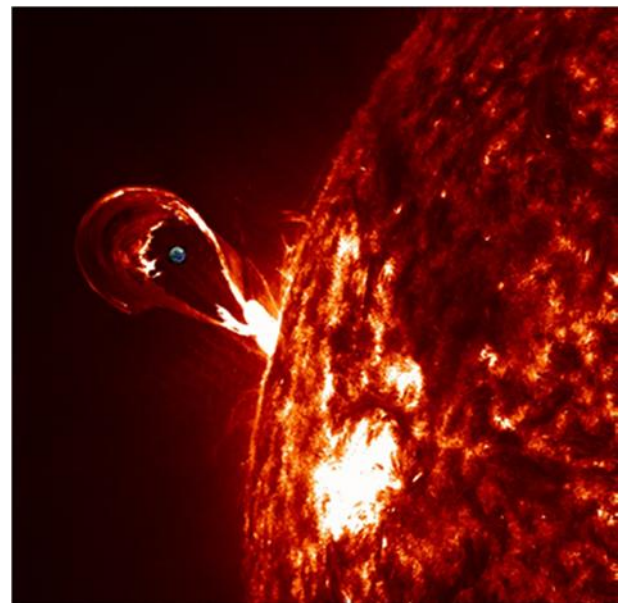


Fig. 5 - "View of a typical solar eruption using data from NASA's Solar Dynamic Observatory spacecraft. Earth depicted for scale. Credit: Tahar Amari / Centre de physique théorique, CNRS École Polytechnique, France." Figure and captions after Choi (2014b). NASA copyright free policy.

Reference, however, has to be made to the size of other planetary objects. For instance, refer to Fig. 7.

In addition, the interplanetary medium is permanently crossed by a multitude of smaller objects that can be eventually observed through photon emission, i.e., by comets.

All these objects are therefore very efficient probes suited to monitor the local state of the solar wind through the whole interplanetary space. Comets are expected to display morphological features associated to a cometosphere (see below).

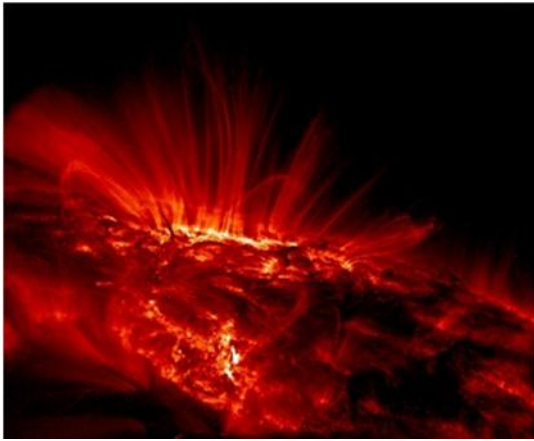


Fig. 6. "Sunspot loops in UV ... shown in UV light, the relatively cool dark regions have temperatures of thousands of degrees Celsius. Large sunspot group AR 9169 is visible as the bright area near the horizon. The bright glowing gas owing around the sunspots has a temperature of over one million degrees Celsius. The reason for the high temperatures is unknown but thought to be related to the rapidly changing **B** loops that channel solar plasma. Sunspot group AR 9169 moved across the Sun during 2000 September and decayed in a few weeks. Credit: TRACE Project, NASA." This is one of several similar pictures often reported of the Sun. It is here claimed that these filamentary structures are the consequence of a domino effect of Cowling dynamos, which also very effectively confine hot plasma, such as it typically occurs inside a laboratory-generated ball lightning (see Gregori et al., 2026d; Gregori and Leybourne, 2025e). Figure and captions after Nemiroff and Bonnell (2006). NASA copyright free policy.

As far as the Earth is concerned, the solar corona expansion is described at Earth's orbit by a spherical surface of radius equal to the average distance of the Earth from the Sun, i.e., $1 AU \sim 2.8 \times 10^{23} m^2$. The Earth captures only a tiny fraction of this whole surface, being equal, say, to some approximate cross-section of the magnetosphere, i.e., say by a circle of radius $\sim 10 R_E$ (where R_E denotes one Earth's radius), or $\sim 1.3 \times 10^{14} m^2$. That is, the Earth - including the entire magnetosphere - monitors a fraction that is only $\sim 0.45 \times 10^{-9}$ the total surface of the expanding solar corona. This is very likely to be much smaller than the minimum size of a solar wind cloud that can be considered with null electric charge.

Electrostatics in the solar corona expansion

Before MHD age and Parker (1958), reference was made to neutral fluids. In general, a vacuum interplanetary environment was supposed to be crossed by sporadic clouds of neutral matter. The argument was that an eventual electrically-charged cloud must expand, by electrostatic repulsion, through space way before reaching the Earth (see Gregori et al., 2026a).

In the 1930s the classical Chapman-Ferraro model of the magnetosphere was envisaged that fairly well explained the sudden commencement (*sc*) feature of geomagnetic storms, although it failed to explain the subsequent development of a geomagnetic storms, or the shorter associated details.

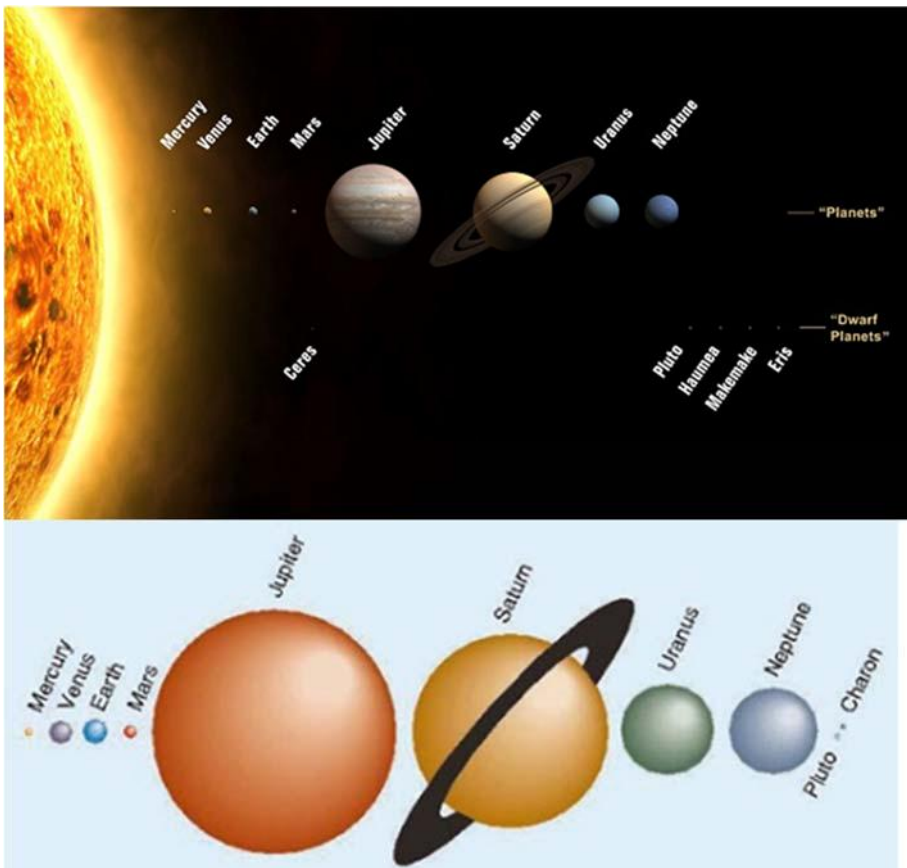


Fig. 7 - "The planets of the Solar System are shown in sequence and in relative size (but not to scale in terms of their true separation from one another)..." A debate in progress is about whether Pluto is a planet or a dwarf planet. Figures and captions after Anonymous (2020d). NASA copyright free policy.

The emanation of the solar wind occurs by thermal release from an exploding system, which is strongly confined by the toroidal \mathbf{B} of the Cowling dynamo (see Gregori et al., 2026d). The system must release the enormous endogenous energy originated by thermonuclear reactions. Hence, the emanation is just a thermal process that opposes the Biermann blocking originated by the Cowling dynamo, by which the Sun ought to keep strictly locked all charged particles to spiral with narrow gyration radii around \mathbf{B} -field-lines.

At equal \mathbf{B} , the gyration radius of a particle is proportional to its mass. Hence, electrons have gyration radii that are several-ten-thousand times smaller than protons and ions. Note that ions are only positive, because - owing to the high temperature - nuclei afford to keep only a limited fraction of electrons bound inside the atomic shells. Negative ions are therefore very unlikely to exist in such an environment.

The thermal emanation process involves particles that are comparatively less firmly trapped around \mathbf{B} -field-lines. Hence, positive ions have a much greater chance of evaporating than electrons: the solar wind is to be expected to contain prevalently positive particles, i.e., protons and positive ions.

In addition, consider the crucial role played by the self-collimation that is observed – and presently it is claimed to be partially unexplained – inside the solar wind flow. Indeed, this collimation is to be expected due to the role of the Cowling dynamo, of the fast solar wind, plus the *EGD* effect due to the much larger mass of protons and positive ions compared to electrons (see Gregori et al, 2026d, and additional details in Gregori et al., 2025w, and Gregori and Gregori, 2025). That is, since the local thermal anomalies generate micro-patterns of convection, these patterns originate a toroidal \mathbf{B} that confines and self-collimates the plasma flow.

Summarizing, the solar wind is to be expected to be mainly composed of protons and positive ions, and to be self-confined in filaments. Hence, the original large scale-size of solar explosions, such as shown in Figs 5 and 6, is maintained inside the expanding solar wind. A planetary object experiences therefore a flux of solar wind that is positively charged.

It is unbelievable that the paradigm of a neutral solar wind firmly survives in the literature, even though since the 1950s the pre-*MHD* age is over. The positive solar wind has some relevant and obvious observed implications, although these features are presently claimed to be unexplained.

Solar morphology

The almost steady exhalation of positively charged solar wind leaves an increasing negative electric charge on the Sun. The electrostatic repulsion is generally confined by the toroidal \mathbf{B} that ought to cause a total self-confinement of the Sun. This cannot occur, due to the need to release endogenous thermonuclear energy. However, in any case, the Sun thus continuously accumulates negative electric

charge. This cannot endure at infinity, as at some suitable time the Coulomb repulsion force ought to prevail.

The phenomenon is therefore to be expected to be cyclic, although of unknown period. In fact, during some time-lag the Sun accumulates negative electric charge. When the total charge attains some threshold, the Sun must release electrons. This must occur through huge van de Graaff accelerators that expel electrons in order to break the confinement by the toroidal \mathbf{B} . The period of such a cyclic feature is unknown. But it can be very easily recognized in solar morphology.

In fact, this is the sunspot cycle. A van de Graaff accelerator ejects electrons that cross through the photosphere. Since no ions are contained in the electron jet, no photons are released. The jet looks therefore black, while it crosses through the photosphere. This is a sunspot.

Sunspots are well-known to appear first at higher heliocentric latitude, and to drift equatorward during the evolution of the solar cycle. This feature is to be explained in a suitable way by the models of Larmor's solar *MHD* (or *MED*) dynamo.

Violent clouds of electrons cross interplanetary environment. They are self-confined – like every kind of solar wind – due to the Cowling dynamo that generates toroidal \mathbf{B} . The greater mobility of electrons - compared to protons and positive ions - is such that self-confinement is even comparatively more effective.

When these clouds of electrons impinge on the Earth - or on a planetary object - spectacular manifestations occur of electron-auroræ, which are the most beautiful auroræ, as proton auroræ are much fainter and only seldom observed, basically due to much fainter intensity, and smaller collimation.

On the other hand, as is well-known, it is impossible to measure the electrostatic charge of a precipitating cloud of particles inside an intense auroral display, as the e.m. environment is severely perturbed. Indeed, a violent perturbation is to be expected, due to the very intense Birkeland currents (see Gregori and Leybourne, 2025g).

This full explanation of several morphological features is original, being in general related to the sunspot cycle that in the past looked like a disquieting challenge for solar and Earth scientists. The logical key of such a simple physical argument is the transition from the surprising survival of the pre *MHD* viewpoint to the post Alfvén age.

Magnetospheres and cometspheres

The interaction of a planetary object with the solar wind generates a magnetosphere that, however, can be more or less structured and developed, depending on the existence of an internal magnetic field \mathbf{B} , originated, e.g., by the *TD* dynamo (Gregori, 2002, and Gregori and Leybourne, 2021 and references therein). Magnetospheres are the concern of extensive literature.

A presently unnoticed feature is, rather, concerned with comets. In fact, the plasma originated from cometary exhalation originates, through Cowling dynamo (see Gregori et al., 2026d), a \mathbf{B} that develops a temporary

magnetosphere – that can be briefly called “cometosphere”. The observation of several morphological features of comets can, perhaps, be used (in preparation) to monitor the state of the solar wind inside a wide 3D space through interplanetary space.

Some relevant aspects implied by a non-vanishing electric charge of the solar wind can certainly affect the interaction of the solar wind with the planetary atmospheres. In fact, whenever no magnetosphere exists that protects the atmosphere like a shield, a spoiling effect on the atmosphere by the solar wind causes a reduction of the total mass of the atmosphere.

In contrast, an increased endogenous energy generation and release – which is associated to a time-varying efficiency of the *TD* dynamo - originates an increase of atmospheric density.

Indeed, the Earth is an effective gauge for such two competing effects, as - during a geomagnetic field reversal (*FR*) - the Earth's atmosphere has no protection by the magnetospheric shield. At the same time, the increased *TD* efficiency originates from a great increase of soil exhalation, hence an increase of atmospheric density. This can be documented by several information provided by extinctions in the biosphere, e.g., by insects inside amber. In fact, the atmospheric density changed, maybe even by several times (e.g., mainly Levenspiel et al., 2000; Levenspiel, 2000 and references therein), and this is, maybe, e.g., the explanation of the extinction of flying large animals, as they missed the needed Archimedean support.⁴ See also Gregori and Leybourne (2025j).

A huge literature exists. Refer, e.g., to several papers announced by Laura Geggel in several short notes on the web (*Live Science*) between 2015 and 2018, or see Gregori (2015a) and references therein for much better details. A few recent findings are reported. The Cenozoic CO₂ Proxy Integration Project (CenCO₂PIP) Consortium (2023a) shows a dramatic decrease of CO₂ concentration in the atmosphere during the Cenozoic (the last 66 *Ma*), relying on a critical re-evaluation of all evidences. They show that an early Cenozoic “hothouse” CO₂ concentration peaked around 1600 *ppm* at ~51 *Ma*. At the onset of Antarctic glaciation, ~33.9 *Ma* ago, the atmospheric CO₂ concentration was 720 *ppm*. Then, atmospheric CO₂ concentration dropped to 550 *ppm* at ~32 *Ma*, corresponding with the onset of radiation in plants that have carbon-concentrating mechanisms and populate grasslands and deserts today. During the remainder of the Cenozoic CO₂ concentration remained below this threshold, continuing the dramatic long-term decrease toward the present value. The middle Miocene (~16 *Ma*) is the last time when CO₂ concentrations were substantially higher than at present; while at that time Greenland was not yet glaciated. According to independent estimates, the sea level is reported as being at that time some 50 *m* higher than today. However, at the Plio-Pleistocene boundary (2.6 *Ma*), the atmospheric CO₂ concentration eventually dropped below 270 *ppm* while the Earth approached our current

“icehouse” state of bipolar glaciation. These findings are a substantial challenge for the present concern about the effects of the increase of atmospheric CO₂ concentration as a primary driver for climate change.

A conspicuous literature exists concerning the effects on other planets of the temporary disappearance of the solar wind. These items are outside the target of the present paper. Let us just mention only a very recent episode reported by Reed (2023).

In addition, several peculiar morphological features are observed, referring to several different kinds of planetary objects that can be affected by a non-null electrical charge of the solar wind. These phenomena are not here discussed due to brevity requirements, as every item ought to require a devoted extensive discussion.

Orbital implications

Two features are related to orbital implications of a planetary object, whenever the object gets electrically charged by the impinging solar wind. Two effects are to be distinguished: (i) an orbiting object is an electric current that generates a magnetic field **B** that interacts with **B_{int}**, and (ii) a spinning charged object has a magnetic moment, hence different spinning objects must interact due to their respective magnetic moments.

A wonderful natural laboratory is the binary system Pluto/Charon, monitored by the *NASA* probe *New Horizons*, which had one-transit and no magnetometer aboard. The Pluto/Charon binary system is useful, and a unique opportunity, to examine three lines of evidence.

The first evidence deals with the time-varying *TD* dynamo efficiency. In fact, consider the great eccentricity of the retrograde orbit, inclined ~ 17° with respect to all other planets, with aphelion 49.31 *AU* and perihelion 29.667 *AU* (e.g., Guo et al., 2015, or Guo and Farquar, 2007). Hence, the efficiency of the respective *TD* dynamo inside either Pluto or Charon changes very much with respect to the heliocentric distance. Therefore, a huge seasonal variation occurs of endogenous energy release during the Hadean year, which lasts ~248 *Earth years*. The Pluto/Charon system has been at its perihelion in 1989. Therefore, in 2015 it was only ~ 16 *years* after perihelion, and its heliocentric distance was ~ 33 *AU*.

Some impressive landscapes are observed. On Pluto the evidence is found of some large regions that remind about frozen swamps of N₂ ice (with evidence of large convection cells) that also show floating icebergs of H₂O ice. The absence of cratering in the frozen swamps denotes a mysterious comparatively much recent freezing. One almost obvious interpretation is that the swamps melt and freeze during the Hadean year, while the floating icebergs of H₂O ice can move only with melt swamps. A more extensive discussion is given in Gregori (2016a).

The second and third evidences refer to the electric charge of the solar wind.

⁴ We are indebted to the late friend Niels-Axel Mörner (1938-2020) for the Levenspiel references.

The orbital motion relative to each other of Pluto/Charon is a circular \mathbf{j} -loop that generates a \mathbf{B} perpendicular to the orbital motion. The orbital motion should therefore be oriented along \mathbf{B}_{int} , i.e., along the Parker spiral. The observed \mathbf{B}_{int} is always located in the ecliptic plane, with a scatter of at most very few degrees.⁵ The \mathbf{B}_{int} intensity is faint, and also the \mathbf{B} generated by the orbital motion of Pluto/Charon. Hence, a faint magnetic perturbation occurs on the orbits that are mainly controlled by gravitation. However, both \mathbf{B}_{int} and \mathbf{B} should be aligned with the same direction.

This happens during one sector of the Parker spiral, while during the opposite sector the orbital motion ought to reverse. In any case, the plane of the orbital motion is observed to be almost perpendicular to the heliocentric orbit of the system that is inclined $\sim 17^\circ$ with respect to all other planets. That is, the orbital motion of the Pluto/Charon binary system is approximately perpendicular to the ecliptic plane (Fig. 8), which is the mean plane of \mathbf{B}_{int} , consistently with a supposed electrically charged solar wind.

The piece of evidence is related to the mysterious 4 tiny satellites that move around Pluto/Charon, i.e., in the same orbital plane as Pluto and Charon. Their bodies are much irregular - of rocky shape - and their size is in the range between 10 and 40 km. In addition, they spin at some incredibly fast speed. They are named (for increasing radial distance) Styx, Nix, Kerberos, and Hydra, respectively (Fig. 9). Owing to the fast spinning, every mini-satellite - which is charged by an eventual non-neutral solar wind - has a magnetic moment, along its spin axis.

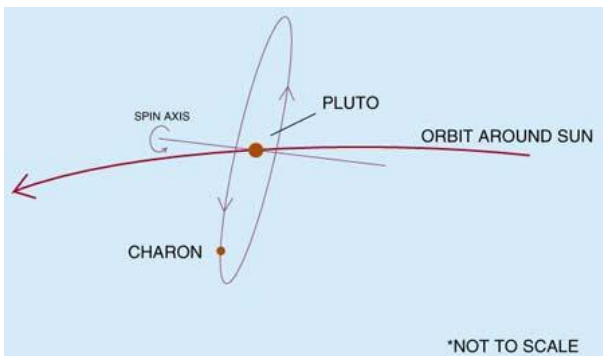


Fig. 8 - Most planets have north poles that point roughly up and out of their orbit planes - except Uranus and Pluto, which rotate on their "sides". Like most satellites, Charon orbits above Pluto's equator, i.e., the plane of the Charon orbit is perpendicular to Pluto's pole axis. From 1985 through 1990 Pluto's equator and Charon's orbit plane were aligned with the line of sight from Earth. Charon would pass in front of Pluto every 6.39 days. After Guo et al. (2015) and Anonymous (2020d). NASA copyright free policy.

The 4 mini-satellites must interact through their magnetic moments. Therefore, they ought to be observed at Hadean longitudes that should be *approximately at equal relative distance*, while every spin axis should be perpendicular to the orbital plane, which is shared altogether by the Pluto/Charon binary system and by the orbits of the 4 mini-satellites. This is, indeed, what is observed (Fig. 10).

It should be stressed that these curious morphological features are reported as being mysterious and unexplained, while they closely fit with the hypothesis of an electrically charged solar wind. Therefore, it can be stated that the Pluto/Charon binary system is an unexpected and clear proof of the non-neutral charge of the solar wind.

A final remark deals with the Hadean magnetosphere. In fact, the solar wind interacts with an intricate planetary magnetic field \mathbf{B} , which is the sum of (i) the TD dynamos that are active inside both Pluto and Charon, plus (ii) the \mathbf{B} generated by the orbital motions of both Pluto and Charon, plus (iii) the \mathbf{B} originated by the 4 mini-satellites, either by the orbital motions or by their fast spinning and magnetic moments.

Therefore, a substantial time-variation has to be expected of the Hadean magnetosphere during the Hadean year, also dependent on the transient sector direction of the Parker spiral.

The Sun and interstellar medium (ISM)

After completing the present paper, we found Smith (2020) who claims that "the Sun lives within a positive space charge sheath with respect to the interstellar medium (ISM): it isolates itself in a cocoon of plasma." He shows Fig. 11 and specifies what follows.

"The Sun is an anode connected to galactic power circuits. Those circuits are of unknown potential, but they probably include energy sources encompassing thousands of cubic light-years. The electrodynamic forces moving through galactic 'transmission lines' (Birkeland currents) are also unknown, but astronomers constantly report their amazement at solar flare output.

The Sun's heliospheric boundary is a double layer 'cocoon', as mentioned, isolating it from galactic plasmas flowing through the ISM. Voltage differences occur within the heliosphere, so the Sun, because it is an electrical terminal, experiences charge/discharge phenomena related to variable electrical input. Sunspots and flares most likely develop from changes in solar electrical supply.

An electrically active Sun means that electric discharges penetrate the solar photosphere, allowing electric charge to flow into its depths. Electromagnetic flux tubes expose the Sun's darker, cooler interior. Those flux tubes connect the Sun's e.m. field directly to Earth's ionosphere

⁵ A reminder is deserved about the present incorrect general agreement by which, in general, \mathbf{B}_{int} is drawn perpendicular to the ecliptic plane, consistently with the Dungey model of the magnetosphere, and with the general assumed "convection" in the magnetosphere. The magnetosphere is not a closed system, hence no

requirement exists for any convective motion. In addition, all available true observations of the interplanetary environment clearly deny such a Dungey/convection model (see Gregori and Leybourne, 2021).

Solar flares can increase Earth's auroral displays because they are composed of charged particles. They

follow Earth's polar cusps, since they are electrical in nature

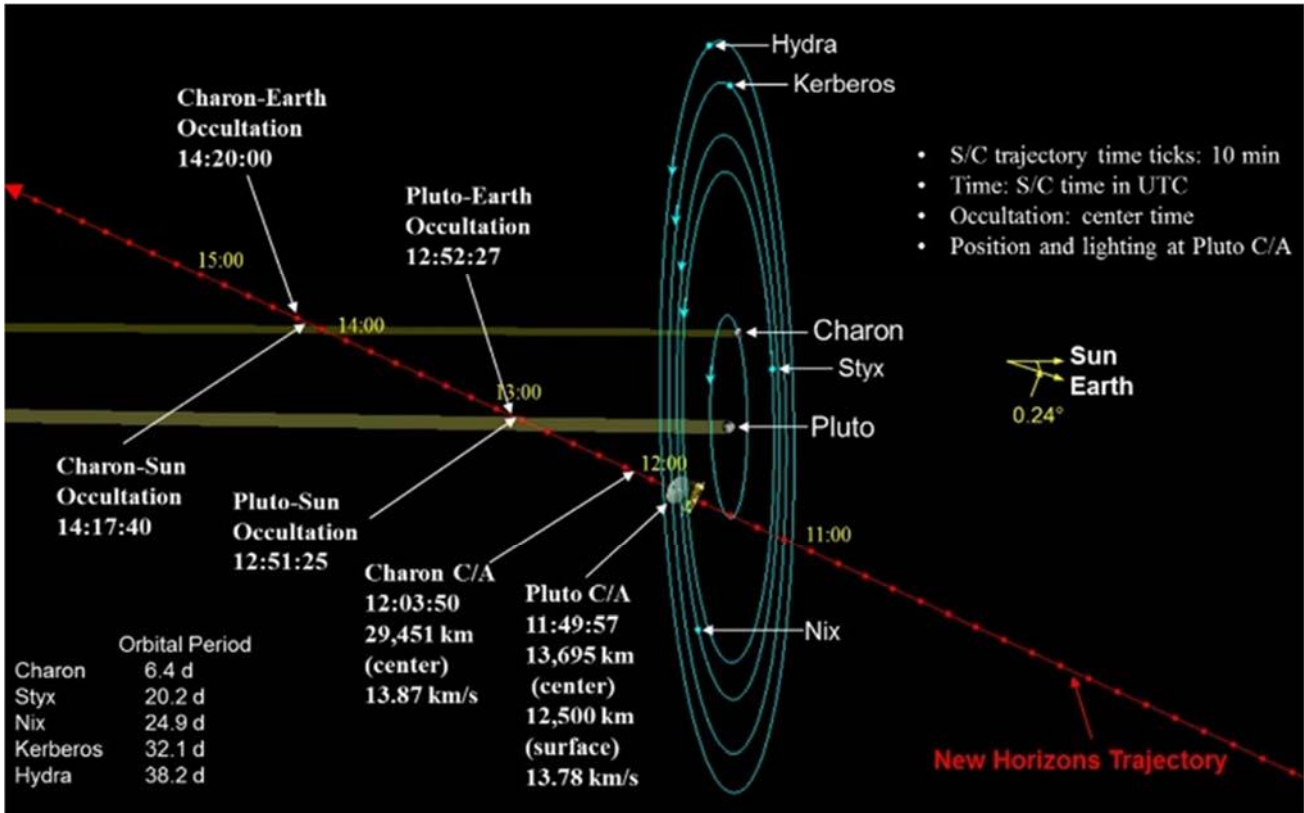


Fig. 9 - Encounter geometry of *New Horizons* with the Pluto/Charon system. After Anonymous (2020d). See also Guo and Farquar (2007). NASA copyright free policy.

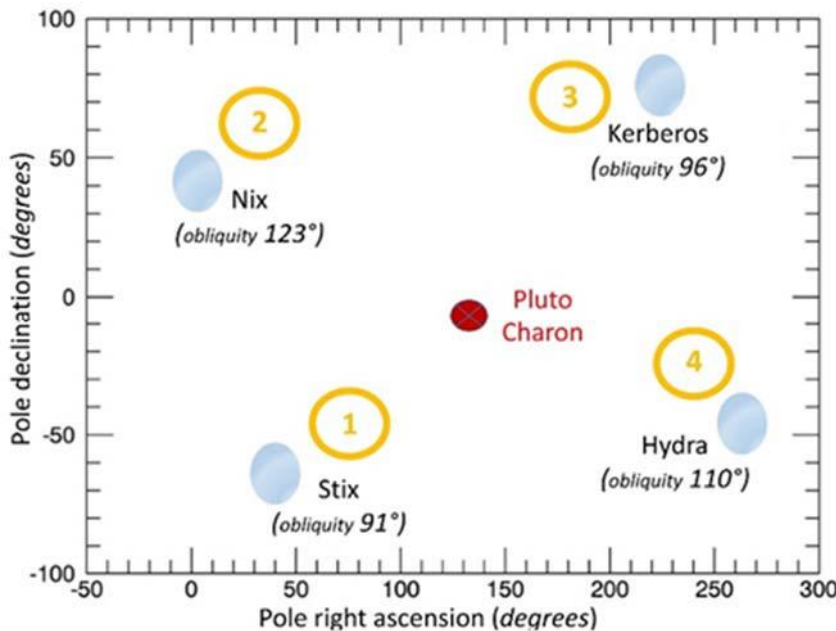


Fig. 10. Rotation pole locations for Pluto/Charon's mini-satellites. The locations of the north poles (i.e., directions determined using the right-hand-rule with the hand curling around in the spin direction and the thumb denoting the north pole) for Pluto/Charon's mini-satellites are plotted on a grid of celestial coordinates in the standard J2000 frame. Every mini-satellite is also associated to a yellow number that denotes the satellite location in the sequence from closer mini-satellite to farther one. The red icon indicates the direction of Pluto's and of Charon's North Pole (which are identical). The obliquity is the angle between the Pluto/Charon pole and the pole direction of every mini-satellite. Values are uncertain by $\pm 10^\circ$. When that angle is $> 90^\circ$, the mini-satellite rotates in the opposite direction from its orbital motion around the barycenter of the Pluto/Charon binary system (i.e., the rotation is retrograde, rather than prograde).

Nominally, all the mini-satellites have retrograde rotation, but Nix is the only one significantly so (i.e., retrograde with $> 1\sigma$ confidence). Also, Hydra is likely to be retrograde (see text), although it is difficult to get a precise estimate by means of a few blurry images. All four planets have rotation poles clustered near their orbital planes (i.e., near the Pluto/Charon orbital plane). Unpublished figure based in information after Stern et al. (2015) and Weaver et al., 2016b).

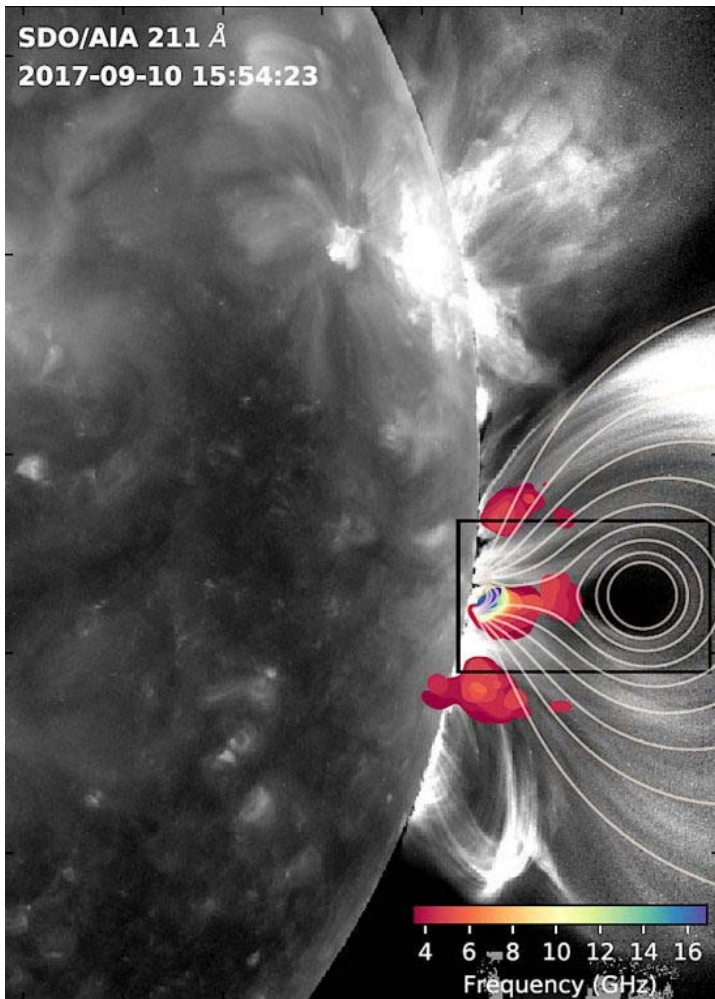


Fig. 11. “An ultraviolet image of a giant solar flare on 2017-09-10 as seen by SDO. These high spatial resolution images confirm that they are the primary locations for accelerating and channeling fast-moving electrons. Credit: NSF, NASA, and Chen et al. 2020.” Figure and captions after Smith (2020).

The Sun is an electric star. When electricity builds up beyond a trigger point within the Sun’s inductive fields, solar plasma discharges at near relativistic velocities—solar flares could be like tremendous lightning bursts on the Sun. Electric Universe advocate, Wal Thornhill wrote:

‘It is obvious from looking at powerful mass expulsion activity in active stars and galaxies that gravitational models are inadequate to explain what is going on. Gravity is an attractive force only. Recourse to magnetic field behavior magically divorced from electric currents serves merely to reinforce the mystical quality of modern physics without telling us anything about the true cause.’ ”

Concerning the impact on Earth’s climate through air-earth currents, Smith (2020) stresses that “on September 7, 2005 an X17 solar flare impacted Earth’s magnetosphere, knocking out radio transmissions and overloading power station transformers. Is it a coincidence that hurricanes Katrina (August 29, 2005) and Rita (September 23, 2005) occurred on either side of the fourth largest X-flare ever recorded?”

Further evidence for solar electrical influence is that, 12 years later, hurricanes Harvey (August 25, 2017) and Irma (with wind speeds of 290 km hour⁻¹ on September 10, 2017) were spawned before and after an X9.3 flare on September 8 (the eighth largest solar flare ever recorded)

and then an X8.2 flare on the same day. At similar periods in the solar cycle, within days of each other, violent e.m. changes in the Sun initiated violent weather events on Earth.”

It is also noteworthy the fact that optical observations of the Sun display precursors of flare activity (Dissauer et al., 2023, Leka et al., 2023).

In addition, a most recent paper reports an unexpected and clear effect associated to the Saturn rings (Ben-Jaffel et al., 2023; the paper is announced and illustrated in *Space Telescope Science Institute*, 2023). They analyzed 40 years of UV data from multiple space missions, including NASA’s *Hubble Space Telescope*, the *Cassini* probe, *Voyager 1* and 2, and the *International Ultraviolet Explorer*. They found that icy ring particles are raining down onto Saturn’s atmosphere, causing heating.

This analysis was possible due to calibration that permits us to compare the measurements carried out by different missions. Ben-Jaffel used measurements from *Hubble*’s *Space Telescope Imaging Spectrograph (STIS)*, which provided precision observations of Saturn UV data from all four other space missions.

An additional finding was that Saturn’s iconic hexagonal storm, first discovered in 1981 by the *Voyager 2*

spacecraft, was difficult to distinguish in 2020, but it is again clearly evident in 2021.

The most feasible explanation is that icy ring particles raining down onto Saturn's atmosphere cause this heating. This could be due to the impact of micrometeorites, solar wind particle bombardment, solar UV radiation, or e.m. forces picking up electrically charged dust. All this happens under the influence of Saturn's gravitational field pulling particles into the planet. When NASA's Cassini probe plunged into Saturn's atmosphere at the end of its mission in 2017, it measured the atmospheric constituents and confirmed that many particles are falling in from the rings." (Space Telescope Science Institute, 2023).

They also found a seasonal variation of the phenomenon. We give a different interpretation of this evidence. In fact, during almost the entire sunspot cycle the solar wind has a dominating positive charge (i.e., proton content). Conversely, only during a few years of the so-called solar maximum, a maximum concentration of electron content occurs, although confined in comparably compacted huge clouds. In fact, these huge electron clouds are self-collimated due to the Cowling dynamo (Gregori et al., 2026d). In addition, they experience an intricate interaction with the huge Saturn's magnetosphere. The phenomenon ought to display substantial variations when comparing different sunspot cycles. All these effects must be observed also in this unexpected and curious impact of the Saturn rings on the Saturn atmosphere.

"The telltale evidence is an excess of UV radiation, seen as a spectral line of hot hydrogen in Saturn's atmosphere. The bump in radiation means that something is contaminating and heating the upper atmosphere from the outside.

Conclusions

The fashionable paradigm of an electrically neutral solar wind is untenable with the present knowledge about the state of the interplanetary environment. The paradigm is, rather, the heritage of the pre-MHD age, i.e., of the state of knowledge before Alfvén and the 1950s.

Sound physical reasons, related to solar processes, very likely envisage a positive charge of the solar wind. The electrical unbalance of the Sun is thus cyclically reset through the ejection of enormous amounts of electrons, inside huge van de Graaff accelerators, and this is the most straightforward explanation of the sunspot cycle.

No detail can be here considered about several morphological features dealing with different kinds of planetary objects. In any case, the Pluto/Charon binary system is found to be a natural laboratory that is an active threefold check of the mechanisms of the interaction between solar wind and a planetary object.

In fact, one check is related to the variation of the efficiency of a TD dynamo depending on the heliocentric distance, because the surface morphology envisages huge changes during the Hadean year - which lasts ~248 Earth years.

Other two checks are more directly related to the electric charge of the solar wind, as both orbital motion and spin, of a charged object, imply the generation of a magnetic field that interacts with B_{int} . The orbital data of Pluto/Charon, and of the 4 mini-satellites, altogether with the fast spinning of the mini-satellites, look to be an almost incredible and unexpected "proof" of the non-neutral charge of the solar wind.

Better observational information ought to require operating a magnetometer in the Hadean environment.

Acknowledgement

We want to acknowledge all co-workers that, in different ways and at different times, contributed to the exploitation of the analyses mentioned in the present study. We are also thankful for the warm encouragement we had from several outstanding scientists. We thank John Ricken ("Rickmo") Wright for the suggestion on the role of fast solar wind, and of the EGD effect due to the much larger mass of protons and positive ions compared to electrons.

Funding Information

G.P. Gregori has been retired since 2005. B.A. Leybourne is a semi-retired self-funded independent researcher.

Author's Contributions

This study derived from a long-lasting cooperation by both authors. The backbone draft was prepared by the first author, although a large number of ideas resulted from the emergence of long-lasting discussions between the authors.

Ethics

This article is original and contains unpublished material. Authors declare that there are no ethical issues and no conflict of interest that may arise after the publication of this manuscript.

References

- Anonymous, 2020d. The Pluto system, The Johns Hopkins University Applied Physics Laboratory LLC, Retrieved on 22 September 2020, <http://pluto.jhuapl.edu/Pluto/The-Pluto-System.php>
- Ben-Jaffel, L., J.I. Moses, R.A. West, K.M. Aye, E.T. Bradley, J.T. Clarke, J.B. Holberg, and G.E. Ballester, 2023. The Enigmatic abundance of atomic hydrogen in Saturn's upper atmosphere. The Planetary Science Journal, 4 (3): 54, DOI:10.3847/PSJ/acaf78
- Chen, Bin, Chengcai Shen, D.E. Gary, K.K. Reeves, G.D. Fleishman, Sijie Yu, Fan Guo, S. Krucker, Jun Lin, G.M. Nita, and Xiangliang Kong, 2020. Measurement of magnetic field and relativistic electrons along a solar flare current sheet, Nature Astronomy, 4: 1140–1147; DOI:10.1038/s41550-020-1147-7
- Chitta, L.P., S.K. Solanki, J.C. del Toro Iniesta, J. Woch, D. Calchetti, A. Gandorfer, J. Hirzberger, F. Kahil, G. Valori, D. Orozco Suárez, H. Strecker, T. Appourchaux,

- R. Volkmer, H. Peter, S. Mandal, R. Aznar Cuadrado, L. Teriaca, U. Schühle, D. Berghmans, C. Verbeeck, A.N. Zhukov, and E.R. Priest, 2023. Fleeting small-scale surface magnetic fields build the quiet-Sun corona, *The Astrophysical Journal Letters*; DOI:10.3847/2041-8213/acf136
- Choi, C.Q., 2014b. Huge magnetic 'ropes' drive powerful Sun explosions, *Space.com*, October 22, 2014
- Clette, F., L. Svalgaard, J.M. Vaquero, and E.W. Cliver, 2014. Revisiting the sunspot number. A 400-year perspective on the Solar Cycle, *Space Science Review*, 186 (1/4): 35–103; DOI:10.1007/s11214-014-0074-2
- Dissauer, K., K.D. Leka and E.L. Wagner, 2023. Properties of flare-imminent versus flare-quiet active regions from the chromosphere through the corona. I. Introduction of the AIA Active Region Patches (AARPs), *The Astrophysical Journal*, 942 (2): 83; DOI:10.3847/1538-4357/ac9c06
- European Space Agency*, 2024. Solar Orbiter's breakthrough: decoding the Sun's million-degree corona, *ESA News*, issued January 16, 2024
- Gregori, G. P., 2002. Galaxy – Sun – Earth relations. The Origin of the Magnetic Field and of the Endogenous Energy of the Earth, with Implications for Volcanism, Geodynamics and Climate Control, and Related Items of Concern for Stars, Planets, Satellites, and Other Planetary Objects. A Discussion in a Prologue and Two Parts. *Beiträge zur Geschichte der Geophysik und Kosmischen Physik*, Band 3, Heft 3: pp. 1-471 [Available at <http://ncgtjournal.com/additional-resources.html>]
- Gregori, G. P., 2015a. Comment on Stephen W. Hurrell: A new method to calculate paleogravity using fossil feathers, *New Concepts in Global Tectonics, Journal*, 3 (1): 68-70
- Gregori, G. P., 2016a. The endogenous energy and the magnetic field of planetary objects: the Pluto/Charon binary system and its seasonal rejuvenation, *New Concepts in Global Tectonics, Journal*, 4, (3): 406-431.
- Gregori, G. P., and B. A. Leybourne, 2021. An unprecedented challenge for humankind survival. Energy exploitation from the atmospheric electrical circuit, *American Journal of Engineering and Applied Science*, 14 (2): 258-291; DOI:10.3844/ajeassp.2021.258.291
- Gregori, G. P., and B. A. Leybourne, 2026c. The solar cycle and MiniMax - Effects on other planets. Present issue of *New Concepts in Global Tectonics, Journal*
- Gregori, G. P., and B. A. Leybourne, 2026e. The physics of electrical discharges – I. Small-scale phenomena - Fog - atmospheric precipitation – BLs. *New Concepts in Global Tectonics, Journal*, 14, (2): 129-152
- Gregori, G. P., and B. A. Leybourne, 2026g. The physics of electrical discharges – III. Sparks and lightning - electrostatics of the ionosphere – TLEs - plasma jets collimation – Birkeland currents & sea-urchin spikes - stellar and galactic alignments. *New Concepts in Global Tectonics, Journal*, 14, (2): 171-207
- Gregori, G. P., and B. A. Leybourne, 2025j. The energy supply to hurricanes. *New Concepts in Global Tectonics, Journal*, 13, (5): 731-786
- Gregori, G.P., B.A. Leybourne, and J.R. Wright, 2026c. The solar cycle and MiniMax. Present issue of *New Concepts in Global Tectonics, Journal*
- Gregori, G. P., B. A. Leybourne, and J. R. Wright, 2026d. Generalized Cowling theorem and the Cowling dynamo. *New Concepts in Global Tectonics, Journal*, 14, (1): 90-112
- Gregori, G.P., B.A. Leybourne, G. Paparo†, and M. Poscolieri, 2026a. The global Sun-Earth circuit. Present issue of *New Concepts in Global Tectonics, Journal*
- Gregori, G. P., W. Soon, V. Straser, and B. A. Leybourne, 2022b. The foundations of physics and axiomatics. I - Axioms. *New Concepts in Global Tectonics, Journal*, 10 (3): 202-235
- Gregori, G.P., C.W. Monckton of Brenchley, W. Soon, R. Tattersall, A. D'Amico†, G. Zimatore, V.M. Velasco Herrera, B.A. Leybourne, and Z.A. Oziewicz †, 2022. Golden Ratio, Variational Principles, Cyclic and Wave phenomena, *Quanta*. In H.M. Colin Garcia, J.-deJ. Cruz Guzman, L.H. Kauffman, and H. Makaruk (eds), *Scientific Legacy of Professor Zbigniew Oziewicz, Selected Paper of the International Conference Applied Category Theory Graph-Operad-Logic* (August 25th to 27th, 2021), 2024 World Scientific Publishing Company; pp: 363-389; DOI:10.1142/9789811271151.0018
- Gregori, G. P., M. T. Hovland, B. A. Leybourne, S. Pellis, V. Straser, B. G. Gregori, G. M. Gregori, and A. R. Simonelli, 2025w. Air-earth currents and a universal “law”: filamentary and spiral structures - Repetitiveness, fractality, golden ratio, fine-structure constant, antifragility and “statistics” - The origin of life, *New Concepts in Global Tectonics, Journal*, 3, (1): 106-225
- Gregori, G.P., and B.G. Gregori, 2025. *The universe out of the box - New foundations of physics - Rhythms, Golden Ratio, origin of life, antifragility*, Europe Books
- Gregori, G. P., W. Soon, V. Straser, and B. A. Leybourne, 2022a. Golden ratio, fractals, and the arrow of time. Irreversibility vs. reversibility - Space, time, antitime - The foundations of physics. *New Concepts in Global Tectonics, Journal*, 10 (3): 158-201
- Gregori, G. P., W. Soon, V. Straser, and B. A. Leybourne, 2022c. The foundations of physics and axiomatics. II - Algorithms and equations, and a comparison with Einstein's theory of relativity. *New Concepts in Global Tectonics, Journal*, 10(3): 236-262
- Gregori, G.P., W. Soon, V. Straser, and B.A. Leybourne, 2022d. The foundations of physics and axiomatics. III - Superluminal phenomena, mechanisms, matter-antimatter, cosmological implications. *New Concepts in Geoplasma Tectonics*, 10(3): 263-283
- Gregori, G. P., W. Soon, V. Straser, and B. A. Leybourne, 2022e. The foundations of physics and axiomatics. IV - The geometrical representation of symmetries -

- Parity, emp, and charge (PEC) “meta-multiverse”. *New Concepts in Global Tectonics, Journal*, 10 (3): 284-299
- Guo, Y., and R.W. Farquar, 2007. New Horizons mission design. *Space Science Review*, 140 (1/4): 49-74; DOI:10.1007/s11214-007-9242-y
- Guo, Y., B. Williams, F. Pelletier, J. McAdams, and W.-J. Shyong, 2015. Trajectory monitoring and control of the New Horizons Pluto flyby, 25th International Symposium on Space Flight Dynamics ISSFD, Munich, Germany, October 19-23, 2015
- Larmor, Sir J., 1919. How could a rotating body such as the Sun become a magnet? *British Association Report*, 159-160, Bournemouth
- Larmor, Sir J., 1920. How could a rotating body such as the Sun become a magnet?, *Rep. Brit. Ass. Adv. Sci.*, Bournemouth Meeting, 1919, pp: 159-160, also in *Mathematical and physical papers*, Vol. II, pp: 611-612, Cambridge University Press, 1929
- Larmor, Sir J., and S. Joseph, 1919. Possible rotational origin of magnetic fields of Sun and Earth. *Elec..Elec. Rev.*, 85, 412
- Leka, K.D., K. Dissauer, G. Barnes, and E.L. Wagner, 2023. Properties of flare-imminent versus flare-quiet active regions from the chromosphere through the corona. II. Nonparametric discriminant analysis results from the NWRA Classification Infrastructure (NCI), *The Astrophysical Journal*, 942 (2): 84; DOI:10.3847/1538-4357/ac9c04.
- Levenspiel, O., 2000. DEPARTMENTS-Learning from the past-Earth's early atmosphere. *Chemical Innovation*, 30 (5): 47-51
- Levenspiel, O., Thomas J. Fitzgerald, and Donald Pettit, 2000. Earth's atmosphere before the age of dinosaurs, *Chemical Innovation*, 30 (12): 50-55
- Owens, M. J., and R. J. Forsyth, 2013. The heliospheric magnetic field, *Living Review of Solar Physics*, 10 (5); DOI:10.12942/lrsp-2013-5
- Parker, E. N., 1958. Dynamics of the interplanetary gas and magnetic fields, *Astrophysical Journal*, 128: 664-676; DOI:10.1086/146579
- Phillips, T., 2013b. The Sun's magnetic field is about to flip, *Science@NASA*, issued August 5, 2013
- Reed, W., 2023. The great solar wind disappearance: groundbreaking discovery by NASA's MAVEN mission, *SciTechDaily*, issued December 13, 2023
- Smith, S., 2020. Space charge, *The Thunderbolt Project*, Picture of the Day, issued July 8, 2020.
- Space Telescope Science Institute*, 2023. Saturn's strange ring-heat phenomenon: Solving a Solar System mystery, *SciTechDaily*, *Space News*, issued April 1, 2023
- Stern, S.A., F. Bagenal, K. Ennico, G. Randall Gladstone, W.M. Grundy, W.B. McKinnon, J.M. Moore, C.B. Olkin, J.R. Spencer, H.A. Weaver, L.A. Young, T. Andert, J. Andrews, M. Banks, B. Bauer, J. Bauman, O.S. Barnouin, P. Bedini, K. Beisser, R.A. Beyer, S. Bhaskaran, R.P. Binzel, E. Birath, M. Bird, D.J. Bogan, A. Bowman, V.J. Bray, M. Brozovic, C. Bryan, M.R. Buckley, M.W. Buie, B.J. Buratti, S.S. Bushman, A. Calloway, B. Carcich, A.F. Cheng, S. Conrad, C.A. Conrad, J.C. Cook, D.P. Cruikshank, O.S. Custodio, C.M. Dalle Ore, C. Deboy, Z.J. B. Dischner, P. Dumont, A.M. Earle, H.A. Elliott, J. Ercol, C.M. Ernst, T. Finley, S.H. Flanigan, G. Fountain, M.J. Freeze, T. Greathouse, J.L. Green, Y. Guo, M. Hahn, D.P. Hamilton, S. A. Hamilton, J. Hanley, A.Harch, H.M. Hart, C.B. Hersman, A. Hill, M.E. Hill, D.P. Hinson, M.E. Holdridge, M. Horanyi, A.D. Howard, C.J.A. Howett, C. Jackman, R.A. Jacobson, D.E. Jennings, J.A. Kammer, H.K. Kang, D.E. Kaufmann, P. Kollmann, S.M. Krimigis, D. Kusnierkiewicz, T.R. Lauer, J.E. Lee, K.L. Lindstrom, I.R. Linscott, C.M. Lisse, A.W. Lunsford, V.A. Mallder, N. Martin, D.J. McComas, R.L. McNutt Jr., D. Mehoke, T. Mehoke, E. D. Melin, M. Mutchler, D. Nelson, F. Nimmo, J.I. Nunez, A. Ocampo, W.M. Owen, M. Paetzold, B. Page, A.H. Parker, J.W. Parker, F. Pelletier, J. Peterson, N. Pinkine, M. Piquette, S.B. Porter, S. Protopapa, J. Redfern, H.J. Reitsema, D. C. Reuter, J.H. Roberts, S.J. Robbins, G. Rogers, D. Rose, K. Runyon, K. D. Retherford, M.G. Ryschkewitsch, P. Schenk, E. Schindhelm, B. Sepan, M.R. Showalter, K.N. Singer, M. Soluri, D. Stanbridge, A.J. Steffl, D.F. Strobel, T. Stryk, M. E. Summers, J. R. Szalay, M. Tapley, A. Taylor, H. Taylor, H.B. Throop, C.C.C. Tsang, G.L. Tyler, O.M. Umurhan, A.J. Verbiscer, M.H. Versteeg, M. Vincent, R. Webbert, S. Weidner, G.E. Weigle II, O.L. White, K. Whittenburg, B.G. Williams, K. Williams, S. Williams, W.W. Woods, A.M. Zangari, and E. Zirnstein, 2015. The Pluto system: initial results from its exploration by New Horizons, *Science*, 350 (6258); DOI:10.1126/science.aad1815
- The Cenozoic CO₂ Proxy Integration Project (CenCO₂PIP Consortium)*, 2023. Toward a Cenozoic history of atmospheric CO₂, *Science*, 382 (6675); DOI:10.1126/science.adi5177
- Weaver, H.A., M.W. Buie, B.J. Buratti, W.M. Grundy, T.R. Lauer, C.B. Olkin, A.H. Parker, S.B. Porter, M.R. Showalter, J.R. Spencer, S.A. Stern, A.J. Verbiscer, W.B. McKinnon, J.M. Moore, S.J. Robbins, P. Schenk, K.N. Singer, O.S. Barnouin, A.F. Cheng, C.M. Ernst, C.M. Lisse, D.E. Jennings, A.W. Lunsford, D.C. Reuter, D.P. Hamilton, D.E. Kaufmann, K. Ennico, L.A. Young, R.A. Beyer, R.P. Binzel, V.J. Bray, A.L. Chaikin, J.C. Cook, D.P. Cruikshank, C.M. Dalle Ore, A.M. Earle, G. Randall Gladstone, C.J.A. Howett, I.R. Linscott, F. Nimmo, J.Wm. Parker, S. Philippe, S. Protopapa, H.J. Reitsema, B. Schmitt, T. Stryk, M.E. Summers, C.C.C. Tsang, H.H.B. Throop, O.L. White, and A.M. Zangari, 2016b. The small satellites of Pluto as observed by New Horizons, *Science*, 351 (6279); DOI:10.1126/science.aae0030

Acronyms

- CME - Coronal Mass Ejection
EGD - or electro-gas-dynamics
EHD – electro-hydro-dynamics
e.m. – electromagnetic
FR field reversal (geomagnetic)

HMF - heliospheric magnetic field, synonymous of IMF
HNS - heliospheric neutral sheet
IMF - interplanetary magnetic field, synonymous of B_{int}
ISM - interstellar medium
MGD - magneto-gas-dynamics
MHD - magneto-hydro-dynamics
NASA – National Aeronautics and Space Administration
NSF - National Science Foundation,
sc - sudden commencement

SDO - Solar Dynamics Observatory
STIS - Space Telescope Imaging Spectrograph (onboard Hubble Space Telescope)
TD – tide-driven (dynamo)
TRACE - Transition Region and Coronal Explorer, Exploring the Upper Regions of the Solar Atmosphere (NASA Project)

ABOUT THE NCGT JOURNAL

The NCGT Newsletter , the predecessor of the NCGT Journal , was begun as a result of discussions at the symposium “Alternative Theories to Plate Tectonics” held at the 30th International Geological Congress in Beijing in August 1996. The name is taken from an earlier symposium held in association with the 28th International Geological Congress in Washington, D. C. in 1989. The first issue of the NCGT Newsletter was December 1996. The NCGT Newsletter changed its name in 2013 to the NCGT Journal . Aims of the NCGT Journal include:

1. Providing an international forum for the open exchange of new ideas and approaches in the fields of geology, geophysics, solar and planetary physics, cosmology, climatology, oceanography, electric universe, and other fields that affect or are closely related to physical processes occurring on Earth from its core to the top of its atmosphere.
2. Forming an organizational focus for creative ideas not fitting readily within the scope of dominant tectonic models.
3. Forming the basis for the reproduction and publication of such work, especially where there has been censorship or discrimination.

